Characterisation of semaphorin 3A-chondroitin sulphate interaction in the central nervous system

Lynda Djerbal

Communauté
UNIVERSITÉ Grenoble Alpes

THÈSE

Pour obtenir le grade de

DOCTEUR DE LA COMMUNAUTE UNIVERSITE GRENOBLE ALPES

Spécialité : **Biologie structurale et nanobiologie**

Arrêté ministériel : 25 mai 2016

Présentée par

« Lynda DJERBAL »

Thèse dirigée par **Hugues LORTAT-JACOB** (DR, UMR5075-IBS-UGA-CNERS-CEA) et **Jessica KWOK** (DR, université de Leeds)

préparée au sein du groupe **Structure et Activité des Glycosaminoglycans à l'Institut de Biologie Structurale-UMR5075**
dans **l'École Doctorale Chimie et Science du Vivant**

Characterisation of semaphorin 3A-chondroitin sulphate interaction in the central nervous system

Thèse soutenue publiquement le **«30 Novembre 2018 »**,
devant le jury composé de :

Pr Dulce PAPY-GARCIA
Professeur d'université, université Paris Est Créteil**, Rapporteur**
Pr Joost VERHAAGEN
Professeur, Netherlands institute for neuroscience, **Rapporteur**
Dr Jean-Maurice MALLET
Directeur de recherche, ENS Paris, **Examinateur**
Dr Anne IMBERTY
Directeur de recherche, CERMAV, **Président**

Summary

Perineuronal nets (PNNs) are the key regulators of neuronal plasticity and regeneration in the mature central nervous system (CNS). They are a unique and highly organised extracellular matrix (ECM) structure, found around sub-population of neurons, composed mainly of chondroitin sulphate proteoglycan (CSPG). Chondroitin sulphate (CS) is a linear polysaccharide belonging to glycosaminoglycans (GAGs) family. The sulphation pattern defines different types of CS, which interact with different signalling proteins including those regulating axonal outgrowth and guidance such as semaphorin 3A (Sema3A). Sema3A is a secreted chemorepulsive protein found accumulated in the PNN through its interaction with CS. This process is believed to potentiate Sema3A signalling through plexin A1 (PlxnA1) and neuropilin 1 (Nrp1) and regulate plasticity and regeneration. The aim of the thesis project is to characterise the interface of Sema3A-CS interaction.

For this purpose, Sema3A is expressed in eukaryote cells and purified. Interestingly, two major forms were obtained: a full length Sema3A (90 kDa) which remains attached to the cell surface GAGs and a truncated form without the C-ter part (65 kDa) which is released to the culture medium. With the use of surface plasmon resonance (SPR), we observed that full length Sema3A binds selectively to CS-E (4,6-disulphated chondroitin) and heparan sulphate with a high affinity (K_D in the sub pM range), while the truncated Sema3A does not bind to any GAG. Four putative GAG-binding sequences were identified in the C-ter of Sema3A and mutated using site directed mutagenesis. SPR analysis then revealed that two out of these four sites are required for the binding to CS-E. The importance of these GAG-binding sequences in inhibition of neurites outgrowth of dorsal root ganglion neurons in culture was also reported, indicating thus the importance of GAG-binding in Sema3A signalling. In parallel, the minimal required sequence of Sema3A-binding of CS-E was determined as being a tetrasaccharide. The Sema3A-CS interface was thus characterized. Furthermore, quartz crystal microbalance with dissipation monitoring analysis suggested that Sema3A could crosslink GAG chains. This suggests Sema3A could be involved in stabilising the PNN network and induces mechanical changes on neuronal surface.

The detail characterization of Sema3A-CS interaction may enable the design of new strategies aiming at enhancing plasticity and regeneration for neurodegenerative diseases or spinal cord injury.

Acknowledgements

Je remercie les membres du Jury : ***Joost VERHAAGEN***, ***Dulce PAPY-GARCIA***, ***Jean-Maurice MALLET*** *et* ***Anne IMBERTY*** *d'avoir accepté d'évaluer mes travaux de thèse.*

Je ne pourrais jamais remercier assez mon directeur de thèse ***Hugues****. Quand je suis venue pour l'entretien et je t'ai vu pour la première fois, je me suis dit « il a l'air très bien ce directeur de thèse» et après trois ans je le pense toujours. Merci de m'avoir fait confiance dès le début et de m'avoir donné l'opportunité de faire une thèse dans des conditions « optimales ». Merci pour tout ce que j'ai appris durant ces trois années de thèse. Merci pour tes encouragements et tes conseils pour les manips, rédaction, présentations... Merci de t'être toujours rendu disponible et cela malgré ton emploi du temps chargé. J'ai vraiment apprécié le travail avec toi sur le plan scientifique et humain. Je suis très contente que mon post-doc sera toujours en collaboration avec toi. Infiniment Merci Hugues !*

Un très grand merci à mon autre directeur de thèse ***Jessica****. Je t'ai aimé dès notre premier skype pour l'entretien. Je me suis aussi dit « qu'est-ce qu'elle est gentille ! » Et cela ne s'est fait que confirmer au cours de ces trois années. Et je n'oublierai pas ce que tu m'as dit au début de ma thèse « fais toutes les erreurs que t'as à faire pendant la thèse, car c'est pendant la thèse qu'on apprend » et cela m'a mis à l'aise. J'apprécie ton dynamisme et ton esprit scientifique. Merci pour tout ce que tu m'as appris. Merci pour ta confiance, ton soutien, tes encouragements et ta gentillesse. Merci pour l'opportunité que tu m'as offerte de poursuivre sur la même thématique que ma thèse et surtout sur ma protéine préférée «Sema3A ». Je suis très contente de poursuivre en post-doc avec toi.*

Je remercie les membres de ma deuxième famille « SAGAG ». ***Rabia****, merci beaucoup pour ton amour, ta gentillesse et tes délicieux gâteaux. Je me rappellerai toujours du premier jour quand je t'ai vu à l'entretien, t'étais adorable comme toujours et je me suis dit j'aimerais bien être prise dans cette équipe. Et merci de m'avoir appris à faire les WB et dot blot.* ***Romain****, t'es le chercheur le plus cool que je connaisse et cela je l'ai su, avant même de te rencontrer, dans le premier mail que tu m'as envoyé. J'apprécie énormément ton enthousiasme, ton raisonnement scientifique et ton sens de l'humour et merci. Merci de m'avoir appris « heparin-beads approach » et l'analyse disaccharidique.* ***Evelyne****, je suis chanceuse que t'as intégré le SAGAG avant que je parte, je suis très contente de t'avoir connue. Merci pour ta gentillesse, ta bonté et ton aide. Rabia et Evelyne, je ne dirai pas vous êtes les mamans du SAGAG mais plutôt les grandes sœurs.* ***Yoan****, quand je t'es vu la première fois je me suis dit « pas très souriant, ce post-doc» mais en fait c'est juste une première impression, t'es sympa et très serviable. Merci d'avoir toujours pris le temps de discuter les difficultés que j'ai rencontrées surtout pendant la purification de la Sema. Merci de m'avoir montré tous les logiciels et tous les sites requis pour mon projet.* ***Rana****, ma petite Rana, j'ai su qu'on allait devenir amies avant même de te rencontrer. Tout aurait été moins drôle si tu n'étais pas là. Je suis très contente de t'avoir rencontrée. Merci pour tous les moments agréables passés au labo surtout après 19h, au bureau, au coin café en dehors du travail. Merci pour ta complicité dans tout et surtout ton amitié.*

Merci à tous les membres du ***SAGAG*** *d'avoir contribué à ma formation scientifique. On dit « il faut tout un village pour élever un enfant » et moi je dis «il faut tout un groupe de recherche pour*

former un étudiant ». Vous allez beaucoup me manquer mais je reviendrai vous voir. Je m'arrête là pour le SAGAG sinon je vais écrire une deuxième thèse de remerciements …

Je remercie les HBB de la « pause 17:00 » : ***Rana*** *(tu vois c'est comme les groupes de FB et WhatsApp, t'es partout),* ***Rida****, je suis très contente d'avoir fait ta connaissance. T'es la libanaise la plus drôle que je connaisse après Rana biensûr. T'es une fille formidable. Merci pour tous les moments géniaux qu'on a passé ensemble à l'IBS ou en dehors de l'IBS et merci pour le GreenMango du mois de juillet.* ***Kevin****, infatigable Kevin, j'étais ravie de rédiger ma thèse au même temps que toi. Merci pour les amandes et ton sens de l'humour.* ***Guillaume****, merci pour ta gentillesse, et les friandises du distributeur et ton sens de détection de fautes d'orthographe.*

Rime *ma compatriote, merci pour ton soutien, ta gentillesse et ta bonté.* ***Ilham****, mon autre compatriote, contente de t'avoir rencontrée. Merci* ***Elodie*** *pour ta gentillesse. Merci aux voisins du SAGAG,* ***IRPAS****, pour les pauses café du matin, leur gentillesse et de partager le matériel de leur labo. Merci à tous les amis que j'ai rencontrés à l'IBS :* ***Muge****,* ***Tomas****,* ***Laura****,* ***Catarina, Amal, Stefaniia, Aldo****,* ***Simon****,* ***Silvia, Quentin, Marko, Justine…***

Je tiens à remercier également tous les gens qui m'ont aidé à la réalisation des manips. Merci à ***Ralf RICHTER*** *de m'avoir accueillie dans son laboratoire à Leeds. Merci à* ***Luke SOUTER*** *de m'avoir montré le fonctionnement du QCM-D. Merci à* ***Chrystel LOPIN-BON*** *pour les oligosaccharides de CS. Merci à* ***Joël BEAUDOUIN*** *pour la mutagenèse dirigée. Merci à* ***Jean-Pierre ANDRIEU*** *pour le « N-ter sequencing » et les mousses au chocolat. Merci au personnel des plateformes SPR et M4D. Merci* ***Joëlle BOENIGEN*** *pour ta gentillesse et ton efficacité pour le traitement des dossiers administratifs. Merci à* ***Mounia****, de m'avoir aidée à construire la table des abréviations. Merci aux deux membres de mes deux CSI :* ***Nicole THIELENS*** *et* ***Alain BUISSON*** pour leurs conseils. *Enfin, merci à tous les gens de l'IBS ou en dehors de l'IBS qui ont contribué d'une manière ou d'une autre pour l'aboutissement de ce projet de thèse.*

Merci à ***Marie-Jeanne*** *et* ***Pierre*** *pour leur présence, gentillesse et soutien pendant ces trois années.*

Enfin merci à ma famille : mes parents, mes deux frères, mes tantes et mes cousins qui ont toujours été là pour moi.

Table of contents

List of abbreviations

a.a: amino acid

A: Alanine

AD: Alzheimer's Disease

ALS: Amyotrophic Lateral Sclerosis

AMPA: α-amino-3-hydroxy-5-methyl-4-isoxazolepropionic acid

AMPAr: AMPA receptor

Aß: Amyloid Beta peptide

ATP: Adenosine Triphosphate

AUC: Analytical Ultracentrifugation Analysis

BBB: Blood–Brain Barrier

BDNF: Brain-Derived Neurotrophic Factor

Bral : Brain-specific link protein

BSA: Bovine Serum Albumin

C: Cysteine

C6ST1: Chondroitin-6-sulphate Sulfotransferase

CAM: Cell Adhesion Molecule

CD: Cluster of Differentiation

Cdk5 : Cyclin-dependent kinase 5

ChABC: Chondroitinase ABC

ChPF: Chondroitin Polymerising Factor

CIH: Colloidal Iron Hydroxide

CMV: Cytomegalovirus

CNS: Central Nervous System

CPC: Cetylpyridinium Chloride

CRAM: CRMP-Associated Molecule

CRMP: Collapsin-Response Mediator Protein

CRP: Complement Regulatory Protein

Crtl: Cartilage link protein

CS: Chondroitin Sulphate

CSPG: Chondroitin Sulphate Proteoglycan

C-ter: C-terminal

DAPI: 4',6-Diamidino-2-Phenylindole, Dihydrochloride

DCN: Deep Cerebellar Nuclei

DEAE: Diethylaminoethyl

DMEM: Dulbecco's Modified Eagle's Medium

DOPC: Dioleoylphosphatidylcholine

DOPE: Dioleoylphosphatidylethanolamine

DRG: Dorsal Root Ganglion

DS-epi: Dermatan Sulphate epimerase

E: Embryonic day

EBNA: Epstein Barr Nuclear Antigen

ECM: Extracellular Matrix

EDC: l-Ethyl-3-(3-Dimethylaminopropyl) Carbodiimide

EDTA: Ethylenediaminetetraacetic Acid

EGF : Epidermal Growth Factor

ELISA: Enzyme-Linked Immunosorbent Assay

Em: Emission

ER: Endoplasmic Reticulum

Ex: Excitation

EXT: Exostosin

FACE: Fluorophore-Assisted Carbohydrate Electrophoresis

FBS: Foetal Bovine Serum

FC: Flow Cell

FGF: Fibroblast Growth Factor

FPLC: Fast Protein Liquid Chromatography

FRAP: Fluorescence Recovery After Photobleaching

GABA: Gamma-Aminobutyric Acid

GAG: Glycosaminoglycan

Gal: Galactose

GalN: Galactosamine

GalNac: N-acetylgalactosamine

GalNacT: N-acteylgalactosaminetransferase

GalT-I: β1,4-Galactosyltransferase I

GAP: GTPase-Activating Proteins

GFP: Green Fluorescent Protein

GlcA: Glucoronic Acid

GlcNac: N-acetylglucosamine

$GlcNH_2$: D-Glucosamine

GnRH: Gonadotropin-Releasing Hormone

GPI: Glycosylphosphatidylinositol

GSK-3: Glycogen Synthase Kinase-3

H: Histidine

HA: Hyaluronic Acid

HAPLN: Hyaluronan and Proteoglycan Binding Link Protein

HAS: Hyaluronan Synthase

HBS: HEPES-Buffered Saline

HBSS: Hank's Balanced Salt Solution

HEK: Human Embryonic Kidney

HGFR: Hepatocyte Growth Factor Receptor

His: Histidine

hMSCs: human Mesenchymal Stem Cells

Hp: Heparin

HPLC: High Performance Liquid Chromatography

HRP: Horseradish Peroxidase

HSPG: Heparan Sulphate Proteoglycan

HYAL: Hyaluronidase

Hz: Hertz

IdoA: Iduronic Acid

Ig: Immunoglobulin

IHC: Immunohistochemistry

ITS: Insulin-Transferrin-Selenium

KO: Knockout

KS: Keratan Sulphate

KSPG: Keratan Sulphate Proteoglycan

LEDCN: Large Excitatory Deep Cerebellar Nuclei Neurons

LRP1: Low-density lipoprotein Receptor-related Protein1

MAM: Meprin A5

MCSP: Melanoma-associated Chondroitin Sulphate Proteoglycan

MD: Monocular Deprivation

MRI: Magnetic Resonance Imaging

MS: Multiple Sclerosis

Mut: Mutant

MW: Molecular Weight

MWCO: Molecular Weight Cut-Off

NG2: Neural/Glial antigen 2

NGF: Nerve Growth Factor

NHS: N-Hydroxysuccinimide

Ni-NTA: Nickel-Nitrilotriacetic Acid

NMDA: N-Methyl-D-Aspartate

NMR: Nuclear Magnetic Resonance

Nptx2: Neuronal pentraxin2

Nrp: Neuropilin

NSC: Neural Stem Cell

NT3: Neutrophin3

N-ter: N-terminal

OD: Ocular dominance

ON: Over Night

Otx2: Orthodenticle homeobox 2

P: Postnatal day

PAGE: Polyacrylamide Gel Electrophoresis

PAPS: 3'- Phosphoadenosine 5'-Phosphosulphate

PBS: Phosphate-Buffered Saline

PCR: Polymerase Chain Reaction

PEI: Polyethylenimine

PFA: Paraformaldehyde

PG : Proteoglycan

pH: Potential of hydrogen

PLC: Phospholipase C

Plxn: Plexin

PNEM: Perineuronal Net of Extracellular Matrix

PNG: Perineuronal Net of Glia

PNN: Perineuronal Net

PNS: Peripheral Nervous System

PPC: Proprotein Convertase

PSF: Penicillin-Streptomycin-Fungizone

PSI: Plexins-Semaphorins-Integrins

PTK: Protein-Tyrosine Kinase

PTPσ: Protein Tyrosine Phosphatase

PV: Parvalbumin

QCM-D: Quartz Crystal Microbalance with Dissipation monitoring

RBD: Rho GTPase-Binding Domain

RGC: Retinal Ganglion Cell

ROS: Reactive Oxygen Species

RPIP-HPLC: Reverse-Phase Ion-Pair High-Performance Liquid Chromatography

rpm: Revolutions Per Minute

RPTPβ: Receptor-type Protein-Tyrosine Phosphate β

RT: Room Temperature

S: Serine

SCI: Spinal Cord Injury

SDS: Sodium Dodecyl Sulphate

SEC: Size Exclusion Chromatography

SEM: Standard Error of the Mean

Sema3A: Semaphorin 3A

SICHI: Semaphorin-Induced Chemorepulsion Inhibitor

SP: Sulpho Propyl

SPAM1: Sperm Adhesion Molecule1

SPR : Surface Plasmon Resonance

SP-sepharose: Sulphopropyl-sepharose

ST: Sulfotransferases

TBS: Tris-Buffered Saline

TCA: Trichloroacetic Acid

TetO: Tet-off and Tet-On

TN-C: Tenascin-C

TN-R: Tenascin-R

Tris: 2-amino-2-hydroxyméthyl-1,3-propanediol

UDP: Uridine Diphosphate

UST: Uronyl 2-O Sulfotransferase

VEGF: Vascular Endothelial Growth Factor

VVA: Vicia Villosa Agglutinin

WB: Western Blot

WFA: Wisteria Floribunda Agglutinin

XylT-I: Xylosyltansferase-I

ΔD: Dissipation shift

Δf: Frequency shift

List of figures

List of tables

List of appendices

Introduction

The central nervous system (CNS) is made of brain and spinal cord. It is responsible for the integration of information sent by all the physiological systems composing the living organism and provision of reaction accordingly. In addition to control the function of other systems, the CNS has to manage its own functions such as learning and memory. This makes it the most complex system in the organism. The functional units of the CNS are neurons and glial cells. Information transmission and storage are performed by the ability of the CNS in establishing, withdrawing and modifying the connections between neurons. This modulation of connection between neurons in response to environmental stimuli is called neuronal plasticity. **Neuronal plasticity** is one of the most important mechanisms in setting up the CNS function and maintaining its integrity during development as well as in the adult. This neuronal plasticity is ensured in part by the **extracellular matrix** (ECM) which occupied a significant part in the CNS. ECM is important in all tissues; in the CNS it plays a role at the same level as the neural cells. The complexity of neural ECM can further be stratified into a specialised structure called **perineuronal nets (PNNs)**. These PNNs are the key regulators of neuronal plasticity and regeneration. How these PNNs regulate plasticity is an open question which is not completely elucidated yet. Compared to classical ECMs, PNNs are enriched in a type of glycosaminoglycan (GAG), **chondroitin sulphates (CSs)** which are important in recruiting of signalling molecules, such **as semaphorin 3A (Sema3A),** and modulating their downstream signal. As such, PNNs could regulate plasticity. In this introduction, we will go through all these highlighted elements starting by neuronal ECM which is the cradle of this project to introduce PNNs. Then, we will detail the PNN and its potential roles in CNS before focusing our description on the main molecules of the project: CS and Sema3A to finish by CS-Sema3A interaction which is the aim of the project.

1. Extracellular matrix in the central nervous system

ECM is the cement which connects cells to form a tissue. It is composed of plethora of molecules secreted by the surrounding cells. In addition to maintain the tissue structure, it is also involved in various physiological and pathological mechanisms. Its composition varies according to cell type constituting the tissue, which enables it to exert a multitude of functions. Moreover, ECM is the entrance and exit gate of all signalling molecules. It represents 50-70% of the dry body mass[1].

It is believed three centuries ago that fibers are alive and constitute the main component of the tissue, this is designated as "fiber theory"[2]. In 1830, Johannes Müller submitted "Bindegewebe" concept, a German term meaning connective tissue. It was then postulated that connective tissue is composed of cells and their products. It is only one century later the term "extracellular matrix" came into use and its components started to be analysed with the apparition of electron microscopy and x-ray diffraction[2]. Collagen is the first analysed molecule and solubilised for the first time by Nageotte at the Collège de France in Paris[3]. At the same time, medical specialties such as rheumatology started to be interested to the GAG[4]. With the development of chemical method and cell biology, other molecules composing ECM were discovered[2].

In this introduction, we focus on neural ECM which includes the background of this thesis project. It is only in 1971 that the existence of brain ECM is reported[5]. Neuronal ECM is unique by its organisation, composition and diversity. It constitutes 20% of the total volume of adult brain, showing its quantitative importance in the CNS[6]. Neural ECM is important in early development and persists in the adult. It is involved in vital functions of the CNS such proliferation, migration, differentiation, plasticity and regeneration of neural cells. In adult CNS, ECM maintains the homeostasis of the brain by playing sometimes opposite roles. However in pathological conditions, ECM undergoes changes in its composition and a reorganisation of its structure. These changes are either the cause or the consequence of the pathology[7] [8]. These changes can occur to overcome the abnormalities or in contrary to promote the spread of the cognitive impairment. For that, neural ECM thus potentially offers a multitude of therapeutic target choices given the diversity of its composition and functions. In addition, it is a much more accessible environment for therapeutic molecules than the

intracellular environment where thousands of signalling pathways are triggered and cross-talk. However given its diversity, complexity and interaction between the different components, it is unlikely to assign a single role to a given molecule to target it. Several researches have been carried out which allowed characterising and understanding more and more the neural ECM and its components. Despite that, there are still many questions to decipher.

1.1 Neural ECM components

Neural ECM is secreted by neurons and glia[9]. In contrary to ECM of other tissues, neural ECM contains less fibrous proteins (such as collagen, laminin, elastin…) and more proteoglycans (PGs)[10]. The ratio of GAGs to collagen is around 10:1[11]. The major components of neural ECM are hyaluronic acid, PGs, link proteins and tenascins[12]. Features of each of these components are detailed below. It is worth noting that in addition to these major classes, other important neural ECM components are also present such as the glycoprotein, reelin, involved in considerable development processes[13] and ECM receptors, integrins.

1.1.1 Hyaluronic acid

Hyaluronic acid (HA) **(Figure 1)**, also known as hyaluronan, is a large linear polysaccharide composed of repeating disaccharide units: glucuronic acid (GlcA) and N-acetylglucosamine (GlcNAc) [-β(1,4)-GlcA-β(1,3)-GlcNAc-]$_n$[14]. It constitutes the only non-sulphated member in the GAG family and non-covalently linked to a core protein[15]. In physiological conditions, HA is made of 2000-25000 disaccharide units which corresponds to 1000-10000 kDa and 2-25 µm of length[16]. HA is synthetized by one of three hyaluronan synthases (HAS: 1-3) and degraded by hyaluronidases. HAS enzymes are transmembrane and synthesise HA chains of different length at different speed and are expressed in different neural tissues[17]. HA chain is extruded through the plasma membrane into ECM while it is being synthesized[18].

HA was long regarded as "goo" holding cells together to form tissue. However, its roles are much more than that[15]. It constitutes the backbone of the ECM on which other ECM molecules aggregate and assemble, thus forming the ECM net. Because of its large size, random-coil structure, and negatively charged and hydrophobic faces due to the carboxyl

groups and a cluster of hydrogen atoms, respectively, HA influences greatly physicochemical and hydrodynamic properties of the tissue[15 16 18 19]. These characteristics confer it an important use in tissue engineering[20]. Moreover, HA interacts with CD44, and thereby influences cell adhesion and migration[18].

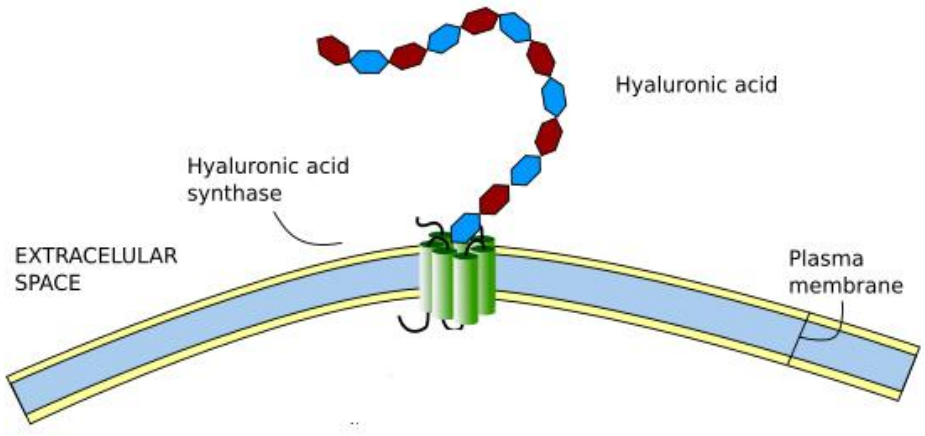

Figure 1: Diagram of hyaluronic acid synthesis by the hyaluronic acid synthase.
(*Modified from Escudero, 2009*[21]).

1.1.2 Proteoglycans

Proteoglycan (PG) is the key component of neuronal ECM. It is made of a core protein linked covalently to one or more GAG chains. GAG chain(s) of PGs contributes to their biological function, while the core protein determines localisation and promotes the interaction with other ECM molecules[22]. The GAG chain can be either heparan sulphate (HS) or chondroitin sulphate (CS) giving rise to HSPG or CSPG, respectively. Hybrid PGs containing both HS and CS chains are also reported. Small amount of keratan sulphate PGs (KSPG) are found in the CNS[23]. In 1985, HSPGs were the first isolated and characterised adult CNS PG by *Klinger et al.*[24 25 26]. In 1990, *Herdon et al*. have identified 25 CSPGs and HSPGs in rat brain[27]. These PGs are distributed over the different level of ECM (ECM compartmentalisation is discussed in section 1.4). Some of them were found in the soluble fraction of the brain (secretory). Others are transmembrane or glycosylphosphatidylinositol (GPI)-anchored[28]. Major species of PGs expressed in the CNS are summarized in **Table 1**. An overview of these typical PGs structure is presented in the next paragraphs.

Table 1: Typical proteoglycans expressed in the central nervous system.

Nature	Name	Core protein size (kDa)	Number of GAG chains	Type
CSPG	Aggrecan	224	~100	secretory
	VersicanV0	370	17-23	secretory
	VersicanV1	262	12-15	secretory
	VersicanV2	180	5-8	secretory
	Brevican	97	0-5	secretory
	Neurocan	133	3	secretory
	Phosphacan	173	3-4	secretory
	RPTPβ	253	3-4	transmembrane
	Decorin	36	1	secretory
	Biglycan	38	1-2	secretory
	NG2	252	0-3	transmembrane
HSPG	Syndecan (4 members)	~ (21, 22, 45 and 32, respectively)	3-8	transmembrane
	Glypican (6 members)	~ 53	2-4	GPI-anchored

1.1.2.1 Chondroitin sulphate proteoglycans

CSPGs are the most abundant PG in the mammalian CNS[28] and are represented mostly by **lecticans family** including aggrecan, versican, neurocan and brevican. Lecticans are determined by globular domains in N- and C-termini. The N-ter part contains HA-binding sites, allowing the lecticans to bind to HA. The C-ter part, which interacts with tenascins, contains complement regulatory protein (CRP)-like domain, lectin and two epidermal growth factor (EGF)-like repeat. The central part includes attachment sites for CS[29] **(Figure 2)**.

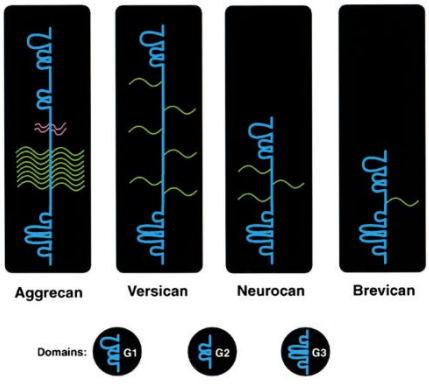

Figure 2: **Domain structures of lecticans.**
All lecticans contain N-ter G1 domains and C-ter G3 domains. Only aggrecan contains the G2 domain. The G1 domain consists of an Ig-like loop and two link modules, whereas the G2 domain consists only of two link modules. The G3 domain consists of one or two EGF repeats, a C-type lectin domain and CRP-like domain. All lecticans contain chondroitin sulphate chains (yellow) in the central domain. Aggrecan also contains keratan sulphate chains (pink) in the N-ter part of the central domain *(from Y. Yamaguchi.2000)*[30].

Receptor-type protein-tyrosine phosphate *β* (**RPTP*β*)** is a transmembrane PG. It is made of a N-ter carbonic anhydrase-like domain, a fibronectin type III domain, a CS attachment site, a transmembrane domain and finally two intracellular tyrosine phosphatase domains. **Phosphacan** results from alternative splicing of RPTP*β* mRNA. It does not contain the intracellular and transmembrane domains, which makes it a secretory protein[12] **(Figure 3)**.

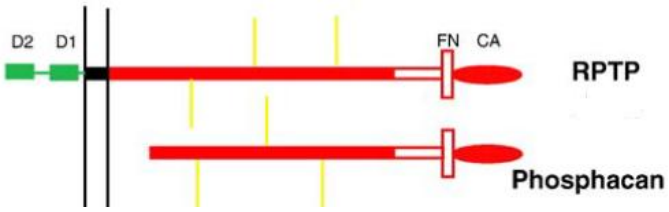

Figure 3: Structure of receptor-type protein-tyrosine phosphate *β* (RPTP*β*) and phosphacan.
RPTPβ has a N-ter carbonic anhydrase-like domain (CA), a fibronectin type III domain (FN), CS attachment regions and two intracellular tyrosine phosphatase domains (D1 and D2). Phosphacan is a soluble form that lacks the intracellular tyrosine phosphatase domains *(modified from Galtry and Fawcett. 2007)*[12].

Biglycan and **decorin** are small leucine-rich PG secreted in ECM. The majority of the core protein (70%) is represented by leucine-rich repeats flanked by cysteine-rich clusters that may oxidize to form disulfide bond. They usually contain one or two CS chains in the N-ter[31] **(Figure 4)**.

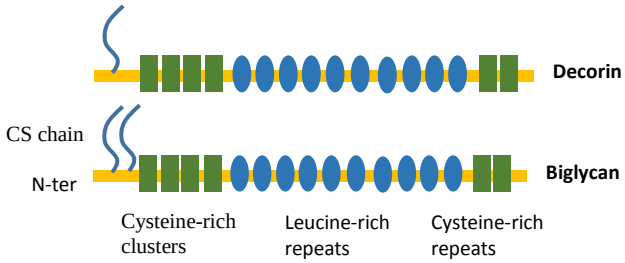

Figure 4: Structure of decorin and biglycan

Neural/glial antigen 2 (**NG2**) is a transmembrane protein, also known as melanoma-associated chondroitin sulphate proteoglycan (MCSP). Its core protein is made of a large ectodomain, transmembrane region and short cytoplasmic domain **(Figure 5)**. The ectodomain is composed of the globular N-ter, the globular C-ter and the rod-like central region which contains CS (CSPG repeats). Intracellular domain interacts with intracellular

ligands and triggers signalling pathways involved in several functions such as proliferation, migration and modulation neuronal network[32].

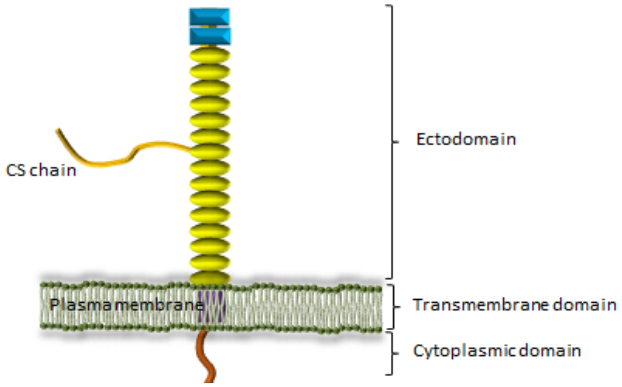

Figure 5: Structure of NG2.

1.1.2.2 Heparan sulphate proteoglycans

The two most reputable HSPG in the CNS are syndecan and glypican. **Syndecan** is transmembrane protein family including four members (Syndican-1, -2, -3 and -4). Syndecan members are composed of a large ectodomain, a transmembrane domain and a short cytoplasmic domain **(Figure 6)**. The ectodomain is poorly conserved among different family members, while the intracellular domain is highly conserved among all family members. Syndecan-3 is the longest member containing at least seven HS chains. In addition to HS chains, syndecan-1 bears CS chains. In syndecan-1 and -3, HS chains are located at the N- and C-ter ends of the ectodomain, while in syndecan-2 and -4, HS chains are tethered to the N-ter only[33].

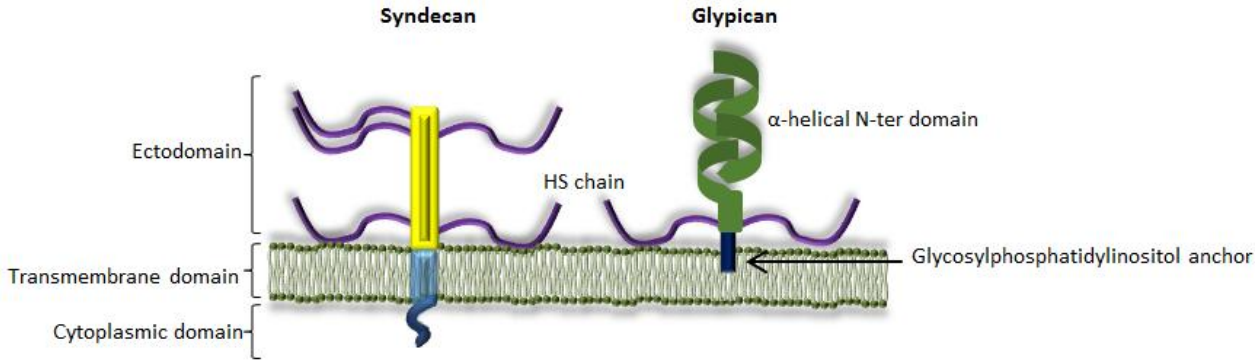

Figure 6: Structure of syndecan and glypican.

Glypican is the other HSPG family in the CNS constituted of six members. They are anchored into the plasma membrane through GPI anchors. The N-ter domains of glypicans adopt an elongated α-helical structure. It undergoes a furin-like convertase cleavage to generate two chains that remain connected by disulfide bonds[34]. HS chains are mainly located at the C-ter part of the ectodomain, close to the membrane[35] **(Figure 6)**.

A significant amount of evidence that PG is an important molecule in ECM has been accumulated, during development as well as in maintaining of adult brain homeostasis. As most of the molecules composing ECM, PGs contribute in the assembly and structure of ECM. In embryonic brain, HSPG, for example, promotes the fibroblast growth factor (FGF)-2-mediated proliferation of neuroepithelial cells[36]. CSPGs, as phosphacan and neurocan, are involved in promoting or inhibiting neurite outgrowth and cell adhesion, depending on cell type[37] [38]. CSPGs interact with a plethora of molecules involved in synaptogenesis, axon guidance and migration. In the mature brain, Versican V2 which constitutes the most abundant CSPG, is described as the major inhibitor of axonal growth[39]. Brevican inhibits neurite outgrowth of cerebellar granule neurons. It is also suggested to control the infiltration of axons and dendrites into the mature glomeruli[40]. PGs are also involved in neurodegenerative disease such as Alzheimer disease (AD) and CNS injury. Both HSPG and CSPG are found in amyloid plaques in AD[28]. Otherwise, many studies have reported the inhibitory effect of CSPGs on axon regeneration after glia scars[41]. After injury CSPGs expression is upregulated around the lesion area[42]. HSPG appears to be increased after CNS injury, but its effect is less investigated than that of CSPG[28].

1.1.3 Tenascin-C and -R

Tenascins are a family of glycoproteins found in the ECM of several tissues, composed of five members: tenascin-C, -X, -R, -Y and –W[43]. Only tenascin-C and -R are reported in the CNS, playing important roles in cell proliferation, migration and differentiation, axonal guidance, synaptic plasticity and myelination[44]. **Tenascin-C** (**TN-C**) is the first discovered member. It is a ~ 1800 kDa protein, assembled from six monomers linked covalently with disulfide bonds. The monomer consists of a tenascin assembly domain, a cysteine-rich domain, 14.5 epidermal growth factor (EGF)-like domains, 8 constitutive fibronectin-type III homologous domains and a fibrinogen-like domain[45] **(Figure 7.A)**. TN-C expression is regulated during development and in the adult brain. It is highly expressed in

early development in the CNS (day 10 in mouse CNS) by different type of cells, mainly immature astrocytes and restricted population of immature neurons[43]. TN-C acts either by its interaction with cell surface receptors such as integrins or by modulation of ECM components such as CSPGs[46]. It is known to be involved in progenitor cells proliferation and migration and neurite outgrowth[47]. Its role in neuronal plasticity is also reported. Indeed, it was identified as one of molecules mediating learning and synaptic plasticity[48].

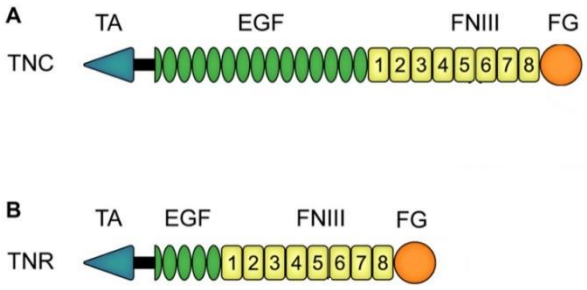

Figure 7: Structures of tenascin-C and tenascin-R monomers.
TN-C: tenascin-C, **TN-R**: tenascin-R, **TA**: amino-terminal tenascin assembly, **EGF**: epidermal-growth factor-like domain, **FN**: fibronectin-like domain, and **FG**: fibrinogen-like domain *(modified from Reinhard et al., 2016[49]).*

Tenascin-R (**TN-R**) is exclusively expressed in the CNS. TN-R is 180 kDa protein from which a 160 kDa form is generated by a proteolytic cleavage. Expression of this two isoforms changes during CNS development.TN-R is assembled from two or three monomers linked with disulfide bonds. As TN-C, the monomer is also composed of a tenascin assembly domain, cysteine-rich N-ter region, 4.5 EGF-like domains, 8 fibronectin type III repeats (FN III repeats), and a carboxyl-terminal region and fibrinogen-like domain[49] **(Figure 7.B)**. TN-R undergoes a post-translational modification consisting in addition of three distinct sulphated oligosaccharides. Among these, one is a CS oligosaccharide which may mediate TN-R interaction with TN-C and fibronectin to inhibit neurite outgrowth[50]. It is expressed by certain subpopulation of neurons and oligodendrocytes in particular cortical region and laminae[51]. TN-R plays sometimes opposite roles, which earned it the name of "Janusin" in reference to Roman god with two faces, according to the type of targeted cells and receptors, and the time of interaction. TN-R plays on one hand an important role in oligodendrocytes differentiation[52]. On the other hand, it is involved in generation of GABAergic neurons. These different effects are mediated by its different domains. The FN6–8 domains inhibit neuronal

stem cells proliferation and differentiation into astrocytes at the expense of neurons, while the EGF domain enhances their differentiation into neurons at the expense of astrocytes and oligodendrocytes[52]. TN-R is also qualified as a neuroprotector after brain injury by modulation microglia function. On one hand EGF-like repeats inhibit adhesion and migration of microglia through a protein kinase A-dependent mechanism. On another hand, fibronectin 6–8 repeats promote adhesion and migration of the primary microglia through a protein kinase C-dependent mechanism[53].

Retina is considered as an excellent model to analyse proliferation and differentiation of neuronal cells as well as axonal guidance and growth. For this purpose, TN-C and TN-R roles were investigated in optic nerve and retinal neurodegeneration. In the optic nerve, huge amount of TN-C is secreted by astrocytes and TN-R is mainly expressed in oligodendrocytes[49]. Expression of these tenascins is found dysregulated in retinal ischemia. In optic nerve damage, TN-C and TN-R have opposing roles in regeneration of optic nerve fibers. TN-C is chemoattractive, whereas TN-R is inhibitory and chemorepulsive[44].

1.1.4 Hyaluronan and proteoglycan binding link proteins

Hyaluronan and proteoglycan binding link protein (HAPLN) family contains four members (HAPLN 1-4). As their name indicate, they stabilise the interaction between HA and CSPG. HAPLNs are 38-43 kDa and made of Ig-like V-type, link 1 domain and link 2 domain **(Figure 8)**. The structure of HAPLNs is homologous to that of G1 domain of lecticans which also binds to HA. Genomic structure revealed that these *HAPLN2* and *HAPLN4* genes were physically linked to the genes encoding brevican and neurocan, respectively supporting thus the hypothesis of common evolutionary origin from an ancestral gene respectively[54]. HAPLN2 and HAPLN4 are restricted in expression to the CNS, hence their other names are the brain-specific link proteins: Bral1 and Bral2, respectively[54]. HAPLN1 is 40 kDa protein initially identified in articular cartilage, hence its other name is cartilage link protein (Crtl1). It interacts with HA and aggrecan. It is also expressed in the CNS where it is crucial for the highly organisation of the specialised matrix, the PNNs that we will discuss in detail in the later chapter. Animals lacking HAPLN1 in the CNS attenuate PNNs[55]. Similar results are observed in animal lacking HAPLN4 which is mainly expressed in cerebellum and brain stem. Moreover, it affects the localization of brevican[56]. HAPLN3 is not detected in the CNS.

Little is known about HAPLNs family. The 3D structure is not yet solved and their interaction with HA and CSPG still poorly characterised as well as its functional role in the CNS.

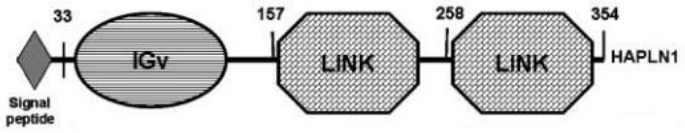

Figure 8: Structure of hyaluronan and proteoglycan binding link protein1 (HAPLN1).
IGv: immunoglobulin-like domain and **LINK**: Link domain.

1.2 Foetal and adult neural ECM components

ECM composition changes with aging, responding thus to brain functions needs **(Figure 9)**. Expression of some components is upregulated, while it is downregulated for others. These components can also play an inhibitory as well as an activatory role depending of the conditions. Alternative mRNA splicing of some ECM proteins leads to numerous combinations of isoforms, thereby increasing the functional diversity at different stages of development and in the adult CNS. Embryonic neural ECM is very dynamic and highly plastic. Indeed, this is required to control different mechanisms occurring in developing CNS such as proliferation, migration, differentiation and synaptogenesis. CNS is the most complex organ responsible of multiple vital functions. In human, its development starts at 4 weeks and it continues until after birth. All these need a dramatical remodelling of ECM components.

HA is the most abundant GAG in foetal rat brain (>60 %) and it decreases after birth[57]. During development of the chick, HA is concentrated in the intermediate zone which gives rise to the white matter[58]. HA is crucial in maintaining neural progenitor cells in an undifferentiated state[59]. Whereas in adult animals, it localizes around myelinated fibers in white matter and it is more diffuse[60]. It is also found in grey matter in PNNs that are involved in neuronal plasticity[61].

HSPG and CSPG function in different way in developing and adult brain. It has been observed that HS represents 25 % of all GAG in the foetal rat brain, this makes it the most abundant Sulphated GAG[57]. In the postnatal brain, it represents only 10 % of all GAGs. CS represents 10 % of all GAGs in the foetal brain, and it becomes the most abundant GAG 20 days after birth[57]. Neurocan and RPTPβ/phosphacan are the most abundant CSPGs in

developing CNS where they are required for cells adhesion and neurite outgrowth. They are exerting an opposite effects on neurite outgrowth. Neurocan and phosphacan inhibit the neurites outgrowth of cortical and dorsal root ganglion (DRG) neurons[38], while phosphacan promotes the neurite outgrowth of mesencephalic and hippocampal neurons[62]. In adult CNS, versican is the major CSPG[63]. It inhibits the neurite outgrowth of granular neurons[40]. CSPGs in adult brain play an important role in neuronal plasticity. Indeed, they are related to synaptic activities. Lacking in neurocan reduces late-phase hippocampal long term potentiation (LTP)[64]. Interestingly, after birth CS chains of neurocan change in size and in sulphation pattern[23]. Furthermore, lacking RPTPβ/phosphacan enhances LTP and impairment in memory task[65].

HSPGs interact with several proteins present in developing brain to achieve their functions. HSPG-FGF is one of the well characterised interactions. Binding to HSPG i) stabilises and protects FGF from proteolysis[66] ii) concentrates FGF locally and thus enhances binding to their receptor, and iii) induces the oligomerization of FGF, thereby receptor dimerization and signalling[67]. FGF1 and FGF2 are required for proliferation, migration and differentiation of neuronal precursor cells. First, HSPG binds to FGF2 to promote neuronal precursors cells proliferation. Then, HSPG switches rapidly its potentiating activity from FGF2 to FGF1 to promote differentiation of neural cells[36]. HSPGs are associated to human mesenchymal stem cells (hMSCs) lineage-specification to neural progenitors[68]. They are also involved in the development of specific synaptic connectivity patterns important for neural circuit function[69]. The four members of syndecan are expressed differently in developing and adult brain. Syndecan-2 is highly expressed in adult brain and concentrated in synapses, while syndecan-3 is highly is expressed in development and concentrated in axons[70]. Syndican-4 is dynamically expressed in the early stages of zebrafish embryonic neurogenesis where it inhibits neural proliferation[71].

TN-C and TN-R are highly expressed during early development of the CNS. TN-C is expressed at early stages of developing brain, while TN-R is expressed later during development and its expression is restricted to the oligodendrocytes[43]. TN-C isoforms are secreted by numerous neural cells during development to accomplish different processes such as migration[43]. Despite expression of TN-C persists in the adult brain, it is restricted to well defined areas where neuronal plasticity and regeneration are still possible such as the nuclei of hypothalamus and olfactory system, respectively[43]. TN-R is detected at one week in postnatal

mice and the peak is reached at 2-3 weeks and remains stable in adulthood[72]. TN-R is considered as a key component of adult CNS matrix. Indeed, it modulates adult but not developmental neurogenesis in the olfactory bulb[73]. Furthermore, TN-R is transiently expressed in peripheral nervous system (PNS) in the sciatic nerve of mice embryos (E14-18) and neonatal[74]. HAPLN1 expression is reported during late embryonic and early postnatal[75].

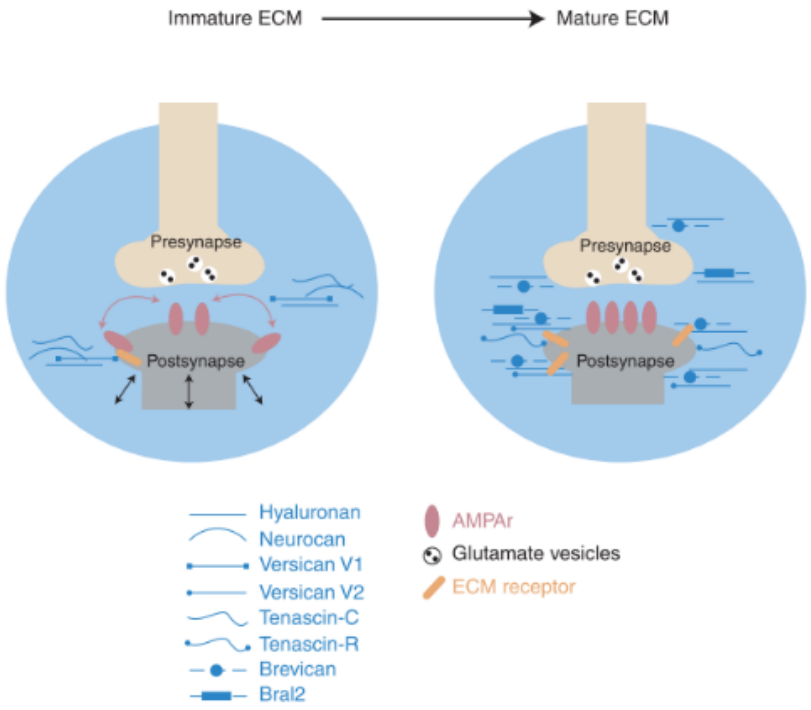

Figure 9: ECM changes at CNS synapses.
Synapses are embedded into an ECM meshwork (blue) composed of hyaluronan, chondroitin sulphate proteoglycans (CSPGs), tenascins, and others. The composition of the ECM changes during development. For example, neurocan, versican V1, and tenascin-C are abundant in the immature CNS, whereas tenascin-R, versican V2, and Bral1 are prominent in the mature CNS. The mature ECM is thought to restrict dendritic spine motility and lateral diffusion of α-amino-3-hydroxy-5-methyl-4-isoxazolepropionic acid (AMPA) receptors (AMPAr) (*from barros et al., 2011*[13]).

1.3 Role of neural ECM

ECM plays a crucial physical barrier for the cells that it surrounds by preventing the infiltration of external agents. It is also a structural support for the cells and maintains the tissue integrity. ECM allows the communication between adjacent cells, but also with distant cells by promoting the transport of different molecules. It offers an adequate environment for enzymes responsible of post-synthesis modifications, signalling molecule cleavage for

activation or inhibition, and degradation. In addition to its structural role, ECM is involved in plethora of physiological and pathological functions.

It is important to mention that cell control by ECM is not one-way. Indeed, the cells are the principal actor of ECM formation and reorganisation. They contribute actively in producing ECM components and the enzyme responsible of its maintenance and restructure, responding thus to changes of conditions in the tissue.

Importance of ECM is reported earlier in development. Regulated spatial and temporal distribution of the components in developing ECM makes it very dynamic. Several studies indicate that the ECM affects all aspects of nervous system development. TN-C-deficient mice show a delay of the developmental program of neural stem due to changes in growth factor responsiveness[76]. ECM components support different migratory trajectories of neural crest cells. Versican isoforms V0 and V1 implanted micromembranes in chick embryos leads to attraction of neural crest cells, while micromembranes of aggrecan retain migratory cells near the implant and thereby perturb their spatiotemporal migratory pattern. Interestingly, this inhibitory effect of aggrecan is mostly due to the GAGs chains (CS and KS)[77]. These observations suggest that neural crest cells may migrate on versican-containing matrix and avoid aggrecan-containing matrix. Pattern expression of these two proteins could be a mechanism of guidance for neural crest cells migration. Neural crest migration is also influenced by laminin. Laminin α5 mutant mice exhibit abnormalities in neural cell migration which demonstrates in expanded neural crest streams. This suggests that laminin α5 may restrict migration into narrow streams[78]. Mice lacking laminin α2 display a detachment of embryonic neural stem cell (NSCs) apical process from ventricular zone[79]. This phenomenon is also observed when β1 integrin function is disrupted. Laminin and integrin thus play a role in anchoring embryonic NSCs in the ventricular surface and maintaining the physical integrity of the neocortical niche[79]. Moreover, conditional β1-integrin gene deletion in neural crest cells causes severe developmental alterations of the peripheral nervous system leading to lethality of mice after birth[80]. ECM provides an adequate microenvironment which controls the NSCs behaviour[11 13]. ECM shapes the niche of stem cells and contributes actively in their maintenance, differentiation and migration.

ECM plays an important role in myelination of axons[13] **(Figure 10)**. Myelination is a vitally important process for the proper function of neurons. It involves the accumulation of

myelin around axons. Myelin is formed by oligodendrocytes in the CNS and Schwann cells in the PNS. Myelination results in the concentration of voltage-gated sodium channels at the nodes of Ranvier, regenerating thus action potential[81]. One of remarkable role of myelination is to enable a very fast action potential propagation in vertebrate[81]. In PNS, ECM components notably laminin and collagen promote myelination of peripheral nerves by regulating Schwann cells proliferation, adhesion and spreading[82 83] as well as neurite outgrowth[83]. In CNS, β1 integrin is required for myelination by promoting myelin sheaths outgrowth through AKT activation[84]. On the contrary, CSPGs are myelination inhibitors by inhibiting oligodendrocytes process outgrowth and myelination[85]. Roles of ECM in the CNS and PNS are innumerable. It influences all the cerebral process in physiological and pathological conditions and from the development to adult.

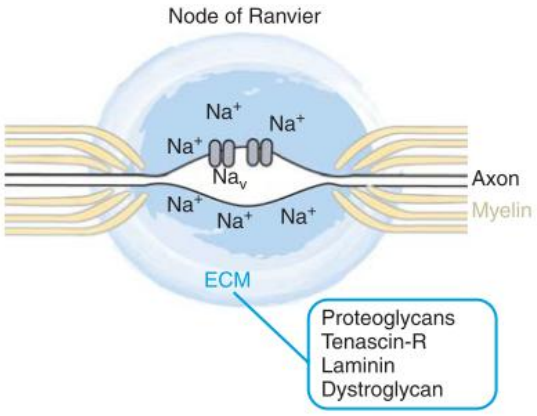

Figure 10: ECM and myelination.
The ECM surrounding nodes of Ranvier may regulate the local concentration of cations and clusters voltage-gated sodium channels, which allow for saltatory electrical conductivity. Several proteoglycans, tenascin-R, laminin and dystroglycan contribute to the formation of nodal matrices. Nav, voltage-gated channel; Naþ, sodium cations (*from Barros et al., 2011*[13]).

Neural ECM undergoes several changes in structure and composition in response to a trauma in the CNS. Expression of certain component is upregulated, while it is downregulated for the other as showed in **Table 2**. These changes can both promote or inhibit the recovery of function. Traumatic brain injury (TBI) induces oxidative stress, leading to the release of reactive oxygen species (ROS). These ROS degrade HA and generate small HA fragments. These biologically active fragments thus modulate angiogenesis[86]. TBI upregulates the expression of domains B and D of fibronectin type III in tenascin-C, thus promoting axonal regeneration and repair processes[87]. However, TBI also results in sulphation pattern

modification of GAG chains carried by PGs. These changes induce the inhibition of axon regeneration, guidance and neuronal plasticity[88]. Role of the sulphation pattern after brain injury is discussed in PNNs section (section 2.7). All aspects of ECM after TBI are reviewed in detail by *George N and Geller HM, 2018*[89].

Table 2: Changes in ECM components after traumatic brain injury (TBI).
(*from George N and Geller HM, 2018*[89])

Matrix protein	Cellular source	Changes after TBI
CSPG		
• Lecticans		
○ Aggrecan	Neurons, astrocytes	Decreased in injury core
○ Brevican	Neurons, astrocytes, oligodendrocytes	Secreted isoform is up-regulated; GPI-anchored isoform unchanged.
○ Neurocan	Neurons, astrocytes	Increased neurocan in a tight band surrounding the injury core
○ Versican-V2	Oligodendrocytes	Increased in the injury core
○ Phosphacan	Neurons, astrocytes, oligodendrocytes	Reduced in the glial scar
• NG2	Oligodendrocyte precursor cells, pericytes, microglia	Increased expression
HSPG		
• Syndecans	Neuron, astrocytes, oligodendrocyte, oligodendrocyte precursors, microglia	Increased immunoreactivity
• Glypicans	Neurons, astrocytes, oligodendrocyte, oligodendrocyte precursors	increased immunoreactivity
• Perlecan	Endothelial cells, astrocytes, oligodendrocytes, oligodendrocyte progenitor cells, microglia	Increased immunoreactivity
• Agrins	Neurons, astrocytes	Increased in reactive astrocytes
KSPG	Neurons and microglia	Increased immunoreactivity
Hyaluronan	Astrocytes, oligodendrocytes, neurons	Altered dynamics in synthesis and degradation.
Fibronectin	Endothelial cells, pericytes, macrophages	Increased levels
Tenascin-C	Astrocytes, oligodendrocytes and neurons	Increased expression in animal and humans
Tenascin-R	Oligodendrocytes	Increased
Laminin	Astrocytes, endothelial cells, pericytes	Immunoreactivity increased
Osteopontin	Astrocytes, microglia	Increased expression

1.4 Types of ECM in the CNS

ECM in the CNS is organised in three different compartments **(Figure 11)**, with difference in composition and function. **Basal lamina** (basement membrane) surrounds the blood vessels and the entire pial surface of the CNS. At the electron microscopic level, the basal lamina is composed of an electron-dense layer called the lamina densa (composed of type IV collagen) and an electron-lucid layer called the lamina lucida (consisting of laminin, dystroglycan and associated proteins)[6]. Basal lamina is involved in neurogenesis, CNS injury repair[90] and nerve regeneration[90 91]. It constitutes a key component in maintaining the integrity of the blood–brain barrier (BBB). Basal lamina is required early in CNS development where it is important for the maturation of endothelial cells required for the BBB[92].

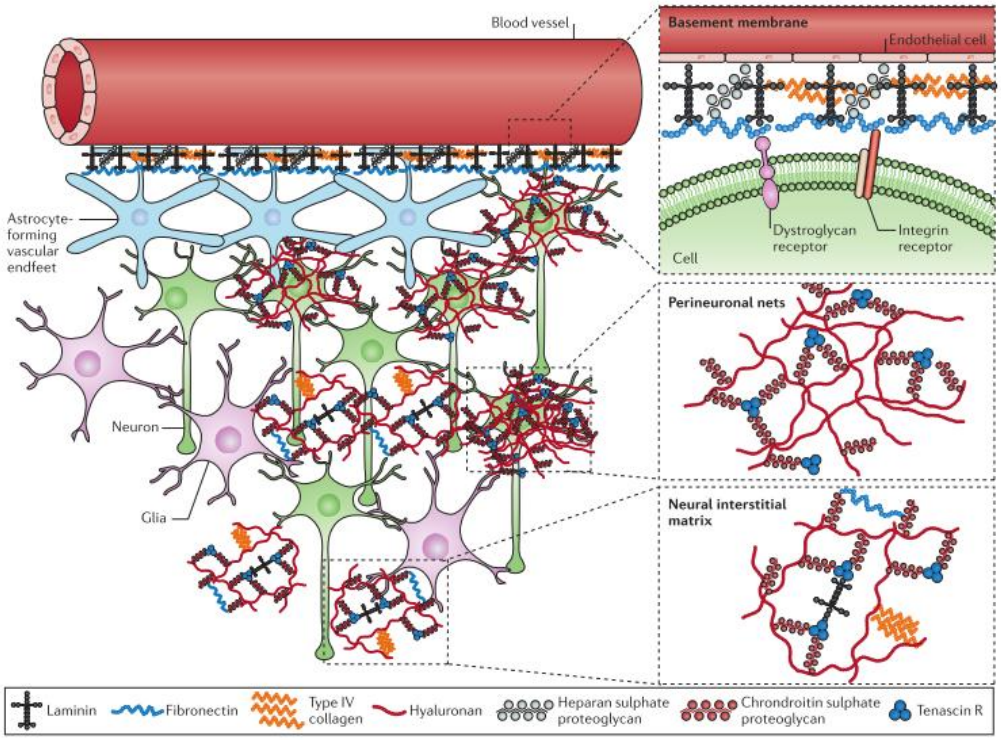

Figure 11: extracellular matrix within the central nervous system (CNS).
The three major compartments of the extracellular matrix in the CNS are the basement membrane, perineuronal net and neuronal interstitial matrix. The basement membrane is found surrounding cerebral blood vessels, the perineuronal net is a dense matrix immediately surrounding neuronal cell bodies and dendrites, and the neuronal interstitial matrix occupies the space between neurons and glial cells (*from Lau L.W et al., 2013*[8]).

Interstitial matrix corresponds to molecules that fill the space between CNS cells in parenchyma. Interstitial matrix is the classical matrix of the CNS whose components and function are described above (section 1.1 and 1.3, respectively). Two different levels of

interstitial matrix can be distinguished: loose matrix and membrane-associated matrix. Loose matrix (diffuse matrix) consists of unbound or loosely attached ECM that can be extracted easily with physiological saline (150 mM NaCl). Membrane-associated matrix consists of ECM molecules bound to the plasma membrane and will only be detached or solubilised with higher salt concentration (1000 mM NaCl) and detergent (0.5% tritonX-100)[93]. In some regions of the CNS, interstitial matrix becomes more complex to give rise to the condensed matrix structure called perineuronal nets (PNNs).

PNNs are the third type of ECM in the CNS. As its name indicates, PNN is a specific and highly organized structure found only on the surface of neurons. PNN is important in controlling neuronal plasticity[61]. PNN components are solubilised only with the combination of 1 M NaCl, 0.5% tritionX-100 and 6 M of urea[93].

2. Perineuronal nets (PNNs)

Camillo Golgi (1843–1926) is known by its discovery of Golgi apparatus which carries his name. However, long before he highlights the existence of Golgi apparatus in the CNS in 1888. He described a particular reticular structure surrounding several neuronal populations, impregnated by his staining "black reaction". He first mentioned his observation in *Enciclopedia Medica* in 1882. In 1892, he announced the existence of reticular network enwrapping cell bodies and proximal dendrites in a publication of *Accademia dei Lincei*. In 1888, during a conference in the *Società Medico-Chirurgica* on the discovery of the Golgi apparatus, Golgi officially stated this reticular structure on neuronal surface as "pericellular net". He described Golgi apparatus as an internal reticular structure of the nerve cell and pericellular net as an external reticular structure. This external structure is described as "delicate covering, mainly reticular in structure, but also in the form of little embraced tiles or an interrupted envelope which covers the body of all the nerve cells continuing along their protoplasmic extensions up to the second and third order arborisations" **(Figure 12)**. At the same time, pericellular net was also observed by other neurobiologists among them Santiago Ramón y Cajal. However, since Golgi and Cajal conflicted about the organization of the nervous system, reticular theory vs neuron doctrine, he postulated then that the pericellular nets were staining artefact claiming that "The pericellular net is not nervous in nature. We do

not think it is neuroglial because there is never a continuity with the ramifications of Deiters' cells and it has not any morphological or histological characteristic of these cells. If we can propose another solution, waiting for a new one, we should say that this net is due to a coagulation of a substance in the pericellular fluid". After these words of the giant of neuronal theory, pericellular nets were fell into oblivion till 1980s[94 95]. Cajal was correct in one sense that the pericelluar nets are coagulation of a substance in the pericellular fluid (i.e. aggregation of ECM molecules). However, he was wrong to disregard the nets as staining artefact. The composition of PNNs started to be elucidated (glycoconjugates[96], hyaluronate-protein aggregates[97] and tenascin[98]) as well as their roles. The number of papers about PNNs has steadily increased since. Discovery of PNNs is reviewed in more detail by *Celio and Blümcke (1994)*[99]*, Celio et al.,(1998)*[94] *and Spreafico et al., (1999)*[95].

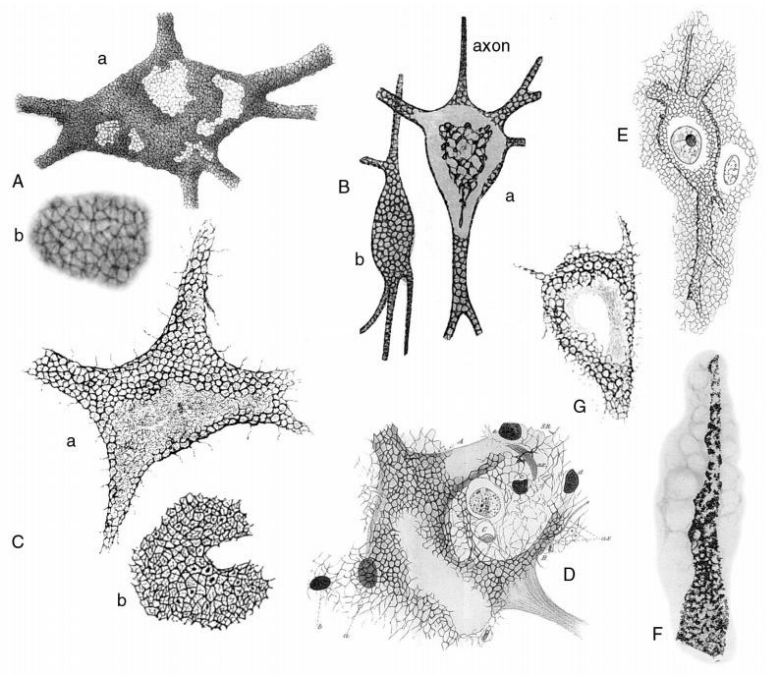

Figure 12: Perineuronal nets as drawn by various authors at the turn of the century.
(A) Nerve cell with reticular covering (anterior horn of cat spinal cord) (a) and (b) enlarged detail of (a) illustrating the fine texture of the perineuronal net. **(B)** Two cerebral cells with short axons (adult cat), stained with reduced silver nitrate after fixation in formol acetone: (a) cell with ascending axon viewed in the equatorial plane; (b) cell with descending axon viewed in the superficial plane. (C) Nerve cell derived from the anterior horns of the dog spinal cord (a). The cartwheel pattern (raggere di Donaggio), formed by thin filaments radiating from a central spot, recognizable within the meshes of the perineuronal net (b). These cartwheel structures probably represent shrunken synaptic endings, which occupy the meshes of the net. **(D)** Cell with Golgi's net and a diffuse net (anterior horn of the spinal cord of a calf embryo), stained according to Bethe's method (Ehrlich's methylene blue and ammonium molybdate). **(E)** Cortical cell of an adult dog, stained according to a modification of Bethe's method. **(F)** Alterations within the perineuronal net of a human cortical cell, derived from a patient with paralytic dementia. **(G)** Cell derived from the nucleus of the vagus (medulla oblongata) of Lacerta muralis. Within the meshes of the peripheral apparatus (or perineuronal net), a typical cartwheel pattern radiating from a central small spot is evident. Filaments originating from the cell surface connect with the surrounding stroma (*from Celio et al., 1998*[94]).

2.1 Composition and organisation of PNNs

PNNs are derived from ECM, thus all PNN components can be found in classical ECM. However, the amount and organisation of PNN components makes it different from the interstitial ECM. It is also important to know that PNN composition and structure vary in time and space. Expression of PNN components such as brevican, phosphacan and TN-R is inhomogeneous in distinct areas of the spinal cord. Moreover, the amount of CS varies significantly in different spinal cord PNNs. This variation is correlated to expression of the fast-spiking neurons marker, Kv3.1b subunit of the potassium channel. Fast-spiking neurons contains more amount of CS in their PNNs[100].

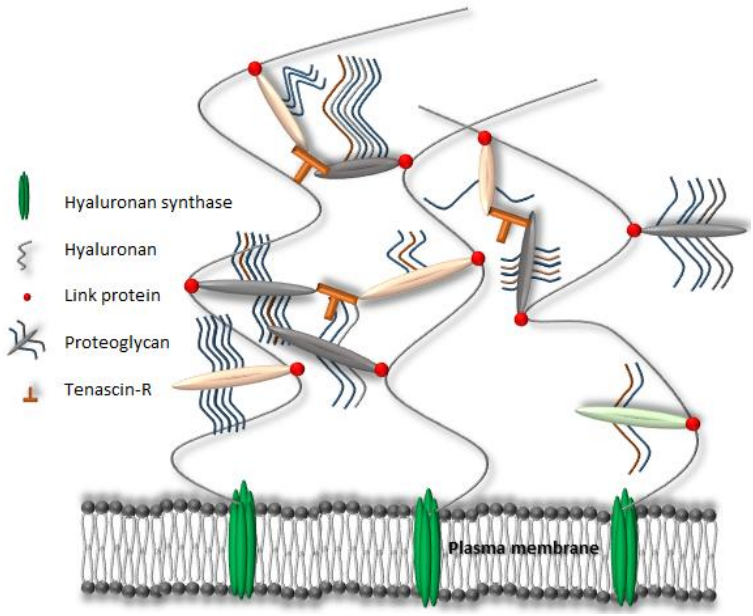

Figure 13: Structure of the PNN.
PNN is composed of hyaluronan (HA) synthetized by hyaluronase synthase. Chondroitin sulphate proteoglycans (CSPGs) interact with HA and this interaction is stabilised by the link protein. Tenascin-R bridges different CSPGs. It is involved in the stabilisation of the PNN.

Identified PNN components so far are: HAS and its synthesized product HA, CSPGs (aggrecan, neurocan, brevican, versican and phosphacan), link proteins (Crtl1 and Bral2) and TN-R[93 101] **(Figure 13)**. HA constitutes the backbone of PNNs. Traditionally, HA can attach to the cell surface either by binding to its receptor such as CD44 or by remaining attached to HAS while being extruded. However, as no expression of CD44 or other HA receptors on the PNNs-bearing neurons have been identified[102], PNN is likely remained attached to neurons *via* HAS[101]. CSPGs are attached to HA and their interaction is stabilised by link proteins.

Link proteins (HAPLNs) are the other PNN components which are important for PNN structural stability. Bral2 (HAPLN4) is required for the proper localization of brevican in the brainstem and cerebellum, and a correct organisation of PNN[56 103]. The trimeric TN-R bridges three CSPGs, thus strengthening the network. Linking PNNs to neurons *via* HAS, stabilising the interaction HA-CSPG *via* HAPLNs and bridging CSPGs *via* TN-R, makes the structure of the PNN highly condensed and stabilised.

2.2 Characterization of PNNs

PNNs were first observed using staining techniques **(Figure 14)**, as mentioned above, using the **"black reaction technique"**[95]**.** This technique consists of incubating the tissue in a silver nitrate solution for one to two days. The silver nitrate solution reacted with the potassium dichromate to form fragments of silver chromate on the cell membrane which are black, hence the name black reaction. These fragments aggregate on the cell membrane of some neurones (presumably those bearing PNNs) stain the entire cell surface. Other scientists interested by PNNs used **methylene blue staining** or its derivatives[95]. It is a cationic thiazine dye with redox-cycling properties. It binds to the dendrites of certain subpopulations of neurons in the brain. The presence of a strong anionic residues in PNNs attracts the cationic dye[104]. ***Wisteria floribunda* agglutinin (WFA)** is currently the most popular staining for PNNs. It is a plant lectin that labels selectively N-acetylgalactosamines of chondroitin Sulphate , enriched in PNNs[105]. ***Vicia villosa* agglutinin (VVA)** is another plant lectin used to stain PNNs[106]. **Colloidal iron hydroxide (CIH) staining** uses an acid-base reaction whereby ferric cations in a colloidal ferric oxide solution are attracted and bound to carboxylated and sulphated substances[106]. This staining can be visualized with light microscopy. **Monoclonal antibodies against CSPGs** are another alternative to visualize PNNs[107]. Labelling PNNs in spinal cord with an antibody directed against aggrecan is better than WFA. Indeed, only ~60% of the CSPG-positive PNNs co-localised with WFA in the spinal motoneurons[108]. For review, a table of markers labelling PNN identified before 1994 is provided by *Celio and Blümcke*[99]. Monoclonal labelling and lecticans staining can visualized in fluorescence in confocal microscopy. PNNs stained with WFA can be visualized with electron microscopy[109] **(Figure 15)**.

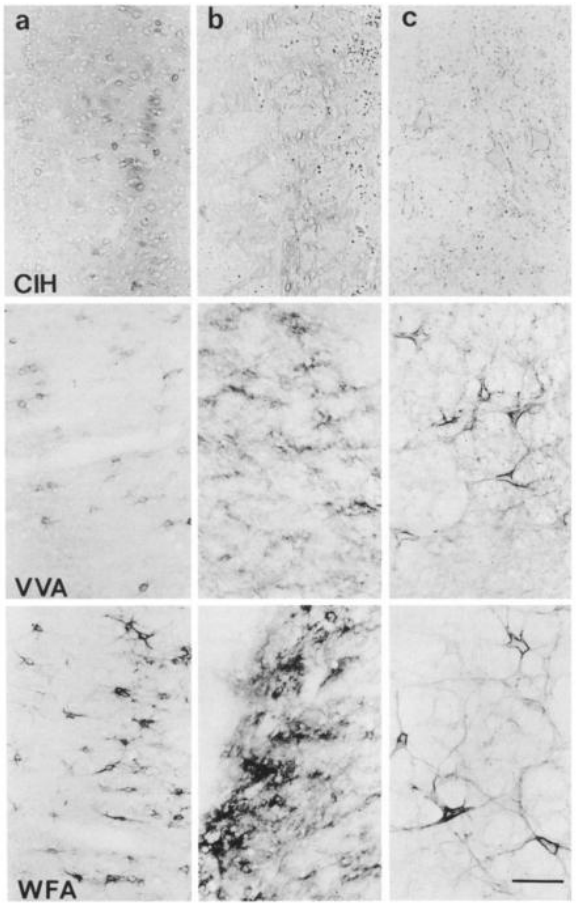

Figure 14: Distribution patterns of PNNs stained by the three methods applied in cortical and subcortial brain regions in light microscopy.
(a) Retrosplenial granular cortex. **(b)** Reticular thalamic nucleus. **(c)** Gigantocellular reticular nucleus are stained with colloidal iron hydroxide (CIH) staining (upper row); *Vicia villosa* agglutinin (VVA) staining (middle row) and *Wisteria floribunda* agglutinin (WFA) staining (bottom row). Scale bar = 100 µm (*from Seeger et al., 1994*[106]).

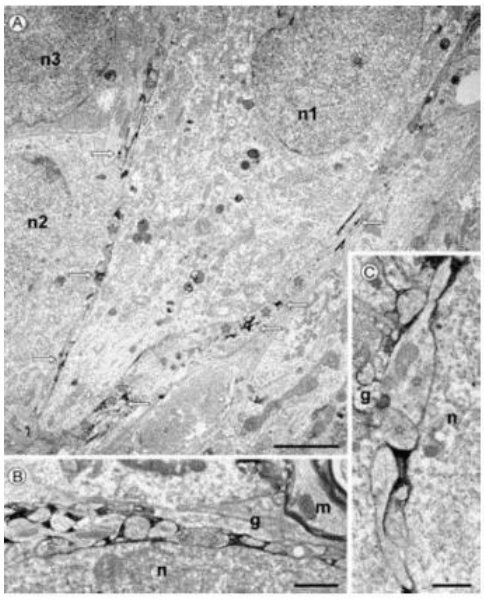

Figure 15: Electron microscopic demonstration of PNN in the hippocampal CA1 region of a slice culture fixed after vital labelling with biotinylated WFA.
(A) The stained components (arrows) of a PNN reveal the contours of a presumed interneuron (n1) which is contacted by numerous synaptic boutons (asterisks). Two adjacent neurons (n2, n3) are devoid of label. (**B)** Somatic part of a PNN. The labelled zone of extracellular matrix is associated with the non-synaptic surface of the neuron (n) but covers synaptic boutons (asterisks) and surrounds clusters of preterminal axon profiles. An astrocytic process containing glial fibrils (g) borders the outer matrix zone. A myelinated axon (m) is seen in its vicinity. **(C)** Two adjacent synaptic boutons contacting a net-associated neuron (n). The labelled extracellular matrix is absent between boutons (asterisks) and in the axosomatic contact area but is accumulated around preterminal axons. Glia profiles (g) can be seen in close proximity to presynaptic boutons. *W. floribunda* agglutinin was applied for 3 days to a 4-week-old slice culture grown in medium with 25 mM KCl. After 7 days, the slice was fixed and the bound lectin visualized with the peroxidase technique. Bars: A, 5µm; B, 2µm; C, 1µm (*from Brückner et al., 2004*[109]).

2.3 Spatial and temporal formation of PNNs

PNNs are expressed in multiple regions in the brain, enwrapping subpopulations of neurons. With the use of lectins (VVA and WFA) and CIH staining, PNNs are mapped in rat brain and they are present in more than 100 regions (see *Seeger et al.*, 1994[106] for the list of identified regions) and recently reviewed by *van't Spijker and Kwok*, 2017[110]. The regions expressing PNNs in the CNS are: cortex, amygdala, hippocampus, cerebellum and spinal cord. Neurons enwrapped by PNNs appear as a mesh or honeycomb **(Figure 12)**. The holes correspond to connection point of nerve terminals on neuron (synaptic boutons). Using lectin staining, population of parvalbumin-containing GABAergic interneurons in the rat cerebral cortex was identified[111]. GABAergic neurons are the main inhibitory neurons in the mature CNS secreting the gamma aminobutyric acid (GABA) neurotransmitter. GABA reduces the excitability of neurons, controlling thus the plasticity. Subpopulation of GABAergic neurons expresses parvalbumin (PV), a calcium-binding protein. PV positive neurons are the largest neuronal population bearing PNN in the brain[112], with 80% being surrounded by PNNs[55] **(Figure 16)**. In the cortex, PV neurons are fast spiking interneurons controlling pyramidal neurons (excitatory neuron whose soma shaped like pyramid able to send their axons for long distances), which in turn project out of the cerebral cortex and provide excitatory signals. PV-GABAergic neurons are the largest population bearing PNNs. However, another population of PNN-bearing neurons could be found in amygdala: calbindin (other calcium-binding protein)-containing GABAergic interneurons[110].

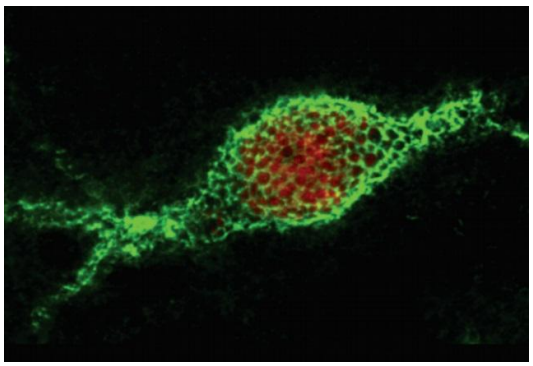

Figure 16: PNNs around a parvalbumin-expressing inhibitory neuron in rat lateral secondary visual cortex.
Green: WFA-stained PNNs and red: neuron *(National Academy of Sciences*[113]).

Contrary to what is often thought, PNNs are not only specific to inhibitory neurons. Indeed, in amygdala regions responsible of emotional learning and memory, PNNs are mainly expressed around excitatory neurons[114]. In the hippocampus, PNNs surround excitatory synapses of pyramidal neurons to supress their plasticity[115]. In cerebellum, in addition to Purkinje cells, Golgi neurons and molecular layer interneurons (GABAergic neurons), PNNs are found enveloping large excitatory deep cerebellar nuclei neurons (LEDCN)[101]. In spinal cord, motoneurons (neurons projecting to control , directly or indirectly, effector organs or gland) express also PNNs on their surface[116] [108]. Widespread expression of PNNs in the CNS demonstrates their importance.

Although PNNs components such as HA, CSPGs and tenascins are detected in the ECM of developing and neonatal CNS, PNN formation occurs late in postnatal development (in rodents 2–5 weeks after birth) and coincides with the closure of the critical period. Critical period is defined as "a maturational time period during which some crucial experience will have its pick effect on development or learning, resulting in normal behaviour attuned to a particular environment to which organism has been exposed". Each individual CNS system has its own critical period **(Figure 17)**. During the critical period, neurons are able to modulate their connections in response to environmental stimuli (high plasticity). At the end of the critical period, PNNs appear and wrap on the neuronal surface when the mature synaptic circuitry is established[107]. Therefore, PNNs stabilize the established connections and the plasticity is restricted. However, this plasticity can be restored by limiting external stimuli or modulating PNNs. For example, in the visual system, the critical period can be delayed by dark rearing or by degrading CS chains of the PNNs in adult visual cortex, thus restores experience-dependant plasticity[117].

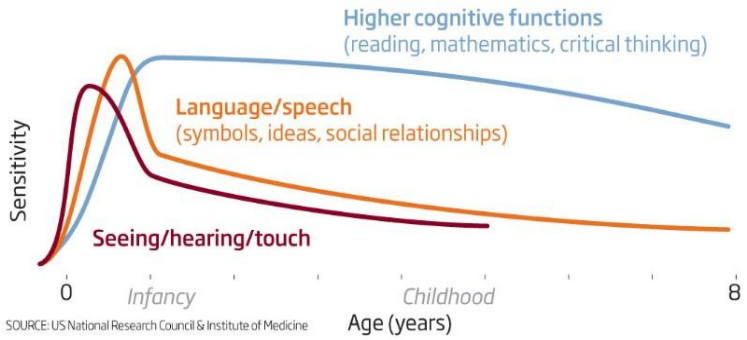

Figure 17: Critical period.

Some components such as CSPGs (neurocan, phosphacan and versican), HAS and TN-R were already expressed at postnatal day 3 (P3)[118]. However, molecules triggering PNN construction are upregulated as the PNN form. PNNs develop around rat deep cerebellar nuclei (DCN) neurons from postnatal day P7, around Golgi neurons from P14 [118] and in the visual cortex at P14 and (at the same age in mice)[55]. In the visual cortex, Crtl1 and Bral2 are the only proteins upregulated at the time of PNNs formation and Crtl1 displays a peak of expression at P14 and Bral2 at P21. Mice lacking Crtl1 have attenuated PNNs and persistent plasticity[55] **(Figure 18).** Crtl1 is a key component in the formation of condensed PNNs in the visual cortex. In rat cerebellum, aggrecan, Crtl1 and HAS are all upregulated during PNNs formation[118].

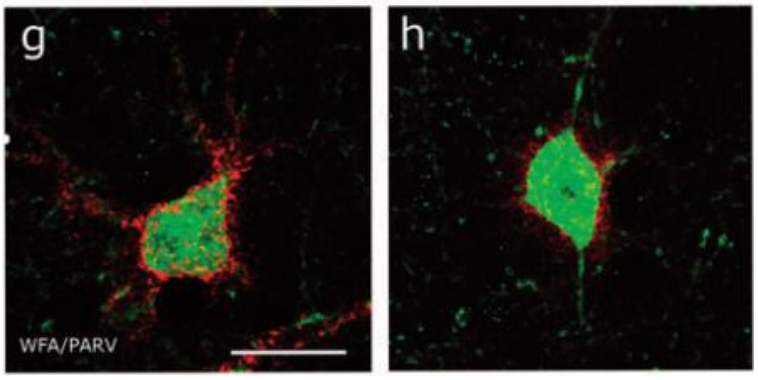

Figure 18: The appearance of PNNs in wild-type and Crtl1 knockout animals.
Left: WT; right: Crtl1 KO. Green: parvalbumin stained neurons; Red: WFA-stained PNN (*from Carulli et al., 2010*[55]*).*

2.4 Cell source of PNNs

Origin of PNNs is one of the first arise questions, neuron and/or glia? In the other hand, PNNs are considered as part of the terminal arborisations of nerve processes[94]. In the other hand, PNNs are observed in continuity with glial cells[119]. Then, it was shown that two reticular structures around nerves cells exist: (i) an outer one consisting in PNN of glia (PNG) and (ii) an inner one consisting in PNN of ECM (PNEM). The two structures are not superimposed, and glial end-feet are sometimes observed to pass through PNEMs. Analysis of the cellular origin of PNN components reveal that both glial cells and neurons provide CSPGs and TN-R of PNNs. However, only neurons express the mRNA of HAS and link proteins (Crtl1 and Bral2)[101] (**Table 3)**. Hence, neurons and glia both are responsible in building PNNs.

Table 3: **mRNA expression of PNN components in adult rat deep cerebellar nuclei (DCN) and large excitatory deep cerebellar nuclei (LEDCN).**
(*from Carulli et al., 2006*[101])

	LEDCN neurons	DCN neurons without nets	Astrocytes	$NG2^+$ cells	Oligo dendrocytes
Neurocan	+	+	−	−	−
Aggrecan	++	−	−	−	−
Brevican	+	−	++	−	−
Versican	−	−	−	++	++
Phosphacan	−	−	−	++	−
RPTPbeta	−	−	−	++	−
TN-R	+	−	−	++	++
Crtl1	++	−	−	−	−
Bral2	++	−	−	−	−
HAS1	−	−	−	−	−
HAS2	+	−	−	−	−
HAS3	+	−	−	−	−

[1]Staining intensity: ++, strong; +, weak; −, not detected.

2.5 Role of PNNs

This highly organised network of PNNs looks optimally designed to accomplish very specific functions. The most known and studied function of PNNs is the plasticity restriction. Three mechanisms by which PNN regulates the plasticity has been proposed: i) PNNs act as a physical barrier inhibiting further synapses formation; ii) attract inhibitory signalling molecules such as Sema3A; iii) restrict the lateral mobility of AMPA receptors[107 120] **(Figure 19)**. Neuronal plasticity is at the basis of learning and memory. Impairment of memory is a result of several neurodegenerative diseases notably AD.

To demonstrate the role of PNNs in plasticity, the most classical model for plasticity which is the reactivation of ocular dominance (OD) plasticity in the adult visual cortex, has been employed. Monocular deprivation (MD) is usually used to analyse experience-dependant plasticity in the CNS. This technique consists of depriving one eye of the animal from light by suture during the visual critical period. This results in a shift of OD plasticity of cortical neurons in favour of the non-deprived eye. However, MD during adulthood (after PNNs surround the established synapses) does not result in OD showing thus absence or diminution of plasticity in the visual cortex. Moreover, the critical period for OD and PNN maturation are delayed for animal reared in complete darkness. MD of adult rats underwent chondroitinase ABC (ChABC) injection results in OD shift toward the non-deprived eye, attesting thus *de novo* plasticity[121].

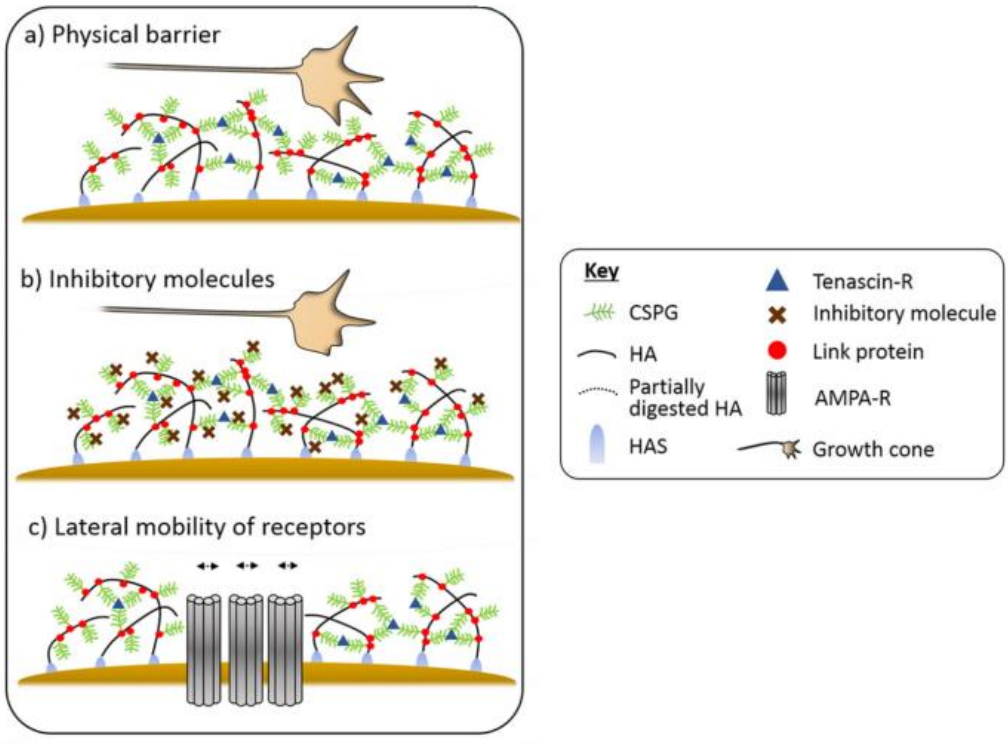

Figure 19: Three possible ways in which PNNs may act to restrict plasticity.
PNNs could regulate plasticity by three mechanisms: **(a)** a physical barrier by PNNs to incoming synaptic inputs; **(b)** binding of molecules *via* specific sites on CSPGs of PNNs (molecules, such as semaphorin 3A, inhibit new synaptic inputs); and **(c)** prevention of lateral diffusion of AMPA receptors, limiting the ability to exchange desensitized receptors in the synapse for new receptors from extrasynaptic sites (*from Sorg et al.,2016*[120]*).*

PNNs are also involved in controlling regeneration. This role is highlighted by disrupting PNN by ChABC treatment. In animals with SCI, ChABC treatment induces *de novo* sprouting in degenerating areas where CSPGs are digested[122]. CSPGs are principal actors in inhibiting axonal growth and sprouting as long as their expression is upregulated around the lesion after SCI and their removing restores the sprouting[123]. In addition to the plasticity control and regeneration, PNNs play several roles described below:

2.5.1 Physical role

One of the first suggested roles of PNNs is a protective and supportive scaffolding[124]. By enwrapping the whole cell body of neuron, PNNs prevent the formation of new neuronal contacts and synapses, restricting thus the plasticity. In addition, PNNs stabilise the existing synapses, ensuring their maintenance. PNNs can act as a physical barrier between the neuron and the extracellular space precluding the penetration of neurotoxic protein species such as amyloid β-protein[125]. The negative charges of GAG chains confer to PNN an ion exchanger

function regulating ion mobility and sorting properties in the brain[126]. They provide an ion buffering capacity around specific subpopulation of neurons notably buffering for cations involved in the neurotransmission of fast spiking interneurons[126 127]. This buffering capacity also prevents oxidative stress by retaining Fe^{3+} ions[128].

PNN constitutes a barrier for the lateral diffusion AMPA receptors[129]. AMPA receptor mobility on plasma membrane is required for the regulation of receptor numbers at the synapse. The compartmentalisation of synaptic membrane by PNNs reduces the availability of naïve AMPA receptors. AMPA receptors are glutamate-gated ion channels and are indispensable for fast excitatory synapses. Glutamate binding to the AMPA receptor results in the opening of the ion channels resulting in a cation influx which depolarizes the post-synaptic membrane. PNNs could also connect ECM components to the cytoskeleton *via* receptors, such as with HA receptor[124].

2.5.2 Functional roles

Immature PNN already acts as a molecule reservoir. It attracts the neurotrophic factors responsible for the survival and the growth of neurones[99]. The diversity of PNN components confers a multitude of protein-binding sites. For example, different GAG motifs enable a specific binding of different type of proteins. Some of these proteins are responsible for the control of plasticity, outgrowth and guidance such as our protein of interest Sema3A and orthodenticle homeobox2 (Otx2)[130]. Sema3A accumulates on PNN through its interaction with CSs. Sema3A on PNN can induce the chemorepulsion of the neurons bearing the PNN as well as the adjacent neurons[130] (accumulation of Sema3A in PNN is detailed in section 4).

In the visual cortex, the transcription factor Otx2 is produced in other areas (retina and dorsal lateral geniculate nucleus) and then transferred to PV-cells *via* thalamocortical axons to be involved in the maturation of PNNs which results in the closure of the critical period. Once PNNs are formed, in turn, they lead to accumulation of Otx2 on the surface of PV-cells thus the mature structure of PNNs and regulate the plasticity for binocular vision in the visual cortex[131] **(Figure 20)**. Otx2 as Sema3A, it is accumulated on PNN *via* its interaction with specific epitopes in CS in addition to its interaction with TN-R[132].

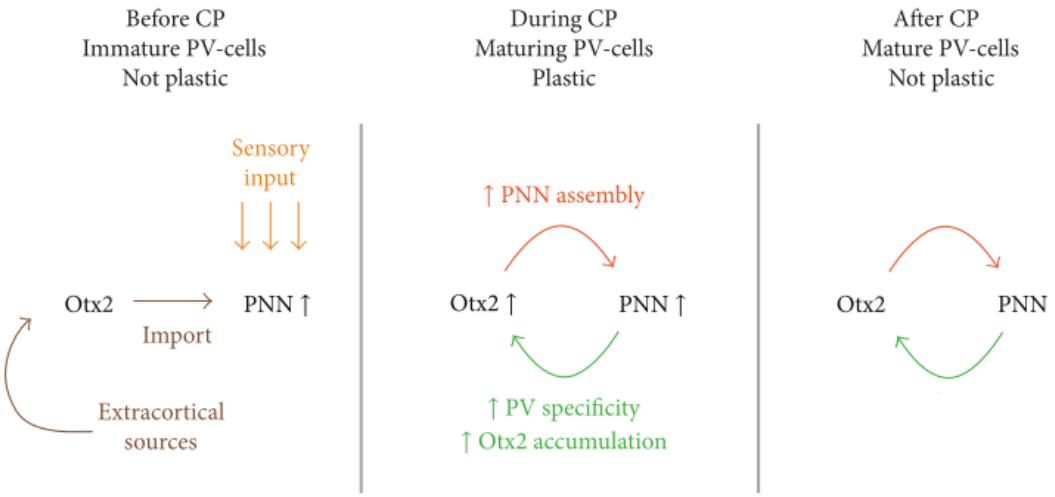

Figure 20: Otx2-PNN feedback loop for critical period plasticity.
At critical period onset (CP), sensory activity induces initial formation of the PNNs, allowing the internalization of extracortical Otx2 by PV-cells. During critical period, the increasing PV-cell Otx2 content enhances PNN assembly. In turn, PNNs ensure the specific accumulation of Otx2 in the PV-cells. In the adult, the constant transfer of Otx2 into the PV-cells, due to the positive feedback loop between the Otx2 and the PNNs, maintains a mature, consolidated, non-plastic state (*modified from Bernard and Prochiantz, 2015*[131]).

Neuronal pentraxin2 (Nptx2, also called Narp) binds and clusters AMPA receptors and accumulates at excitatory synapses on PV-interneurons[133]. PNNs are implicated in Nptx2-mediated AMPA receptors clustering in mature PV cells as a homeostatic response to elevated circuit activity[133]. In addition to the physical barriers that PNN constitutes to regulate AMPA receptors, PNN could regulate these receptors with a molecular way, through Nptx2. Recent data from the lab also shows that the binding of Nptx2 to neuronal surface facilitates the formation and maturation of PNNs (unpublished data).

PNN concentrates specifically all these plasticity regulating actors. Each molecule has its own expression pattern in time and space and triggers different signalling pathways. It is not known yet if they could act in dependant or independent ways, but certainly they are all required for the regulation of plasticity.

2.6 PNNs in pathology

Only some notes from Nissel and Alzheimer reported on an alteration of PNN in case of dementia before 1911. Besta (1911) and Belloni (1933) are the pioneers in PNN and

pathology. Baesta highlighted that PNNs are resistible to brain injury and remain intact even after a destruction of axonal endings. In addition, modifications occurring within PNNs are independent of those observed in neurons. Belloni mentioned that PNNs are altered and disintegrated in dementia, diffuse gliosis and psychiatric cases[94]. These last two decades, the number of papers analysing the behaviour of PNNs in cerebral pathology is dramatically increased. PNN is a dynamic structure that responds to changes of its environment. Expression of PNN components is regulated and likely their rearrangement as well. As it was discussed earlier, PNN recruits signalling molecules involved in different processes. These molecules require a specific binding site. Thus, PNN should adapt its composition, modulating the availability of these binding sites for recruiting the adequate molecules to the environmental conditions. PNN is considered as double edged sword because on one hand it protects the neuron against disorders and abnormalities, but on other hand it promotes the spread of the disease and the perpetuity of the disorder. PNN is involved in lot of pathologies of the CNS among them neurodegenerative diseases such as AD and CNS trauma such as spinal cord injury (SCI).

2.6.1 Neurodegenerative diseases

Neurodegenerative diseases are a group of chronic, progressive disorders characterized by the gradual loss of neurons. Mechanisms underlying their progressive nature remain unknown. Millions of people worldwide are affected. AD is the most common type[134]. AD is a chronic degenerative disorder that destroys memory and other important mental functions. It is the most common cause of dementia. AD is characterized by beta aggregate fibrillary of neurotoxic elements: amyloid beta peptide (Aß) and Tau-protein. Among the neuroprotective role of PNN: they are able to restrict the processes of distribution and internalization of Tau protein, thus protecting the neuron that they surround[135]. Neurons enwrapped by PNNs are not affected by the accumulation of neurofibrillary tangles despite the severity of damaged region[136]. This could explain the selective neuronal vulnerability of most neurodegenerative diseases[137] **(Figure 21)**. This neuroprotective effect in AD usually assigned to CSPGs. Neurons in culture expressing CSPGs-rich PNNs withstand to Aß treatment, while neurons devoid PNN succumb to the treatment[125]. CSPGs protect also neurons in culture from delayed cell death induce by glutamate, AMPA and N-methyl-D-aspartate (NMDA)[138]. Moreover, brevican expression is upregulated in PNNs of AD. Other non-CSPG components are also upregulated such as Crtl1[139]. These upregulated components could be the actors of the

neuroprotective effect of PNNs. Furthermore, PNNs protect the neurons that they enwrap from oxidative stress in normal-aged brain and AD. The negative charges of HA and CS neutralize ions generated from the oxidative stress such as iron[140]. Several examples presented in **Table 4** show the neuroprotective effect of PNNs.

Figure 21: Distribution of aggrecan-based PNNs compared to AD-typical neurofibrillary degeneration in the human cortex.
Area 20– 22. Complementary pattern of aggrecan-immunoreactive PNN and neuropil (HAG, gray/black) with anti-tau phosphospecific immunoreaction (pT205, brown) becomes clear. PN-rich regions are not or less affected by tau-pathology, whereas regions with less or no PNNs display high amounts of pathology. *(from Suttkus et al., 2016[137]).*

Table 4: **Overview of the most important findings regarding the different experimental approaches using human postmortem tissue, *in vitro* trials, or animal models to investigate the protective action of ECM components.**
(from Suttkus et al,. 2016[137]).

	Experimental design	Results
Studies using postmortem tissue	Immunohistochemical and histological staining proceeded on AD affected tissue	PNs-associated cortical neurons are unaffected by NFT formation
		tau pathology is mostly found in regions with a low proportion of PN
		PN-ensheathed neurons are lesser affected by lipofuscin inclusion
In vitro studies	Exposure of cultured neurons to excitotoxic concentrations of NMDA, AMPA, and kainate	CSPGs reduce the delayed cell death
	Treatment of human neuroblastoma 5H-SY5Y cells with H_2O_2 or a combination of rotenone and oligomycine to induce oxidative stress	purified chondroitins 4 and 6 reduce significantly the generation of free radicals
	Incubation of cultured neurons with toxic concentrations of ß-amyloid	sulphated GAGs attenuate the neurotoxic effects of ß-amyloid
		PNs protect neurons against ß-amyloid toxicity
Approaches using animal models	Stereotactical injection of trimethyltin into the hippocampus	PN-enwrapped neurons persist in the vicinity of the lesion
	Immunohistochemical studies on the AD mouse model Tg2576	Aggrecan-based PN-associated neurons are not affected by amyloid plaques
	Induction of oxidative stress by GBR using the schizophrenia mouse model Gclm KO	PNs limit induced oxidative stress
	Stereotactical injection of iron chloride to induce oxidative stress	PNs protect neurons against oxidative stress

AD: Alzheimer's disease, PN perineuronal net, NFT: neurofibrillary tangle, NMDA: N-methyl-D-aspartic acid, AMPA: α-amino-3-hydroxy-5-methyl-4 isoxazoleproprionic acid, CSPG: chondroitin Sulphate proteoglycan, GAG: glycosaminoglycan.

On the other hand, PNN is described as noxious for neurons in AD. For example, disruption of the PNN in the hippocampus or peripheral cortex by digesting CS chains with injection of ChABC restores the memory lost in mice AD[141 142]. Furthermore, the depletion of Crtl1 KO mice enhances long term object recognition memory and facilitates long-term depression in the perirhinal cortex[143]. In contrary to CSPG, HSPGs are found co-localising with Aß promoting AD by accumulation of Aß and hyperphosphorylation of Tau protein[144 145]. HSPGs act in cooperation with low-density lipoprotein receptor-related protein 1 (LRP1) to mediate cellular Aß uptake[146]. PNNs are also involved in other degenerative diseases such as multiple sclerosis and Parkinson disease.

On one hand PNNs protect neurons from oxidative stress and accumulation of Aß. On the other hand, PNNs removal by ChABC enhances plasticity to compensate for the function of the lost neurons, thus memory. This aspect should be considered to target PNN in neurodegenerative disease.

2.6.2 Traumatic CNS injury

Traumatic CNS injury (SCI and TBI) comprises disorders resulting from spinal cord and brain trauma (*e.g* car crash and fall), stroke or cancer. SCI is the most common. According to the WHO (World Health Organization) the annual global incidence ranges from 40 to 80 cases per million inhabitants. Up to 90% of these cases are due to traumatic causes. Men are most at risk in early adulthood (20 to 29 years) and in old age (over 70). For women, the risk is greatest in adolescence (15 to 19 years), then from the age of 60. Most spinal cord injuries result in permanent impairment of some degree or loss of sensation in areas of the body below the level of the lesion. The degree of disability depends on the severity of the injury and the location in the spinal cord. There is no effective treatment to date. SCI causes deleterious secondary injury mechanisms including glutamate-induced excitotoxicity, inflammation and oxidative stress, in addition to the primary pathology due to the initial impact which results in cut axons, then degeneration. This secondary injury leads to failure of axonal sprouting and progressive neuronal death. After SCI, the BBB is disrupted due to rupture of the blood vessels and the site of the lesion is rapidly infiltrated by blood neutrophils. This process leads to formation of glial scar and contributes to the secondary alteration that follows the primary lesion[147 148]. Thus, the primary injury affects the lesion site leading to axonal degeneration and cell death. The secondary injury resulted from the glia scar

broadens this lesion through the chronic inflammatory and oxidative stress and prevent the axonal regeneration. Despite some surviving cut axons which are able sprouting but they cannot traverse the glial scar tissue to connect to other neurons[149] **(Figure 22)**.

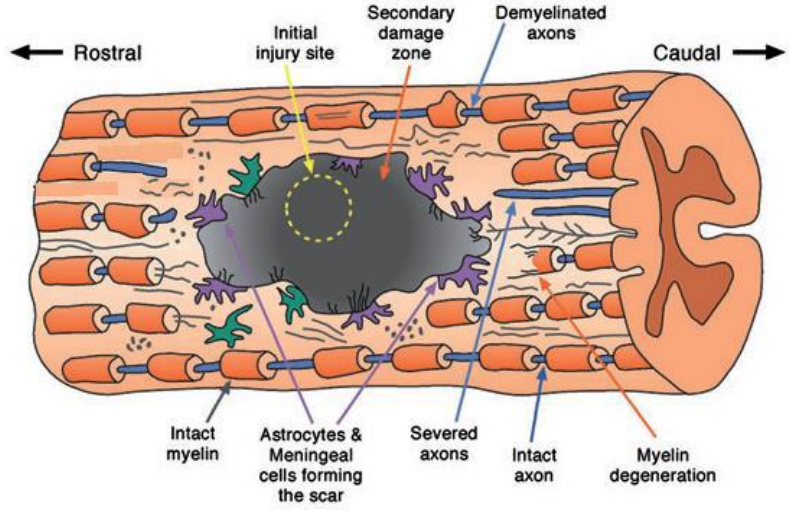

Figure 22: Schematic representation of the spinal cord injury.
The site of the primary lesion is often restricted and secondary injury mechanisms such as inflammation, oxidative stress, and glutamate-induced excitotoxicity contribute significantly to broaden the primary lesion site (*from Mueller et al., 2006*[150]).

The composition of PNNs changes drastically after CNS injury notably CSPGs. CSPGs are inhibitory for axonal regeneration and neurite outgrowth[40] [151]. Phosphacan, neurocan, brevican, versican and NG2 are upregulated following SCI[152] [153]. In addition to these CSPGs, TN-C are found upregulated[153]. Furthermore, axotomy (cutting axons) of nigrostriatal tract (one of the major dopaminergic pathway in the brain) induces an increase of CSPGs expression[154]. Removing CS chains of CSPGs by injecting ChABC promotes sprouting of spinal system and the functional recovery after SCI[122] [155]. In nigrostriatal tract axotomy, ChABC treatment enables dopaminergic nigral axons regeneration[154].

In conclusion for PNNs in pathology, PNNs should be modulated according the context of the pathology. Traumatic CNS injuries result in axon cut. The injury environment, whose upregulation of PNN CSPGs, constitutes a barrier for functional recovery by preventing the axonal regeneration and the reconnection between neurons. Hence, disrupting these PNNs through ChABC digestion promotes the functional recovery. However, first this

treatment does not target only CSPGs of the PNN, second it targets only CS chains of CSPG and potentially HA, hence the core protein and the other components remain intact and third we do not know about the inhibitory effect of the other PNN components in traumatic CNS injury. Thus, we cannot attribute an inhibitory effect to the whole PNN structure. In addition, in AD, PNN seems to be neuroprotective and protects neurons that it surrounds against oxidative stress. This oxidative stress is also a consequence of the primary injury and the cause of the secondary injury in TBI and SCI. Hence, the question is what about the protective role of PNNs against the oxidative stress following the trauma?

2.7 Modulation of PNNs

The most common way to modulate PNNs in order to analyse their role is ChABC treatment. The role of PNN in plasticity and regeneration is thus highlighted. In 2001, Fawcett lab treated rat injured in the brain with ChABC which results in axonal regeneration[154]. In 2002, *Bradbury et al.* have demonstrated the benefit of ChABC treatment in functional recovery following SCI[155]. In the same year *Pizzorusso et al.* have shown the reactivation of plasticity in visual cortex through ChABC treatment[121]. Since, a multitude analysis of ChABC treatment effect on different functions in the CNS was performed and some examples are summarised in **Table 5**.

ChABC digests the CS chains of CSPGs, but also it acts slowly on HA which constitutes the backbone of the net (ChABC, Sigma, C3667) resulting thus in the disruption of the organisation of the net **(Figure 23)**. However, it is hard to know if the observed results are due to the disruption of the 3D organisation of the net or due to the absence of CS chains and HA, or both. Although, this is the question which should be asked when we modulate one of the PNN components (tenascins, link proteins and CSPGs KOs), since the effect of PNN is not due only to the role played by each component individually but also to their disposition and interaction. Despite the efficiency of ChABC treatment and its importance to analyse the involvement of CSPGs in plasticity and regeneration, it could not be used as a treatment because of i) it is not targeting a specific region, since CSPGs are present in the whole ECM and in addition PNNs cover different type of neurons, ii) it is degrading all CS types and some of them are promoters rather than inhibitors and iii) PNN plays a neuroprotective effect on the neuron that it surrounds. Thus, other treatment(s) more targeted and more specific need to be elaborated.

Table 5: **Effect of chondroitinase ABC treatment on neuronal plasticity.**
(*from Karetko and Skangiel-Kramska et al., 2009*[156]).

Species	Place of ChABC action	Effect of PNs degradation
mouse	hippocampal slices	reduction of LTP
rat	axotomized nigrostriatal pathway	long-distance regeneration of interrupted dopaminergic nigral axons
rat	visual cortex	restoration of ocular dominance plasticity in adult
rat	injured spinal cord	functional recovery of locomotor and proprioceptive behaviors
rat	injured spinal cord	sprouting of injured and intact spinal cord projections
rat	injured spinal cord	regeneration of damaged dorsal root fibers
rat	injured spinal cord	sprouting of intact dorsal root fibers; restoration of sensory function
mouse	amygdala	abolishment of spontaneous recovery and context-dependent renewal of conditioned fear in adult
mouse	amygdala	impairment of LTP at thalamo-LA inputs
rat	culture of hippocampal neurons	increase of lateral diffusion of AMPA receptors

(ChABC) chondroitinase ABC; (LA) lateral amygdala; (LTP) long term potentiation; (PNs) perineuronal nets

PNN can also be modulated by exercise training. While exercise is usually used to improve the functional recovery after SCI in human patients, ChABC treatment enhances the functional recovery after SCI in rat. Combining these two treatments, promotes the greatest recovery of rat with SCI. Exercise training alone leads to an increase in the level of Crtl1 and WFA staining, likely for the consolidation of an efficient circuitry. However, administration of ChABC during the rehabilitation removes PNNs and prevents their upregulation during the exercise. Moreover, ChABC treatment induces sprouting and reconnection which can be strengthen with the exercise training[157]. However, exercise training regulates differently PNNs expression in different region of the CNS. Indeed, exercise training decreases expression of PNN in the brain, while it increases it in the spinal cord. This divergence indicates different regulatory mechanisms of plasticity *via* PNN in the brain and the spinal cord[116].

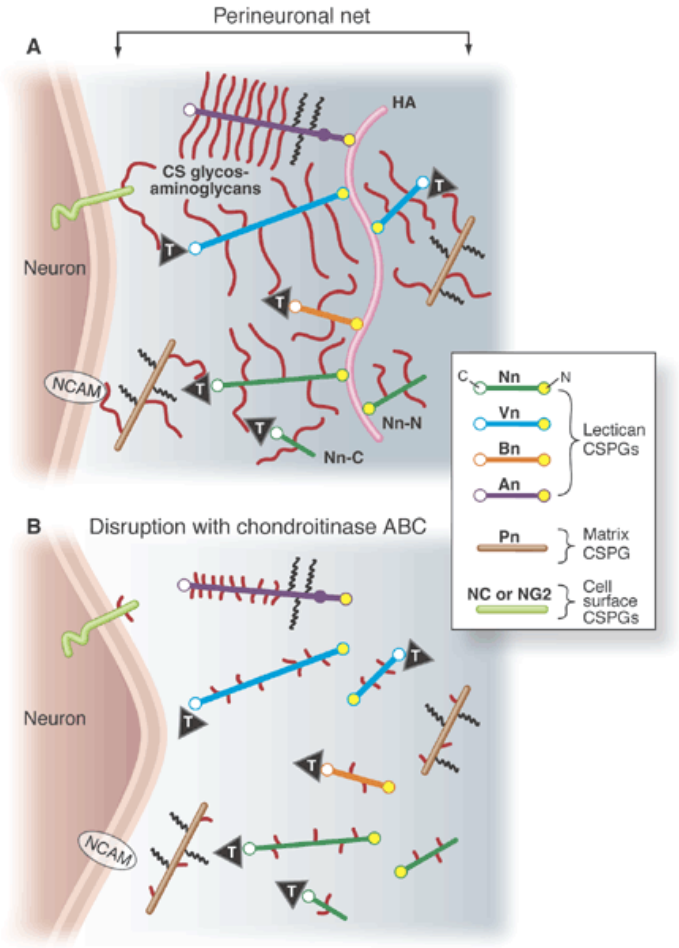

Figure 23: Chondroitinase ABC treatment of the PNN.
ChABC treatment of the PNN degrades all of the CS (red line) as well as all of the matrix hyaluronan (pink line), which causes major disruption to the macromolecular heterophilic interactions that hold the PNN together. Disruption of PNN may allow extension of axons into the vacated space and closer interactions between the membranes of neighbouring neurons, contributing to a restoration of neuronal plasticity (*from Fox and Caterson, 2002*[158]).

One of mechanism by which PNN regulates plasticity is by recruiting signalling molecules such as Otx2 which is important for PNN maturation and stability. The effect of PNN can be modulated by manipulating the recruitment of these signalling molecules. The Otx2-binding motif in CS is already determined as well as the CS-binding site on Otx2. Based on the CS-binding sequence, a peptide mimicking this sequence has been conceived. This peptide is able to inhibit the Otx2 transfer *in vivo* restoring then the visual cortical plasticity in adult mice[159]. Modulation of PNN through the interaction of its CS chains and signalling molecule requires an understanding of the expression, distribution, function and specifically the structure of both the signalling molecule and CS chains. In the next chapter we detail the CS in the CNS.

3. Glycosaminoglycans and central nervous system chondroitin sulphate

CS belongs to GAGs family. It is an important component of the cartilage and CNS matrix notably PNNs. CS was first obtained from cartilage in 1861 by Fisher and Boedecker and then isolated in 1884 in purer form by Krukenburg[160]. In 1913, Levens published a paper discussing already the composition and structure of sulphuric acid (the name at that time) and developed a method to isolate one component which is GlcA[161]. The correct composition of CS was then elucidated by the same author in 1925. He found that CS is composed by GlcA and galactosamine (GalN) conjugated to sulfuric acid[160]. Before to identify its correct structure, it was thought that the CS is a tetrasaccharide[162], then a complex molecule represented in branched chain[160].The correct structure was only identified later. Furthermore, the linkage between CS molecule and its conjugated core protein remained a mystery for a while. It was thought that protein-CS interaction was an ionic bond[162]. In 1965, Lindahl has reported the nature of CS-4S (CS isoform)-protein linkage[163]. With the progress in structural biology notably the progress in sugar field, the structure of CS is increasingly analysed. The crystal structure of CS-4S was reported in 1978 by *Winter et al.*[164]. Furthermore, benefits and the virtues of CS were then highlighted notably in osteoarthrosis. Cartilage notably marine animal cartilage is the principal source of CS.

3.1 Generalities on glycosaminoglycans

GAGs are an important family of linear polysaccharides found mostly in the glycocalyx and ECM of most animal tissues. They are made of repeating disaccharide units: hexosamine and uronic acid (except keratan sulphate) which can be epimerized and sulphated at different positions. The nature of hexosamine (glucosamine or galactosamine) gives rise to two principal subfamilies: glucosaminoglycan and galactosaminoglycan. Glucosaminoglycan subfamily contains heparin (Hp)/ HS, KS and HA (detailed in section 1), the only non-sulphated GAG member. Galactosaminoglycan subfamily contains chondroitin/dermatan sulphate (CS/DS) **(Figure 24)**. Except HA, other GAGs are synthetized as a part of the proteoglycan molecule composed of a core protein and at least one chain of GAG. Hp/HS and CS/DS are linked covalently to serine residue (by O-glycosylation posttranslational modification) of the core protein at specific amino acid sequence Gly-Ser-Gly *via* a specific linkage tetrasaccharide. This tetrasaccharide consists in xylose (Xyl) - galactose (Gal) – Gal - GlcA[163 165].

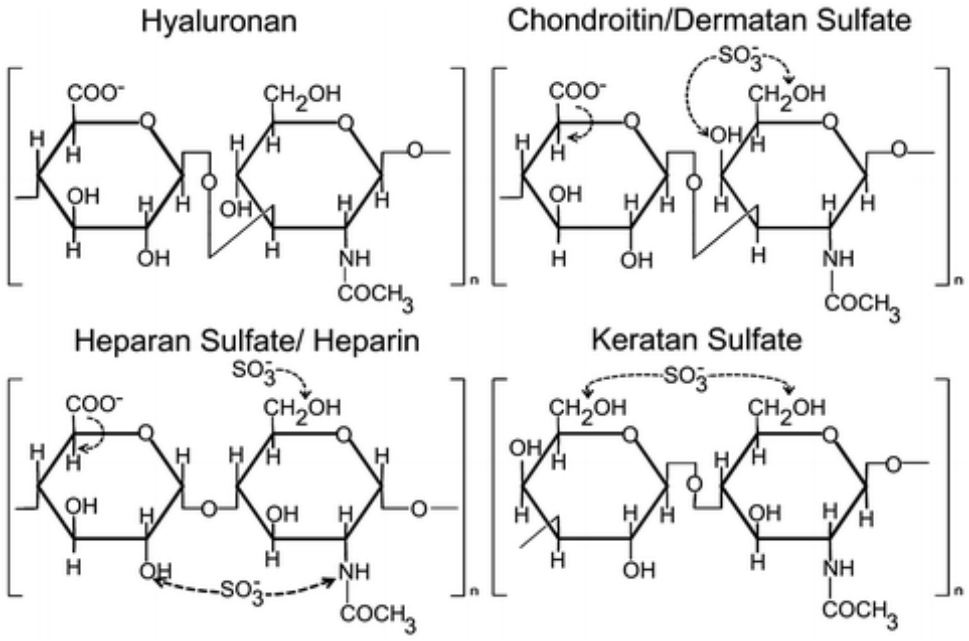

Figure 24: Structure of disaccharide unit of GAG members.
Hyaluronan: β(1,4)-GlcA-β(1,3)-GlcNAc. **Chondroitin Sulphate:** β (1,4) GlcA-β (1,3) N-GalNAc, **heparin sulphate and heparin**: α(1,4) GlcA- β (1,4) N-GlcNAc / α(1,4) IdoA-(1,4) N-GlcNAc and **keratin Sulphate:** β(1,4) Gal-β(1,3) GlcNAc.

3.2 Modification of glycosaminoglycan backbone

Sulphation consists of the transfer of a sulphate group (SO_4^{2-}) at specific positions on the disaccharide unit. The process occurs in the Golgi apparatus *via* specific sulfotransferases (STs) enzymes which transfer the sulfo group from the universal sulphate donator 3'-phosphoadenosine 5'-phosphosulphate (PAPS) to the GAG backbone. PAPS is synthetized in the cytosol and then translocated to the Golgi apparatus by PAPS translocase where it serves as sulphate donator **(Figure 25)**.

Epimerisation is the other modification that GAG backbone can undergo during its synthesis in the Golgi apparatus to generate astereisomers. It consists in inverting the configuration of the asymmetric centre at C5 position of the glucuronic acid to give rise to its epimer iduronic acid (IdoA). This reaction is catalysed by glucuronyl C5-epimerase. Its occurrence may require specific sulphation modification beforehand.

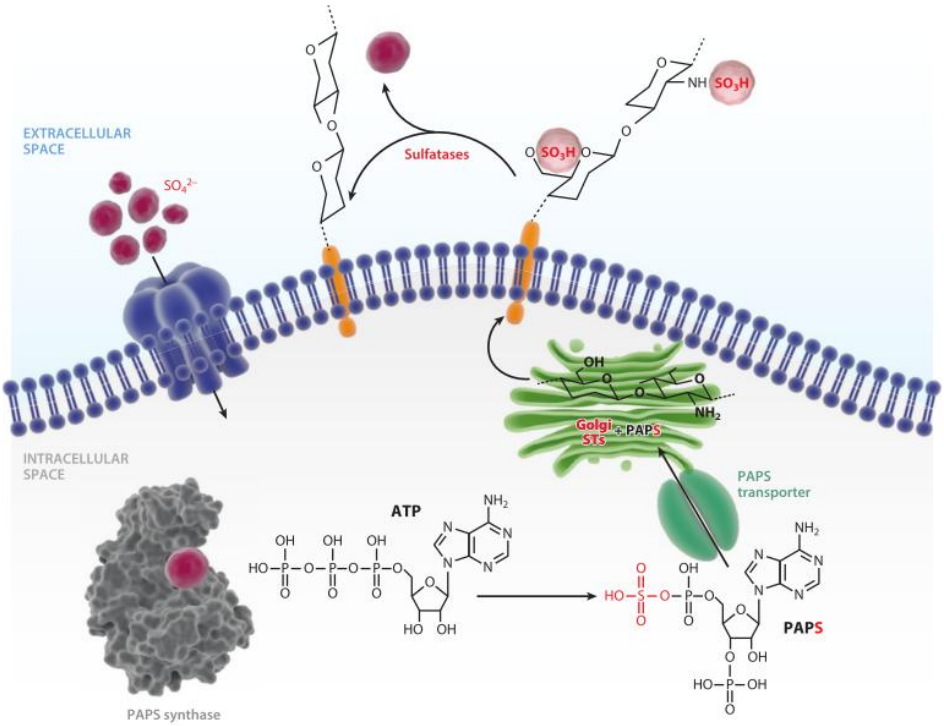

Figure 25: The sulphation cycle in mammalian cells.
3'-Phosphoadenosine 5'-phosphosulphate (PAPS) is synthesized in the cytosol and then transported into the Golgi apparatus by a specific transporter known as PAPS translocase. In this cellular compartment, the carbohydrate sulfotransferases (STs) catalyse the transfer of a PAPS sulfonyl group onto a hydroxyl or amino group(s) of the nascent glycoconjugates, which are then secreted into the extracellular matrix or inserted into the plasma membrane. So far, more than 30 Golgi-associated STs have been identified *(from Soares da Costa et al., 2017*[166]).

The structure of the GAG backbone is simple by itself. However, the epimerisation of the uronic acid, the position and number of sulphate on one monosaccharide and the size variety between molecules results in plethora isoforms within subfamilies and infinite variation within the same isoform. Moreover, since in contrary to the DNA and protein molecule, GAG synthesis is not template-based model, the structure of each molecule could be unique. Furthermore, this variability notably in sulphation pattern allows a specific interaction with numerous proteins. Sulphation pattern encodes molecular recognition and activity. This makes GAGs involved in a multitude of physiological and pathological processes.

3.3 Glycosaminoglycan types

- **Hyaluorinc acid:** detailed in ECM chapter (section 1.1.1)

- **Heparin and heparin Sulphate**

HS constitutes the most abundant sulphated GAG in several tissues. The disaccharide unit of Hp/HS is composed of α1, 4 GlcA which can be epimerised to give rise to iduronic acid (IdoA) and β1, 4 N-GlcNAc which undergoes an N-deacetylation to give rise to glucosamine ($GlcNH_2$). They undergo also an O-sulphation (at C6 of $GlcNH_2$ and C2 of GlcA/IdoA) and N-sulphation (at C2 of $GlcNH_2$). These modifications occur in clusters resulting thus in sulphated (S-domains) and non-sulphated (NA-domains) domains **(Figure 26)**. Difference between Hp and HS is the degree of these modifications. Hp is most modified with 2.7 sulphates per disaccharide unit on average[167] and he N- and 2,6-di-O-sulphated structure (-IdoA2S-GlcNS6S-) as generally the predominant disaccharide unit. However, IdoA2S-GlcNS6S is minor unit in most HS[168]. With other words the majority of uronic acid of Hp is IdoA, while it is GlcA in HS. HSs are involved in lot of mechanisms notably the interaction host-pathogen[165]. HS plays an important role in the CNS. Mice deficient for the expression of exostosin1 (EXT1) glycosyltransferase, mediating polymerisation of HS chain during biosynthesis, failed to gastrulate and died by embryonic day (E) 8.5[169]. HSs are also involved in signalling of FGF which is indispensable for neural cell proliferation[169]. HSs are also known for their role in AD by modulating brain amyloid-β clearance and aggregation[170].

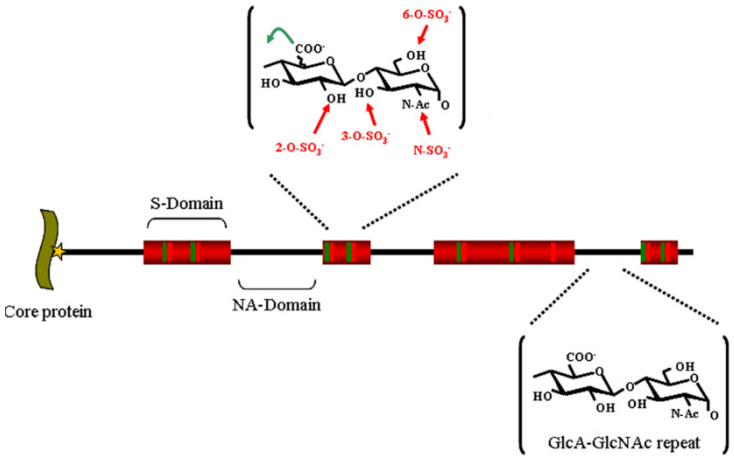

Figure 26: Heparan sulphate structure.
HS, whose biosynthesis is initiated by the attachment of xylose (star) to specific serine residues in HSPG core proteins, followed by the formation of a linking tetrasaccharide (xylose-galactose-galactose-glucuronic acid), is initially polymerized by an enzyme complex composed of Ext1 and Ext2 as a GlcA-GlcNAc repeat (black). In restricted regions, called S-domains (shown in red), the chain is extensively modified by a series of enzymatic reactions that remove the acetyl group from GlcNAc residues and substitute the resulting free amino groups with sulphates, epimerize the adjacent GlcA into L-iduronic acid (IdoA) and add sulphates on various positions: the C2 of the IdoA (and less frequently that of the GlcA), the C6 of the GlcNS (and less frequently that of the GlcNac), and finally at the C3 of GlcNS or GlcN units. Altogether, these modifications can generate (the theoretical number of) 48 different disaccharides, whose combination within the S-domain gives rise to a large diversity of structures and make up binding sites for protein ligands (*from Connell and Lortat-Jacob. 2013*[165]).

- **Keratan Sulphate**

KS is the most particular GAG member with a lot of exceptions comparing to other GAGs: the disaccharide unit of KS is composed of β1, 4 Gal instead an uronic acid and β1, 3 GlcNAc; the sulphation can occur at C6 of both Gal and GlcNAc but GlcNAc sulphation is most abundant. There are three types of KS: KS I (identified in cornea), KS II (identified in cartilage) and KS III (identified in CNS). KSs are attached to their core protein in two different ways: N-glycosylation (KS I) and O-glycosylation (KS II and III). The KS displays usually a ramification and can be capped by sialic acid [171].

- **Chondroitin Sulphate /dermatan Sulphate**

CS and DS are the only two members of galactosaminoglycan subfamily. CS is the second most known sulphated GAG member after HS. CS disaccharide unit is composed of β (1,4) GlcA-β (1,3) N-acetylgalactosamine (GalNAc). GlcA can be epimerized at C5 and gives rise to DS unit. CS unit can be sulphated at different positions resulting in different isoforms summarized in **Table 6**. Most of them are obtained from marine invertebrate.

Table 6: **Structure of disaccharide units derived from chondroitin sulphate and dermatan sulphate by Chondroitinase digestion.**
(*from Volpi 2006*[172])

			Hexuronic acid				*Galactosamine*		
No	*Name*	*Other names*	R^2	R^3	R^6_G	R^6_I	R^2	R^4	R^6
1	**ΔDi-nonS$_{GlcA}$**	**ΔDi-0S$_{CS}$**	**H**	**H**	**COOH**	**H**	**Ac**	**H**	**H**
2	**ΔDi-nonS$_{IdoA}$**		**H**	**H**	**H**	**COOH**	**Ac**	**H**	**H**
3	**ΔDi-mono4S$_{GlcA}$**	**ΔDi-4S/ A unit**	**H**	**H**	**COOH**	**H**	**Ac**	**SO$_3$H**	**H**
4	**ΔDi-mono4S$_{IdoA}$**		**H**	**H**	**H**	**COOH**	**Ac**	**SO$_3$H**	**H**
5	**ΔDi-mono6S$_{GlcA}$**	**ΔDi-6S/ C unit**	**H**	**H**	**COOH**	**H**	**Ac**	**H**	**SO$_3$H**
6	**ΔDi-mono6S$_{IdoA}$**		**H**	**H**	**H**	**COOH**	**Ac**	**H**	**SO$_3$H**
7	**ΔDi-mono2S$_{GlcA}$**		**SO$_3$H**	**H**	**COOH**	**H**	**Ac**	**H**	**H**
8	**ΔDi-mono2S$_{IdoA}$**		**SO$_3$H**	**H**	**H**	**COOH**	**Ac**	**H**	**H**
9	ΔDi-mono3S$_{GlcA}$		H	SO$_3$H	COOH	H	Ac	H	H
10	ΔDi-mono3S$_{IdoA}$		H	SO$_3$H	H	COOH	Ac	H	H
11	ΔDi-monoNS$_{IdoA}$		H	H	H	COOH	SO$_3$H	H	H
12	**ΔDi-di(2,6)S$_{GlcA}$**	**ΔDi-diS$_D$/ D unit**	**SO$_3$H**	**H**	**COOH**	**H**	**Ac**	**H**	**SO$_3$H**
13	**ΔDi-di(2,6)S$_{IdoA}$**		**SO$_3$H**	**H**	**H**	**COOH**	**Ac**	**H**	**SO$_3$H**
14	**ΔDi-di(2,4)S$_{GlcA}$**		**SO$_3$H**	**H**	**COOH**	**H**	**Ac**	**SO$_3$H**	**H**
15	**ΔDi-di(2,4)S$_{IdoA}$**	**ΔDi-diS$_B$ / B unit**	**SO$_3$H**	**H**	**H**	**COOH**	**Ac**	**SO$_3$H**	**H**
16	**ΔDi-di(4,6)S$_{GlcA}$**	**ΔDi-diS$_E$ / E unit**	**H**	**H**	**COOH**	**H**	**Ac**	**SO$_3$H**	**SO$_3$H**
17	**ΔDi-di(4,6)S$_{IdoA}$**	**ΔDi-diS$_H$ / iE unit**	**H**	**H**	**H**	**COOH**	**Ac**	**SO$_3$H**	**SO$_3$H**
18	ΔDi-di(3,6)S$_{GlcA}$	ΔDi-diS$_L$ / L unit	H	SO$_3$H	COOH	H	Ac	H	SO$_3$H
19	ΔDi-di(2,3)S$_{IdoA}$		SO$_3$H	SO$_3$H	H	COOH	Ac	H	H
20	ΔDi-di(3,4)S$_{GlcA}$	ΔDi-diS$_K$ / K unit	H	SO$_3$H	COOH	H	Ac	SO$_3$H	H
21	ΔDi-di(2,N)S$_{IdoA}$		SO$_3$H	H	H	COOH	SO$_3$H	H	H
22	**ΔDi-tri(2,4,6)S$_{GlcA}$**	**ΔDi-triS**	**SO$_3$H**	**H**	**COOH**	**H**	**Ac**	**SO$_3$H**	**SO$_3$H**
23	**ΔDi-tri(2,4,6)S$_{IdoA}$**	**ΔDi-triS$_{iT}$ / iT unit**	**SO$_3$H**	**H**	**H**	**COOH**	**Ac**	**SO$_3$H**	**SO$_3$H**
24	ΔDi-tri(3,4,6)S$_{GlcA}$	ΔDi-triS$_M$ / M unit	H	SO$_3$H	COOH	H	Ac	SO$_3$H	SO$_3$H
25	ΔDi-tri(2,6,N)S$_{IdoA}$		SO$_3$H	H	H	COOH	SO$_3$H	H	SO$_3$H

Subscripts G and I show the GlcA and IdoA origins of Δ-disaccharide, respectively. The IdoA- or GlcA- derived disaccharides have obtained the same structure at C-5 after digestion with chondro-/dermatolysases. The commonest disaccharides are those in bold. The others have been determined only in CS/DS chains from marine invertebrate.

The most common sulphation pattern is C-4 and/or C-6 of the GalNAc and C-2 of the GluA or IdoA resulting in monosulphated or disulphated units. Disaccharide unit sulphated at C-4, C-6, C-4 and C-6 or C-6 and C-2 are called CS-A, CS-C, CS-E and CS-D unit, respectively. CS-A unit can be epimerized and results in CS-B or DS unit **(Figure 27)**[172]. CS chains are referred by the name of the most abundant unit constituting the chain *e.g* a chain is referred as CS-E chain when CS-E units are the most abundant in the chain.

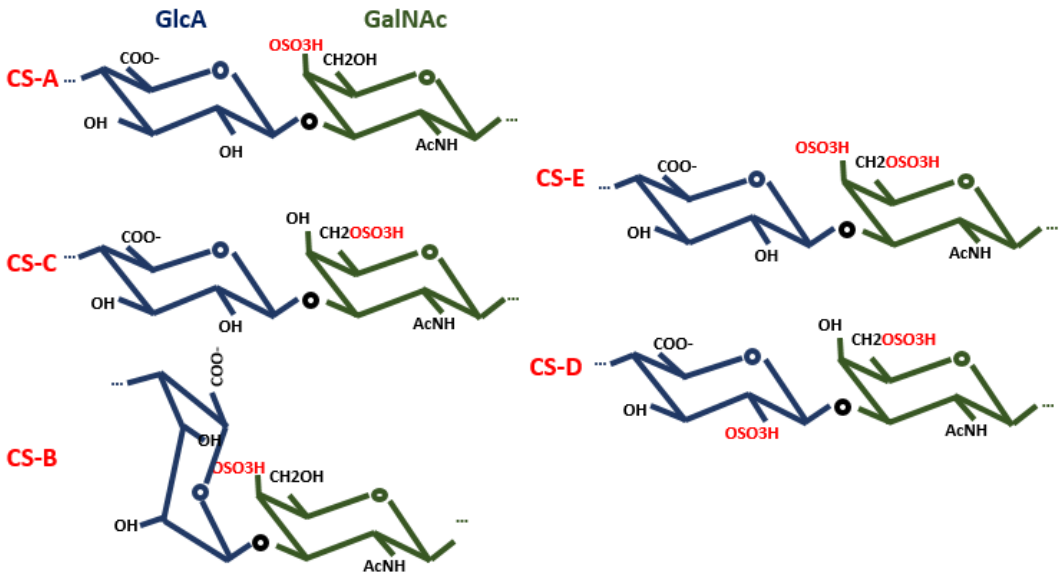

Figure 27: Structure of chondroitin sulphate disaccharide units.
Disaccharide unit of the chondroitin sulphate is made of glucuronic acid (GlcA) and N-acetylgalactosamine (GalNAc). Sulphation can take place on the C4 and/or C6 of the GalNAc and C2 of GlcA. Disaccharide unit can be mono or disulphated resulting in numerous isoforms: CS-A (4S), CS-C (6S), CS-E (4S6S) and CS-D (6S2S). GlcA of CS-A can be epimerised at C5 to give rise to CS-B or dermatan sulphate (DS).

3.4 Chondroitin sulphate biosynthesis

Chondroitin sulphate (CS) biosynthesis was investigated since 1960s with the isolation of the PAPS and sulfokinase (transfers the sulphate from PAPS to nitrophenol). At that time, PAPS was demonstrated as a sulphate donor in GAG, notably in CS synthesis. Moreover, uridine diphosphate (UDP)-GlcA and UDP-GalNAc were also demonstrated as sugar unit donors for the CS chain synthesis. The mechanism of the CS biosynthesis has been started to be elucidated i) as consisting of an equimolar and simultaneous incorporation of GalNAc and GlcA; ii) GlcA was added to the non-reducing end of GalNAc and iii) the enzymes involved in the chain polymerisation and sulphation were located together and work together which leads to understand that the sulphation occurs simultaneously with the polymerization[172 173].

As CS is synthetized as a part of CSPG, CS synthesis does not take place without the core protein. Once the core protein is formed in the endoplasmic reticulum (ER) and transferred to the Golgi apparatus, CS chain is synthetized in three steps detailed below: formation of the linkage region, polymerization and modification (sulphation and epimerization) of the nascent polysaccharide. CS biosynthesis requires a multitude of specific enzymes: glycosyltransferases, sulfotransferases and epimerases **(Figure 28)**.

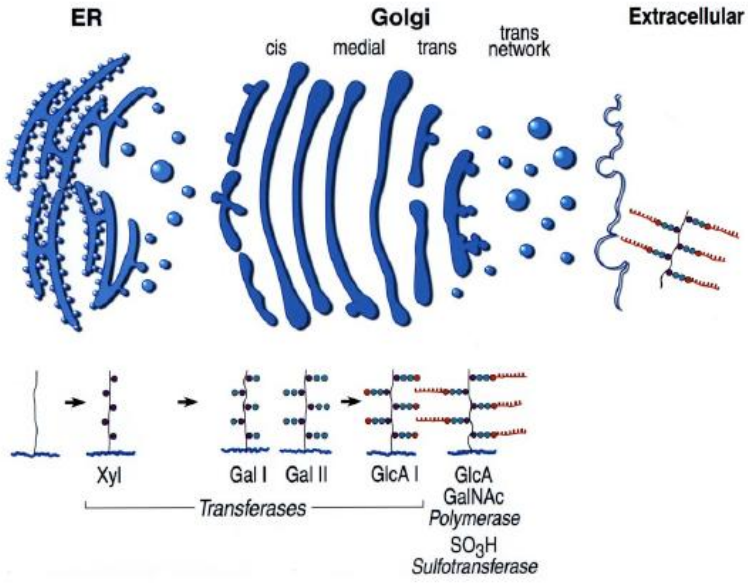

Figure 28: Subcellular localization of proteochondroitin/dermatan Sulphate.
ER: endoplasmic reticulum, Xyl: xylose, Gal: galactose, GlcA: glucuronic acid, GalNAc: N acteylgalactosamine formation (*from Silbert et al., 2002*[174]*).*

3.4.1 Biosynthesis of the core protein

As most proteins, the CSPG core protein is first translated from the mRNA in the cytosol then translocated to the ER lumen where disulfide bonds are made and the folding of the protein occurs, in addition to the N-glycosylation (which consists of attaching an N-linked oligosaccharides to asparagine residues from dolichol phosphate intermediates). Correctly folded proteins are transferred to Golgi for gagosylation (enzymatic reaction which consists in synthesis a GAG chain on a core protein) by a mechanism that is not clear[174]. Another point needed to be elucidated is what determines the gagosylation of the core protein. An alignment of amino acid (a.a) primary sequence over 50 chondroitin sulphate attachment sites from 19 different core proteins generated the consensus sequence XXXXGSGXYX (with X = E or D and Y = G, E, or D). Numerous exceptions to this consensus sequence were found: A residue

can substitute to G residues of the consensus sequence, potential consensus sequences escape commonly to the gagosylation and xylosyltansferase may transfer xylose to a T residue instead S residue. This indicates that they are likely other mechanisms regulating the gagosylation decision[174 172].

3.4.2 Synthesis of the linkage region

The biosynthesis of CS chain initiates with the formation of the linkage region in ER and Golgi apparatus. The linkage region is a tetrasacchride made of: Ser-O- β1 Xyl 4 -> β1Gal 3 -> β1 Gal 3 -> β1 Glc A **(Figure 29)**. The assembly of this oligosaccharide on the core protein proceeds by direct transfer of a monosaccharide from their donor to the core protein. Glucose and galactose are the main precursor for all sugars of CS through formation of UDP-Xyl, UDP-Gal, UDP-GlcA and UDP-GalNAc. The addition of the xylose to the hydroxyl group of serine, followed by a first Gal then a second to terminate with ClcA is catalysed by O-xylosyltansferase-I (XylT-I), β1,4-galactosyltransferase I (GalT-I), β1,3-galactosyltransferase II (GalT-II) and β1,3-glucuronyltransferase I (GlcAT-I), respectively. Solubilisation of the xylosyltrasferase was easily achieved, while it was complicated for GalT-I and GalT-II indicating that the galactosyltransferases are more attached to the Golgi membranes[175 174 172]. Xylosylation (xylose addition) begins in ER and continues in Golgi where the two Gal and GlcA were added[176]. It was postulated that XylT-I interacts with GalT-I in early Golgi but not with GalT-II and GalT-I does not interact with GlcAT-I indicating that GalT-I and GalT-II are located in different part of the Golgi. GlcA addition occurs in medial/trans Golgi where the polymerisation takes place. Hp/HS and CS/DS share the same linkage region. Thus, the fate of the GAG chain being synthesized is determined by the type of the first transferred hexosamine to the tetrasaccharide, if it is a GalNAc, the chain will be a CS[174]. However, what is the molecular signal determinant for the type of hexosamine to be added is poorly known. Investigating about this, it was found that the linkage region undergoes a post-translational modification. Indeed, the galactose residues can be sulphated at position O-4 and O-6 in CS chain synthesis but not HS. This could constitutes the molecular signal for the type of GAG chain that will be synthetized[177]. Moreover, N-acteylgalactosaminetransferase (GalNAcT-I) could recognise the sulphated galactose of the linage region[172]. Phosphorylation of the xylose can also take a place but in both HS and CS synthesis[177]. Xylose is phosphorylated only once the first Gal is added and dephosphorylated

just after GlcA addition[172]. Furthermore, the structure of the core protein could also influence the type of the GAG chain that will be synthetized.

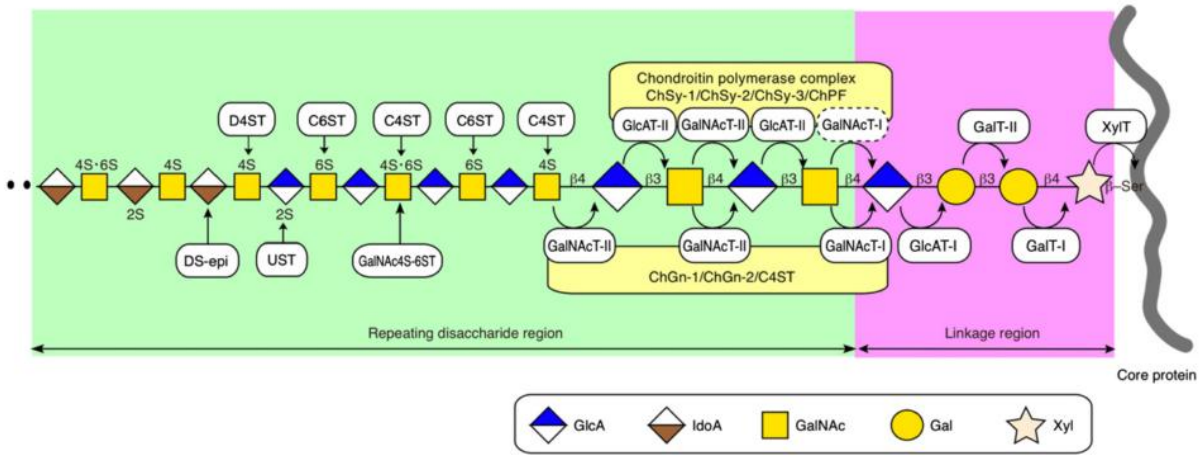

Figure 29: Conventional scheme for CS biosynthetic machineries.
A number of glycosyltransferases participate in the synthesis of the common tetrasaccharide linkage region and repeating disaccharide region characteristic to CS chains. The Chain backbone is further modified by specific sulfotransferases and epimerases. XylT, xylosyltransferase; GalT-I, β1,4-galactosyltransferase-I; GalT-II,β1,3-galactosyltransferase-II,GlcAT-I, β1,3-glucuronyltransferase-I; GalNAcT-I,GalNAc transferase-I; GlcAT-II, GlcA transferase-II; GalNAcT-II, GalNAc transferase-II; ChSy, chondroitin synthase; ChPF, chondroitin polymerizing factor; ChGn, chondroitin GalNAc transferase; C4ST, chondroitin 4-O-sulfotransferase; C6ST, chondroitin 6-O-sulfotransferase; D4ST, dermatan 4-O-sulfotransferase; UST, uronyl 2-O-sulfotransferase; GalNAc4S-6ST, GalNAc 4-sulphate 6-O-sulfotransferase; DS-epi, GlcA C-5 epimerase (DS epimerase) (*from Mikami and Kitagawa. 2013*[175]*).*

3.4.3 Chain initiation, polymerization and sulphation

The transfer of the GalNAc to the linkage region by GalNAcT-I constitutes the **initial step** for the polymerization of the CS chain. Then, the **polymerization** occurs in alternative highly organized process orchestrated by two types of polymerases, GlcAT-II and GalNAcT-II, to synthetize the repeating disaccharide motif GlcA-GalNAc, respectively **(figure 29)**. These enzymes add an individual sugar to the non-reducing end of growing nascent chain. GalNAcT-I is not able to polymerize the CS chain, the same applies to GalNAcT-II which is not able to recognize the tetrasaccharide of linkage region. This is also noticed for GlcAT-I and GlcAT-II. Another type of enzyme in human referred as a chondroitin synthase displaying both GalNAcT-II and GlcAT-II activities was reported. This enzyme is able to transfer GalNAc to GlcA *via* β1, 4 linkage and GlcA to GalNAc *via* β1,3 linkage. Nevertheless, no polymerisation activity was observed *in vitro* with the recombinant protein. *In vivo*, this enzyme is probably associated to another protein as chondroitin polymerising

factor (ChPF) to allow the polymerisation. Indeed, the co-expression of chondroitin synthase and ChPF leads to a polymerisation on the linkage region of α-thrombomodulin. Furthermore, this enzyme appears to act on longer acceptors, while GalNAcT-II acts on the shorter, suggesting that they are involved at different stages of the polymerisation[172 174 175]. The size of the synthetized chain can reach 70 kDa. However, to get this extensive polymerization a core protein is required. Indeed, in experiment of cell culture where CS chains, xylosides or oligosaccharides were added as acceptors they accepted only few sugar units[174].

Modifications such as epimerization and sulphation occur during the synthesis of CS backbone by glycosyltransferases **(Figure 30)**. As we mentioned above, GalNAc and GlcA can be sulphated at different positions which involves several CS sulfotransferases. In the same chain, all sulphation patterns can be found. **Sulphation** at position 6 is catalysed by chondroitin-6-sulphate sulfotransferases (**C6STs**). C6ST1 is the first characterized enzyme. It transfers the sulphate group on GalNAc at position O6 in GlcA-rich regions, resulting in CS-C units. Moreover, it is also able to sulphate the KS galactose residues. Other homologues of C6ST1 have been identified later and they are involved in 6-sulphation in different regions *e.g* in residues adjacent to IdoA or in non-reducing end GalNAc 4-sulphate residues. The enzyme acting on non-reducing end GalNac-4S is referred as chondroitin 6-O-sulphate sulfotransferase (GalNAc4S-6ST) and is involved in the generation of highly sulphated non-reducing terminal sequence in CS-4S, thus CS-E (4S6S) motif in non-reducing end **(Figure 30)**. The 6-sulphation occurs in the *medial/trans* Golgi while 4-sulphation occurs in a later *trans* Golgi region.

4-O sulphation is catalysed by 4-O sulfotransferases (**C4STs**) and it consists in the most common sulphation in CS and DS chains. Similar to C6ST, different isoforms of C4ST exist and sulphate different region: C4ST-1, C4ST-2 and C4ST-3 catalyse the 4-O sulphation on GlcA-rich region, while the D4ST-1 catalyse the 4-O sulphation on GalNAc residues adjacent to IdoA[174 172] **(**Figure 30**)**. C4ST-1 is also involved in cooperation with GalNAcT-II in the amount of CS synthesis since its loss can be compensated by C4ST-2 and C4ST-3 and affects drastically the amount of synthetized CS which results probably from the shorter chain length. 4-O-sulphation by C4ST-1 promotes the CS chain elongation[175]. C4ST-2 cooperates with GalNAcT-1 to increase the number of CS chains. Furthermore, the 4-sulphation in IdoA-rich region prevents back epimerization into GlcA[175].

2-O sulphation of the uronic acid occurs more on IdoA than on GlcA. This reaction is catalysed by uronyl 2-O sulfotransferase (**UST**). It 2-O sulphates either the GlcA adjacent to 6S-GalNac (in the CS-C unit) to give rise to CS-D unit (6S2S) or the IdoA adjacent to 4S-GalNAc to give rise to iB unit (4S2S) **(Figure 30)** Since 2-O sulphate occurs after the GalNAc sulphation, it is likely the last sulphation step in CS and DS biosynthesis. Thus, it occurs in a relatively late Golgi trans network[174 172 175].

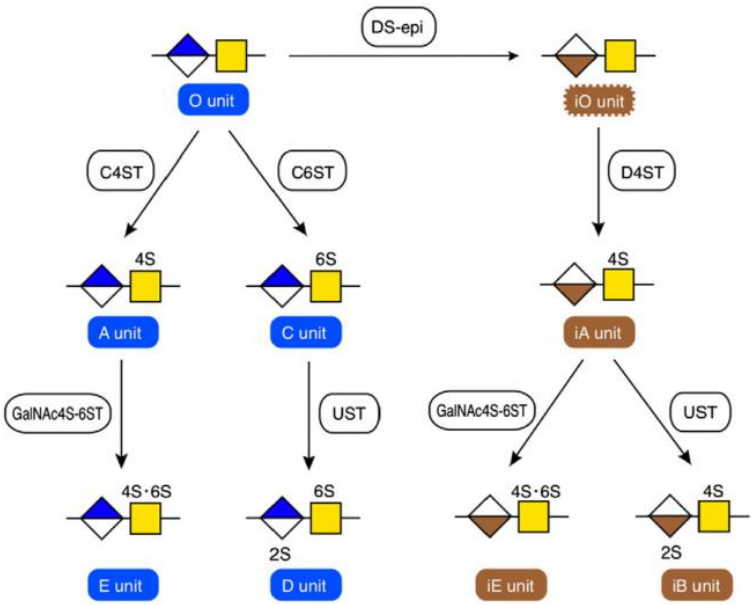

Figure 30: A schematic diagram of pathways for biosynthetic modification of CS/DS chains.
On the basis of the substrate specificities of the sulfotransferases, the biosynthetic pathways for CS-type disaccharide units can be classified into the initial "4-O-sulphation" and "6-O-sulphation" pathways. In contrast, the DS-type disaccharide units are synthesized through the intermediate iO units formed by GlcA C-5 epimerases, DS-epi1 and DS-epi2 *(from Mikami and Kitagawa, 2013[175]).*

The presence of 0.2 mM sulphate in the culture medium is the minimal required concentration for the normal sulphation of CS, while the sulphation of HS is affected only at very lower concertation. DS is also less affected by lower PAPS concentration. In addition, CS and DS involve distinct sulfotransferases. All these suggest that the lower sulphate concentration in the organism would affect first the sulphation of CS before DS and HS[174]. CS sulphation degree depends also to anchoring of nascent CSPG at the site of the membrane-bound enzyme. Indeed, when β-xyloside, compound derived from xylose able to interfere with proteoglycan synthesis by acting as an artificial acceptor for glycosaminoglycan synthesis, is added to the culture cell, the resulted xyloside-CS chain is less sulphated than the

concurrent CS chain of the CSPG[174]. Furthermore, sulphation of the same core protein is tissue-dependant *e.g* of decorin from bovine which contains 6-O sulphated Glc-A rich domains in sclera, while it contains 4-O rich domains in cartilage and bone[172].

DS is resulted from the conversion of the GlcA to its IdoA (**epimerization)** at the C-5 of GlcA **(Figure 30)**. This reaction is catalysed by two C-5 epimerases: DS-epi1 and DS-epi2. IdoA residues are either altering with GlcA forming thus hybrids structure or clustered together to form IdoA blocks[178]. Epimerization occurs usually in concomitant with the 4-sulphation, even that the 4-sulphation increases the epimerization. Epimerization is affected by monensin which inhibits the secretory pathway in the *medial* Golgi region as well as the 4-sulphation, indicating that 4ST and C5 epimerase are juxtaposed[174].

3.4.4 Chain termination

There is no universal motif at the end of CS chain as a termination signal of the CS biosynthesis. It can terminate with GlcA, GalNAc, GalNAc-4S, GalNAc,-6S and GalNAc-4S6S. Nevertheless, GalNAc-4S6S (CS-E) motif seems to be a predominant terminal structure[172]. Indeed, this motif is found in several mammalian species *e.g* in human cartilage aggrecan, *in vitro* culture of chick and rat embryo cartilage and in rabbit thrombomodulin[172]. These CS-E motif are 60 times more abundant in the non-reducing end than interior of the chain[179]. In support to CS-E motif as a termination signal is the existence of GalNAc4S-6ST which adds 6-O-sulphate to the non-reducing GalNAc4S[172]. Moreover, GalNAc4S-6ST KO mice display larger CS chains and heterologous terminal structure[180].

From all that has been described on CS biosynthesis, it is clear that all these enzymes cross-talk and work together in order to elaborate an adequate CS length and pattern of sulphation and epimerization. Lot of evidences pointing the existence of "GAGosome" notion, complex of membrane-bound enzyme working together. Furthermore, despite all we know about the GAG biosynthesis in general and especially CS, it remains a lot to know about the detailed location of each step, the mechanisms of their regulation and how these enzymes communicate? Understanding all these will enable us to modulate it, thus controlling length, numbers and epimerization/sulphation pattern of CS in order to understand their role in physiological condition or their modulation in pathological conditions. The chemical synthesis is not enough developed yet to be able to synthetize a long polysaccharide. Even

oligosaccharide synthesis is very challenging. Indeed, more than 40 chemical steps have been required to create a single oligosaccharide[181].

3.5 Chondroitin sulphate catabolism

Mechanisms of CS catabolism are even less known than the CS biosynthesis mechanism. CS/DS degradation is supposed to occur mainly in lysosomes to generate monosaccharides which are used again in the biosynthesis. There are two types of enzymes degrading CS: CS/DS-hydrolases and CS/DS-lyases. These two families act on glyosidic bond β GalNAc 1-> 4-β GlcA. Degradation of CS/DC in mammal is based only on hydrolases, since no lyases in vertebrates are identified so far. CS can be degraded by β-glucuronidase which cleaves the β -GlcA residue. Sulphate groups of non-reducing GalNAc at position O-4 and O-6 are removed by GalNAc-4-sulfatase and GalNAc-6-sulfatase, respectively, followed by β-N- acetylhexosaminidase to cleave the GalNAc. DS catabolism is achieved with iduronate-2-sulfatase which removes 2-sulphate groups of idoA, then followed by α-iduronidase which cleaves terminal non-reducing IdoA. No mammalian endoglycosidases specific for CS/DS have been reported[182]. Nonetheless, some hyaluronidases (HYAL), which hydrolyse initially HA, can catalyse CS chain depolymerisation: HYAL-1, HYAL-4 and sperm adhesion molecule1 (SPAM1) corresponding to PH-20 testicular hyaluronidase **(Figure 31)**. These enzymes act at the initial step in the catabolism of CS at cellular level *in vivo*. HYAL-1 and SPAM1 degrade CS to a limited extent. Interestingly, HYAL-4 does not show activity on HA, while it degrades the CS. Indeed, human HYAL-4 is a CS hydrolase acting as endo-β-N-acetylgalactos-aminidase[183]. HYAL-4 is expressed after SCI in rat model in areas surrounding CSPGs, suggesting thus its involvement in degrading CSPGs[184]. Defect in expression of these enzymes leads to a disorder in the catabolism and accumulation of polysaccharides in lysozymes and then pathology such as mucopolysaccharidose[182].

CS/DS lyases (chondroitinases) exist only in bacteria and regroup several members: Chondroitinase-C (cleaves CS-C units), chondroitinase-AC (cleaves CS-A and CS-C units), chondroitinase-B (cleaves DS unit) and ChABC (cleaves CS-A, CS-C, CS-E, CS-D and DS units) **(Figure 31)**. Chondroitinase-C, -AC and –ABC are also able to depolymerize HA. Resulted products varying from degree of polymerization (dp) 2 to 4-6. However, higher dp can be obtained. These enzymes serve to generate oligosaccharides libraries. ChABC is

frequently used for the disaccharide composition analysis of CS chain in high performance chromatography (HPLC) in a particular cells or tissues. Moreover, it shows a great benefit in treatment of SCI *in vivo* models. Unlike lyases, chondroitinases result in unsaturated disaccharides units which absorbs at 232 nm[172].

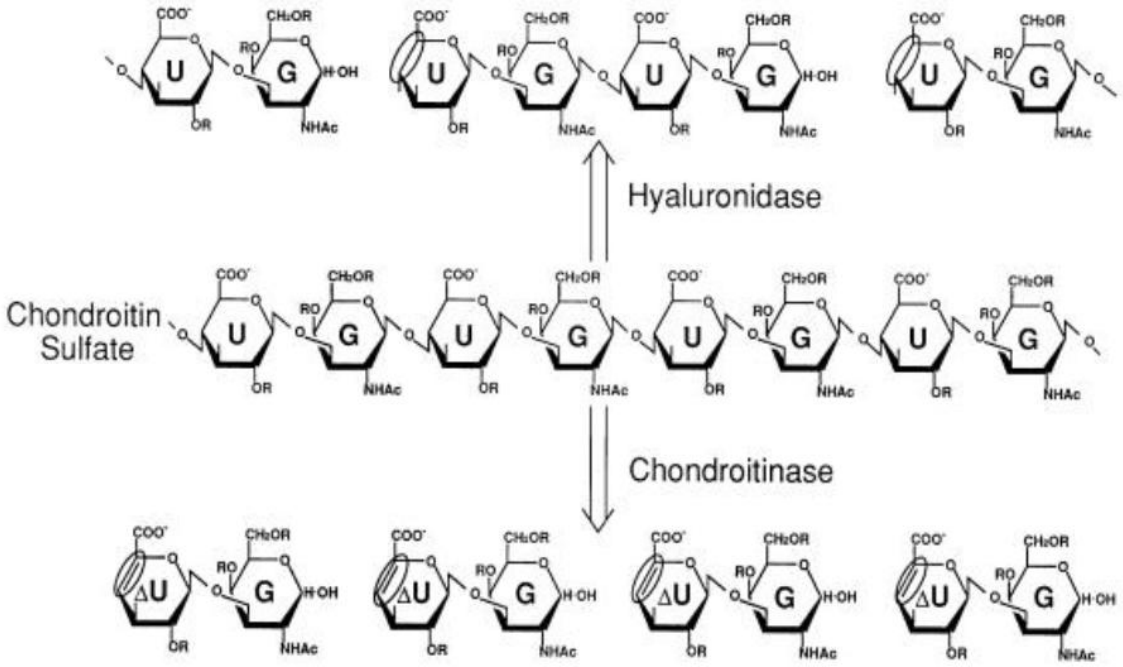

Figure 31: Action of hyaluronidase and chondroitinase.
Testicular hyaluronidase cleaves the *N*-acetyl-D-galactosaminidic linkages in CS chains in a hydrolytic fashion to yield tetra-, hexa-, octa-, deca-, and polysaccharides with glucuronic acid at the non-reducing ends as major products. In contrast, bacterial chondroitinase is a lyase that cleaves *N*-acetyl-D-galactosaminidic linkages in an eliminative fashion to give unsaturated disaccharides as major products. G: *N*-acetyl-D-galactosamine, U: glucuronic acid, ΔU: unsaturated uronic acid (*https://jcggdb.jp/GlycoPOD/protocolShow.action?nodeId=t19).*

3.6 Chondroitin sulphate in the CNS

3.6.1 Sulphation pattern of CS in the CNS

CS is the most abundant sulphated GAG in the ECM matrix notably in PNN (70% CS and ~ 30% HS)[185]. Its sulphation pattern varies dynamically from embryo to adult CNS of vertebrate, from physiological to pathological conditions indicating thus the importance and role of the sulphation pattern in the CNS. The monosulphated units are the most abundant units in mammals, while the disulphated units represent negligible amounts. Indeed, the 6-sulphation (CS-C) is enriched in the CNS during embryogenesis and decreases progressively

over development until ~ 2.5% of total CS in adult brain, while the 4-sulphation (CS-A) expression increases over development to constitute the predominant unit in adult CNS (~ 92% of the total CS units)[55 88 93 186] **(Table 7)**. These changes are essentially due to the changes in expression and activity of C4ST and C6ST, which supports the idea that the resulted sulphation pattern is mainly due to the availability and activity of sulfotransferases[186]. Disulphated units (CS-E and CS-D) are present in tiny amounts during ontogenesis of mammals. However, they are upregulated over the development[88] **(Table 7)**. Important changes of sulphation pattern occurs between P21 and adulthood, but no changes are observed between birth and P21 in rat cortex[55]. Interestingly, CS-E and CS-D amounts decrease in the rat cortex during postnatal development[55 187]. Moreover, CS-E profile expression correlates perfectly with GalNAc4S-6ST expression indicating thus CS-E unit apparition is regulated by this enzyme[187]. In the postnatal developing cerebellum, GalNAc4S-6ST expression decreases as well as CS-E units[188].

Table 7: CS-GAG proportions: changes with development of rat brain.
(*from Properzi et al., 2005[88]*)

	Distribution (%) of disaccharide components		
Disaccharide components	Embryonic day 18	Postnatal day 0	Adult
Di-0S and Di-4S	84.7	87.2	95.5
Di-6S	14.2	11.6	2.4
Di-diSD	0.1	0.1	0.6
Di-diSE	0.7	0.9	1.1

Sequential extraction of CS from different brain ECM compartments using four different buffers (buffer 1: normal saline; buffer 2 containing detergent: loose matrix; buffer 3 containing 1 M NaCl: membrane-bound matrix and buffer 4 containing 6 M urea: PNN) was developed in Fawcett lab. Disaccharide CS composition of each compartment is analysed anion exchange HPLC **(Table 8)**. Results show while the CS-A units decreases over the buffers, CS-C units increases. In addition, the disulphated units are enriched in the late buffers

notably in 6 M urea (PNNs). Furthermore, PNNs-associated CSs represent a tiny amount of the total CS (~ 1.3%)[185]. Sulphation profile in PNNs changes with aging. CS-A units increases progressively from 3 to 18 months rat, while CS-C units proportion decreases in PNNs. Furthermore, PNNs from aged rats are more inhibitory for axon growth than younger rat[189]. This is likely due the increase CS-A/CS-C ration. The role of the 6 sulphation in cortical plasticity is highlighted by an interesting study with transgenic mice that overexpress human C6ST-1, thus CS-C units amount decreases and a decrease of CS-A units (decrease of CS-A/CS-C ratio). This adult mice retains the ocular dominance plasticity by reducing PNNs formation and failure accumulation of Otx2 in PNNs overexpressing CS-C, indicating thus the importance of sulphation pattern of PNNs in Otx2 accumulation[190]. However, in this study the authors did not investigate the expression of the disulphated units CS-E and CS-D to which Otx2 binds with a high affinity. The failure of Otx2 accumulation in PNNs overexpressing CS-C units could due to a defect in CS-D/CS-E expression in these transgenic mice.

Table 8: **Disaccharide composition of CS/DS-GAG chains in buffer 1, 2, 3, and 4 extracts from adult rat brain.**
(*from deepa et al., 2006*[185])

	Buffer 1 extract	Buffer 2 extract	Buffer 3 extract	Buffer 4 extract
		nmol/g brain		
ΔDi-0S[a]	2.51 (3.6%)	1.29 (6.6%)	0.39 (6.8%)	0.13 (10.4%)
ΔDi-6S	1.57 (2.3%)	0.54 (2.8%)	0.22 (3.9%)	0.06 (4.9%)
ΔDi-4S	62.90 (91.2%)	16.97 (87.0%)	4.87 (85.5%)	1.03 (80.6%)
$\Delta Di\text{-}diS_D$	0.45 (0.7%)	0.15 (0.8%)	0.06 (1.0%)	0.02 (1.2%)
$\Delta Di\text{-}diS_B$	0.48 (0.7%)	0.10 (0.5%)	0.03 (0.6%)	0.01 (0.8%)
$\Delta Di\text{-}diS_E$	0.98 (1.4%)	0.43 (2.2%)	0.13 (2.3%)	0.03 (2.1%)
ΔDi-TriS	0.06 (0.1%)	0.02 (0.1%)	ND[b]	ND
Total disaccharides	68.95 (72.3%)[c]	19.50 (20.4%)	5.7 (5.9%)	1.28 (1.3%)
Sulfation degree[d]	0.99	0.97	0.97	0.94

[a]ΔDi-0S, ΔHexUA-GalNAc; ΔDi-6S, ΔHexUA-GalNAc (6-O-Sulphate); ΔDi-4S, ΔHexUA-GalNAc (4-O-Sulphate); ΔDi-diSD, ΔHexUA (2-O-Sulphate)-GalNAc (6-O-Sulphate); ΔDi-diSB, ΔIdoUA (2-O-Sulphate)-GalNAc (4-O-Sulphate); ΔDi-diSE, ΔHexUA-GalNAc (4,6-O- diSulphate); ΔDi-TriS, ΔHexUA (2-O-Sulphate)-GalNAc (4,6-O-Sulphate).
[b]ND, not detected.
[c]The values in parentheses represent the percentage of disaccharides in the four extracts, taking the sum of CS/DS disaccharides found in all four extracts as 100%.
[d]Sulphation degree was calculated as the average number of sulphate groups per disaccharide unit.

CS expression is upregulated in damaged CNS. Moreover, changes in sulphation pattern are observed. Indeed, the sulfotransferase C6ST as well as its product CS-C are upregulated in glial types around cortical injuries in mammalian model. CS-E units are the first motif upregulated after CNS injury **(Table 9)**. In addition, CS-C units are enriched in oligodendrocytes, oligodendrocyte precursors cells and astrocytes cell lines (A7 and Neu7) which are inhibitory for axon regeneration[88]. Interestingly Neu7 astrocytic cell line, the most

inhibitory for axon regeneration[151], contains 7.5% of CS-E units[88]. Furthermore, CS-E units are reported to be upregulated (17% of total CS, analysed in fluorophore-assisted carbohydrate electrophoresis: FACE) in glial scar of injured cortex analysed at day 30 post injury, while this sulphation is not detectable in normal cortex[191]. These CS-E units, on one hand, are inhibitory of neurites extension, induce growth cone collapse and repel axons of embryonic day E7[192] and E9[191] chick DRG neurons in culture in dose-dependent manner, while CS-A and CS-C do not affect neurites outgrowth even when used at concentration 100 times higher than CS-E. This suggests the importance of sulphation pattern rather than high overall negative charges[192]. CS-E could mediate its inhibition through transmembrane protein tyrosine phosphatase PTPσ[192]. Treatment of mice displaying an optic nerve crush injury, which upregulates CS-E expression around the lesion site, with an antibody directed against CS-E promotes axon regeneration[192]. On the other hand, CS-E promotes neurites outgrowth of E16 mouse hippocampal neurons[193]. Moreover, CS-E synthetic tetrasaccharide stimulates the outgrowth of hippocampal neurons neuons[181]. CS-E mediates neurites outgrowth *via* its interaction with contactin-1, a cell adhesion molecule (CAM)[194]. Furthermore, CS-E with CS-B appear to promote proliferation of neural stem cells *via* FGF-2 at E14[195]. CS-E may play different roles according to the surrounding environment.

Table 9 : CS-GAG proportions: changes with brain cortex lesion of adult rat.
Analyses were performed 4, 7 and 14 days post-injury. Control consist in GAG of non-injured hemisphere (*from Properzi et al., 2005*[88]).

Disaccharide components	Control	Day 4	Day 7	Day 14
di-0S	11.2	14.5	10.6	9.2
di-6S	2.4	3.8	4.5	3.7
di-4S	83	78	81	84
di-SD	0.9	0.7	1.2	0.8
di-SE	2.2	3.1	2.8	2.4
(Total GlcA in pmol/mg dry tissue)	(350)	(364)	(454)	(447)

CS expression profile is analysed in goldfish spinal cord lesion model in which descending axons regenerate beyond the lesion to connect with distal spinal neurons. CS-A-positive PNN is maintained after the lesion, while CS-C-positive PNN population decreases

progressively. Moreover, the regeneration of descending axons occurs preferentially on neurons not enwrapped with CS-C-positive PNN, suggesting the inhibitory role on formation of new contacts[196].

Sulphation pattern over the brain is heterogeneous. Labelling of mouse cerebral cortex and cerebellum with an antibody against CS-D units (MO-225) has revealed a differential expression of CS. In addition, it has showed a differential expression of CS-D units which are enriched in the cerebellum **(Figure 32)**. These results are confirmed by disaccharide composition analysis[197]. This is consistent with the upregulation of UST (responsible for the synthesis of CS-D units) during development[188]. Analyses of sulfotransferases, responsible of disulphated CS (GalNAc4S-6ST, UST and D4ST), expression in different cell population: granule cells, Purkinje cells and inhibitory interneurons in cerebellum mouse shows a great inter-diversity between cell population and intra-diversity according the stage of development[188].

Figure 32: Immunohistochemical localization of chondroitin sulphate-D in the developing mouse brain after birth.
Sagittal sections from P7 mouse brains were stained immunohistochemically MO-225 monoclonal antibodies. The staining varies between cerebral cortex (Cx) and cerebellum (Ce) (*modified from Maeda et al., 2003*[197]*).*

3.6.2 Role of chondroitin sulphate in the CNS

CSs in the CNS have drawn attention of neurobiologists, since the observation that their digestion using ChABC promotes the persistence of plasticity in adulhood[121] and allows regeneration of axons following SCI[198]. This highlights the CS part importance of the CSPG in the CNS. Indeed, ChABC treatment highlighted plethora roles of CSs in the CNS. CS are

involved in the guidance of axons by repulsion in the optic chiasm of mouse embryo[199]. Furthermore, neural pathfinding is sulphation-dependent. Hippocampal cells growing on different sulphated CS chains show a preference to CS-A, CS-B and CS-E, but ovoid CS-C substrate. This indicates the variation in sulphation pattern contributes to the pathfinding of neurons[200]. CSs are also required for early embryonic cell devision[169]. CS-D units enriched in the cerebellum retains pleiotrophin, growth factor promoting neurites outgrowth, around Purkinje cells and could be required for pleitrophin signaling[201]. During embryogenesis, CS-E units appears to have a positive role on neural cell proliferation[195] and neurites outgrowth of hippocampal neurons[181 193]. Several studies used synthetic CS-E tetrasaccharide as a substrate for hippocampal and dopaminergic culture[181 202]. CS-E tetrasaccharide promotes neurites outgrowth of these neurons through midkine, pleiotrophin, tyrosine phosphatase ζ and brain-derived neurotrophic factor (BDNF) pathways followed by activation of phospholipase C (PLC) pathways[202], while the disaccharide or unsulphated tetrasaccharide have no effect, suggesting thus tetrasaccharide is the minimal required motif to promote the neurite outgrowth[202]. Synthetic oligosaccharides allow analysis of any sulphation pattern effect. In addition, oligosaccharide could be a promising therapeutic approach in the CNS. Some roles of the sulphation pattern on neurons are summarized in **Table 10.**

Table 10: **Influence of CS variants on neuronal growth and guidance.**
(*from Swarup et al., 2013*[200])

CS variant	sulfation or disulfation	observed effect on neurons
CS-A	4S	presented negative guidance and growth cues to cerebellar granule neurons
CSA/CSB/CSE	4S	stimulated neurosphere formation in EGF dependent mouse embryonic neuronal stem cells
CS-B/CS-D/CS-E	4S	CS-B and CS-E significantly promoted FGF-2 mediated cell proliferation. CS-D led to a slight increase in proliferation
CS-E/CS-B	4S	interacts with pleiotrophin; promoted neurite outgrowth in hippocampal neurons by interacting with pleiotrophin
CS-C	6S	expressed in barrier tissues to axons in avian embryo; upregulated after CNS injury; up regulation was associated to axonal regeneration in nigrostriatal axons of mice; resulted in schwann cell motility
CS-D/CS-E	2S,4S or 4S,6S	promoted growth in embryonic rat hippocampal neurons
CS-E	4S,6S	stimulated outgrowth in neurons by binding to several CNS growth factors; assembled neurtophin-Trk complex; inhibited rat cortical cell binding by interacting with midkine, inhibited hippocampal neurons

In some cases, it is not obvious to assign a role for CS alone, since it is a part of PG molecule. Moreover, their enzymatic digestion highlights partially their importance, as it is

discussed before, chondroitinases can act on HA which is present in all matrices, thus resulted consequences could due to the HA digestion. To overcome the effect of chondroitinases on HA and since the ChABC digestion is not complete by leaving an inhibitory "stub" carbohydrate behind, a DNA enzyme targeting mRNA of XylT-1 (involved in the first step of linkage region biosynthesis) was designed. Its application on injured mouse spinal cord reduces CS amounts in the lesion and improves axon regeneration[203]. However, CS and HS share the same linkage region, hence this DNA enzyme inhibits the HS synthesis as well. Thus, HS may be involved. Furthermore, mutation of CS biosynthesis enzymes is not a better way, since some enzymes are redundant. In addition, since one motif into CS chain can bind to several proteins, mutation of one enzyme responsible for a specific sulphation will affect the interaction with numerous proteins involved in different mechanisms, hence difficulties in evaluating the role.

CSs, thanks to their structure and negatives charges, are involved in most of physical roles of ECM and especially of PNN. However, their importance and involvement in regulation of the functional mechanisms is mainly due to their specific interaction and with a high affinity with signalling molecules regulating different processes in developing and adult CNS. Indeed, CS interacts with growth factors crucial for the neural cells survival, proliferation and differentiation, with receptors involved in axonal outgrowth and guidance, with adhesion molecules and finally with guidance protein such as Sema3A. Indeed, Sema3A accumulates in PNNs *via* its interaction with CS-E motifs[204]. In a review published in 2017 **(Appendix 1)**, we described most of proteins found interacting with CSs in the CNS[205] in developing and adult brain, in physiological and pathological conditions. Specific motifs on both protein and CS are involved in the interaction[205]. Multiple consensus sequences basic a.a rich, linked by a peptide bond or approximated by the secondary and tertiary structure, are found on the protein binding GAG: XBBXBX, XBBBXXBX and XBBBXXBBBXXBBX where B is a basic residue and X is a hydropathic residue. These proteins bind selectively to different CS motifs. A specific binding motif is required for the interaction to take place[205]. For example, Otx2 involved in PNN formation and plasticity binds selectively to CS-E and CS-D motif *via* specific R and K-rich sequence: RKQRRER[159]. Interestingly, such sequence is also found in Sema3A RKQRRQR [708-714]. This specificity of CS-interaction is mainly due to the spatiotemporal variation of CS sulphation pattern. Although, epimerization, length and number of chains, and especially the distribution of the sulphated motif over the chain are less investigated but should be considered as being important in CS functions.

4. Semaphorins and their receptors

Sema3A belongs to semaphorin (Sema) family. The name "semaphorin" is derived from "semaphore", which refers to a method of visual signalling with lights or flags used in maritime and rail transportation. Semaphorin members are secreted, transmembrane or GPI-linked proteins. They all share a "Sema domain" of approximately 500 a.a in their N-ter[206]. The first semaphorin member is discovered in 1992 in Grasshopper embryo axons and it is referred fasciclin IV (Sema I later). It is a transmembrane repulsive guidance protein[207]. Indeed, it is believed that the guidance of the growth cone can be achieved by a repulsive signal during development and also in damaged adult CNS. One year later, the first vertebrate semaphorin is reported in chick brain and referred as a "collapsin" since it induces the collapse of the neuronal growth cone *in vitro* (Sema D, Sem D or Sema3A in mammals)[208]. It is described as a 100 kDa secreted glycoprotein with an immunoglobulin (Ig)-like domain and highly basic regions in its C-ter and N-ter sharing similitudes with fasciclin IV. Collapsin is responsible for the repulsive guidance cues in chick[208]. Then, semaphorin family began to expand by the identification of other members such as Sema II in drosophila, viral Sema[209] and five members of mammalian Sema (Sem A-Sem E), where most of them share the Ig-like domain[210]. Sem F and Sem G were later characterized and confirmed that they do not contain Ig-like domain but a thrombospondin motif known to promote neurites outgrowth suggesting thus Semas can also act as attractive guidance cues[211]. Comparing their sequences showed certain diversity allowed to class them under eight classes. The gene encoding Semas are highly conserved during evolution. Common functions of semaphorin members are targeting the cytoskeleton and modulation of microtubules, and actin polymerization. Semas mainly signal through plexin (Plxn) and its co-receptor neuropilin (Nrp)[206]. Semas were first considered as CNS proteins involved in axon guidance, but their involvement in other physiological processes are reported afterward notably in immune response, angiogenesis, cardiovascular development, bone remodelling and tumour progression[206].

4.1 Semaphorin classes

Semas are a large family of guidance molecules grouped in eight classes and each class is composed of 1 to 8 members. While classes 1 and 2 are invertebrate Semas encoded by 8 genes, classes 3 to 7 are vertebrate Sema (with an exception for Sema 5C found in invertebrates) encoded by 21 genes and the last class are viral Semas[206] **(Figure 33)**. Genes encoding Semas are found dispersed throughout the genome containing several exons.

Diversity of Semas is a result of an alternative splicing[206]. Classes 1, 4, 5 and 6 are transmembrane proteins. Class 7 are GPI-anchored molecules, and Class 2, 3 and viral Semas are soluble[206]. Some members of class 4, 5 and 7 members could be proteolytically cleaved into soluble forms which are biologically active such as Sema4D[212], Sema5B[213] and Sema7A[214]. The N-ter Sema domain is common to all Semas. It is made of seven-bladed β-propeller. It constitutes the principal part interacting with their receptors and thus mediates semaphorin effect[206]. Crystal structure of some members is already solved. Sema3A and Sema4D are the first solved structure in 2003 by *Antipenko et al*.[215] and *Love et al*.[216], respectively. In 2010s, crystal structures of Sema3A, Sema4D, Sema6A and Sema7A ectodomain on their receptors are solved (most of them by Jones's lab)[217] [218] [219]. These structures indicate a homophilic dimerization between Sema domains which seems to be important for Semas function. In addition to sema domain, Semas share another domain which is plexins-semaphorins-integrins (PSI) domain containing a cysteine-rich region forming a knot based on three conserved disulfide bond. PSI domain is so called because it is also found in Plxns and it is homologous to the β chain of integrins. PSI domain appears to couple tightly to the sema domain. Ig-like domain is found only in some classes: 2, 3, 4 and 7 and viral at the C-ter to the PSI domains. Interestingly, Sema and PSI domains are also found in the extracellular part of Plxns and MET receptor which is tyrosine kinase receptor for hepatocyte growth factor receptor (HGFR)[220].

Figure 33: The semaphorin family.
Semaphorin protein family (Semas) members are grouped into 8 classes based on their domain structure. Class 1 and 2 Semas and Sema5C are found in invertebrates, Class 3–7 Semas are found in vertebrates and Class V Semas are found in viruses. Plexin receptors, the predominant receptors for Semas, are grouped into 4 classes (A–D) and each plexin receptor class interacts with a particular Sema class or classes to mediate signalling. A number of other membrane-associated receptors and co-receptors are also important for Sema signal transduction. These proteins directly bind Semas and initiate signalling (*e.g.*, integrins), act as ligand binding co-receptors (e.*g.*, Npn1, 2), and/or work as part of multimeric receptor complexes (*e.g.*, RTKs). At least some transmembrane Semas also function as receptors in reverse signalling (*e.g.*, leftward arrows) and participate in *cis* (within the same cell) interactions with plexin receptors (*e.g.*, asterisk). Semi-transparency of Class V semaphorin Ig and PSI domains indicates that these domains are present in some, but not all, viral semaphorins. Sema (semaphorin domain), PSI (plexin-semaphorin-integrin domain), Ig (immunoglobulin domain), Basic (basic domain), PDZ (PDZ domain), TSP (Thrombospondin domain), GPI (glycosylphosphatidylinositol linkage), RTK (receptor tyrosine kinase), Npn1 (Neuropilin 1), Npn2 (Neuropilin 2), CAM (cell adhesion molecule) Tim-2 (T-cell Ig and mucin domain containing protein 2), CD72 (B cell differentiation antigen CD72), CLCP1 (CUB, LCCL-homology, Coagulation factor V/VIII homology domains protein 1), TREM2 (Triggering Receptor Expressed on Myeloid Cells 2), DAP12 (DNAX activating protein of 12 kDa) (*from Alto and Terman, 2017*[220]).

4.2 Sema domain

Sema domain is composed of approximately 500 a.a, common to all semaphorin members and also found in Plxns receptors. It constitutes the N-ter which is required for the binding and triggering a signal. Sema domain topology consists in seven blades arrayed sequentially around a central axis and each blade is composed of four anti-parallel β sheets. This arrangement earned him the name of β-propeller. The inner strand of each blade lines the channel at the center of the propeller. The blades are arranged in a locked circle by N-ter β strand completing the C-ter blade **(Figure 34)**. This organization of β-strands provides a high rigidity and stability platform. One of the features of Sema domain revealed by crystal structure is their homodimerization. A two-fold symmetric interface results from an off-center "face-to-face" interaction between the top surfaces of the two propellers **(Figure 34.C)**. However, this dimerization behaviour is not reported for non-semaphorin proteins (Plxns and MET). Furthermore, the dimerization of Sema-Sema is quite specific since variation in the exact composition at the level of individual residues of the interface is reported. This thus excludes the heterodimerization between classes but not within class members. Disruption of the dimerization by point mutation of the residues involved in the dimerization generated monomers. The monomer kept the binding capacity to its Plxn receptor without inducing a signalling pathway, hence the importance of dimerization in biological activity. Crystal structure of Semas revealed also that the stability of Sema dimer is variable between classes *e.g* of Sema3A which has less hydrophobic dimer interface comparing to Sema4D. However, this dimerization can be strengthened by other mechanism(s). Indeed, some classes such as class 3 contain an Ig-like domain which tends to dimerize contributing thus to the stability of the dimerization. Moreover, Sema3s form a covalent dimer by a disulfide bond in their C-ter. At least six independent crystal structures of Sema domain are available and allowed us to gain insight on the mechanism of function of this large family[220 221 222]. However, there is still a lot to know about the other members, if they also share the same similitude or no.

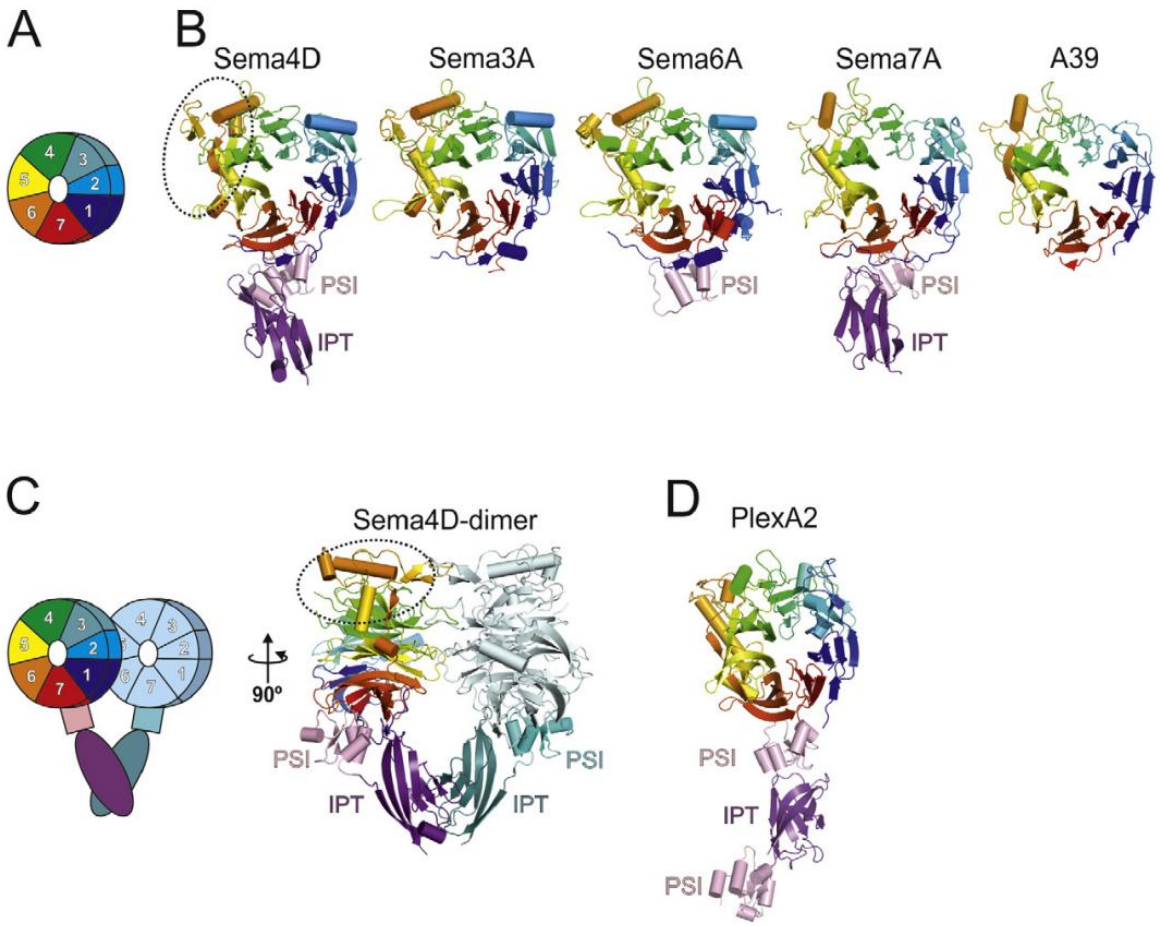

Figure 34: The sema domain: common feature of the extracellular regions of semaphorins and plexins.
(A) Schematic of the sema domain, a seven-blade - propeller. **(B)** Cartoon representation of semaphorin family members. The Sema domain is coloured in rainbow (blue: N-ter, red: C-ter), PSI domains are depicted in light pink, IG-like (or IPT) domains in violet. PDB IDs are as follows: Sema4D: 1OLZ, Sema3A: 1Q47, Sema6A: 3OKW, Sema7A: 3NVQ. **(C)** Schematic (left) and cartoon representation (right) of the Sema4D dimer. Orientation of the right panel is 90◦ rotated around the y axis compared to Figure. 1B left panel. **(D)** Cartoon representation of the PlxnA2 ectodomain (D; PDB ID: 3OKT). Colour-coding is as in (B) (*from Siebold et al., 2013*[222]).

4.3 Semaphorins signalization

As indicated in **Figure 33,** several proteins can bind to Semas and act as receptors or coreceptors. The major known receptors to Semas are Plxns and all Semas are found to interact with them **(Figure 34)**. However, while most of classes bind directly to specific Plxn, class 3 need to bind to Nrp as a coreceptor to signal *via* Plxns[220]. Nrp is the common co-receptor. Here we describe some features of both Plxns and Nrps.

4.3.1 Plexins

The Plxn receptors are grouped in 2 classes in invertebrates: A and B and in 4 classes in vertebrates: Plxn-A 1-4, Plxn-B 1-3, Plxn-C1 and plxn-D1. Plxn molecule is single-pass protein which consists of N-ter ectodomain made of Sema domain, PSI domains (PSI1), IPT (Ig domain shared by Plxns and transcription factors) domains and second PSI (PSI2), a transmembrane segment predicted to be α helical and finally an intracellular C-ter domain which contains guanosine triphosphatase (GTP)ase-activating proteins (GAP) domain[222]. Plxn-B contains PDZ-binding motif[220]. Several crystal structures of the ectodomain are reported for plxnA2 (in complex with Sema6A[218 223] and Sema3A[217]), PlxnB1(in complex with Sema4D)[218] and PlxnC1 (in complex with Sema7A)[219]. Biophysical analysis of these complexes revealed their mechanisms of interaction and signalling. *Janssen et al., 2010* analysed the crystal structure of the complexes: human PLXNB1–SEMA4D and murine PlxnA2-Sema6A. Sema6A and Sema4D are both transmembrane proteins whose dimers bring together two Plxn monomers to allow their dimerization and form a symmetric 2:2 complex and allow a further oligomerization *via* a *cis* interactions of the intracellular domains of Plxns **(upper panel of Figure 34)**. Indeed, the Sema domain of Plxn is not predisposed to dimerization as seen in Sema domain of Semas. However, some regions in the ectodomain of Plxn presents sufficient flexibility enabling it to have *cis* interaction with other Plxns leading to oligomerization **(lower panel of Figure 34)**[218]. The *trans* interaction "head-to-head" between transmembrane Semas and Plxns receptors promotes the signalling in opposing cells. It has also reported that unlike Semas, the PSI1-IPT1-PSI2 segment in PlxnA2 extends away from the sema domain[218].

The binding of Semas to their Plxn receptors induces their dimerization which is required to trigger a signalling cascade by engaging the intracellular part to a Rho GTPase (intracellular small protein binds and hydrolyses GTP to GDP to trigger signal). Crystal structures of Plxn cytoplasmic region have now been obtained for PlxnA3 and PlxnB1[222]. The intracellular part of Plxn consists of ~ 600 a.a organized in two segments (A1 and A2) separated by Rho GTPase-binding domain (RBD) with coiled-coil propensities[222]. A1 and A2 domains form GAP domain for Rap, another member of small GTPases catalysing GTP hydrolysis on Rap[220 224]. The Rap GAP activity of Plxns is regulated by the induced dimerization of Plxns[224]. The intracellular signal could also be triggered by the binding of Rac1, a small Rho GTPase at the RBD of one Plxn and in the same time interacts with an adjacent binding site on a second Plxn, which suggests that the role of Rho GTPase in

clustering Plxn monomers[225]. PlxnA modulates the cytoskeleton for repulsive axon guidance through MICAL1, multidomains protein found in axons and induces oxidation of actin molecules[226]. This could be a mechanism by which the interaction of semaphorin to Plxn affects the cytoskeleton to mediate the guidance.

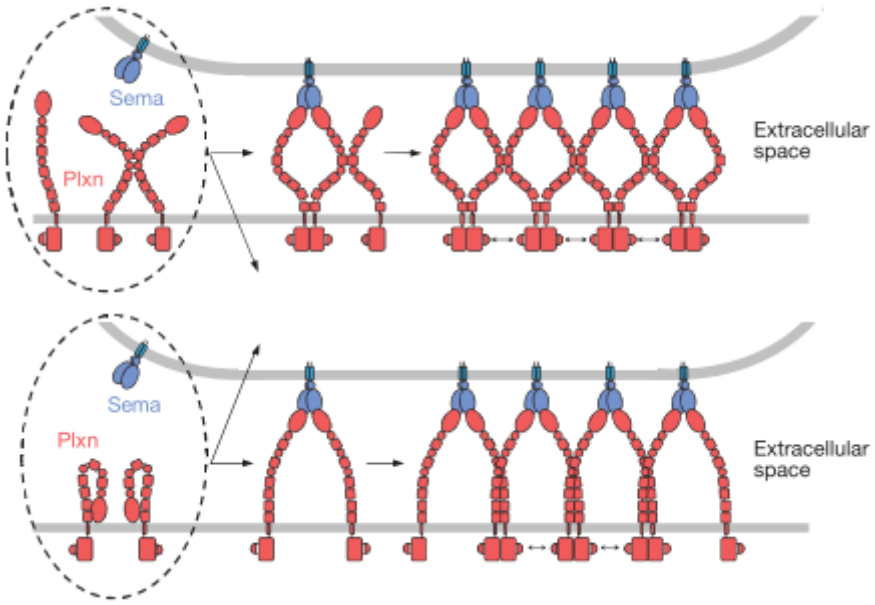

Figure 34: Model for semaphorin-stabilized plexin signalling.
Binding of semaphorin stabilizes plexin dimerization, sufficient plexin ectodomain flexibility may enable plexin-to-plexin *cis* interaction in their membrane-proximal regions (upper panel) and seed further oligomerization. Possibly, dimerization is preceded by a 'switch-blade' conformational change in the plexin ectodomain (lower panel) exposing *cis* interaction sites leading to extracellular clustering. Two types of initial binding events (dotted enclosures) could result in the dimer and cluster architecture of either the upper or lower panel. The precise arrangement of the cytoplasmic region in the active state triggered by extracellular clustering cannot be specified (*from Janssen et al., 2010*[218]).

4.3.2 Neuropilins

Nrp was first postulated as the semaphorin receptors[227]. However, the binding of chicken Sema3A (collapsin-1) to Nrp through its C-ter is not responsible for the specific binding *in situ*, while Sema domain does, suggesting thus Nrp alone is not the functional receptor for Semas[228]. Indeed, the short intracellular domain of Nrp does not allow a signal transduction. Plxns are thus complexed to Nrp to transduce the signal resulted by Sema 3 binding. Nrp is a single-pass transmembrane receptor. Nrp family comprises two members neuropilin 1 and 2 (Nrp1 and Nrp2) which share 44% a.a sequence identity in humans. Nrp ectodomain is made of two CUB (for complement C1r/C1s, Uegf, Bmp1) domains (referred

as a1 and a2 domains) at the N-ter followed by two coagulation factor V/VIII homology-like domains (referred as b1 and b2 domains) and a meprin A5 (MAM) domain (c domain)[220 229 230]. The a2, b1, and b2 domains form a tightly packed core that is only loosely connected to the a1 domain[229]. The MAM domain was first proposed as involved in Nrp1 and Nrp2 homo/hetero dimerization and oligomerization[231]. However, the crystal structure of MAM is solved recently and showed that no evidence for dimerization[230]. Transmembrane part of Nrp is single helix which contains a GXXXG sequence required for Nrp dimerization and oligomerization[232]. The intracellular part consists in a short cytoplasmic tail of 42-44 a.a without a catalytic activity but presents a PDZ binding site for Nrp binding proteins **(Figure 35)**. Nrp1 binds to all class 3 Semas, while Nrp2 binds to Sema3B, Sema3C, Sema3D, Sema3E, and Sema3F but not to Sema3A[233]. Nevertheless, the binding to Nrp1 and Nrp2 is very heterogeneous. Nrp1 preferentially interacts with SEMA3A, SEMA3B, and SEMA3E, whereas Nrp2 has higher affinity for SEMA3F and SEMA3G, but SEMA3C binds both Nrps with similar affinity[234]. Moreover, different Sema3F domains show a differential binding to Nrp1 and Nrp2. The binding of the truncated form, Sema-Ig domain, binds with a higher affinity to Nrp2, while the C-ter basic tail binds effectively to Nrp1 but not Nrp2[231].

In addition to class 3 Semas, Nrps are also coreceptors for proangiogenic factors, including several vascular endothelial growth factors (VEGF) which signal through VEGF receptor (VEGFR). Nrp KO mice are embryonic lethal due to abnormalities in the cardiovascular system and neural vascularization[235 236]. Their implication in angiogenesis makes them also involved in tumorigenesis. They are also involved in the attractive guidance of axons during CNS development[237]. VEGF and Semas are structurally unrelated. While the first two domains a1 and a2 in Nrp are the Sema3s binding site, the b1 and b2 are $VEGF_{165}$ (VEGF isoform resulted from alternative splicing) binding site[229 238 239] **(Figure 35)**. Indeed, the mutation at the N-ter of Nrp-1 affects dramatically the binding of Sema3A, but not $VEGF_{165}$[239]. A soluble form of Nrp1 consisting of only a1/a2 and b1/b2 portions of ectodomain is reported and may act as a natural antagonist for VEGF, promoting thus an antitumor activity[240]. Interestingly, Nrp1, but not Nrp2, can carry a single CS or HS chain at S^{612} (between b2 domain and MAM domain), with CS chain as the more common modification. This Nrp1 GAG modification enhances VEGF binding to Nrp1 and regulates VEGFR protein expression. In addition, this GAG chain could induce the oligomerization of Nrp1 receptor[241]. Further experiments should be performed to characterize in detail the role of this modification notably in the CNS.

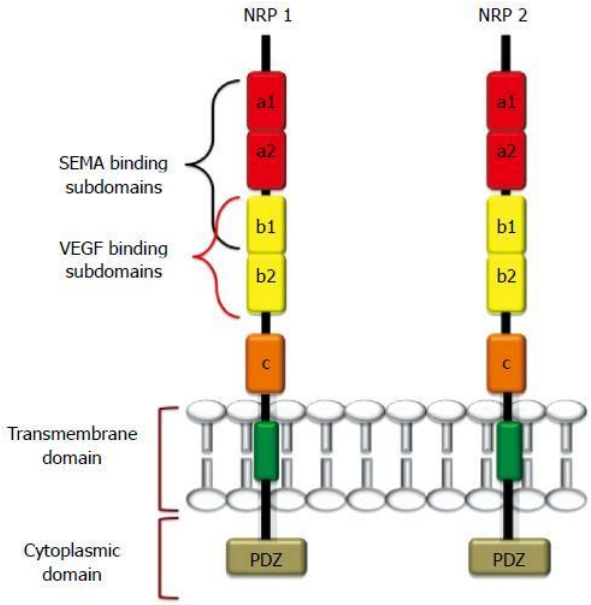

Figure 35: Structure of neuropilin-1 and neuropilin-2.
These proteins contain five extracellular domains, a single-pass transmembrane domain, and a short cytosolic tail that lacks tyrosine kinase activity. SEMA3s bind to the a1/a2/b1 segment, and vascular endothelial growth factors (VEGFs) bind to b1/b2 (*from Elpek, 2015*[242]).

4.4 Semaphorins roles

Semas are involved in physiological and pathological mechanisms during development and in adult[227]. Semas are required for neural circuit assembly in the CNS development and even in the adult. They are considered one of the 4 classes of canonical axon guidance molecules in addition to netrins, ephrins, and slits[220] **(Figure 36)**. During development, axons follow specific paths to reach their corresponding targets in order to establish connections. A mistake in the neural paths and circuits could result in numerous disorders in development or in adult CNS such as autism spectrum disorder and AD[243 244]. The human brain contains about 100 billion of neurons, how can each one of them find its appropriate target neuron is a key question and already been asked more than one century ago by Ramón y Cajal. Indeed, neuronal pathfinding is achieved by several molecular mechanisms consisting mainly in receptors expressed by axons in their growing type, growth cone, responding to the molecular environment. This results in their guidance by attraction or repulsion and a switching between them[245]. The target could be local (short-range guidance) and reached easily by the axon, or it can be distant (long-range guidance) and in this case intermediates targets are required. The role of this intermediate target is not to establish

connections with them but providing a guidance information allowing to continue the path and even to switch from an attractive cue to repulsive cue[246].

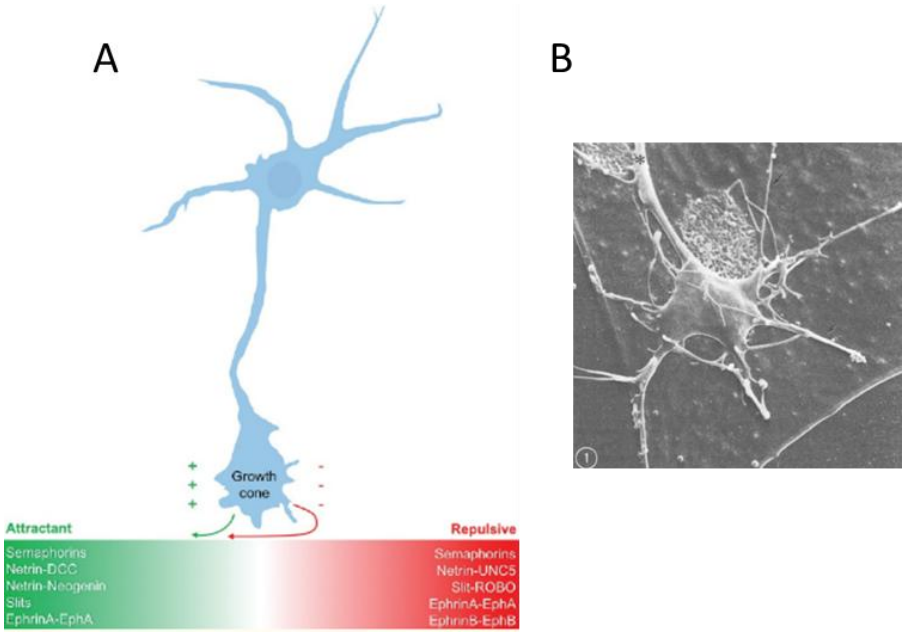

Figure 36: Growth cone guidance.
(A) Schematic representation of growth cone response to classic family of axonal guidance cues: semaphorins, netrins, slits, and ephrins. Guidance cues can trigger an attractant response (green) or a repulsive response (red) in the traveling axonal growth cone (*from Gamboa et al., 2017*[247]). **(B)** Scanning electron micrograph of a growth cone of a sympathetic neuron in culture (*from Landis, 1983*[248]).

Semaphorin molecules signalling through Plxns and Nrps could be either a repulsive or attractive cue, while some of them can be both according to the environment and stage of development such as Sema3E[249], Sema3F[250] and Sema5A. Indeed, Sema5A which is able to interact with CS and HS of PGs through its thrombospondin repeats and elicits either a repulsive or attractive response respectively[251]. Sema5A and other transmembrane Semas such as Sema5B and Sema6A are required for establishment neural circuit formation within mammalian visual system notably retina lamination. Lamination is the biological process by which cells are arranged in layers (stratification) within a tissue during development and governed mainly by migration and axon guidance. Laminated structures in the nervous system include the cerebral cortex, retina and hippocampus. Sema5A and Sema5B are involved in this process by inhibiting retinal neurites outgrowth through PlxnA1 and PlxnA3 receptors and provide a repulsive guidance cue[252]. Sema6A and its receptor plxnA4 trigger also a

repulsive guidance for the correct stratification of neurons[253]. Retinal ganglion cells (RGCs) are initially guided by attraction with netrin-1 then by repulsion with Sema3A. The responsiveness of RGCs to Sema3A is regulated by Nrp1 expression which is in turn upregulated by miRNA[254]. Guidance role of Semas in the developing CNS is also reported for the olfactory system with members of class 3 such as Sema3A[255]. Semas play crucial role in all aspects of neural circuity assembly in the brain.

Semas are also involved in axons guidance in the spinal cord. Sema3A are expressed in the ventral region of the developing spinal cord[210]. Sema3A repulses cutaneous but not proprioceptive axons of sensory neurons, whose their cell bodies are located in DRG, preventing thus their extension to the ventral region during embryogenesis. Indeed *in vitro*, Sema3A acts as a repulsion signal for nerve growth factor (NGF)-induced cutaneous axons but not for neutrophin3 (NT3)-induced proprioceptive axons[256]. DRG belongs to PNS which is located between the dorsal root and the spinal nerve. It contains pseudounipolar sensory neurons that transmit sensory information from the periphery to the CNS **(Figure 37)**. Inhibition of the NGF-induced DRG axonal sprouting by Sema3A through Nrp1 persists in the adult[257]. This is interesting as NGF is upregulated after SCI and induces sprouting of nociceptive axons (sensors of the pain) resulting in chronic pain. Sema3A maintains its inhibitory effect on the sprouting and acts upon sprouting in a dose-dependent manner of NGF. Sema3A could be used therapeutically to attenuate the pain after SCI[258]. Sema3A is also involved in the guidance and correct extension of motor neuron axons during spinal nerve development of the chick embryo[259].

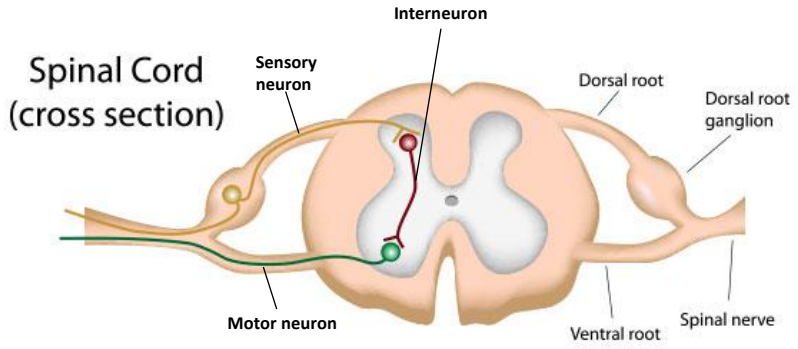

Figure 37: schematic representation of dorsal root ganglion (DRG).
(medical dictionary.thefreedictionary.com).

Semas are also involved in cell migration in the CNS. There are two main types of migration: radial migration consisting in the migration along radial glia and tangential migration consisting in migration independently of radial glia. For example, Sema3A is a chemoattractive cue in radial migration of cortical neurons in developing CNS[260]. Sema4D promotes the migration of cells secreting gonadotropin-releasing hormone (GnRH) originally from the outside the CNS[261]. The role of Semas notably Sema3A as a guidance cue in the CNS development as well as in adult is innumerable and here we have listed only a few main examples.

Semas are related to several neurodegenerative diseases. Sema3A is involved in amyotrophic lateral sclerosis (ALS). ALS is characterized by a progressive loss of motor neurons in the spinal cord and brain. Patients are initially paralyzed, followed by death due to breathing problems. Sema3A might be upregulated within the neuromuscular junction where ALS starts and leads to the repulsion of axons from motor neuron resulting in degeneration[262]. In AD, Sema3A is upregulated and induces growth cone collapse resulting again in neurodegeneration. Moreover, Sema3A enhances the phosphorylation of collapsin-response mediator protein-2 (CRMP-2), belonging to Sema3A signalling pathway which induces the growth cone collapse. Indeed, CRMP-2 is found upregulated in AD[262]. Involvement of other members is also reported such as Sema5A in Parkinson disease; Sema3A, Sema3F, Sema4A, Sema4D, Sema6D and Sema7A in multiple sclerosis[262].

Semas and their receptors have a multitude of roles outside the CNS. Semas are involved in immune system regulation. Sema4D is the first characterized member with immunoregulatory function. Sema4D and other members including Sema3A, Sema4A, Sema6C, Sema6D and Sema7A enhance the activation of B-cells, T-cells and dendritic cells[263]. Semas play also an important role in bone homeostasis. Osteoblasts and osteoclasts are the two types of bone cells found in bone tissue. Osteoblasts are responsible for bone tissue formation, while osteoclasts are responsible in breakdown of bone tissue. Sema4D derived from osteoclast inhibits the differentiation of osteoblasts[264], while Sema3A, mainly expressed in osteoblasts, inhibits osteoclasts differentiation[265], thus maintaining the bone homeostasis. As mentioned above Semas notably Sema3A are involved in angiogenesis. VEGFs family are the major angiogenesis regulators. It has been hypothesised that Sema3A competes with VEGF in binding to Nrp1 in order to inhibit VEGF-induced angiogenesis[266]. Indeed, it was shown recently that Sema3A is able to partially reverse the VEGF effects *via*

binding to Nrp1[267]. However, Semas and VEGF have different binding sites on Nrp1. This leads to the suggestion that Sema3A may also activate its own signalling pathway independent of VEGF. Other members such as Sema3E, Sema3F and Sema4D are also involved in angiogenesis modulation[266]. Furthermore, Semas affect several mechanisms in tumour progression including tumour angiogenesis. While some Sema members display pro-angiogenic and pro-tumorigenic effects (Sema4D, Sema5A and Sema6D), class 3 Semas show antiangiogenic and antitumorigenic properties (Sema3A, Sema3B, Sema3F and Sema3E), both *in vitro* and *in vivo*, and by several mechanisms which trigger apoptosis in endothelial cells[268].

4.5 Semaphorin 3A

Sema3A, the first vertebrate semaphorin, is a one of the best characterized member of semaphorin family. Since its discovery, the numbers of studies reporting its involvement in different vital processes steadily increased. However, the mechanisms of its signalling notably in the CNS are not yet completely elucidated. Sema3A is a secreted covalent dimer of two ~90 kDa (86.5 kDa without post-translational modifications) monomers. Similar to other class 3 members, Sema3A monomer is composed of a Sema domain, a PSI domain, an Ig-like domain and a C-ter basic tail **(figure 38)**. Sema3A is most known for its role as a chemorepulsive cue and inhibitor of the growth cone in the CNS. However, as described below, it is involved in other different mechanisms in or outside the CNS notably as anti-angiogenesis.

4.5.1 Semaphorin 3A activity

Sema3A is naturally cleaved by a ubiquitous protease called furin. Sema3A monomer has two furin-cleavage sites KRRRTRR at amino acid 535 and KKGRNRR at amino acid 741. Complete cleavage of Sema3A by furin could results in three peptides with theoretical MWs of 60.8 kDa (N-ter domain of 65 kDa after post translational modifications), 24.4 kDa and 1.3 kDa[269] **(Figure 38)**. This process occurs *in vivo* as well as *in vitro* during the recombinant expression of Sema3A. Furin is a ubiquitous subtilisin-like proprotein convertase (PPC) belonging to Ca^{2+}-dependent serine protease family which cleaves preferentially upstream of a consensus sequence "R-X-K/R-R". It is the major processing enzyme of the secretory pathway and is mainly localized in the *trans*-Golgi network but can be found on the cell surface. It cleaves precursors of many functional proteins such as enzymes[269 270 271 272].

Class 3 Semas have two highly conserved sequences for furin or related PPC. The most known study on the activity of Sema3A cleaved by furin is realized by Adams *et al.1997*[269]. In this study, it was suggested that Sema3A undergoes a differential proteolytic processing which determines the magnitude of its repulsive activity. In the suggested model, Sema3A is synthetized as a precursor with limited chemorepulsion activity, it undergoes a first cleavage at the second furin cleavage site (release the 1.3 kDa peptide) to acquire the maximum of its activity and finally inactivated by the cleavage in the first furin-cleavage site (release the N-ter domain of 65 kDa)[269]. In addition, in this study they performed several mutations, and the one at the first furin-cleavage site (R532A and R535A) prevents the cleavage. This is the most used mutation to prevent the furin-cleavage of Sema3A and it even used in commercial Sema3A[269]. Sema3A activity is also dependant of its covalent dimerization. The disulfide bond at C^{703} in the C-ter allows a covalent dimerization of Sema3A. Mutation of C^{703} to A results in Sema3A monomer and abolishes repulsion activity[273].

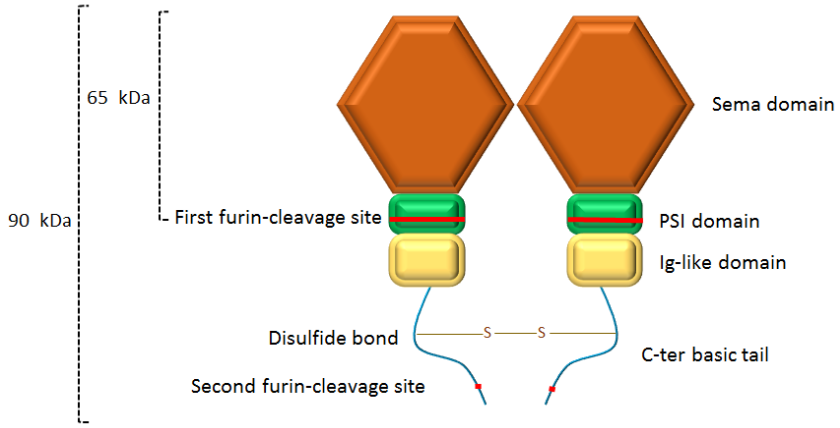

Figure 38: Schematic diagram of semaphorin 3A structure.
Sema3A is made of Sema domain, PSI (plexin-semaphorin-integrin) domain, Ig (immunoglobulin)-like domain and C-ter basic tail. It is a covalent dimer (90 kDa X 2) with one disulfide bond at C^{703}. Sema3A contains two furin cleavage sites in PSI domain and in C-ter basic tail. It is thus physiologically cleaved by this protease. The cleavage at the first site releases the N-ter domain of 65 kDa.

4.5.2 Semaphorin 3A structure

Sema3A domains are characterized as early as its discovery in chick brain. Its cloning revealed the presence of the conserved N-ter Sema domain of 500 a.a, Ig-like domain and C-ter basic tail[208]. The first crystal structure of Sema domain is reported for Sema3A in 2003 at 2.8 Å resolution[215] **(Figure 39.A)**. In this study, only the Sema domain and a part of PSI

(Sema3A-65: 26-546 a.a residues) are expressed in insect cells using the baculovirus system and its binding to Nrp1 was analysed. Interestingly, Sema3A-65 interacts very weakly to a1a2 or b1b2 of Nrp1 alone comparing to Nrp1 (a1a2/b1b2). As described above Sema domain adopts a seven-bladed β-propeller structure with approximate dimensions of 60 X 40 X 45 Å. Each blade is constituted of ~ 70 a.a arranged in a secondary structure. For example, the first strand and first helix of the first blade (1S1 and 1h1, respectively), the second blade has two inserted helices (2H1 and 2H2), the fourth blade has an extra helix (4H1), and the fifth blade has the largest insertion composed of three helices (5H1, 5H2, and 5H3) and two strands (5S5 and 5S6). This domain is also characterized by some very long loops connecting the secondary structures. The shape of central tunnel is slightly conical with the top face defined by the N-ter part and the bottom face determined by the C-ter part. To lock the circle, Sema domain use "loop and hook" system with its N-ter. The 3D structure of Sema domain is stabilized by four disulfide bonds (C^{103} - C^{114}, C^{132} - C^{44}, C^{269} - $C^{381}$and C^{293} - C^{341}). The identified post-translational modification consists in glycosylation (N-acetyl-β-D-glucosamine) at N^{53} and N^{125}. Residues 515-568 corresponding to PSI part are not well ordered, thus not included in the Sema model[215].

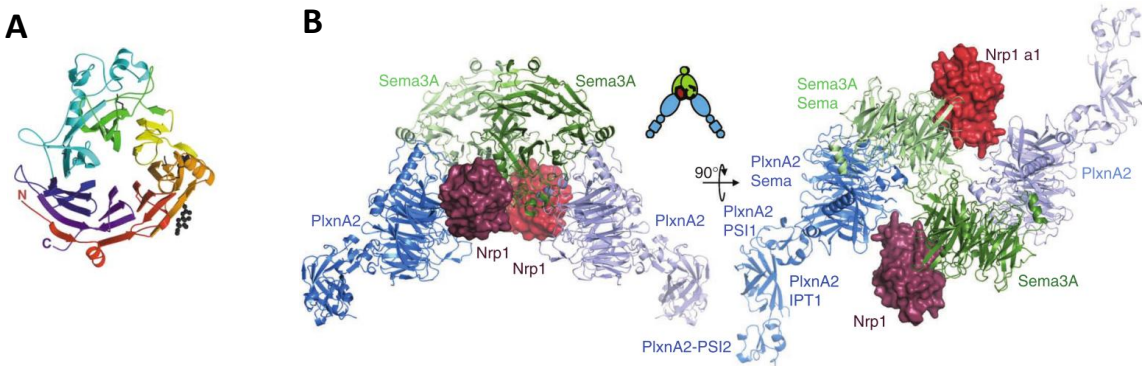

Figure 39: Crystal structure of Sema3A and Sema3A in complex with Neuropilin1 and plexinA1.
(**A)** The structure of Sema3A-65K viewed from the "top" face of the molecule. The disulfide bonds and the N-acetyl-β-D-glucosamine moieties are coloured in grey (*from Antipenko et al., 2003*[215]). **(B)** The Sema3A PlxnA2–Nrp1 complex, with Sema3A and PlxnA2 in ribbon representation, Nrp1 in surface representation and a schematic drawing (middle) (PDB 3OKY) (*from Janssen et al., 2012*[217]).

This Sema3A-65 is found as a noncovalent homodimer (K_D=3 µM). Homodimer interface contains ~ 40% of hydrophobic residues. The dimer breaks down into monomers in order to bind to the soluble Nrp1 (a1a2/b1b2) (K_D= 0.23 µM) to form 1:1 complex. Deletion of residues 252-260 corresponding to strand 3 and 4 of the fourth blade or deletion of residues

359-366 corresponding to the stand 5 and 6 of the sixth blade prevent the dimerization of Sema3A-65. These deletions do not affect the correct folding of the protein, but affect Nrp1 binding and Sema3A activity[215]. From these data and previously published work, they constitute a model for Sema3A signalling initiation **(Figure 40)**.

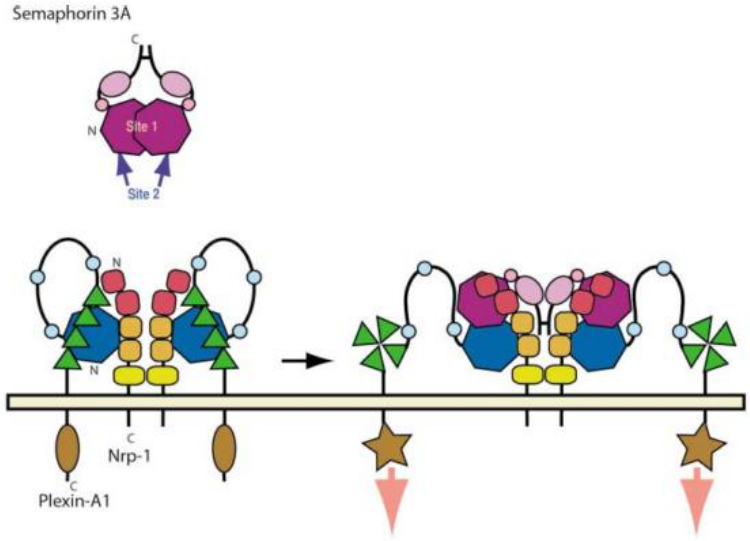

Figure 40: Model for Semaphorin 3A Signalling complex.
Initiation of Sema3A-mediated signalling *via* the Nrp-1/Plexin-A1 complex. Sema3A is in magenta (Sema domain, heptagon; PSI domain, circle; Ig domain, oval). In plexin, the Sema domain is in dark blue, the IPT domains in green, and the PSI regions in light blue. The intracellular Plexin domain is in brown, and the star corresponds to the activated form (the red arrow indicates signalling directing growth cone collapse). In Nrp-1, the A1 and A2 domains are in red, B1 and B2 are in orange, and the MAM domain is in yellow. Sema3A binding results in a 2:2:2 ligand/receptor/coreceptor complex formation and the release of the plexin membrane-proximal extracellular region, which in the absence of constrains adopts an active conformation (right panel) (*from Antipenko et al., 2003*[215]).

The binding of the ligand to its receptor(s) constitutes the first step of signalling. Crystal structure of Sema3A complexed to Nrp1 and PlxnA2 is reported. Different length of Sema3A (residues 21-555) and soluble part of Nrp1 (residues 22-586) and PlxnA2 (residues 35-703) were expressed in HEK293-F. The interaction between different components of the ternary complex was analysed in surface plasmon resonance (SPR) separately. Sema3A does not interact with PlxnA2, while it interacts with Nrp1. Nrp1 interacts with PlxnA2 in the absence of Sema3A. The crystal structure is defined for the ternary complex Sema3A, Nrp1 and Plxn2A **(Figure 39.B)**. This structure revealed the role of Nrp1 in bridging and stabilizing Sema3A-PlxnA1 interaction. Sema domain of Sema3A interacts with Sema domain of PlxnA2 and this is assembled by Nrp1 a1 domain which serves as cross braces. Complex

formation does not induce conformational changes. They also crystalized the Sema3A (21-675: Sema -PSI-Ig-like domains) with the mutation of the first furin-cleavage site. In addition to Sema domain, PSI domain is ordered and showed a clear electron density, but not the Ig-like domain. In the previous crystal structure of Sema3A (crystal structure of 2003[215] and the one of the ternary complex), the PSI domain is partially present, it is thus disordered[217]. However, the probability that Sema3A binding induces oligomerization of Plxns to trigger a signal is not discussed.

4.5.3 Semaphorin 3A signalling

It was first postulated that Sema3A binds mainly to Nrp1 *via* its C-ter. Indeed, truncated collapsin-1 (chick homologue of Sema3A) containing Ig-basic tail binds to Nrp1 with almost the same affinity as the full length, whereas truncated collapsin-1 missing this part binds very weakly the Nrp-1. Moreover, it was suggested that the positive charges of the basic tail of the Sema3A interacts with the negative charges of MAM domain. However, this fragment (Ig-basic tail) is not enough to trigger a signal[228]. Further study has shown that Sema domain of Sema3A binds to Nrp1 at CUB and MAM domains. Moreover, it was suggested in this study that Sema3A needs another receptor to transduce its signal[274]. Furthermore, structural studies presented above, analysing the interaction of the purified Sema3A-65 kDa (without the C-ter domains) to Nrp1, reported the correct binding of this Sema3A-65 to Nrp1[215 217]. The functional receptor of Semas notably Sema3A was identified as a Plxn family. The first identified Plxn as a functional receptor was for semaphorin virus[275]. In drosophila, two Plxns are identified as receptors for class 1 Semas[276]. Subsequently, plxnA1-Nrp1 complex is characterized as a functional receptor for Sema3A. PlxnA1 increases the affinity of Nrp1 to Sema3A and the Nrp1 MAM domain is required for Sema3A signalling[277]. Sema3A signals through Plxn A (1-4)[278 279 280 281] and Plxn D1[282] according to the triggered function and the tissue. Sometimes their role is redundant[279]. Taken together, these studies demonstrate that Sema3A binds to Nrp1 and one of the Plxns to induce an intracellular signal *via* the intracellular part of Plxns. Interestingly, plxnA1 is able to induce autoinhibition through its Sema domain. This inhibition is removed with Sema3A-Nrp1[278].

Sema3A is involved in different signalling pathways[283 234] **(Figure 41)**. The most common one is its effect in the reorganization of the cytoskeleton. CRMP-2 is the first identified member to be involved in the growth cone collapse[284]. CRMPs are intracellular

proteins exclusively expressed in the CNS[284 285]. Another partner of CRMP was identified and referred as CRAM for CRMP-associated molecule. It has been proposed that CRMP and CRAM form a ternary complex with an unidentified molecule bearing the protein-tyrosine kinase (PTK) activity[286]. The identity of the PTK molecule is later revealed as Fes tyrosine kinase which interacts with PlexA1. Moreover, Sema3A binding enhances the binding of Fes to PlexA1 and phosphorylation of PlxnA, CRAM and CRMP2[285]. This complex acts on microtubule polymerization. CRMP-2 by itself is able to bind to tubulin and regulates microtubule assembly[287]. Rho GTPase Rac1 is also identified to mediate the collapse induced by Sema3A[288]. Moreover, Plxns have a Rho GTPase-binding domain (RBD)[222]. Fyn (a member of the Src family of nonreceptor tyrosine kinases) and cyclin-dependent kinase 5 (Cdk5) (a member of the serine/threonine kinase) participate also in Sema3A signalling. Fyn interacts with Plex-A2 and phosphorylates Cdk5 to trigger the Sema3A signal and reorganize the cytoskeleton and induce the repulsion[289]. In addition to microtubules, Sema3A leads to depolymerisation of the F-actin and its loss, hence the growth cone collapse[290]. This could be mediated through the subsequent phosphorylation/dephosphorylating of cofilin, highly expressed actin-binding protein in the CNS and induce the actin depolymerisation, by LIM kinase and induce the growth cone collapse.

Phosphatase and tensin homologue deleted on chromosome ten (PTEN), known for its tumour suppressor role, is identified to be involved in Sema3A signalling to control growth cone behaviour. Indeed, the binding of Sema3A activates PTEN which in turn inhibits phosphatidylinositol 3-kinase (PI3K) responsible of phosphorylation, thus inhibition of glycogen synthase kinase-3 (GSK-3). GSK-3 mediates axon elongation, determination and maintenance of axonal identity[291]. Sema3A can induce two types of response: growth cone collapse and retraction. These two responses are mediated by different type of myosin II. Collapse is associated with the movement of myosin IIA, while retraction is associated to myosin IIB[292].

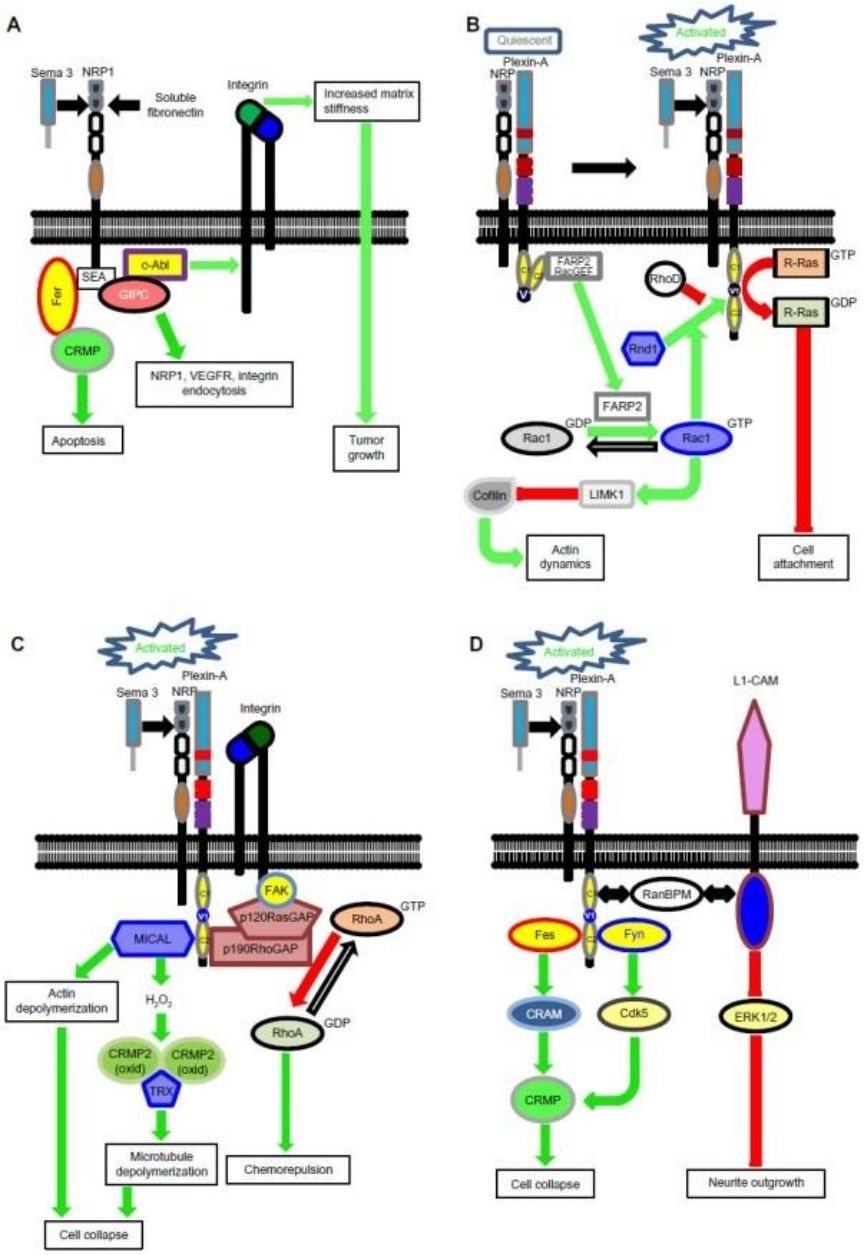

Figure 41: Main signal transduction pathways activated by class 3 semaphorin binding to neuropilins.
Notes: These pathways involve either neuropilin alone **(A)** or neuropilin/plexin receptor complexes **(B–D)**. In the absence of plexins **(A)**, semaphorins can signal through neuropilin interactions with Fer and GIPC, which regulate cell viability, matrix stiffness, and tumour growth. This latter mechanism involves integrin activation by the protein c-Abl. However, class 3 semaphorin function has been mainly described to involve plexins **(B–D)**. In this context, cell migration **(B)** is regulated by the release and activation of the protein FARP2 from the plexin cytoplasmic domain, which leads to the activation of the small G-protein Rac1. In addition, R-Ras is inhibited by interacting with plexin GAP domain, and this inhibition prevents cell adhesion. The binding of the proteins MICAL **(C),** Fes, and Fyn **(D)** to the cytoplasmic domain of plexins affects actin dynamics and induces cell collapse through molecular mechanisms involving CRMPs. Sema 3 binding to neuropilin-plexin complex is also known to promote cell repulsion (or chemorepulsion) **(C)**. This mechanism involves the interaction of a p190RhoGAP-p120RasGAP-FAK complex with plexins and integrins, and inactivates the small G-protein RhoA. Finally, in neural cells **(D),** the protein L1-CAM has been shown to inhibit neurite outgrowth through a mechanism involving interactions of RanBPM with plexins and L1-CAM itself, and inhibition of the MAP kinases ERK1/2 by L1-CAM. Green arrows: activation; red bars: inhibitory mechanisms. Abbreviations: CRAM, CRMP-associated molecule; CRMP, collapsin response mediator proteins; MAP, mitogen-activated protein; MICAL, mono-oxygenase molecule interacting with CasL; NRP, neuropilin; VEGFR, vascular endothelial growth factor receptor; oxid, oxidized (*from Nassar et al., 2014*[234]).

4.5.4 Expression of Semaphorin 3A in the CNS

Sema3A is found concentrated in the PNN and suggested to be one of the mechanisms by which PNN modulates plasticity during and beyond the critical period[130 204] **(Figure 42)**. Expression of Sema3A in the brain is reported in early development, before PNNs formation. It is involved in setting up the neural circuity of the CNS as presented above[259 260]. Sema3A expression persists in the adult CNS[130 293]. Several regions in brain are enriched in Sema3A, cerebral cortex, hippocampus and olfactory system, where Sema3A immunoreactivity varies between different subpopulation of neurons[293]. Immunohistochemistry (IHC) in adult rat brain using antibodies recognizing selectively Sema3A shown that Sema3A staining is colocalized with WFA staining of PNNs, around inhibitory interneurons. In addition, the colocalization of Sema3A staining and other PNN components such as aggrecan, versican, phosphacan and TN-R was observed. These results showed that Sema3A is a component of PNN[293]. Sema3A staining is only observed around cells bearing PNN in the adult CNS. Nevertheless, not all PNNs contain Sema3A[130]. Sema3A is commonly present in PNN enwrapping PV-positive neurons[130].

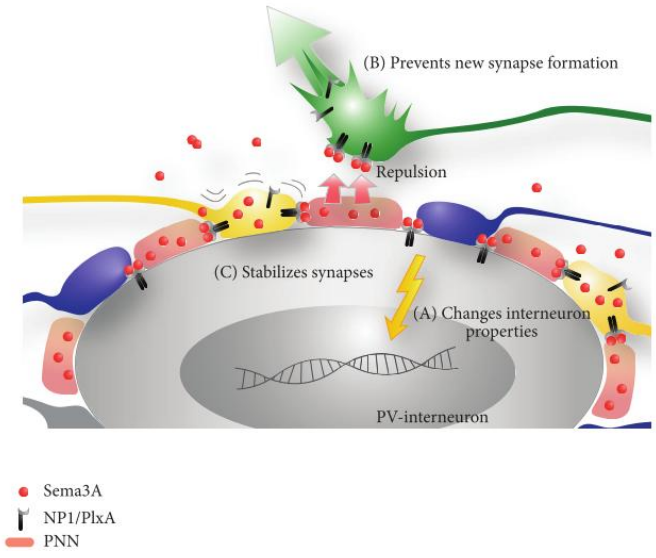

Figure 42: Schematic view of possible roles for Sema3A in PNN related plasticity.
Sema3A protein molecules (red spheres) derived from the more distant cells in the environment, that is, meningeal cell or cells of the choroid plexus, or secreted along axons or by presynaptic terminals (yellow) integrate in the PNN surrounding parvalbumin (PV) positive interneurons. PV-interneurons express Sema3A receptor components (Nrp1/PlxnA) which may trigger an internal response upon Sema3A binding that eventually may change the properties of the PV cell **(A)**. Alternatively, Sema3A may act on (new) presynaptic terminals. Sema3A bound to the PNN may repel growing axons (green) away from the PV cell membrane and thereby prevent the formation of new synapses between PV-interneurons and ingrowing axons **(B)**. Sema3A in the PNN may also "stabilize" synaptic contacts on the PV-interneuron surface by preventing local rearrangements of existing synaptic terminals **(C)** (*from De winter et al., 2016*[130]).

The origin of PNN-Sema3A is not well characterised. Indeed, cells expressing mRNA of Sema3A do not necessarily have Sema3A-positive PNN and vice versa. It was then supposed that Sema3A is produced elsewhere and transported to PNNs[130]. This phenomenon is already seen with Otx2[131], another PNN binding molecule. Moreover, existence of secretory vesicles transporting Sema3A is reported. Punctate distribution is reported for Sema3A at axon and growth cone of immature neurons and at cell body and neurites in more mature neurons[294 295]. Another study supports the existence of vesicle transporting Sema3A. Glioblastoma (highly vascularized brain tumours) releases extracellular vesicles expressing at their surface Sema3A that promotes vascular permeability[296]. It has been hypothesized that Sema is produced by cells in the choroid plexus or the meninges and diffuse over the brain to bind to PNNs as Otx2[130]. Further studies should be performed to elucidate the origin of PNN-Sema3A.

Several studies have reported the upregulation of Sema3A expression in glia scar after CNS trauma due to its high expression in invading fibroblasts and is an inhibitor of axonal regeneration and sprouting, and neuronal plasticity[297 298 299]. Moreover, Sema3A inhibits the differentiation of oligodendrocytes, thus leading to remyelination failure, notably in MS[300]. Sema3A negatively influences immune cells, for example it triggers the apoptosis of macrophages[297]. These place Sema3A as a therapeutic target for CNS recovery.

4.5.6 Semaphorin 3A-glycosaminogan interaction

In addition to Sema3A, its receptors are also expressed by PV-positive neurons of the visual cortex[130]. Hence, the question that Sema3A is found in PNN through the binding to their receptor or retained by other components of PNN. Disruption of PNNs with ChABC removes Sema3A from PNNs[293], suggesting binding to CSs. Moreover, Sema3A displays a high binding to the GAGs isolated from PNNs than any other compartments. Sema3A binds with a high affinity to commercial CS-E chain. It has been postulated that Sema3A accumulates in PNNs *via* its interaction with CS-E motif, enriched in PNNs[204]. Interaction of Sema3A with brain CSs was already reported before. Treatment of neuronal culture with ChABC or GAGs displaces the cell surface Sema3A[295]. Furthermore, IHC and co-immunoprecipitation assay demonstrated that a fraction of total CS binds to Sema3A. Sema3A and CS act together to induce repulsion guidance[301]. It was suggested that Sema3A binds to CSs through its C-ter because of the positive charges of the C-ter tail and negative

charges of the CS. According to this, recently two peptides bearing two different basic sequences of the C-ter basic tail were produced and their binding to GAG was analysed. Both of them interact with GAGs. Besides of this, a peptoid referred semaphorin-induced chemorepulsion inhibitor (SICHI) charged positively at neural pH inhibits selectively the chemorepulsion and growth cone collapse mediated by Sema3A. Interestingly this peptide interferes between Sema3A and GAG, but not between Sema3A and its receptors, suggesting thus the importance of GAG in Sema3A signalling[302 303].

5. Aim of the project

As we can conclude from this introduction, neural ECM notably the PNN, which is responsible in maintaining the plasticity homeostasis in the CNS, contains and recruits a wide variety of molecules with equally important roles. In this project, we are particularly interested in two molecules of different nature. The first molecule is of a GAG nature, CS, and the second molecule is of protein nature, Sema3A. CS, a permeant component of PNN, adapts its sulphation pattern according to spatiotemporal changes of the environment, hence recruits a variety of signalling molecules which participate in inhibition of plasticity and regeneration of neurons mediated by PNNs. Sema3A, which is an important member of a large family of axon guidance proteins, is one of those molecules. Its importance is proven since early development and persists in adult. Indeed, recruiting Sema3A in PNN *via* CS could be one of mechanisms by which PNN inhibits plasticity. The aim of this project is to characterise the interaction interface of CS-Sema3A in the perspective of developing inhibitors of a GAG or a protein nature. The inhibitor(s) could serve against CNS pathology like SCI. Moreover, interaction of Sema3A with CS of Nrp1 or CS of adjacent CSPGs could be involved in the first step of Sema3A signalling *via* its receptors, thus characterising the Sema3A signalling complex in the CNS and the other tissues where Sema3A is involved **(Figure 43)**.

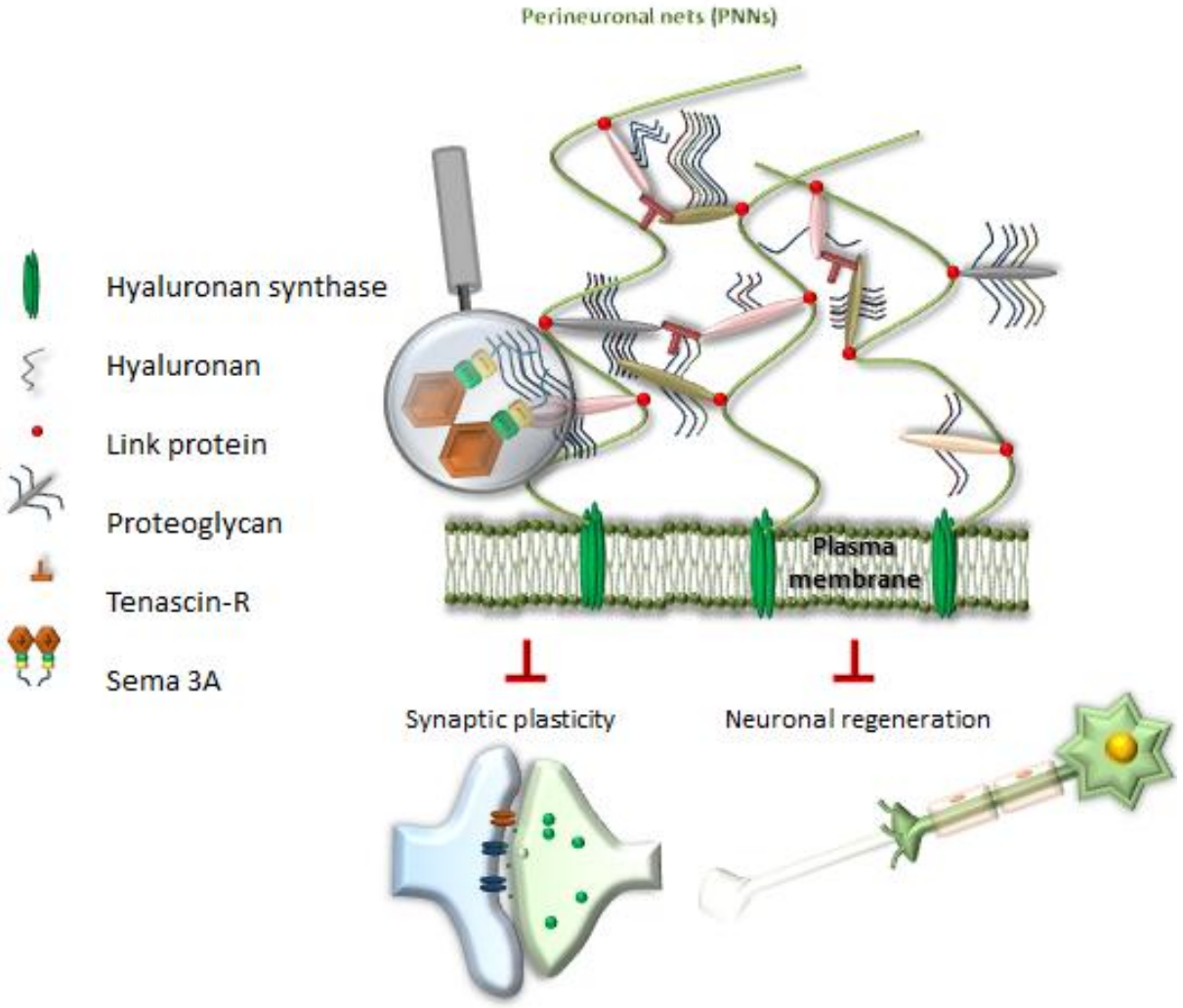

Figure 43 : Schematic representation of the aim of the thesis project.
The aim of the project consists in characterization of chondroitin sulphate (CS: the most abundant sulphated GAG in the CNS, synthetized as a part of proteoglycan) and semaphorin 3A (Sema3A: secreted chemorepulsive protein) interaction in perineuronal nets (PNNs). PNNs (highly organized ECM) are the key regulators of neuronal plasticity and axonal regeneration in the mature CNS. Binding to CS may potentiate Sema3A signalling to regulate the plasticity and regeneration. This could be one of mechanisms by which PNNs regulate the plasticity.

Materials and methods

1. Recombinant semaphorin 3A (Sema3A)

1.1 Sema3A-WT subcloning and expression

Rat Sema3A cDNA was subcloned downstream of CMV5 2xTetO promoter in pTT22SSP4 **(Appendix 2 and Appendix 3)** mammalian expression vector (NRCC, Biotechnology Research Institute) containing a secreted alkaline phosphatase signal peptide and a N-ter 8 x His tag. 250 ml of HEK293-EBNA1-6E (HEK293-6E) cells growing in suspension (NRCC, Biotechnology Research Institute) at 1.5-2 x 10^6 cells/ml were transfected with 250 µg of the recombinant plasmid using 500 µl of 1 µg/µl linear polyethylenimine (PEI, Polysciences, 23966-1). The cells were cultivated in FreeStyle™ F17 Expression Medium (Thermo Fisher scientific, A1383501) supplemented with 4 mM L-glutamine, 0.1% Kolliphor P188 (Sigma, K4894) and 25 µg/ml G418, in a humidified incubator at 37°C with 5% CO_2 under stirring at 120 rpm. 0.5 % Tryptone TN1 (Organotechnie, 19553) was added 24 h post-transfection. One tablet of protease inhibitors cocktail ethylenediaminetetraacetic acid (EDTA)-free (Roche, 5056489001) was added at 1 and 3 days post-transfection to minimise protease degradation of Sema3A. Sema3A expression was followed by collecting 500 µl of cells during 5 days post transfection and was analysed by western blotting using an antibody against the Sema3A domain (1:1000, Abcam, Ab23393). At 4 days post-transfection, where the expression was maximal, cells were collected for protein purification

In some cases, stable Sema3A expressing HEK-6E cell line was obtained by adding 5 µg/ml puromycin 2 day post-transfection and maintaining the selection for 30 days. Dead cells were eliminated by dilution and centrifugation for 3 min at 300 xg.

1.2 Cell clusterisation analysis

100 µl of HEK293-6E cells transfected or not with Sema3A were collected at day 3 post transfection and centrifuged. Cell pellet was washed, resuspended in PBS, deposited on coverslip and left to settle. Coverslips containing cells were mounted on slide and observed in epifluorescence microscope equipped with an interference contrast (DIC) at magnification 20X.

1.3 Sema3A labelling in overexpressing HEK cell

1 ml of Sema3A transfected HEK cells were collected and centrifuged. Cell pellet was washed 2 times in PBS before fixing with 4 % paraformaldehyde (PFA) for 10 min. After PBS washing to remove PFA, cells were permeabilized by incubation 30 min at room temperature (RT) in PBS-0.2 % tritonX-100. No-specific sites were blocked by incubation 30 min at RT in PBS-1% bovine serum albumin (BSA)-1 mM EDTA. Cells were first labelled for 1 h at RT with the primary antibody against the Sema3A domain (Abcam 23393) diluted at 1:1000 in PBS-1% BSA-1mM EDTA. After 3 washes, Cells were incubated 1 h at RT with the secondary goat anti rabbit antibody diluted at 1:2000. After several washes, cells were mounted on slides with ProLong Gold Anti-fading mountant containing 4',6-Diamidino-2-Phenylindole, Dihydrochloride (DAPI). The slides were observed with an epifluorescence microscope (V-M4D, Olympus and Perkin-Elmer) using DAPI and green fluorescent protein (GFP) filters. The images were recorded with 20x magnification and with sCMOS camera (Hamamatsu Orca Flash4, Volocity).

1.4 Sema3A WT purification

Three tablets of protease inhibitors were added to 250 ml of cells 1h before harvesting cells from the incubator. Cells were first centrifuged for 5 min at 300 xg at 4°C (low speed prevents cell damage and cell content release notably proteases). Both supernatant (culture medium) and pellet (cells) were collected. Supernatant which contains Sema3A truncated form was re-centrifuged for 30 min at 6000 xg at 4°C. It was collected and dialysed (3.5 K MWCO) 3 times against 2 L of PBS (10 mM phosphate-150 mM NaCl, pH 7.4). To dissociate Sema3A full-length which remains attached to the cell surface, cell pellet was treated with 20 ml of PBS-1 M NaCl pH 7.2, incubated on ice for 30 min and centrifuged at 3000 xg for 30 min at 4°C and the supernatant was collected. Both supernatants (culture medium and 1M NaCl wash) were subjected to different steps of chromatography.

1.4.1 Nickel-affinity chromatography

Supernatants were loaded separately on 1 ml of Ni-NTA (Nickel-nitrilotriacetic acid) column chromatography (Qiagen, 30210) equilibrated in PBS, pH 7.2. The column was washed with 50 ml of PBS-1 M NaCl, 50 ml of PBS-0.5% triton X-100 and then 50 ml of PBS-25 mM imidazole. Sema3A was eluted with 10 ml of PBS-300 mM imidazole, pH 7.2.

All Ni-NTA chromatography steps were performed in gravity-flow at 4°C and all buffers used here contain protease inhibitors (1 tablet: 50 ml).

1.4.2 Sulpho-Propyl cation exchange chromatography (SP-sepharose)

Eluates of Ni-NTA column were injected at 0.5 ml/min on 1 ml of SP-sepharose (GE Healthcare, 17072901) on AKTA fast protein liquid chromatography (FPLC) system equilibrated in PBS, pH 7.2 at RT. The column was washed with 20 ml of PBS and the protein was eluted with NaCl gradient: 150 mM NaCl-1 M NaCl in 30 min. Fractions of 1 ml were collected and placed immediately at 4°C. Fractions of interest (full length Sema3A) were pooled and centrifuged at a high speed for 5 min and the absorbance at 260 and 280 nm was measured, from which the concentration was calculated. Protein samples were stored at -80°C until use.

1.4.3 Size exclusion chromatography (Superdex 200)

The flow through of SP-sepharose which contains the Sema3A truncated form was concentrated using Millipore Centricon (30 K MWCO) up to 500 µl and injected at 0.5 ml/min over 1 ml loop in 20 ml superdex 200 10/300 GL (GE Healthcare, 17517501) on AKTA FPLC system equilibrated with PBS, pH 7.2. Fractions of 1 ml were collected and placed immediately at 4°C. Fractions of interest were pooled, concentrated and stored at -80°C until use.

To follow the purification, 15 µl were collected at each step, run on SDS-PAGE (10 % acrylamide gel) and stained with InstantBlue protein stain.

1.5 Furin inhibitor-treatment of Sema3A transfected HEK cells

One day post transfection, 100 µM of furin inhibitors "Dcanoyl-R-V-K-R-chloromethylketone" (bachem N1505) were added to the cell culture, in addition to EDTA-free protease inhibitors cocktail. At 2, 3 and 4 days post transfection, an aliquot of culture was centrifuged and the cell pellet was treated with 1 M NaCl to release Sema3A from the cell surface. Both culture medium and cell surface-associated protein were analysed in western blot (WB) with an antibody directed against Sema3A domain.

2. Recombinant Neuropilin1 (Nrp1)

2.1 Nrp1 expression

Recombinant plasmid pCMVi-SV40ori-Nrp1, coding for the expression of the soluble domain of mouse Nrp1 with an Fc and poly-His tag was a gift of Woj Wojtowicz (Addgene plasmid # 72097, **Appendix 4**). 250 ml of Floating HEK293-F at 1.7 – 2 x 10^6 cells/ml were transfected with 250 µg of this recombinant vector using 500 µl of 1 µg/µl linear PEI. The cells were cultivated in FreeStyle™ 293 Expression Medium (Thermo Fisher scientific, 12338-026) in a humidified incubator at 37°C with 5% CO_2 under stirring at 120 rpm. 0.5 % Tryptone TN1 was added 24 h post-transfection. Nrp1 expression was followed by collecting 500 µl of cells during 5 days post transfection and was analysed by WB with an antibody against poly His-horseradish peroxidase (HRP). 4 days post-transfection cells were collected for protein purification.

2.2 Nrp1 purification

Three tablets of protease inhibitors were added 1 h before harvesting cells from the incubator. Floating cells were centrifuged for 5 min at 300 xg and 4°C and the pellet was thrown. The supernatant which contains secreted Nrp1 (protein sequence is **Appendix 5**), was centrifuged again for 30 min at 6000 xg at 4°C and purified using nickel-affinity chromatography (Ni-NTA column). The Ni-NTA column (1 ml, equilibrated in PBS, pH 7.2) was loaded with the supernatant and washed with 50 ml of PBS-1 M NaCl and 50 ml of PBS-25 mM imidazole. Nrp1 was eluted with 10 ml of PBS-300 mM imidazole, pH 7.2. All Ni-NTA chromatography steps were performed in gravity-flow at 4°C. Imidazole of Ni-NTA eluate was removed by a serial dilution in PBS and concentration using Millipore Centricon (30 K MWCO). To follow the purification, 15 µl were collected at each step, run on SDS-PAGE (8 % gel) and stained with InstantBlue protein stain. The absorbance at 260 and 280 nm was measured, to calculate the concentration, in spectrophotometer and the protein was stored at -20°C until use.

2.3 Chondroitinase ABC digestion of Nrp1

95 µl of 4.8 µM purified Nrp1 was treated with 5 µl of 25 U/ml ChABC (Sigma, C3667-10UN) in ChABC buffer containing 50 mM tris HCl-50 mM NaCl-2 mM $CaCl_2$ pH 7.5, ON at 4°C. Control was Nrp1 in ChABC buffer without the enzyme. After treatment, the protein was checked in WB with an antibody directed against poly-His tag.

3. Identification of GAG-binding sites in Sema3A (strategy of "the beads approach")

Identification of GAG-binding sites was performed according to the method published by *Vives et al.* [304] **(Appendix 6)**. 30 µl of Heparin coated beads: HyperD® M (particle size=80 µm, PALL Life Sciences, 20029-062) were washed (suspension in 1 ml of buffer and pelleting by a quick centrifugation in a mini centrifuge) 3 times with PBS before use. This method comprises the following steps:

- Heparin beads activation

Heparin was activated by incubating the beads in 80 µl of 100 mM N-hydroxysuccinimide (NHS) and 80 µl of 400 mM l-ethyl-3-(3-dimethylaminopropyl) carbodiimide (EDC) for 10 min under stirring. Excess of EDC and NHS was removed by 3 washes in PBS. Water soluble-EDC reacts with the carboxylic acid group to form an unstable reactive ester which is stabilised by addition of NHS **(Appendix 7)**.

- Heparin beads-Sema3A crosslinking

Sema3A was then crosslinked to the activated heparin beads. Amine-reactive NHS ester formed in the precedent step reacts with primary amine ($-NH_2$) of lysine or arginine through amine bond **(Appendix 7)**. For that purpose, full length Sema3A, which was stored in high salt conditions (about 700 mM NaCl), was diluted 4 times in HBS-P (10 mM HEPES pH 7.4, 150 mM NaCl and 0.005% v/v Surfactant P20) and incubated 2 h at RT under stirring with the activated heparin beads. 4 batches of protein were used at these final concentrations: 25, 24, 35 and 40 µM which correspond respectively to 86, 108, 189 and 86 µg of protein.

Sema3A truncated form, which was stored in PBS, was directly incubated with the activated heparin beads. 4 batches of protein were used at these concentrations: 1.2 and 4 µM which correspond respectively to 40 and 104 µg of protein.

The reaction was stopped by adding 10% of 1 M tris pH 7.5 and incubating for 10 min at RT. the beads were centrifuged to remove the unbound proteins.

- Sema3A denaturation

The crosslinked protein was denatured by incubation in 1 ml of PBS - 2 M NaCl - 1% tritonX-100 - 6.5 % 2-mercaptoethanol for 15 min at RT under stirring, this step was repeated 2 times without incubation. The beads were then washed with PBS before incubating in PBS-2 M urea for 1 h at 100°C.

- Sema3A digestion with thermolysin

The denatured protein was digested with 2 µl of 1 mg/ml thermolysin in 50 µl of PBS at 50°C overnight (ON) under stirring. Released peptides were removed by washing the beads 3 times with PBS.

An additional denaturation step with PBS - 2 M NaCl - 1% tritonX-100 - 6.5 % 2-mercaptoethanol and thermolysin-digestion were carried out. The beads were washed 5 times with PBS and resuspend in Milli-Q H_2O.

- Heparin-binding site(s) identification

Crosslinked GAG-binding sites were identified by Edman degradation automated N-ter sequencing performed directly on the beads in the protein sequencing platform of IBS, Grenoble.

4. Sema3A mutants

4.1 Sema3A site directed mutagenesis

The GAG-binding sites, as identified by the beads approach and primary a.a sequence analysis (4 potential GAG-binding sites in the C-ter, **Appendix 3**) were mutated individually. Mutations consist in deletion of the whole site or substitution of basic a.a by alanine (A) or serine (S) present in this site **(Table 11)**. Generated mutants were labelled Mut 1, Mut 2, Mut 3 and Mut 4 respectively according to their position starting from N-ter (5'). Double mutant, missing sites 3 and 4, referred as Mut 3/4, was also generated. Mut C consists in the substitution of the cysteine (C), responsible for the disulfide, by a serine (**Table 11)**. Mutations were realized by PCR quick change using pTT22SSP4-Sema3A as a template and phusion hot Start II high-fidelity PCR master mix (ThermoFisher scientific, F565S). PCR conditions were provided as indicated in ThermoFisher data sheet.

Table 11: Generated mutations in Sema3A.

Label	Type of mutation	Initial amino acid sequence	Generated amino acid sequence	Secreted
Mut 1	Deletion	K R R T R R	-	No
Mut 1	Substitution		K **S S** T R R	No
Mut 1	Substitution		K **S S** T **S A**	No
Mut 1	Substitution		**A S S** T **S A**	Yes
Mut 2	Deletion	R R N E D R K	-	No
Mut 2	Substitution		**SA** N E D R K	Yes
Mut 2	Substitution		**SA** N E D **A A**	No
Mut 3	Deletion	K R D R K Q R R Q R	-	Yes
Mut 4	Deletion	K K G R N R R	-	Yes
Mut 3/4	Deletion	K R D R K Q R R Q R …K K G R N R R	x…x -	Yes
Mut C	Substitution	M D E F **C** E Q V W	M D E F **S** E Q V W	Yes

Basic amino acids are shown in red and those underlined represent the realised substitution. "-" represents the deletion.

4.2 Sema3A mutants expression and purification

Mutants were expressed in HEK-6E as Sema3A-WT (see above Sema3A WT expression and purification sections). Not all generated mutated constructs leads to a soluble and secreted protein to be purified. Thus, the purified mutants were:

- Mut 1: substitution of all basic a.a of the site (A S S T S A)
- Mut 2: substitution of 2 basic a.a of the site (SA N E D R K)
- Mut 3: deletion of the site
- Mut 4: deletion of the site
- Mut 3/4: deletion of 2 sites (3 and 4)
- Mut C: substitution of C^{703} by S

5. Rat brain chondroitin sulphates (CSs)

5.1 Rat brain GAGs extraction

Male Sprague Dawley rat 3 months old brains were used to extract GAGs. GAGs were extracted according to the method published by *Kwok et al*.[305] They were stored at -80°C until their use. Extraction lasted five days:

- Day 1: homogenization and dialysis

Four sequential extraction Buffers were prepared freshly from 10x tris buffer saline (TBS) stock solution which can be stored at RT for 1 month: 500 mM tris buffer saline (TBS) and 1.5 M of NaCl in d-H_2O.

- ✓ Buffer 1 (B1, extraction of soluble ECM): TBS 1X +2 mM EDTA. pH was adjusted to 7 with NaOH. This solution was filtered using 0.22 µm filter.
- ✓ Buffer 2 (B2, extraction of membrane-associated molecules): 100 ml of B1 + 500 µl of tritonX-100 (0.5 % v/v).
- ✓ Buffer 3 (B3, extraction of membrane-associated molecules): 100 ml of B1 + 1 M NaCl. This solution was filtered using with 0.22 µm filter. Then, 500 µl of was added.
- ✓ Buffer 4 (B4, extraction of PNNs): 100 ml of B1 + 6 M urea. This solution was filtered using with 0.22 µm filter. Then, 500 µl of TritonX-100 was added.

Two rat brains were thawed out on ice. Then, one brain was cut into small pieces using a scalpel and transferred into the homogenizer. 5 ml of B1 was added. The mixture was homogenized gently one time with homogenizer piston on ice. Then, Pasteur pipettes of decreasing diameter were used to homogenize gently until obtaining a smooth homogenous solution. The second brain was manipulated in the same way. Homogenates of the two brains were pooled and centrifuged at 23000 xg for 20 min at 4°C. The supernatant was collected in 50 ml falcon tube and kept on ice. The pellet was resuspended again in 10 ml of B1 and centrifuged at 23000 xg for 30 min at 4°C. The supernatant was pooled with the previous one. The same steps are followed using B2, B3 and B4. At the end of treatment, four solutions of 20 ml were obtained and dialysed (3.5 K MWCO) against 8 L of 25 mM tris-HCl, 5 mM EDTA, pH 7.8 at 4°C ON. To check that PNNs were extracted with the right buffer (B4), 30 µl of each solution were analysed by WB with an 1 µg/ml of HAPLN1 antibody (*R&D* ,AF2608) in PBS-0.05 % tween 20 -5 % milk.

- Day 2: Pronase treatment

After dialysis, the samples were collected in 50 ml Falcon tubes. Pronase (Sigma, P5147) was added to a final concentration of 2 mg/ml. The digestion was performed at 37°C with shaking, ON.

- Day 3: protein precipitation

After pronase digestion, samples were centrifuged at 23000 xg and 4°C for 15 min and the supernatants were collected. Ice-cold 100 % trichloroacetic acid (TCA) was added to a final concentration of 5% (v/v). Samples were incubated for 1 h on ice. Then, they are centrifuged at 15000 xg and 4°C for 20 min. Supernatants were collected and kept on ice. Pellets were resuspended in 10 ml of ice-cold 5% TCA and centrifuge again at 15000 xg and 4°C for 20 min. supernatants were pooled with the previous ones. This last step was repeated one more time. The acidity resulted from TCA was neutralized after the last centrifugation with 1 M sodium carbonate until pH 7 was reached.

To eliminate fats from the samples, diethyl ether was added to final concentration 50 % and shacked vigorously and settled for 1 min. The upper phase was discarded. This step was repeated until there are no micelles forming in the upper phase (about 5 times). The remaining diethyl ether was evaporated in the fume hood ON.

- Day 4: GAGs precipitation

Sodium acetate and cold absolute ethanol were added to a final concentration of 5 % and 75 % respectively. Samples were incubated ON at 4°C.

- Day 5: GAGs collection

Samples were centrifuged at 2000 xg for 15 min at 4°C. Supernatants were discarded and pellets containing GAGs were air-dried at RT to be resuspended in 300 µl of milli-Q H_2O. The presence of GAGs at the end of extraction was checked in PAGE (20% gel) and azure A staining.

- GAGs quantification

GAGs extracted with each buffer were quantified using cetylpyridinium chloride (CPC) turbidity assay. 1 µl (B1, B2), 2 µl (B3) and 3 µl (B4) of extracted GAGs were diluted in H_2O to a final volume of 25 µl in 96-wells plate in triplicate. CS-A concentrations ranging from 0 to 0.06 µg/ml of H_2O (8 concentrations) were also prepared in triplicate in 96-wells plate to constitute the standard curve. 25 µl of CPC reagent, composed in an equal ratio of 0.2 % CPC and 133 mM $MgCl_2$, was added to each well and mixed. The absorbance was measured at 405 nm in a plate reader spectrophotometer. The quantity of extracted GAGs was calculated from the linear regression equation of CS-A standard.

5.2 Rat brain CSs purification

To purify CS from the GAGs brain, extracted GAG were first treated with 10 mU/ml heparinase I and III (Grampian enzymes, Orkney, UK) in 5 mM tris-50 mM NaCl-2 mM $CaCl_2$-1 mg/ml BSA, pH 7.5 for 5 hours at 30°C. 100 mM sodium acetate-5 mM $MgCl_2$ were added afterward for a digestion with DNaseI (Roche, 10832500) for 15 min at 37°C to remove potential DNA contaminants.

To remove the digestion products, the samples were loaded at 12 ml/h on 2 ml of anion exchange chromatography, diethylaminoethyl (DEAE)-sepharose (GE healthcare, 17-0709-01), equilibrated beforehand with 20 mM phosphate, pH 6.5. The column was washed with 1 column volume of 20 mM phosphate, pH 6.5, then for 2 h (24 ml) with 20 mM phosphate-0.3 M NaCl, pH 6.5. CSs were eluted with 5 ml of 20 mM phosphate-1.5 M NaCl, pH 6.5 and lyophilized. The powder was resuspended in 2 ml of milli-Q H_2O and split in 3 fractions (670 µl). Each fraction was loaded into Sephadex G-25 in PD-10 desalting column (GE healthcare, 17085101) washed with 2 ml of H_2O and CSs were eluted with additional 2.5 ml of H_2O. Eluates of the 3 fractions were pooled and lyophilized again to be resuspended in 500 µl of H_2O.

5.3 Rat brain CSs disaccharides analysis

100 µl of purified CSs were centrifuged using the SpeedVac system to evaporate the H_2O under vacuum and resuspended in 40 µl of milli-Q H_2O. To generate disaccharides units, CSs were digested with 100 mU of ChABC at 37°C for 24 h in 10 µl of buffer containing 50 mM tris HCl-50 mM NaCl-2 mM $CaCl_2$ pH 7.5.

1 µl (B1 and B2) and 2 µl (B3 and B4) of digested CS diluted in 100 µl of milli-Q H_2O were used for the disaccharides analysis using reversed-phase ion-pair high-performance liquid chromatography (RPIP-HPLC). Samples were injected in a Luna 5µm C18 reversed phase column (4.6 × 300 mm, Phenomenex) equilibrated beforehand at 1.1 ml/min for 2 h in 1.2 mM tetra-*N*-butylammonium hydrogen Sulphate -8.5% acetonitrile pH 3. Disaccharides were eluted using multi-steps NaCl gradient: 0–30 mM in 1 min, 30-90 mM in 39 min, 90–228 mM in 2 min, 228 mM for 4 min, 228–300 mM in 2 min, 300 mM for 4 min. Eluted disaccharides underwent a post column derivatization using 0.25% of fluorogenic 2-cyanoacetamide in 0.5% NaOH at 0.35 ml/min flow rate, at 130°C for 4 min. Resulted fluorescent disaccharides were detected by an excitation at 346 nm and emission at 410 nm. The column is calibrated with a mix of CS disaccharide standards (1pmol/µl each): 0S, 4S, 6S, 2S, 6S4S, 4S2S, 6S2S and tri S (Iduron, Alderley Edge, UK) to assign the results peaks.

1 µl of 125 ng/µl commercial CS-E (Amsbio, AMS.CSR-NACS-E2.SQC-10) and CS-D (Seikagaku, 400676) were also analysed by RPIP-HPLC as purified brain CSs.

6. Sema3A-GAGs interaction analysis

6.1 Commercial GAGs biotinylation

Commercial CS-E (30 kDa, Squid cartilage, Amsbio, AMS.CSR-NACS-E2.SQC-10), CS-D (38 kDa, ,Shark cartilage, Seikagaku, 400676), CS-B (porcine intestinal mucosa, Sigma, C3788-25 MG) and HS (12 kDa, porcine intestinal mucosa, Celsus laboratories, Cincinnati Ohio) were biotinylated on their reducing end essentially according to *Saesen et al.*[306]**.** Biotinylation reaction was achieved by reacting 5 mg/ml of GAG with 10 mM of EZ-link Alkoxyamine PEG4-SS-biotin (Thermo Scientific, 26138) in the presence of 20 mM aniline in the coupling buffer (50 mM sodium acetate) in 200 µl of reaction final volume at 37°C ON. Excess of biotin and other reagents were removed by dialysis against water and biotinylation level was estimated by a dot blot as described below in rat brain CS biotinylation section.

6.2 Rat brain CSs biotinylation

400 µl of purified CSs were centrifuged using the SpeedVac system to evaporate the H_2O under vacuum and resuspended in 95 µl of biotinylation buffer (20 mM Hepes-150 mM NaCl, pH 8). 5 µl of 100 mM Sulfo NHS-LC-LC-biotin (Pierce Biotechnology, 21338) was

added to the solution. The reaction was performed during 3 h at room RT. 10 µl of 1 M ethanolamine-HCl, pH 8.5 (to final concentration of 100 mM) was then added and incubated 15 min at RT before dialysis (3.5 K MWCO) 3 times over 24 h against 2 L of milli-Q H_2O to remove excess of biotin and other reagents.

A dot blot was performed to check the efficiency of biotinylation. For this purpose, 10 µl of dialyzed CSs (B1 and B2) and 20 µl (B3 and B4) were diluted in milli-Q H_2O to final volume of 250 µl. Serial dilution (8 dilutions) was carried out (dilutions of 1: 5) for each sample and in the range 0.0003-10 ng/ml for the positive control (biotinylated commercial CS-B; Sigma, C3788). 100 µl/well of each sample was spotted on Nylon transfer membrane (hybond-N+) mounted on dot blot system and pre-equilibrated with TBS (50 mM tris-150 mM NaCl). Two washes were performed afterward with 200 µl of TBS/well. The membrane was incubated first in TBS-5% of skimmed milk for 20 min at 37°C and washed 2 times with TBS to remove the milk. Then, the membrane adsorbed biotin was revealed by incubation with 1:4000 diluted extravidin-peroxidase (Sigma, E2886)-TBS-0.05% tween20 for 1 at RT under shaking. After incubation, the membrane was washed 5 min x 6 in TBS-0.05% tween20 and incubated in 2 ml of Luminata classico western HRP substrate (Millipore, WBLUC0500) for 3 min. Revelation was performed by exposition of the membrane to X-ray film for 30 s and soaking the film in developer bath, water, fixer bath, water (GBX Developer, Fixer and Replenisher - Carestream Dental, 310-1458) in a darkroom.

6.3 Preparation of synthetic, size-defined CS-D and CS-E oligosaccharides

Oligosaccharides used in this study were synthetized in university of Orleans by Chrystel Lopin-Bon. CS-D, CS-E oligosaccharides were prepared from a single disaccharide precursor bearing a benzylidene acetal on the GalN moiety and a naphylmethyl group as aglycon that was prepared by semisynthesis from commercially available chondroitin sulphate polymer. Di, tetra and hexasaccharides were then synthesized after several selective protection and deprotection steps followed by sulphation of hydroxyl group and deprotection as previously described[307]. In some cases, oligosaccharides were biotinylated. For that purpose, 2-benzyloxycarbonylaminoethyl group was introduced on the key disaccharide and after similar steps of selective protection/deprotection, sulphation, biotinylation and deprotection, the biotinylaed oligosaccharides were isolated as described[308].

6.4 Surface Plasmon Resonance (SPR)-based binding assay

SPR analysis were performed using Biacore SPR technology (T3000) on CM4 sensor chips (contains 4 flow cells: FC1-FC4) with HBS-P (10 mM HEPES pH 7.4, 150 mM NaCl and 0.005% v/v Surfactant P20) as a running buffer at 25°C. The surface has a carboxymethylated dextran matrix covalently attached to a gold film. The free carboxyl groups of dextran were activated by 50 µl of 100 mM NHS and 400 mM EDC and then coupled covalently to the primary amine of 80 µg/ml streptavidin (Sigma, S4762) in 10 mM sodium acetate buffer, pH 4.2 which results in 1000 resonance units (RU) of coupled streptavidin. Remaining activated groups were blocked with 50 µl of 1 M ethanolamine hydrochloride-NaOH, pH 8.5.

- GAGs immobilisation

5 µl of biotinylated commercial GAGs (CS-D, CS-E or HS), biotinylated CS-E (di, tetra or hexasaccharide) oligosaccharides and 10 µl of biotinylated rat brain CSs were immobilized separately on the streptavidin-functionalized chip at concentration of 2.5 µg/ml, 1 µM and 10 µg/ml, respectively, in 10 mM Hepes-300 mM NaCl, pH 7.4 and at 10 µl/min flow rate. GAGs immobilization resulted in about 60 (commercial GAGs) and 70 (synthetized oligosaccharides) RU shift. FC1 was left as a negative control. Before injecting protein, 2 washes with HBS containing 2 M NaCl were performed. All solution used were filtered (0.22 µm) and degassed.

- Sema3A binding

Sema3A-WT, commercial Sema3A or mutants were injected in “kinject” mode at 60 µl/min for 5 min (250 µl) with a concentrations range of 0 - 10 nM. Dissociation time of the complex protein-GAG lasted 300 s.

- Regeneration

The GAG surfaces were regenerated with several injections of 250 µl of 2 M NaCl at 60 µl/min. Control sensorgrams were subtracted on line from GAG sensorgrams. The data were analysed by fitting both the association and dissociation phases for each Sema3A concentration to a 1:1 Langmuir model using the biaeval 3.1 software, to determine the

association and dissociation rate constants (k_{on} and k_{off}) from which the affinity ($K_D = k_{off}/k_{on}$) was calculated.

6.5 Quartz Crystal Microbalance with dissipation monitoring (QCM-D) measurement

Q-sense E4 system was used for QCM-D analysis as previously described in *Migliorini et al.*[309] 4 NV (normal volume) flow cells connected *via* tubing to a pump were passivated with 10 mg/ml of BSA at 50 µl/min for 10 min then washed with 2 ml of milli-Q H_2O at 100 µl/min until dry. 4 SiO2 sensors washed beforehand with ethanol and milli-Q H_2O and exposed at least for 30 min to UV light were placed in the flow cells under a continuous flow of HBS (10 mM Hepes-150 mM NaCl, pH 7.4) at 20 µl/min. Before starting measurement, all resonances of each sensor were searched and checked. Once a stable baseline was obtained (30 min after starting running buffer), GAG film formation was carried out in 3 steps:

- Bilayer formation

300 µl of 50 µg/ml dioleoylphosphatidylcholine (DOPC): dioleoylphosphatidyl-ethanolamine (DOPE)-CAP-biotin in a molar ratio 95:5 solution were injected on each sensor at 20 µl/min. Spreading of the lipid vesicles leads to for liposomes formation. Lipid bilayer was washed for at least 10 min with HBS.

- Streptavidin layer formation

300 µl of 20 µg/ml streptavidin (Sigma, S4762) was injected at 20 µl/min through each flow cell. The formed streptavidin layer covered the whole lipid bilayer. It was washed for at least 10 min with HBS.

- GAGs layer formation

Before adding GAGs, running buffer was changed for PBS containing 220 mM NaCl, pH 7.2 and ran for 20 min. 400 µl of 10 µg/ml biotinylated CS-E or CSD, or 200 µl of 10 µg/ml biotinylated HS were then injected at 20 µl/min (until to reach the equilibrium). Formed GAGs film was washed for at least 10 min with the running buffer before injecting the protein. One of the four flow cell was left as a negative control.

- Protein binding

20 µg/ml Sema3A WT, truncated form (65 kDa), Mut1, Mut 2, Mut 3 or Mut 4 were injected at 20 µl/min for 20 min over the assembled film.

Changes in frequency Δf and dissipation ΔD were recorded at six overtones (3, 5, 7, 9, 11 and 13). The data are presented in results by Δf and ΔD of the 3rd overtone since all overtones provide a similar changes. Q-tool software was used to analyse data.

7. Furin cleavage assays

Furin enzyme cleaves Sema3A in 2 specific cleavage sites: KRRTRR and KKGRNRR (on the right of amino acid 535 and 741, respectively) releasing three peptides with theoretical MWs of 65 kDa, 24.4 kDa and 1.3 kDa. To investigate if GAGs protect Sema3A from furin cleavage, 2 assays were performed on the cell expressing Sema3A and on purified Sema3A protein. Furin activity was checked by its ability (4 U) to cleave 0.5 or 100 µM fluorogenic peptide substrate Boc-RVRR-AMC (Ex: 360-380 nm, Em: 440-460 nm; Enzo, ALX-260-040) for incubation time of 0, 1/2, 1, 2.5, 6, 8 and 21 h.

10^6 of stable Sema3A WT expressing HEK-6E cells were centrifuged for 3 min at 300 xg and washed one time with PBS to remove the remaining culture medium. Cell pellet was resuspended in 200 µl of furin buffer (25 Mm tris, pH 7.5 -10 mM CaCl2 - 0.5% Brij-35), 2 µl of 110 ng/µl furin (R&D, 1503-SE-010) were added or no (negative control) and incubated at 37°C for 5 h. 0, 1, 2 and 5 h post-furin treatment, 30 µl of sample was taken, centrifuged for 3 min at 300 xg. Supernatant was collected and cell pellet was treated with PBS-1 M NaCl for 10 min and centrifuged again at high speed for 20 min and the supernatant was collected. WB with an antibody directed against Sema3A N-ter (1:1000, Abcam, Ab23393) was performed to follow the cleavage kinetic.

0.25 µM purified Sema3A WT (4.5 µg=50 pmol) was treated with 2 µl of 110 ng/µl furin (molar ration furin: Sema3A = 1:15) in furin buffer and in the presence or no of 2.5 µM CS-E (16.8 µg) or HS (5.8 µg) (molar ration Sema3A: GAG = 1:10) in 200 µl final reaction volume. Samples were incubated at 37°C for 8h. 30 µl of sample was taken at 0, 1h, 2 h, 5 h and 8 h post-furin treatment, and ran on SDS-PAGE for an InstantBlue staining or a WB against Sema3A N-ter.

8. Effect of Sema3A WT and mutants on dorsal root ganglion neurons

Male Sprague Dawley rats 3 months old were used and the experimental procedure in this study was approved by the animal ethic committee of university of Leeds.

- DRGs extraction

Animal were killed by an overdose of Pentoject (animalcare). The spinal cord was quickly removed, cleaned of the flesh, cut in 3 pieces and placed in cold Dulbecco's Modified Eagle's medium (DMEM). Each piece was cut off in sagittal plane and then desiccated in cold Hank's Balanced Salt Solution (HBSS) under dissection microscope. DRGs were removed one by one by their nerves (to avoid damaging DRGs) using a micro-scissor and fine point forceps #5 and kept in HBSS on ice until all DRGs were removed (about 40 DRGs). A supplementary cleaning was realised to remove nerves and remaining arachnoid matter and transferred to DMEM medium.

- DRGs dissociation into individual neurons and culture

DRGs were incubated in 2 ml of 0.2% collagenase (Sigma, C9407) - 1 ml of DMEM in the incubator at 37°C for 90 min. 2 ml of 0.1% trypsin (Sigma, T0303) were added and incubated for 10 min at 37°C. Trypsin activity was stopped by resupending DRGs in 1 ml of DMEM containing 10 % foetal bovine serum (FBS, Invitrogen, 10500064)-1% *penicillin-streptomycin-fungizon* (PSF, Invitrogen, 15240062). Loose DRGs were then triturated with decreasing diameter Pasteur pipettes until to obtain a homogenous solution. To remove enzymes, cell suspension was centrifuged at 2000 xg for 2 min and the pellet was resuspended in 1 DMEM-10 % FBS -1% PSF. To separate debris from cells, the suspension was laid down carefully on 2 ml of DMEM-15 % BSA and centrifuged at 1000 xg for 15 min. Pelleted alive cells were resuspended in 2 ml of DMEM-1 % *insulin-transferrin-selenium* (ITS, VWR, 734-1315) - 1% PSF- 0.1% NGF (Sigma, N2513) and centrifuged at 2000 xg for 2 min. The cells were resuspended again in 12 ml of DMEM- 1 % ITS - 1% PSF- 0.1% NGF and distributed over 24 wells plate (500 µl/well) containing coverslips coated beforehand with 1 ml/well of 20 µg/ml Poly-D-lysine (Sigma, P1149) ON and then with 500 µl/well of 1µg/ml laminin (Sigma, L2020) for 1 h. DRGs neuros were cultivated in an humidified incubator at 37°C with 5% of CO_2 for 24 h.

- Sema3A proteins treatment

Once neuros have adhered to the coverslips (3h post-culture), Sema3A WT was added at final concentration of 0.5, 0.125 and 2 µg/ml , while Mut 1, Mut 2, Mut 3 or Mut 4 were added at final concentration of 2 µg/ml and incubated 48 h before fixing with 4% PFA for an immunostaining. The negative control was PBS and each condition was repeated in 3 wells x 3 different rats.

- Immunocytochemistry : against BIII tubulin

B III tubulin antibody (Sigma, T8660) recognises an epitope of βIII tubulin specific to neurons microtubules. The fixed cells were rinsed with PBS two times and incubated in 500 µl/well of PBS - 0.1 % triton X-100 - 3% normal donkey serum (NDS) for 30 min at RT to block the nonspecific sites. Then, they were incubated for 2h at RT under stirring in the primary antibody solution: 250 µl of PBS - 0.1 % triton X-100 - 3% NDS-0.2% B III tubulin antibody. The excess of primary antibody was removed by 3 washes of 5 min in 500 µl/well of PBS. Cells were then incubated 1 h at RT under stirring with the secondary antibody: 0.2% of donkey anti-mouse-alexa 488 in PBS - 0.1 % triton X-100 - 3% NDS. The excess of secondary antibody was removed by 3 washes of 5 min in 500 µl/well of PBS and 2 washes of 5 min in 500 µl/well tris non saline buffer. Dried coverslips were mounted on slides with ProLong Gold Anti-fading mountant containing DAPI. The slides were examined in epifluorescence microscope as previously described (section 1.3) and the number of neurons with neurites was quantified (only neurons which have neurite length 2 times longer than the cell body were taken into account). Data were obtained from culture of 3 rats, 3 coverslips per rat and 5 views per coverslip. Percentage of neurons with neurites was counted. One-way Anova test was used to confirm the variation between different conditions.

Results and discussion

1. Semaphorin 3A

1.1 Sema3A WT expression

Sema3A was overexpressed in HEK293-6E cells that were transfected with a pTT22SSP4 mammalian expression vector, containing the secreted alkaline phosphatase signal peptide and a poly-His tag in the N-ter (see the purification protocol of **Figure 44.A)**. As Sema3A is a secreted protein, its expression was analysed into the collected culture medium. Interestingly, WB screening at 1 to 5 days post transfection with an antibody directed against the poly-His tag revealed the existence of two forms of Sema3A, with molecular mass of 90 kDa and 65 kDa, the latter being the most represented **(Figure 44.B)**. As the antibody used to detect the protein was directed against the N-ter His-tag, the Sema3A-65 is likely a truncated form of Sema3A without its C-ter domains **(Figure 38)**. The existence of such form has been reported in both mouse embryo[269] and adult rat brain[204], and presumably corresponds to a furin-cleaved fragment of Sema3A. There are two furin cleavage sites of which (RX[K/R]R) being found in the Sema3A sequence at position 535 and 741, which can be cleaved by furin-like proprotein convertase (PPC) mediated processing. The cleavage in the first site releases an N-ter domain of 65 kDa composed of Sema domain and a part of PSI **(Figure 38)**. It is worth noting that commercial full length Sema3A (R&D) is mutated in the first cleavage site (R532A & R535A) to prevent processing at this position.

We then postulated that full length Sema3A, which contains the highly basic C-ter tail, may remain on the cell surface by its interaction with cell surface GAGs. We thus treated cell pellet with PBS containing 1 M NaCl to disrupt GAG-protein interaction and analysed the presence of the Sema3A in the high salt washes, using antibodies directed against both the N- (anti His-tag) and C- (C17) terminal domains **(Figure 44.C-D)**. WB data confirm our hypothesis that Sema3A-90 remains attached to the cell surface and Sema3A-65 is released in the culture medium. Sema3A-65 is not observed in C17 WB confirming thus the specificity of this antibody to the C-ter domain of Sema3A. In addition, the WB screening with these two antibodies at 1 to 5 days post transfection of Sema3A expression on the cell surface and the culture medium shows that the expression of both forms are higher at day 4 **(Figure 44.C-D)**. To further support that Sema3A-90 remains associated to the cells surface, we labelled

permeabilized HEK cells expressing Sema3A at day 3 with C-17 antibody. Immunostaining images show that Sema3A accumulates on the cell surface notably in the areas between cells **(Figure 44.E)**. Sema3A-90 remains attached to the cell surface probably by electrostatic interaction of the C-ter domains with GAGs of the cell surface. These results are the first indication of importance the C-ter domain in the binding to HEK cell surface.

Furthermore, other information can be deduced from Sema3A expression in HEK cells. We noticed that HEK cells expressing Sema3A are forming clusters **(Figure 44.F)**. This suggests that Sema3A on the cell surface oligomerises with Sema3A molecules from adjacent cells or that Sema3A binds and cross-links GAG chains from different cells, thus bridging them. This last suggestion will be investigated in a later chapter (section 1.9). Control presented in **Figure 44.E and F** were naive HEK cells without transfection, while a comparative control should be transfected cells expressing another protein. In order to confirm that the clustering phenomenon is specific to Sema3A expression, a proper control with the expression of another protein should be performed. However, transfected cells with the same vector (pTT22SSP4) expressing another protein were used in the lab, but no cells clusters were noticed. HEK cells tend naturally to form clusters. However here, we supplemented the culture medium with kolliphor P188 which protects cells from shear stress and hydrodynamic damage, preventing thus clusters formation.

Stable cell line expressing Sema3A was created from transfected cells. Some difference in expression were noticed in this stable line comparing to the transient expression: i) Furin cleavage is more prominent in this line: only Sema3A-65 is found in the supernatant and the cleavage in the second furin-cleavage site is stronger in Sema3A-90 found in the cell surface and ii) clustering phenomenon is more obvious in the stable line. Thereby, in order to be able to compare the expression with the other proteins (Sema3A mutants in section 1.5), we opted for a transient expression of Sema3A WT, as long as we do not have stable line for the other proteins.

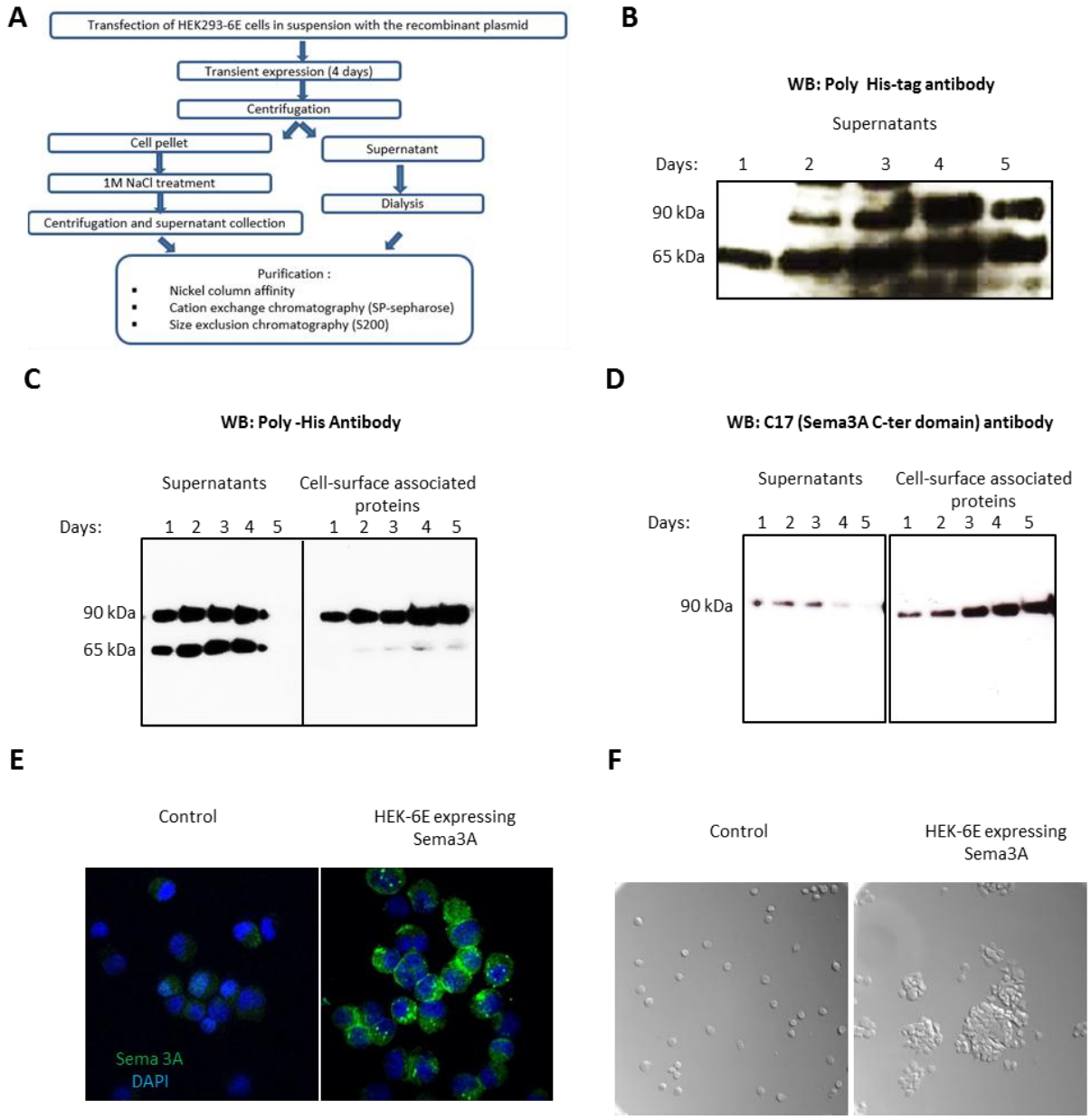

Figure 44: Sema3A heterologous expression in HEK293-6E cells.
(A) Schematic diagram of Sema3A purification protocol. Two samples were collected: from the cell surface and from the culture medium supernatant. **(B-C-D)** Kinetic of Sema3A expression in HEK293-6E cells during 5 days examined by western blotting using a poly-His antibody (B and C) and C-17 (D) antibody recognising the C-ter domain of Sema3A. Both supernatant and cell surface-associated protein, detached by washing with 1 M NaCl, were analysed in C and D. Absence of band in condition "poly-His, Supernatants, day 5" is probably due to an issue in transfer. Two forms of Sema3A were identified in the supernatant: 90 kDa and 65 kDa, while, on the cell surface only Sema3A-90 is present. **(E)** Immunocytochemistry of Sema3A expression on HEK293-6E cells surface using an antibody directed against the N-ter Sema3A domain (green), nuclei were stained with DAPI in blue, at magnification x 40. Control represents non transfected HEK293-6E cells. **(F)** Sema3A induces HEK cells clusterisation during Sema3A expression (pictures were taken 3 days after transfection, in differential interference contrast (DIC), at magnification x 20.

1.2 Sema3A cleavage by furin

As previously mentioned, Sema3A-65 form is likely resulted from a cleavage by endogenous furin. To check this, furin inhibitors "Dcanoyl-R-V-K-R-chloromethylketone" was added to transfected cell culture 1 day post-transfection and culture medium aliquots were collected at days 2, 3 and 4 post-ransfection and centrifuged. The cell pellet was treated with PBS containing 1 M NaCl to release the bound Sema3A from the cell surface. Both the culture medium and cell surface-associated protein were analysed in WB with an antibody directed against Sema3A domain. Sema3A-65 form was neither found in the cell surface-associated protein, nor in the supernatant with furin inhibitor treatment **(Figure 45.A)**, whereas the full length Sema3A-90 was detected in both fractions. Furin is therefore responsible of Sema3A-90 cleavage in HEK293-6E expressing Sema3A to generate Sema3A-65.

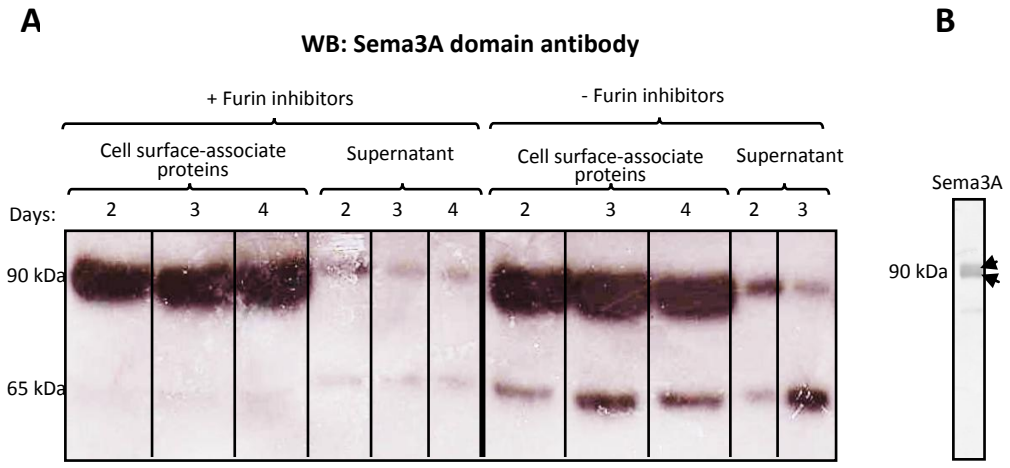

Figure 45: Sema3A cleavage by furin.
(A) WB with an antibody directed against Sema3A domain (N-ter) analysing the cleavage of expressed Sema3A in HEK293-6E cells by the endogenous furin in the presence or not of furin inhibitors "Dcanoyl-R-V-K-R-chloromethylketone". At day: 2, 3 and 4 post-transfection, fraction of cells was collected, centrifuged and the cell pellet was treated with PBS containing 1 M NaCl to release Sema3A from the cell surface. Both culture medium and cell surface associated proteins were analysed. **(B)** Example of coexistence of Sema3A full length and Sema3A missing1.3 kDa peptide in purified sample analysed by InstantBlue staining. Overlapping of the two protein bands is indicated by two arrows.

Sema3A contains two furin cleavage sites. Cleavage in the first site releases Sema3A-65 and a peptide of 25 kDa **(Figure 38)**. Cleavage in the second site releases a small peptide of 1.3 kDa. Difference between the full length Sema3A and Sema3A missing this peptide is generally insignificant in SDS-PAGE. Using this inhibitor could overcome the confusion

between these two forms, in addition to increasing the yield of Sema3A-90. However, this inhibitor commercially available is very expensive and requires to be used at high concentration of "100 µM" for a total inhibition. It is thus not practical for Sema3A purification. Nevertheless, we can purify a significant quantity of full length Sema3A-90 from the cell surface without resorting to furin cleavage inhibition. Surprisingly, the small difference between the full length and Sema3A missing 1.3 kDa peptide can be detected in SDS-PAGE. Indeed sometimes, overlapping of the two forms can be observed **(Figure 45.B)**.

1.3 Sema3A purification

Since Sema3A is conjugated with a poly-His tag at the N-ter, supernatant and cell-surface proteins were first subjected to Ni-NTA chromatography for purification. Protein was eluted with 10 ml of 300 mM imidazole and analysed in SDS-PAGE with InstantBlue staining **(Figure 46)**. Results show that two forms of Sema3A were purified from the supernatant: small fraction of 90 kDa and a large fraction of 65 kDa, while only Sema3A-90 is purified from cell surface-associated protein sample. Contaminants of different MW are also observed **(**gels of **Figure 46.A and Figure 46.B)**. As Sema3A contains a C-ter basic tail which could allow interaction with negative charges, a second step of purification using cation exchange chromatography onto SP-sepharose was performed. Sema3A-65, which does not contain the C-ter basic tail, is found in the flow through of SP-sepharose, whereas Sema3A-90 is eluted with ~ 700 mM NaCl **(**chromatograms of **Figure 46.A and Figure 46.B)**. SP-sepharose purification allows likewise elimination of contaminants of Ni-NTA elution resulting in pure Sema3A **(**gels of **Figure 46.A and Figure 46.B)**. Two forms of Sema3A were purified with high yield: ~ 5.5 mg/L of culture Sema3A-65 and ~ 5 mg/L of Sema3A-90. Altogether, these results show the importance of C-ter domains positive charges to interact with SP-sepharose.

Initially, Sema3A-65 from the SP-sepharose flow through (containing imidazole of the Ni-NTA elution) was stored without exchanging the buffer. After thawing out, we observed that the protein precipitates, suggesting that the high concentration of imidazole induces protein precipitation. To overcome this issue, Sema3A-65 collected from the SP-sepharose flow through was subjected to size exclusion chromatography (SEC) S200 in order to exchange the buffer against PBS. Using these conditions, we do not observe Sema3A-65 precipitation anymore and therefore the protein can be stored using these conditions (gel of **Figure 46.A**). Sema3A-90 was eluted from SP-sepharose with ~ 700 mM NaCl. NaCl

concentration was decreased down to physiological concentration (150 mM NaCl) by either dialysis against PBS or by dilution in PBS (more than 100 times) and then concentration using Millipore Centricon (30 K MWCO). In both cases, Sema3A-90 precipitates. We concluded that the stability of purified Sema3A-90 is salt-dependant. Sema3A-90 is thus stored in PBS containing 700 mM NaCl. Moreover, Sema3A-90 is sensitive to the concentration using centrifugal filters likely because of its interaction with the filter membrane. Therefore, Sema3A-90 is stored as eluted from SP-sepharose.

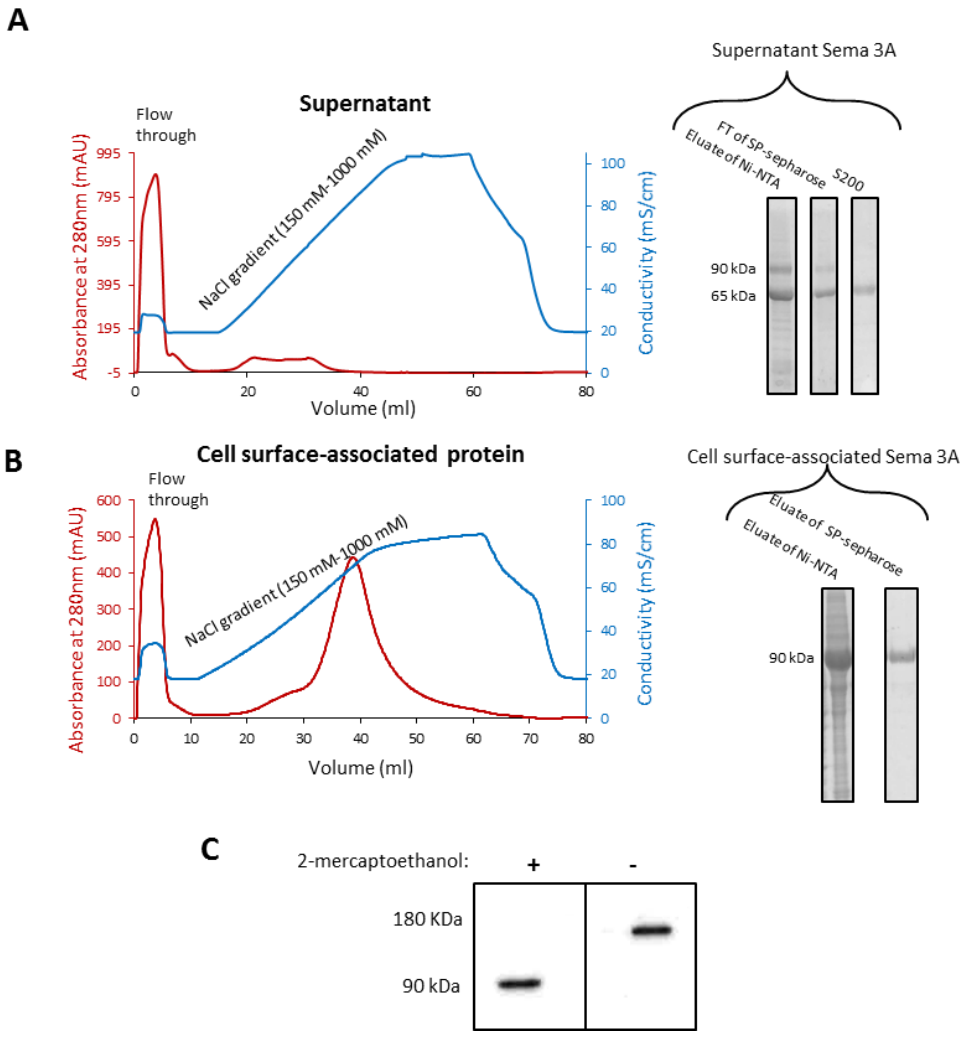

Figure 46: Sema3A WT purification.
(A-B) Supernatant and cell surface-associated protein detached with 1 M NaCl, respectively, were subjected to Ni-NTA column affinity (Elution with 300 mM imidazole), then cation exchange chromatography SP-sepharose (elution with NaCl gradient: 150 mM-1M). FPLC chromatograms (absorbance at 280 nm and conductivity) of supernatant protein (A) and cell surface-associated protein (B) are presented in the left. In the supernatant, Sema3A cleaved form of 65 kDa was found in the flow through of SP-sepharose. In cell surface-associated protein, Sema3A full length of 90 kDa was eluted at ~ 700 mM NaCl from SP sepharose. Eluates of each purification step were analysed in InstantBlue staining of 10% gel. Sema3A of the culture medium supernatant underwent a supplementary purification step in SEC S200. **(C)** Covalent dimerization of purified Sema3A-90 was analysed in WB (C-17 antibody directed against the C-ter domain of Sema3A) in +/- reducing conditions.

It was previously described that Sema3A full length is a covalent dimer. To check if purified Sema3A is a covalent dimer, we analysed in WB the dimeric state of purified Sema3A using C17 antibody in the presence or absence of reducing agent (2-mercaptoethanol). Purified full length Sema3A is 180 kDa without 2-mercaptoethanol treatment and, while it is 90 kDa in reducing conditions. This indicates that the purified Sema3A is covalent dimer as reported before[273] **(Figure 46.C)**.

To our knowledge, this is the first time full length Sema3A is purified without resorting to mutation of furin cleavage site. Indeed, given that Sema3A is a secreted protein, it is automatically collected from the culture medium in predominantly cleaved form (Sema3A-65) which contains the receptor-binding domain, thus the activity[215]. Once the full length is needed, the first furin cleavage site is mutated[269 217]. However, this does not prevent the cleavage in the second furin cleavage site, thus there is no control on the cleavage at this second site by the furin. Here, we reported for the first time a protocol of the full length Sema3A purification without any modification of amino acids composition. Moreover, Sema3A purified from the cell surface is protected from furin cleavage in both sites.

1.4 Identification of GAG-binding sites in Sema3A

Protein-GAG interaction is of great importance to several of physiological processes including that of Sema3A. This interaction constitutes generally the first step before triggering a signalling pathway. Characterising this interaction enables a better upstream control on the signalling pathway. Electrostatic forces usually contribute significantly to protein-GAG interactions, and binding sites are thus commonly enriched in basic residues. Multiple consensus amino acids sequences were discovered, mostly heparin-binding sequences such as XBBXBX, XBBBXXBX and XBBBXXBBBXXBBX where B is a basic residues and X is a hydropathic residue[310 311]. Sema3A has previously been shown to bind to CS-E[204]. To order to elucidate the GAG-binding domain on Sema3A, we examined the amino acid sequence of Sema3A and revealed the presence of four such basic clusters, herein referred as clusters 1 to 4 (red sequences in **Figure 47.A**), two of which (clusters 1 and 4) are also the furin cleavage sites. These clusters, KRRTRR [residues: 530-535], RRNEDRK [residues: 593-599], KRDRKQRRQR [residues: 708-717] and KKGRNRR [residues: 735-741] are located in the PSI domain, the Ig like domain and the downstream unstructured C-terminal sequence of the protein respectively **(Figure 47) (Appendix 3)**.

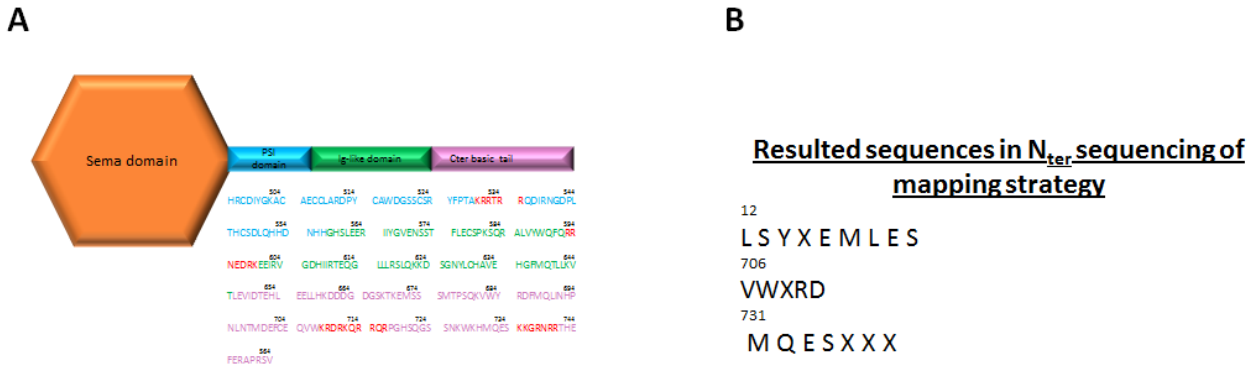

Figure 47: Sema3A-90 binds to GAG *via* specific sequences located in the C-ter domains.
(A) Schematic diagram of Sema3A domains and the sequence of the C-ter domains: PSI domain (blue), Ig like domain (green) and C-ter basic tail (purple). Numbering starts from the first amino acid of Sema3A sequence. Four basic amino acids-rich clusters (red) designed as cluster 1 to 4 are identified based on primary sequence in the C-ter domains and postulated to be the potential GAG-binding sites. **(B)** Identification of potential GAG-binding sequence(s) using heparin beads approach **(Appendix 6)**. This strategy is based on crosslinking of K/R residue(s) of heparin-binding sequence with the carboxyl group of heparin. X residue of resulted sequences represents the crosslinked residues K or R which are not visible in the N-ter sequencing or another unidentified amino acid. n=2 for Sema3A-65 and n=4 for Sema3A-90.

To analyse the possible involvement of these clusters in GAG recognition, we used a mapping strategy based on the formation of cross-links between heparin carboxyl groups and protein side chain-primary amine (of K or R). The bound material is subjected to proteolytic digestion, the resulting complexes and the identification of the polysaccharide-covalently bound peptides are performed by N-ter sequencing[304]. For this analysis we used both Sema3A-90 and Sema3A-65. N-ter sequencing results yielded several sequences. Only sequences containing a cross-linked K residue(s) are presented here (the cross-linked K is represented by an X): sequence 1 [residues 12-20: LSYXEMLES], sequence 2 [residues 706-710: VWXRD] and sequence 3 [residues 731-737: MQESXXX] (**Figure 47.B)**. Sequence 1 is found in both Sema3A-90 and -65 analyses. Sequence 2 and 3 are generated from Sema3A-90 and encompass clusters 3 and 4, respectively, identified by Sema3A primary sequence analysis. Revelation of other sequences which do not contain a cross-linked K could due to an incomplete digestion by thermolysin. They are maintained on heparin through crosslinked K or R of the next involved sequence.

Mapping strategy results confirm in part the potential GAG-binding sites identified by analysing the primary sequence. Altogether, these results confirm the importance of the C-ter in GAG-binding using heparin as a ligand. However, GAG-binding sites might be different

according to GAG type and the current method is only able to analyse heparin binding. To further analyse the Sema3A-GAG interaction, to identify potential CS-binding sites, and evaluate their respective importance in the interaction, site directed mutagenesis of the 4 identified consensus sequences was performed in the next section.

1.5 Sema3A mutants expression and purification

Further investigation of GAG-binding sites in Sema3A was performed using PCR-based site directed mutagenesis. This technique allows an analysis of the involvement of the mutated amino acid(s) or even a full sequence in a binding site or a role in function. Herein, we mutated individually the previously identified potential GAG-binding sequences to analyse if their deletion or modification influences GAG-binding of Sema3A.

1.5.1 Deletion/mutation of the potential GAG-binding sequences

Since there are 4 potential GAG-binding sites and each sequence is composed of 6-10 amino acids, we opted in the first place for deletion of the entire individual sequences. The four resulting mutated constructions were expressed in HEK293-6E as the WT. In the cells transfected with constructions carrying a deletion of cluster 1 or 2, Sema3A was neither found in the culture medium nor at the cell surface, but remained intracellular. We thus tried to purify it from cellular extract using different detergents but the protein remains insoluble **(Figure 48.A)**. This suggests the importance of these 2 clusters in the correct folding of the protein and/or in the secretion. Cluster 1 and 2 are located in structured domains PSI and Ig like domain, respectively **(Figure 48.B)**. The deletion of a whole sequence of 6 or 7 amino acids could drastically influence the protein structure and hence, an unfolded or misfolded protein could aggregate inside the cells. To our knowledge, there is no study reporting the role of these 2 sequences in secretion. Further investigation should be done to highlight this phenomenon. Furthermore, we noticed that the cells expressing these 2 mutants do not display clusterisation as observed in the cells expressing Sema3A-WT. This demonstrates that i) the clusterisation phenomenon in Sema3A WT condition is due to the secreted Sema3A itself but not to another phenomenon that would be linked to the manipulation required for transfection, and ii) on the other hand, the clusterisation constitutes an indication of success of transfection and protein secretion.

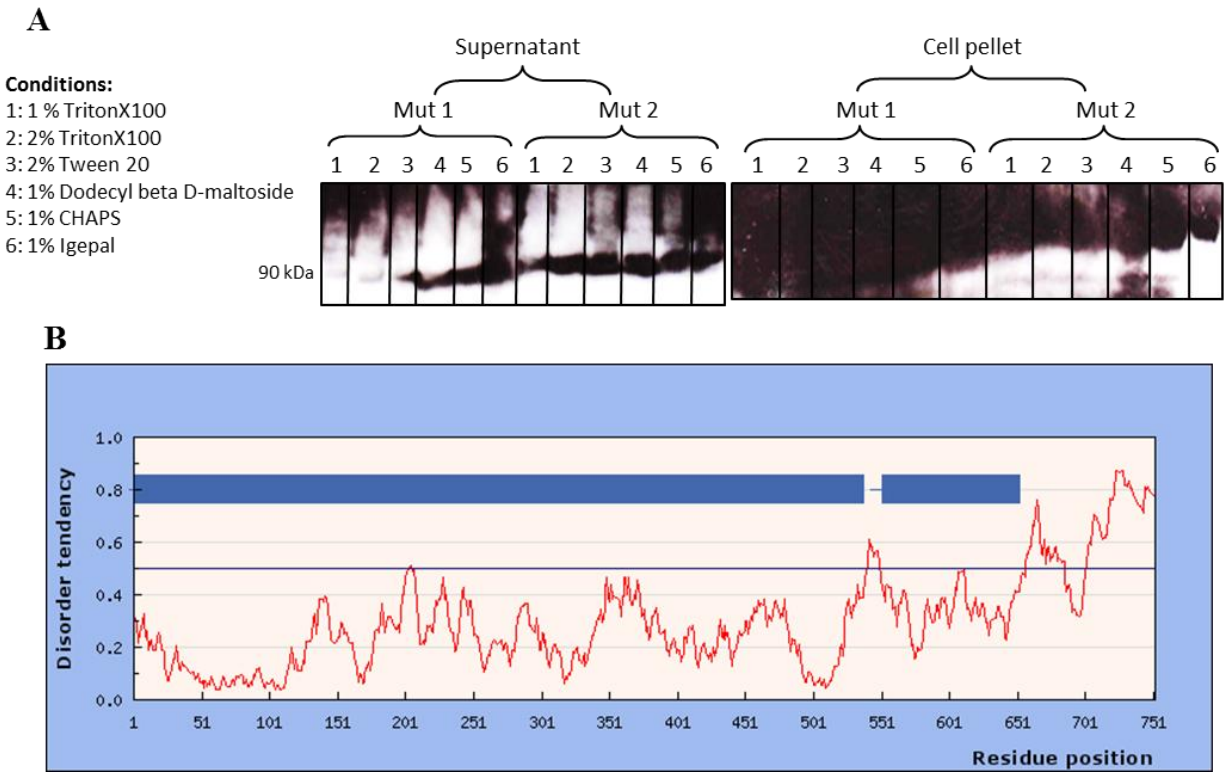

Figure 48: Deletion of cluster 1 and 2.
(A) WB using an antibody directed against Sema3A domain, of Mut 1 and Mut 2 (deletion of cluster 1 and 2, respectively). Cells expressing Mut 1 or Mut 2 were treated with different detergents (conditions: 1-6) to solubilise the non-secreted protein and then centrifuged. Both the cell pellet and supernatant were analysed. Most of protein remains insoluble into the cell pellet. **(B)** Prediction of intrinsically unstructured Sema3A-90 using IUPred software (http://iupred.enzim.hu/). Disorder tendency: [0-0.5] refers to structured region and [0.5-1] refers to disordered regions. Structured regions are shown in blue on the top of the plot. Amino acid residues position is represented in horizontal axis. Numbering starts from the first amino acid of Sema3A. Cluster 1 [residues 530-535] and cluster 2 residues [593-599] are located in structured regions. Cluster 3 [residues708-717] and cluster 4 [residues 735-741] are located in disordered regions.

In contrast to the deletion of cluster 1 and 2, deletion of cluster 3 or 4 does not affect the solubility and the secretion of the protein. Resultant proteins are designated Mut 3 and Mut 4, respectively **(Figure 49)**. The same strategy of expression and purification for Sema3A-WT was used **(Figure 44.A)**. Both full-length Sema3A of ~ 90 kDa bearing the mutation and truncated form of 65 kDa were resulted, but only Sema3A full length was purified since Sema3A-65 was already purified from the WT. Interestingly, most of Mut 3 and 4 were found in the culture medium, unlike Sema3A-WT which is remains attached to the cell surface. They were also eluted from the SP-sepharose at lower NaCl concentration (~ 450 mM NaCl) than the WT (~ 700 mM NaCl) **(Figure 49.A and B)**. Small fractions of Mut 3 and 4 remain attached to the cell surface are also eluted at 450 mM of NaCl in SP-Sepharose.

However, this fraction was contaminated with other proteins which are not eliminated in SP-sepharose **(Appendix 8)**. Hence, we did not use Mut 3 and Mut 4 proteins purified from the cell surface for subsequent analysis. As WT expression and purification profile indicated the importance of C-ter domains, Mut 3 and Mut 4 expression and purification profiles provide evidence that these 2 deleted sequences are important in binding to the cell surface and SP-sepharose. Deletion of both of them abolishes the binding. Furthermore, as clusters 3 and 4 are located in the unfolded C-ter basic tail of the protein **(Figure 48.B)**, we assumed that their elimination did not cause structural modifications to the tertiary structure of the protein.

Double mutant containing deletion of cluster 3 and 4 was designed and referred as Mut 3/4. Similar to individual Mut 3 and Mut 4, this double mutant did not remain at the cell surface, and was thus purified from the culture medium. As for Sema3A-65, the deletion of the charged sites in Mut 3/4 abolished its binding to SP-sepharose. Mut 3/4 sample, purified form culture medium, is thus contaminated with Sema3A-65 that results from furin cleavage within the cluster 1. To separate Sema3A-65 from Mut3/4 Sema3A-90, the flow through of SP-sepharose was subjected to SEC-S200 **(Figure 49.B)**. This observation shows that Sema3A-90 remains bound to cell surface and SP-sepharose through cluster 3 and 4. In addition, Sema3A-65 is released in the culture medium and SP-sepharose because of absence of cluster 3 and 4 and not because of the absence of the whole C-ter domain.

To analyse the involvement of cluster 1 and 2 in GAG-binding and to overcome the resulted issue from their deletion, we secondly opted for the substitution of all basic amino acids of each cluster by an alanine or serine. This substitution interrupts the consensus GAG-binding sequences. We substitute cluster 1 [KRRTRR] by [ASSTSA] or cluster 2 [RRNEDRK] by [SANEDAA]. While the substitution in cluster 1 resulted in secreted protein, substitution in cluster 2 yielded to the same problem as a deletion **(Figure 50)**. This result further suggests amino acids within cluster 2 are in involved somehow in the structure and/or secretion of the protein. We then decreased the number of mutated amino acids by substituting just the two first amino acids [i.e: SANEDRK]. Finally, the protein is successfully secreted **(Figure 50)**.

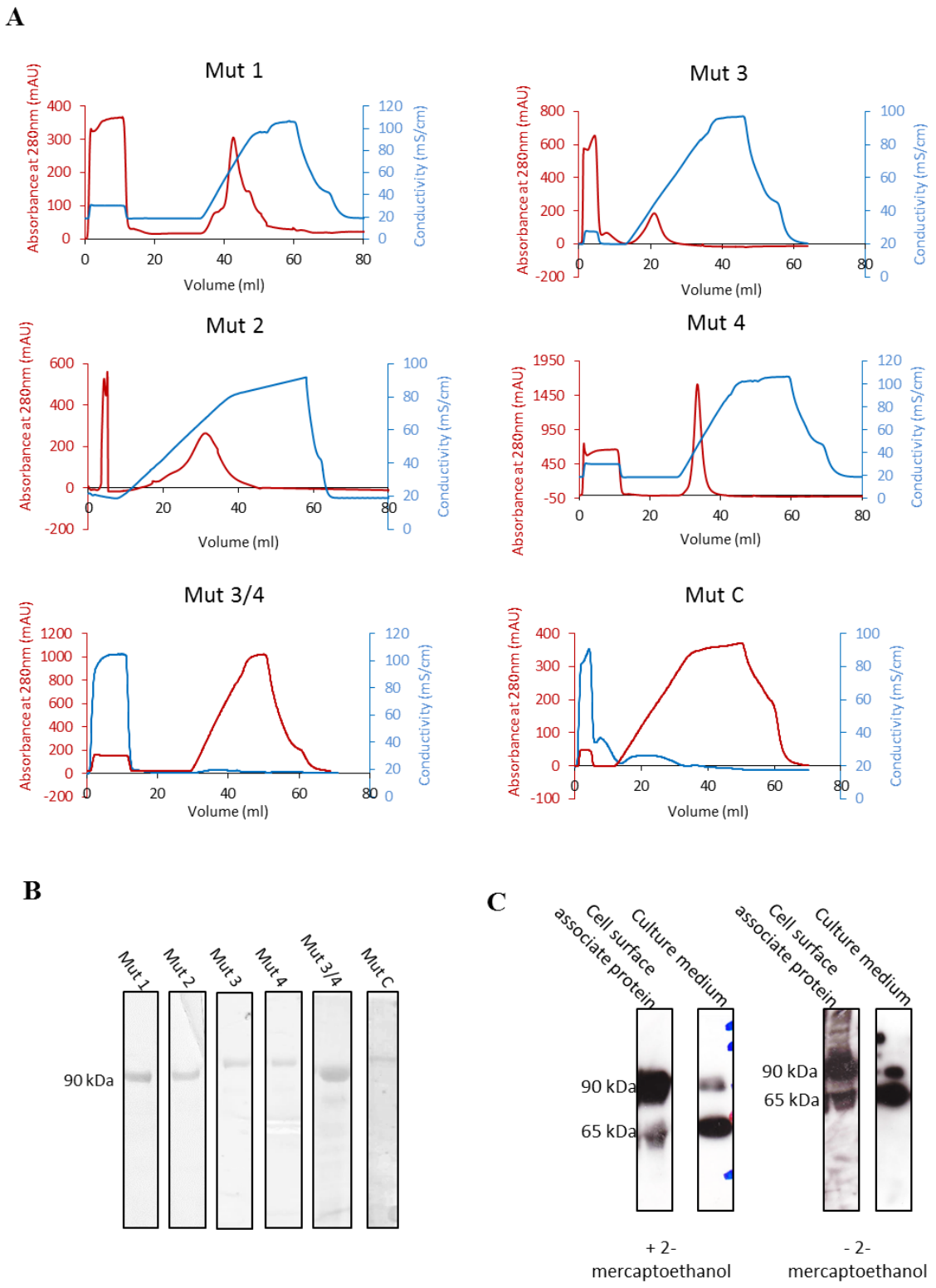

Figure 49: Sema3A mutants purification.
(A) Examples of FPLC chromatograms (absorbance at 280 nm and conductivity) of Sema3A-90 mutants: Mut 1, Mut 2, Mut 3, Mut 4, Mut 3/4 and Mut C. Sema3A-90 of Mut 1, Mut 2 and Mut C were found on the cell surface and detached with PBS containing 1 M NaCl. Mut 1 and Mut 2 were eluted at ~ 700 mM NaCl from SP-sepharose, while Mut C was eluted at ~ 500 mM. Sema3A-90 of Mut 3, Mut 4 and Mut 3/4 were purified from the culture medium. Mut 3 and 4 were eluted at ~ 450 mM NaCl from SP-sepharose, while Mut 3/4 did not bind. **(B)** InstantBlue staining of purified Sema3A-90 mutants (10 % acrylamide gel in reducing conditions). **(C)** WB with an antibody directed against Sema3A domain of cell surface and culture medium Mut C, in reducing or not conditions (+/- 2-mercaptoethanol).

This suggests that the two last amino acids "RK" of the cluster 2 or at least one of them are required for the correct folding and/or the protein secretion. Resulted proteins from the substitution in cluster 1 and 2 are designated as Mut 1 and Mut 2, respectively. Mut 1 and Mut 2 expression and purification profile is as the WT. In Mut 1, full length Sema3A is purified from the cell surface and eluted at ~ 700 mM NaCl as the WT. As cluster 1 is the first furin-cleavage site, Sema3A-65 form does not exist in Mut 1. In Mut 2, full length Sema3A is also purified from the cell surface and eluted at ~ 700 mM NaCl, while Sema3A-65 was found in the culture medium as the WT **(Figure 49.A and B)**. These expression and purification profiles of Mut 1 and Mut 2 indicate that cluster 1 and 2 are not required for the binding to the cell surface and SP-sepharose. Furthermore, Mut 1 and Mut 2 bear a complete or partial substitution mutation of basic amino acids, respectively. Substitution affects less the structure than deletion, especially cluster 1 and 2 are located in structured domains **(Figure 48.B)**.

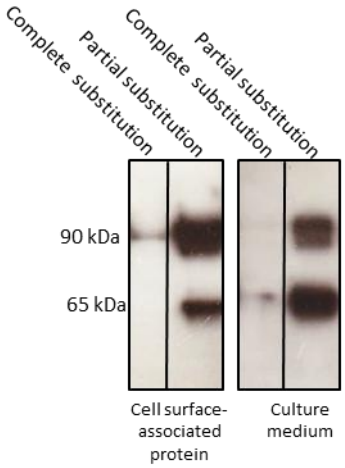

Figure 50: **Comparison between complete and partial substitution of cluster 2 basic amino acids.**
Comparison in WB, using an antibody directed against Sema3A domain, between Mut 2 displaying a substitution of all basic amino acids and substitution of the two first basic amino acids of cluster 2. Both the cell surface-associated protein, detached with PBS containing 1 M NaCl, and culture media were analysed. Sema3A is found on the cell surface and culture medium in "partial substitution condition", but not in "complete substitution condition".

To summarise this section, we expressed and purified five mutants. Mut 1 and Mut 2 bear a complete or partial substitution of basic amino acids of cluster 1 and cluster 2, respectively and Mut 3 and Mut 4 bear a deletion of cluster 3 and cluster 4, respectively. Mut 3/4 bears deletion of both cluster 3 and 4. Mut 1 and Mut 2 were purified from the cell surface

and eluted at ~ 700 mM NaCl from SP-sepharose as the WT, while Mut 3 and Mut 4 were purified from the culture medium and eluted at ~ 450 mM NaCl from SP-sepharose. These results indicate that cluster 3 and 4 are required for the binding to the cell surface and the strong binding to SP-sepharose, while cluster 1 and 2 are not.

1.5.2 Substitution of the cysteine (C) responsible for the disulfide bond

Sema3A-90 is a covalent dimer with a disulfide bond at position C^{703}. To study the role of this covalent dimerization in GAG-binding, we mutated this C by substituting it with S, we called this Mut C. Sema3A-90 was purified from the cell surface as the WT, but eluted at lower salt concentration (~ 500 mM NaCl) from SP-sepharose. This weaker binding to SP-sepharose comparing to the WT could be explained by the fact that positive charges from both monomers composing the dimer are involved in the interaction with the column and these charges are 2 times lower in mutant, hence the binding is weaker. Sema3A-65 was found in the culture medium as in the WT. However, total protein quantity is lower in this mutant than in the WT, especially the Sema3A-90 form whose yield was 200 µg/L of culture compared to that of the WT (5 mg/L of culture) **(Figure 49.A and B)**. Absence of disulfide bond in the purified protein was checked in non-reducing condition in WB with Sema3A domain antibody. WB data show that the band at 90 kDa corresponding to full length Sema3A remains unchanged in non-reducing conditions confirming thus the full length Mut C is not a covalent dimer **(Figure 49.C)**.

Eluates of Ni-NTA and SP-sepharose of cell surface-associated proteins and culture medium proteins of different mutants are appended **(Appendix 8)**.

1.6 Interaction analyses of Sema3A WT and mutants to GAGs using SPR (GAG-binding)

1.6.1 SPR (Biacore) principle

Biacore system measures interaction between two biomolecules in real time, using SPR: one of the two partners is immobilised on the gold sensor chip surface, another one flowing in solution, over the surface. The increase in mass on the sensor chip surface, that occurs upon binding induces changes in the refractive index at the surface of the sensor chip which results from angle incidence alteration (SPR angle), displaying thus the interaction

(Figure 51.A). Binding response is quantified in resonance unit (RU) which indicates a shift in the angle, 1 RU = 10^{-4} ° shift or 1 pg/mm^{2}[312]. The binding is interpreted in a sensorgram composed of association-dissociation phase. Fitting the resulted sensorgrams to an adequate binding model allows calculation of various parameters (R_{max}, K_D, k_{on}, k_{off}..). Herein, we immobilized GAGs chain on the sensor chip (ligand) and proteins of interest (Sema3A WT and mutants **(Figure 51.C**) were injected in solution in the flow (analyte).

1.6.2 GAG-surface preparation for interaction analysis

GAGs were biotinylated at their reducing ends (CS-E, CS-D and HS) **(Figure 51.B)** and immobilised on streptavidin-coated surfaces. This type of immobilization of GAGs *via* their reducing end mimics the orientation of GAGs at the cell surface or within the ECM and present the GAGs as in their natural orientation, i.e. all GAG chains are facing up allowing for a homogeneous disposition and exposition for interaction. Indeed, GAG chains are attached to the core protein by their reducing ends. We started our investigation by immobilizing ~ 3000 RU of streptavidin and ~ 200 RU of GAGs without having reached surface saturation. We injected the protein at 10 µl/min flow rate in a concentration range of [5 - 100 nM].

With these conditions, we could analyse and compare interactions between Sema3A and different GAGs, whose results are discussed below. However, resulted curves do not fit to any model to calculate affinities, presumably because of mass transfer phenomenon **(Figure 51.D)**. Binding of the protein delivered in the flow to the GAG on sensor chip takes place in two steps. The first one consists in the transfer of the protein from the bulk to sensor chip surface. The second step consists in the binding with the immobilized ligand. First step is also known as mass transfer **(Figure 51.D)**. Mass transfer depends on diffusion coefficient of the protein and the flow rate. If the association rate is higher than the diffusion rate, binding is limited by mass transfer. Sensorgram measures the rate of protein diffusion rather than association to the ligand. Three common ways can limit mass transport effect on kinetic data. The first one is to decrease the surface density of GAGs thus reduce the number of binding sites. Less protein needs to diffuse to interact with the GAG. To this purpose, we reduced the amount of streptavidin on the surface to immobilise less GAG chains (~ 1000 RU) and we immobilised ~ 60 RU of GAG **(Figure 51.E)**. A second way is to increase the flow rate, providing thus more proteins in a short time for interaction. We then increase the flow rate

from 10 µl/min to 60 µl/min. The last way is to include mass transfer in the fitting model correcting thus the association rate to the GAG. We then fitted the resulted data to Langmuir binding model 1:1including mass transfer step.

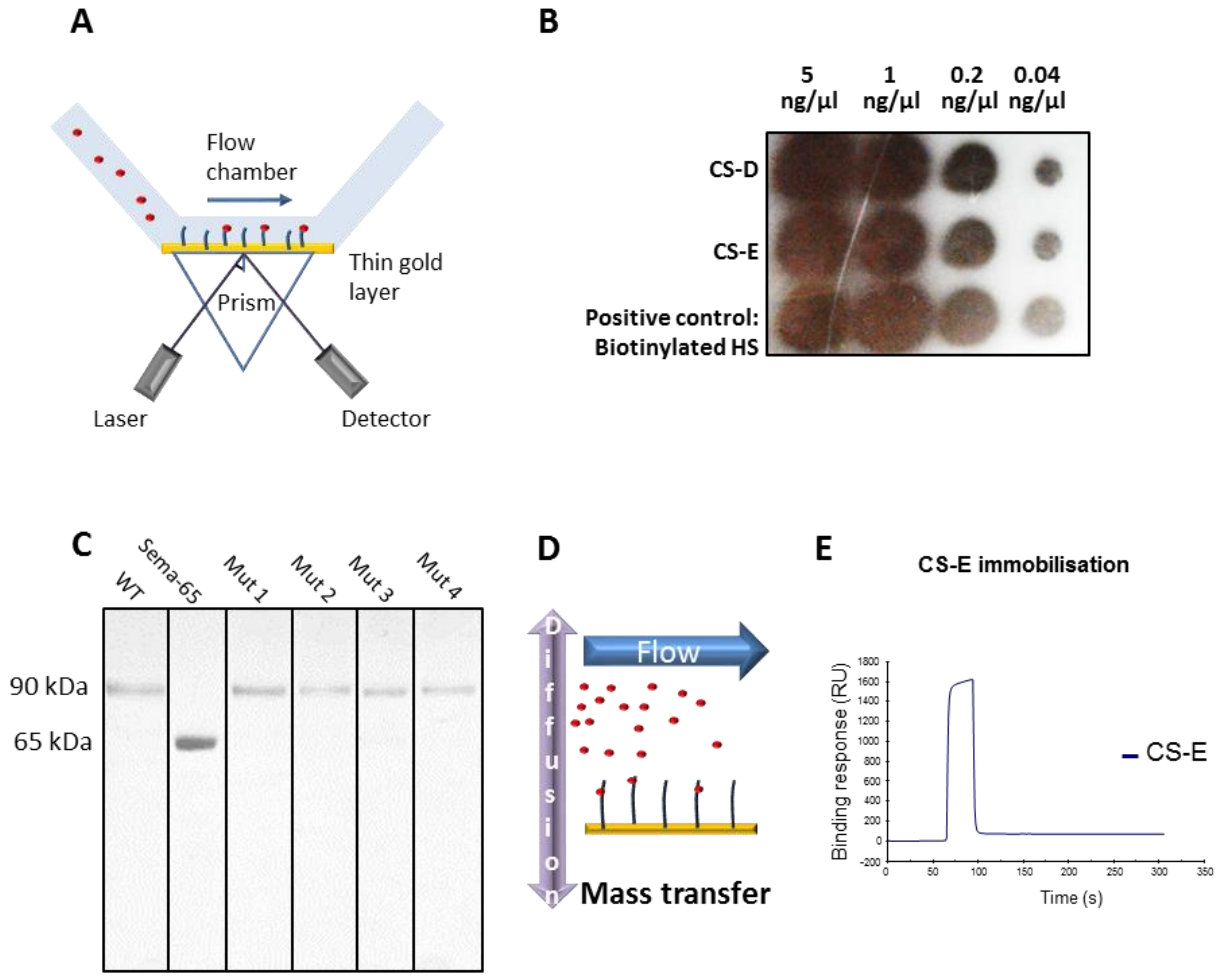

Figure 51: Surface plasmon resonance (SPR) and GAG-surface preparation for interaction analysis. **(A)** Schematic diagram of SPR technique. GAG are immobilised on SPR sensor chip and Sema3A is injected in the flow. **(B)** Dot blot showing the biotinylation of commercial CS-E and CS-D. Positive control is a biotinylated HS. Blots of each lane correspond to a serial dilution of biotinylated GAG. **(C)** SDS-PAGE (10 %) in reducing conditions of analysed proteins in SPR after freeze-thaw, stained by InstantBlue (Sema3A- WT, Sema3A-65, Mut 1; Mut 2, Mut 3 and Mut 4) used in SPR analysis. **(D)** Schematic representation of protein delivery from the bulk to the GAG surface which takes place in two steps: mass transfer and binding to the ligand. **(E)** Example of SPR sensorgrams of commercial CS-E immobilisation on CM4 sensor chip which results in ~ 60 RU shift.

All these modifications in working conditions enabled us to limit the mass transport effect and obtaining sensorgrams with curvatures that we can fit to a binding model to calculate kinetic parameters. This also reduced 10 times the injected concentration range to

[2-10 nM]. Moreover, with the starting conditions high amount of protein bounds to the GAG, generating thus an important binding response (> 1000 RU). To elute the bound protein from GAGs chains (regeneration), we have injected 0.05% SDS and 2 M NaCl. With the new conditions, lower amount of protein bound to GAG, hence lower binding response (<500 RU). In addition, only 2 M NaCl is sufficient to elute the protein from GAGs.

1.6.3 Sema3A WT and mutants –GAG interaction analysis

1.6.3.1 Sema3A WT-GAG interaction

As it has been reported that Sema3A binds to CS-E in ELISA and carbohydrate microarray assays[204], we hence analysed this interaction in SPR to determine the K_D. We first analysed the binding of purified Sema3A-90 WT and commercial Sema3A as a positive control of binding to CS-E, CS-D and HS. CS-E chains (from squid cartilage) are enriched in disulphated units CS-E (4S6S). CS-D (from shark cartilage) enriched in another type of disulphated units (2S6S) was used as a control for a sulphation pattern (position of sulphate)-dependent binding. As HS-protein interaction is the most studied GAG-protein interaction, we analysed also the binding to HS. SPR data show that Sema3A binds to CS-E and HS with a high affinity in pM range **(Figure 52.A-C and Table 12).** However, Sema3A does not bind to CS-D **(Figure 52.A)**. This very high affinity to CS-E and HS is mostly due to both high association rate and weak dissociation rate. Indeed, the resulted complex is stable over time. Plethora of proteins in the CNS were reported to interact with CS-E with high affinity as in the case of Sema3A, for example the multi-functional fibroblast growth factors involved notably in neurons proliferation: FGF-16, FGF-18, and HB-EGF ($K_D \approx$ 47.2, 8.9 and 16 nM, respectively)[205]. These affinities were measured using different techniques. It is thus difficult to compare with our own results. It is worth noting that Sema3A binds to GAGs with much higher affinity.

The large difference of K_D between the binding to HS and CS-E is due to the difference in analysis conditions. Indeed, the binding to HS was analysed with starting conditions (200 RU of GAG, 10 µl/min flow rate and concentration range [5-100 nM]), while the results of the binding to CS-E presented in **Figure 52.B** were obtained with the new conditions (60 RU of GAG, 60 µl/min flow rate and concentration range [2-10 nM]). In addition, a comparable K_D to HS was obtained for CS-E with the starting conditions (K_D= 414.68 ± 128.8 pM).

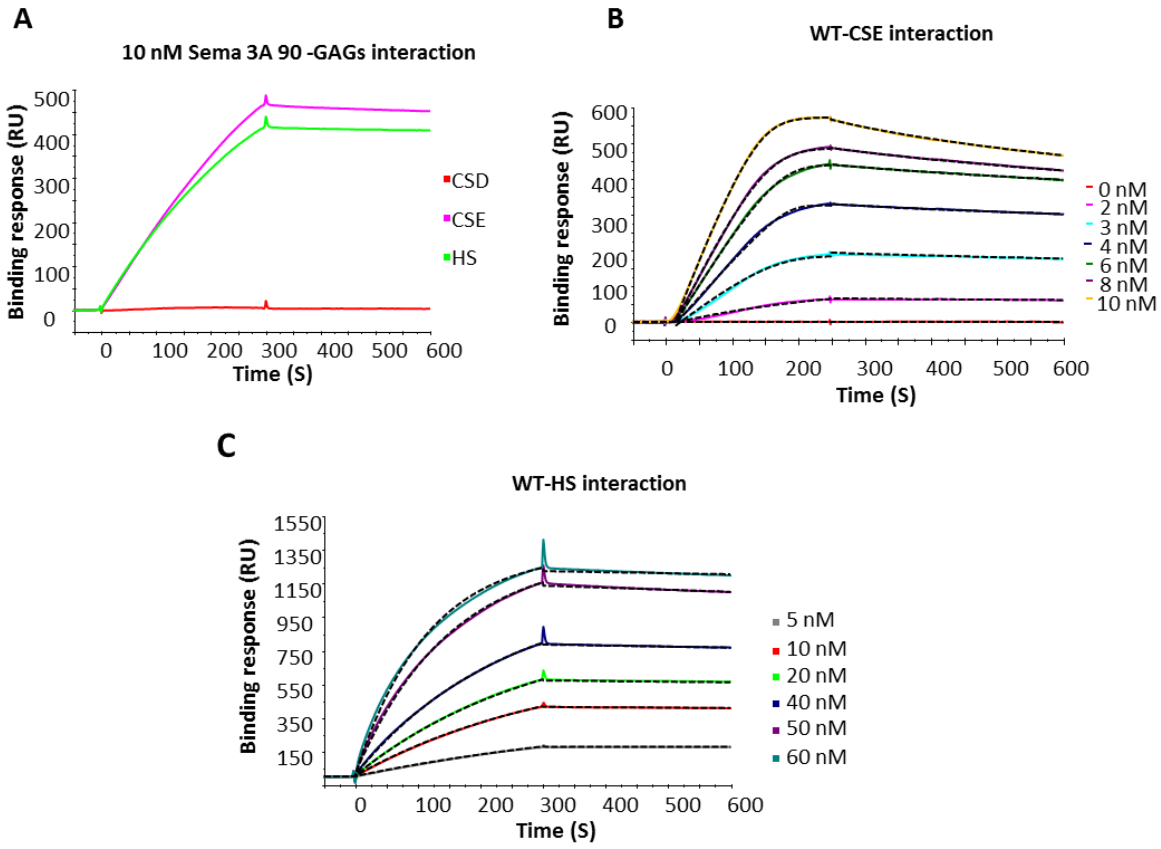

Figure 52: Sema3A WT-GAG analysis in SPR.
(A) 10 nM Sema3A-90 was injected over HS, CS-E and CS-D. Sema3A-90 binds selectively to CS-E and HS and does not bind to CS-D. **(B-C)** Sema3A-90 was injected over immobilized CS-E and HS, respectively. Binding curves (coloured lines) were fitted to1:1 Langmuir binding model with mass transfer (dotted lines). Binding parameters were calculated from the fit are listed in **Table 12**. In these experiments, 200 RU (A and C) or 60 RU (B) of GAGs were immobilized on CM4 sensor chip *via* their biotinylated reducing extremity. Sema3A proteins were injected at 10 µl/min (A and C) and 60 µl/min (B) for 300 s. The complex protein-GAG was left for dissociation for 300 s. All the experiments were repeated at least two times.

Table 12: Kinetic parameters resulting from the fit to 1:1 Langmuir binding model with mass transfer of Sema3A WT, Mut 1 and Mut 2 – CS-E/HS interaction in SPR.

	CS-E			HS		
	K_{on} ± SEM (1/Ms)	K_{off} ± SEM (1/s)	K_D ± SEM (pM)	K_{on} ± SEM (1/Ms)	K_{off} ± SEM (1/s)	K_D ± SEM (pM)
WT	$1.11E^{7} \pm 3.05E^{6}$	$5{,}28E^{-4} \pm 9.78E^{-5}$	73.75 ± 26.10	$3.11E^{5} \pm 8.26E^{4}$	$1.84E^{-4} \pm 2.57E^{-5}$	1371. 16± 424.34
Mut 1	$1.54E^{7} \pm 5.82E^{6}$	$6{,}21E^{-4} \pm 7.18E^{-5}$	56 ± 10.9	-	-	-
Mut 2	$6.93E^{7} \pm 1.54E^{6}$	$5.60E^{-4} \pm 1.94E^{-4}$	74.28 ± 15.20	-	-	-

k_{on}: association constant expressed in $M^{-1}s^{-1}$; k_{off}: dissociation constant expressed in s^{-1}; K_D: Dissociation equilibrium constant expressed in pM, resulting from the ratio k_{off}/k_{on}. Values present the mean of two experiments ± standard deviation of the mean. "-": not analysed yet. CS-E and HS kinetic parameters values are obtained in different conditions.

According to SPR results, Sema3A binds specifically to CS-E and not to CS-D suggesting that the binding is not charge-dependent but sulphation pattern-dependent. However, purified CS chains are made of mixt of different disaccharide CS units. It is important to analyse the percentage of CS-E and CS-D units in commercial CS-E and CS-D chains, respectively, to be able to compare their interaction with Sema3A. For this purpose, a disaccharide composition analysis of the commercial CS-E and CS-D used in binding assays was performed (see disaccharide analysis principle in section 2: brain CS). Results show that CS-E chains are enriched in CS-E units (~70 % of 4S6S and 30 % of 0S units**) (Figure 53.A)**, while, CS-D is made only of ~ 30 % of the 2S6S units. It is composed in addition, of 50 % of 6S and ~20 % of 0S **(Figure 53.B)**. These results indicate that the CS-E and CS-D samples also differ in the level of disulphated disaccharide (70% for CS-E versus 30 % for CS-D). Therefore, they do not feature the same global charge. In addition, this analysis does not indicate how such units are distributed within the polymer. Protein binding to GAGs usually requires a continuous stretch of 2 to 5 sulphated disaccharides units. With 70 % of 4S6S disulphated disaccharide, such stretches are likely to be present along the CS-E chain. In contrast, for CS-D, which contains only 30% of disulphated 2S4S disaccharides whose the distribution is unknown, the existence of such stretches can only be hypothetical. It is therefore not possible to definitively conclude that Sema3A specifically binds to CS-E units and not to CS-D units. The absence of Sema3A binding to CS-D chains may due to the low percentage of CS-D units distributed in homogenous way along the chain, preventing thus CS-D-enriched domain formation. Analysis of Sema3A binding to oligosaccharide CS-D would elucidate the presence or no of interaction. Indeed, oligosaccharide is size-defined and contains a homogeneous sulphation pattern.

In a previous study, *Dick et al.*, reported the binding of Sema3A-90 to CS-E[204], and also that Sema3A does not bind to HS, while we observed such interaction in SPR. This contrasting data could be explained by the difference in HS sources. We used HS from porcine intestinal mucosa which is 50% sulphated, while in in this previous study they used bovine kidney HS which are less sulphated. Once again, in the absence of knowledge on the chain organisation, it is difficult to bring definitive conclusions solely based on the overall composition of the various samples used in binding assays.

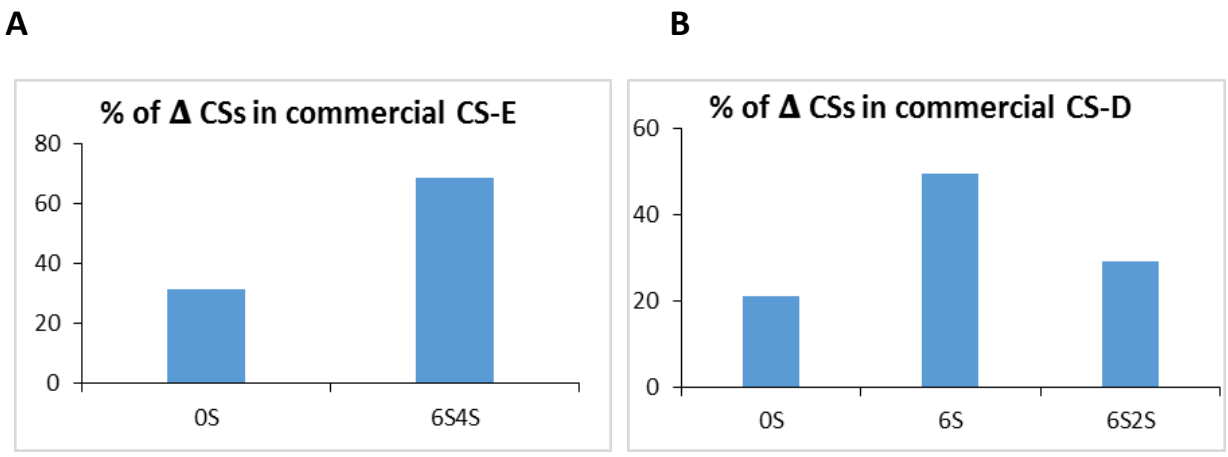

Figure 53: Disaccharide composition of commercial CS-E and CS-D.
(**A-B)** Disaccharide composition analysis of commercial CS-E and CS-D, respectively. CS chains were digested with chondroitinase ABC to generate disaccharides units (**Δ** CS) and analysed using RPIP-HPLC. 0S: non-sulphated units. 6S: CS-C units. 4S6S: CS-E units. 2S6S: CS-D units. CS-E is composed of ~70 % of 4S6S units. CS-D is composed only of ~ 30 % of 2S4S units.

We next compared the binding response of purified Sema3A-90 kDa with that of the commercial Sema3A. This analysis showed that the resulted binding is five time higher in purified Sema3A than commercial Sema3A **(Figure 54)**. The commercial Sema3A is mutated in the first basic cluster (furin cleavage site): R532A & R535A and lacks thus two basic residues compared to the WT. We can however exclude that it caused the observed reduced binding as we showed that this cluster 1 is not involved in GAG-binding **(Figure 56.A)**. It is worth noting that the commercial Sema3A is linked to a FC-domain, which could affect its structure and/or the orientation of the two monomers. Finally, information obtained from R&D company, revealed that the commercial preparation contains no more 20.4 % of full length Sema3A of 120 kDa (90 kDa of full length Sema3A + 30 kDa of the FC-tag in the C-ter) the remaining being 53.6% of the cleaved form at the second furin cleavage site (without the FC-tag and small part of the C-ter) and 23.7% of the FC-tag and small part of the C-ter of the Sema3A. This is likely the reason for the low binding of commercial Sema3A to CS-E.

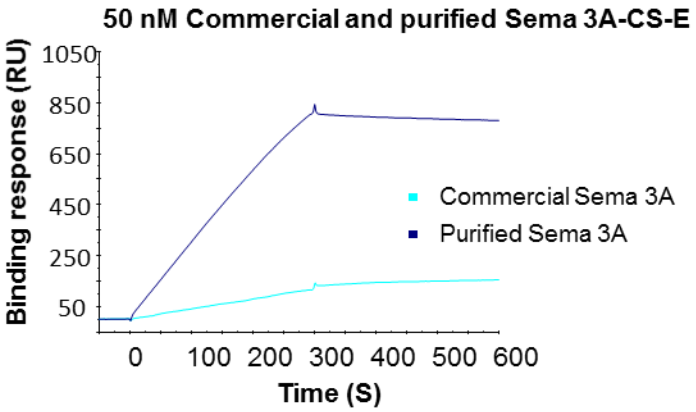

Figure 54: Comparison between purified and commercial Sema3A-90 binding to CS-E.
50 nM of full length purified Sema3A or commercial Sema3A was injected over CS-E. Binding response of commercial Sema3A is lower than the purified Sema3A. In this experiment 200 RU of CS-E is immobilized on CM4 sensor chip *via* its biotinylated reducing extremity. Sema3A proteins were injected at 10 µl/min for 300 s. The complex protein-CS-E was left for dissociation for 300 s.

Having set up a CS-E-Sema3A binding assay that enables us to quantify the kinetics and the affinity of the interaction, we next analyse the importance of the C-ter domain of the protein for the interaction. Binding experiments were first performed with purified Sema3A-65 **(Figure 55.A)**. SPR data show that Sema3A-65 does not bind to any GAG. This indicates that the GAG binding sites are not present within the Sema3A domain of the protein but at the C-ter domains. In particular, as cluster 1 is present in Sema3A-65 (furin cleaves on the right of KRRTRR), this result further indicates that cluster 1 is not involved in GAG binding. In addition, this finding does not support the involvement in the GAG-binding of the sequence LSYKEMLES, that was identified by N-ter sequencing during the "heparin-bead approach" described above (section 1.4). The crosslinked K of this sequence could be a part of a basic sequence resulted from the tertiary structure of Sema domain. However, electrostatic surface analysis of Sema3A-65 reveals a homogenous distribution of positive charges **(Figure 55.B)**. Nevertheless, it is near the poly-His-tag, which might be positively charged (usually below pH 6.5) and could have interact with the negative charges of heparin that is much more electronegative than CS-E. We could thus postulate that poly-His tag could have approximated the K residue of this peptide to heparin and as such promote cross-linking.

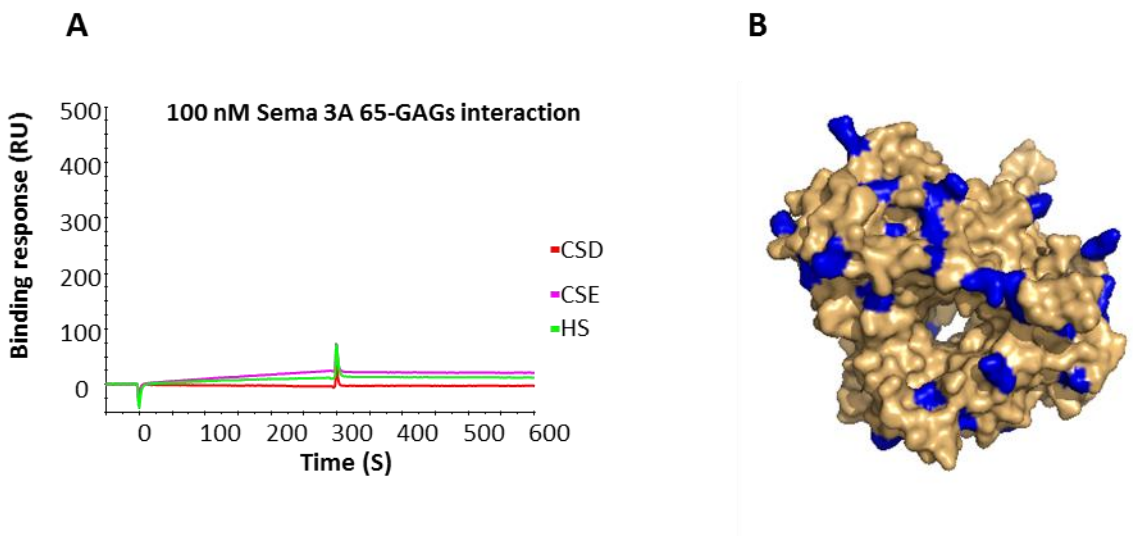

Figure 55 : Sema3A-65 binding to GAGs.
(A) 100 nM Sema3A-65 was injected over HS, CS-E and CS-D. No binding is observed at this concentration. In this experiments 200 RU of GAGs were immobilized on CM4 sensor chip *via* their biotinylated reducing extremity. Sema3A-65 was injected at 10 µl/min for 300 s. The complex protein-GAG was left for dissociation for 300 s. This experiment was repeated at least two times. **(B)** Distribution of K and R (blue) residues on Sema3A-65 monomer (beige).

1.6.3.2 Sema3A mutants- GAG interaction

To determine GAG-binding site(s) in Sema3A, we next examined the interaction of full length Sema3A Mut 1, Mut 2, Mut 3 and Mut 4 to CS-E. As observed for the WT, Mut 1 and 2 bind with a high affinity to CS-E **(Figure 56.A and B, Table 12).** In contrast, both Mut 3, Mut 4 and Mut 3/4 do not bind at all to CS-E in the investigated concentration range **(Figure 56.C and D)**. These results are in accordance with the "heparin beads experiments" exposed above (section 1.4). Altogether, these results indicate that cluster 3 and 4 are the GAG-binding sequences on Sema3A. Deletion of one of them is sufficient to abolish the GAG-binding of Sema3A, demonstrating thus both of them are required for the interaction to take place. Cluster 3 and 4 are located in unstructured C-ter basic tail, and separated by only 17 amino acids containing two K. It is therefore interesting to know if cluster 3 and 4 belongs to one long GAG-binding sequence or they constitute two independent sites. Mutation of the two K residues within the sequence in between the 2 clusters could confirm this.

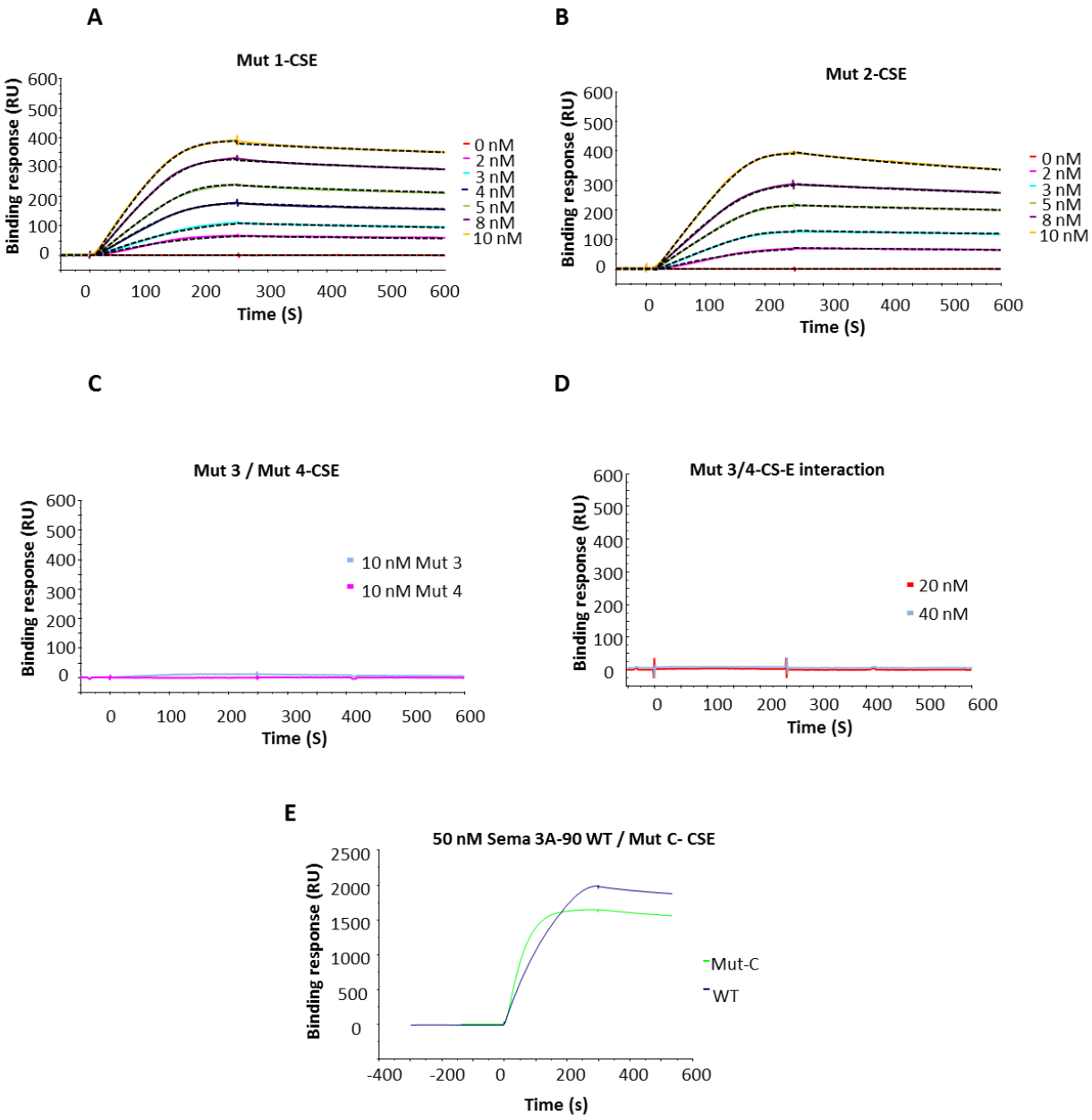

Figure 56: Sema3A Mutants-CSE interaction analysis in SPR.
(A-B) Full length Mut 1 and Mut 2 bind highly to CS-E. Binding curves were fitted to1:1 Langmuir binding model with mass transfer. Binding parameters calculated from the fit are listed in **Table 12**. **(C-D)** Mut 3, Mut 4 and Mut 3/4 do not bind to CS-E at analysed concentrations. **(E)** Comparison between full length WT and Mut C at 50 nM. In these experiments 60 RU (A-D) and 200 RU (E) GAGs were immobilized on CM4 sensor chip *via* their biotinylated reducing extremity. Sema3A proteins were injected at 60 µl/min (A-D) and 10 µl/min (E) for 300 s. The complex protein-GAG was left for dissociation for 300 s. Coloured and dotted lines represent the binding data and the result of the fit, respectively. All the experiments were repeated at least two times.

We also compared the binding of Mut C (mutation in C involved in disulfide bond) and the WT, and no significate difference was concluded **(Figure 56.E)**. Mutation of C^{703} prevents the formation of the disulfide bond but not the dimerization. Indeed, non-covalent

dimerization can take a place between two Sema3A domains[215]. To study the effect of dimerization on GAG-binding, mutation of the dimerization interface, which have been already reported by *Antipenko et al*., would be required[215].

1.6.3.3 Limits of SPR study

Despite the originality of this interaction study, orientation of CS chains on SPR sensor chip which mimics the orientation in ECM, we are far from reproducing the ECM conditions. We are able to control the quantity of GAG on SPR surface but not their distribution and disposition. Density of GAGs on the cell surface potentially influences the protein binding. In addition to the "immobilization heterogeneity" and "mass transfer", binding of the analyte to several GAG chains and "crosslink" them can also affect the data. "Re-binding" of the protein to the unoccupied site, before diffusing out, distorts the k_{off} which becomes slower than the true k_{off}. On the other hand, association rate are very high (over 10^7) which is the limit of the instrument measurement. The affinity of Sema3A to CS-E could be much higher than what we obtained.

1.7 Sema3A WT – CS oligosaccharides interaction analysis using SPR (CS oligosaccharides-binding)

To identify the minimal oligosaccharide length Sema3A requires to bind to CS-E, we made use of size defined CS-E molecules (di-, tetra-, or hexa- saccharides) that were produced and biotinylated by chemical synthesis by Chrystel Lopin-Bon lab, Orleans[308] **(Figure 57.A)**. Injection of Sema3A over these size-defined oligosaccharides that were immobilized at a level of 70 RU, demonstrated that Sema3A binds well to the tetra- and hexa-saccharides, for which K_D of 96.72 ± 35.16 pM and K_D=74.67 ± 23.23 pM, respectively, were calculated. However, Sema 3A does not bind to the disaccharide **(Figure 57.B-D**). Hence, tetra CS-E motif is the minimal oligosaccharide length sufficient for Sema3A binding.

This analysis allows us a better understanding of interaction between well-defined CS structure and Sema3A. However in physiological conditions, CSPGs are usually composed of long CS chains containing different type of CS units, hence a plethora of combinations arises. For example, we do not know about two units of CS-E separated by one unit of CS-A. We do

not know how the rest of chain, surrounding the potential binding domain, could influence this binding.

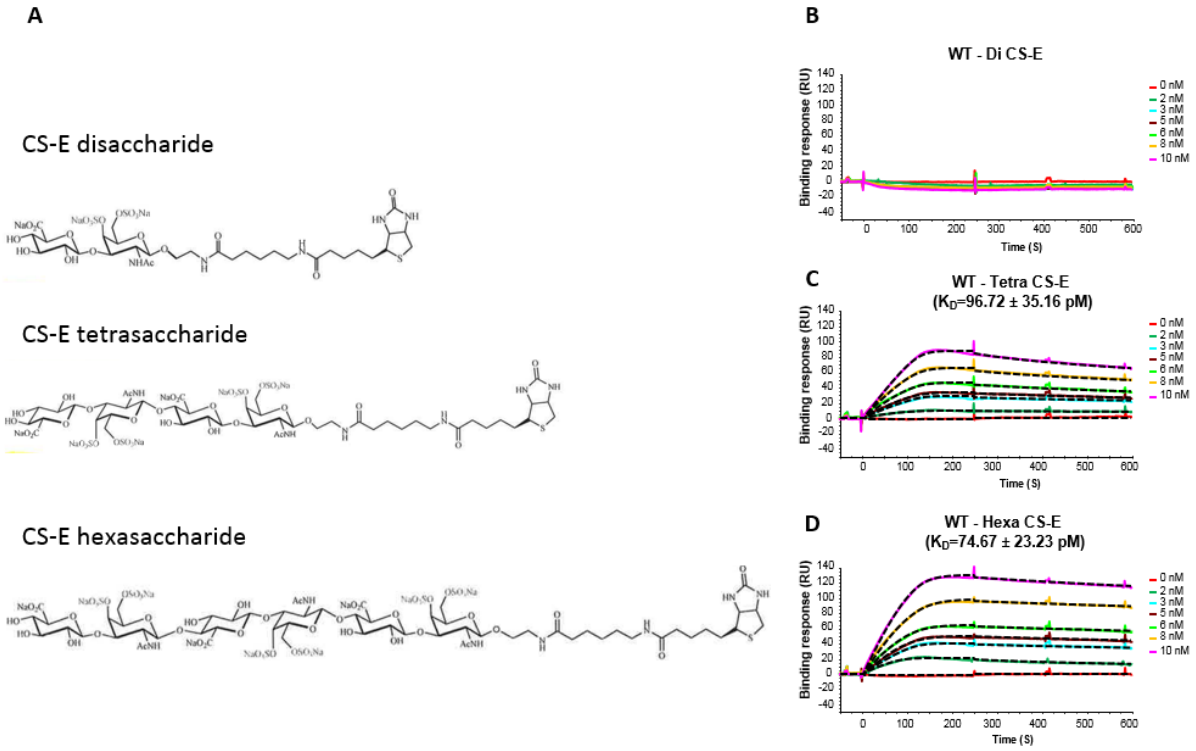

Figure 57: Sema3A requires a minimal motif of tetrasaccharide to bind to CS-E.
(A) Synthetic biotinylated chondroitin sulphate CS-E (di, tetra and hexasaccharide) oligosaccharides. **(B)** Sema3A-90 does not bind to di-CSE in [2-10 nM] range**. (C and D)** Sema3A-90 binds with a high affinity to tetra and hexa CS-E respectively. 70 RU of oligosaccharides were immobilised by their biotinylated reducing end. [0-10 nM] range of concentrations for Sema3A-90 were injected at 60 µl/min. K_D values were determined by fitting to1:1 Langmuir binding model with mass transfer. Coloured and dotted lines represent the binding data and the result of the fit, respectively. K_D value presents the mean of two experiments ± standard deviation of the mean.

Further analysis with CS-D oligosaccharides should be performed. Indeed, we have a synthetic di and hexa-saccharide of CS-D which are not and cannot be biotinylated. We tried to set up competition assay between immobilised CS-E and CS-D in solution. We incubated Sema3A-90 with CS-D or no (as a control) in [150-350 mM] NaCl concentration. Resulted data showed that the binding is decreased in both CS-D condition and control. Incubation of Sema3A-90 in lower salt concentration leads to its precipitation, thus a decrease in the CSE-binding. Other alternatives should be considered to overcome this issue such adding BSA which may stabilise the protein and prevents Sema3A to stick to the tube wall. As CS-D chains contain only 30 % of CS-D units and no interaction was observed between these chains

and Sema3A in SPR, it will be very interesting to analyse CS-D oligosaccharide-Sema3A interaction.

1.8 Role of GAGs in furin-cleavage of Sema3A

The role of Sema3A binding to GAG remains poorly known. Here we hypothesised that GAG could protect Sema3A from furin cleavage, hence a role of Sema3A binding to the GAG. To experiment this, we first treated HEK293-6E cells expressing Sema3A with furin after washing them with PBS. After different time, a fraction of cells was taken for centrifugation. The cell pellet was treated with PBS containing 1 M NaCl to release the bound Sema3A from the cell surface. Both the culture medium and cell surface-associated protein were analysed in WB with an antibody directed against Sema3A domain. Results show that Sema3A-65 fraction increases over time in cell surface-associated protein and supernatant in furin-treated cells condition **(Figure 58.A)**. GAGs on HEK cells surface do not protect Sema3A from furin cleavage at least at the first furin-cleavage site (since we only analysed the release of the 65 kDa fragment). This is consistent with the observation that the first furin cleavage site is not involved in binding to GAGs and thus should remain accessible to furin mediated processing. Sema3A-65 of the supernatant is probably resulted from the cleavage of cell surface Sema3A-90 and from the cleavage of Sema3A-90 released in furin buffer that we observed already in T=0 h.

Another experiment was performed, in solution, to analyse the role of CS-E in furin-cleavage of Sema3A at site 1. Purified Sema3A-90 was incubated with CS-E and treated with furin. Furin cleaves Sema3A-90 in the presence of CSs **(Figure 58.B)**. Thus, CS does not protect Sema3A from furin cleavage.

Together, these two furin cleavage assays, on cells expressing Sema3A and purified Sema3A, show that binding to GAGs does not prevent the furin cleavage, hence GAG binding is likely having another role. However, we cannot exclude the fact that CS could help the furin-cleavage especially in physiological conditions.

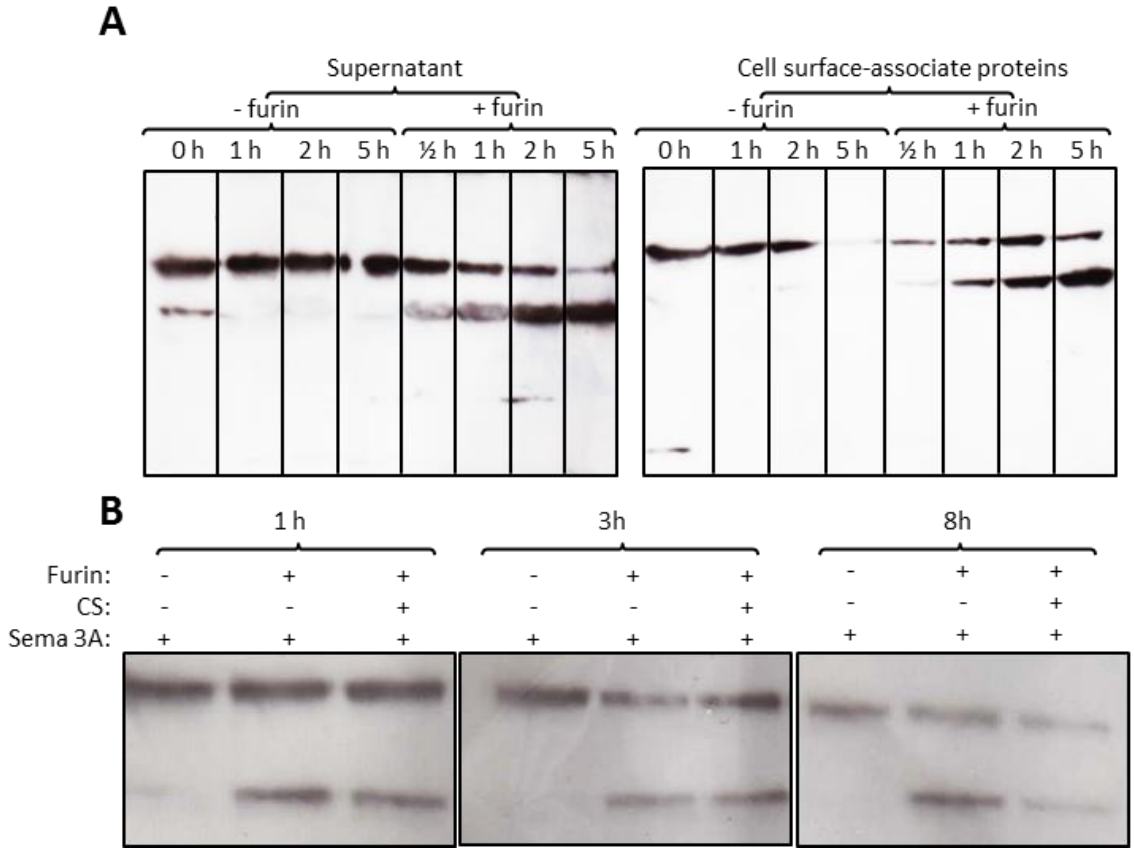

Figure 58: Sema3A cleavage by furin.
(A) WB analysis of the cleavage of Sema3A in HEK293-6E cell surface by an addition of commercial furin. HEK293-6E cells expressing Sema3A were washed with PBS and treated with furin. After 0, 1/2, 1, 2 and 5 h, fraction of cells was centrifuged and the cell pellet was treated with PBS containing 1 M NaCl. Both culture medium and cell surface associated protein were analysed. **(B)** Purified Sema3A-90 was treated with furin in the presence or not of CS-E for 1, 2 and 8 h and analysed by WB. WB analysis was performed with an antibody directed against a Sema3A domain.

1.9 Sema3A WT and mutants-GAG interaction analysis using QCM-D (rigidification of GAG film)

We have reported earlier that Sema3A-transfected HEK293-6E cells clusters once Sema3A is secreted **(Figure 44.F)**. We hypothesized that the Sema3A on the cell surface interacts with GAG chains from different cells, which results in cells clusterisation. To test this hypothesis, we first analysed in QCM-D the changes in GAG (HS, CS-E or CS-D) film thickness and softness induced by full length Sema3A WT and mutants (1-4), and Sema3A-65.

1.9.1 QCM-D principle

QCM-D is an acoustic technique measuring frequency (Δf, Hz) of oscillating quartz crystal and energy loss (dissipation, ΔD) per oscillation. Changes in mass (*e.g.* through binding of molecules) on the quartz surface induces changes in frequency of oscillating crystal and dissipation. Δf measures the binding of molecules to the quartz surface, and ΔD measures viscoelasticity properties related to the film thickness and softness **(Figure 59)**. In this analysis, as in SPR, biotinylated GAGs: CS-D, CS-E and HS are immobilized on streptavidin layer supported by lipid bilayer. This disposition allows the GAG chains movement in the film. Sema3A proteins were injected over the film **(Figure 59)**. For example, here if Sema3A binds to the GAG film, the oscillation frequency will decrease and dissipation will increase (the film becomes thicker due to the binding of protein). However, dissipation can decrease if Sema3A induces the collapse of the film (the film becomes thinner) upon binding, hence more rigid. This rigidification could be the result of crosslinking of several GAG chains.

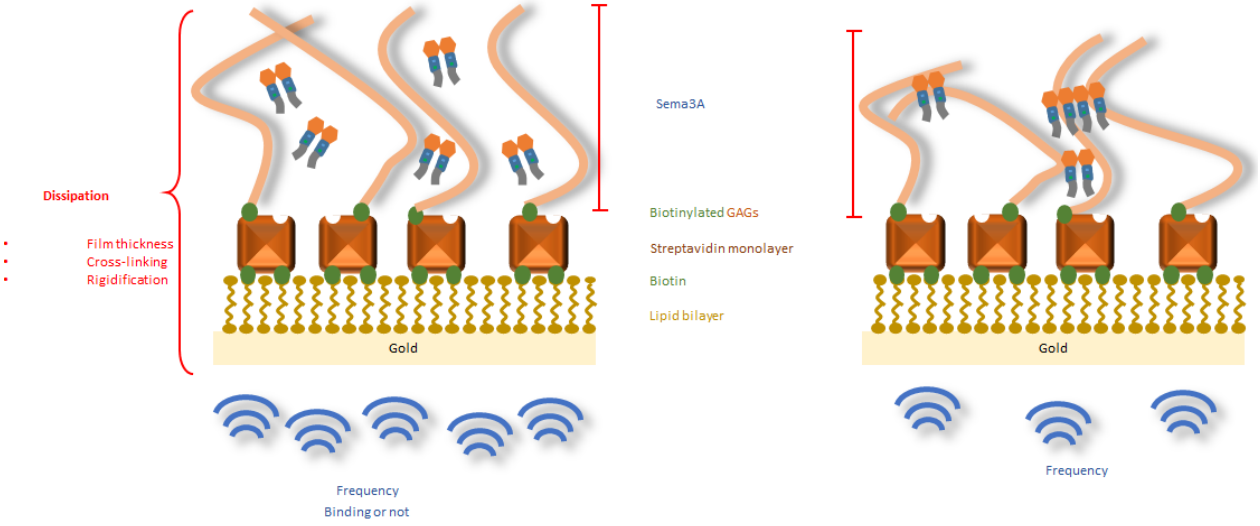

Figure 59 : Schematic representation of QCM-D principle measuring frequency and dissipation.
GAGs are immobilized on a streptavidin layer supported by lipid bilayer. Sema3A is injected over the film.

While SPR measures only one parameter which is the interaction of two molecules, QCM-D measures in addition to the binding, the energy dissipation providing us information about the film thickness and rigidification. Moreover, GAGs are immobilised on lipid bilayer that mimics the plasma membrane and allows the movement of GAG chains. In contrast to

SPR, QCM-D (although it is quantitative) will not provide information on the binding affinity (K_D) of Sema3A to the GAG film. QCM-D measures the change of total mass. This mass includes amount of H_2O varying between 10-90 %. Dissipation could inform us if the formed film is rigid (less water) or soft (water rich). Furthermore, as in SPR, four conditions can be analysed in the same time. Nevertheless, the flow cells are completely independent from each other in QCM-D, in contrary to SPR sensor chip where the flow cells are connected.

1.9.2 GAG film formation

To form the GAG film, first lipid bilayer, which serves as a support for the GAG film, was constituted by injecting biotinylated vesicles which spread to form lipid bilayer. Adhesion of the lipid on the sensor reaches -50 Hz of frequency shift and +4 x 10^{-6} of dissipation shift in ~ 3 min after injection **(Figure 60.A)**. Then, the frequency increases to -25 Hz and dissipation decreases to regain its initial value (0), indicating thus the spread of vesicles and rigid lipid bilayer formation. Formed bilayer was then coated by streptavidin which engages at least two biotin-binding sites for a stable immobilisation[313]. Streptavidin was added up to saturation, allowing thus a homogeneous streptavidin monolayer formation which serves as tool of GAG anchoring in the lipid bilayer. Addition of streptavidin leads to a consistent -25 Hz of frequency shift and ~ 0.5 10^{-6} of dissipation shift **(Figure 60.B)**. Biotinylated GAGs (HS, CS-E or CS-D) were then immobilised by their biotinylated reducing end, as in SPR. They were also injected up to saturation at 10 µg/ml concentration. HS saturates the surface in > 10 min and induces a decrease of dissipation to ~ -20 Hz and increase of dissipation to +4 x 10^{-6}, confirming HS binding to the surface, while CS-E and CS-D saturate the surface in 20 min and the association rate is slower than HS. CS-E and CS-D decrease frequencies to ~ -40 and -43 Hz, respectively and increase dissipation to 12 and 9 x 10^{-6}, respectively **(Figure 60.C and D)**. Difference in saturation rate between HS and CS-E/CS-D is due to MWs difference (HS ≃ 12 kDa, CS-E ≃ 30 kDa and CS-D ≃ 38 kDa) resulting differences in molar concentrations. Frequency shift induced by the GAG is proportional to the MW, while the dissipation shift is related to MW and sulphation pattern of GAGs, as observed with CS-E and CS-D. Indeed, despite the higher MW of CS-D, dissipation shift is higher in CS-E and this could due to the higher sulphation in CS-E as reported above. The resulted values (frequency and dissipation shifts) after each step of the film formation are reproducible in all experiments and constitute an indication of correct film formation.

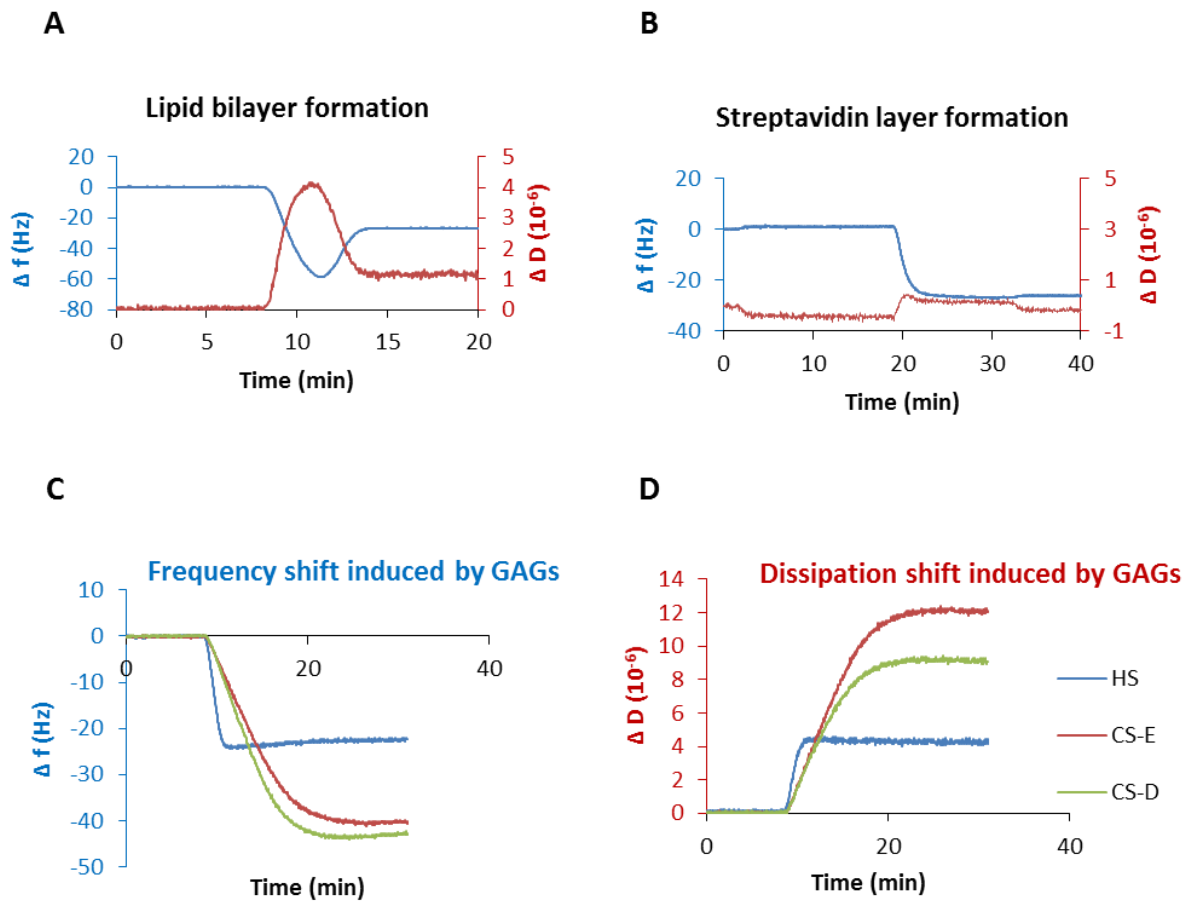

Figure 60: different steps of GAG film formation in QCM-D.
(A-B) Frequency and dissipation shift induced by lipid bilayer and streptavidin layer formation, respectively. **(C-D)** Frequency and dissipation shift, respectively, induced by different types of GAG (HS, CS-E and CS-D).

1.9.3 Sema3A proteins binding analysis

To analyse the effect of Sema3A and its mutants on the GAG film, proteins were injected at 20 µl/min up to reach equilibrium. Sema3A-90 WT and Mut 1 bind to HS and CS-E as seen in SPR, but also to CS-D **(Figure 61.A; Table 13)**. In parallel, they induce a strong decrease of dissipation in HS and CS-E film but weaker in CS-D film **(Figure 61.B; Table 13)**. This indicates that Sema3A rigidifies HS and CS-E film and it is confirmed by the parametric plot, measuring ratio ΔD /-Δf versus -Δf, indicating thus changes in the film softness **(Figure 61.C)**. Immobilisation of the GAG (blue and green dots) results in unchanged ΔD /-Δf ratio showing formation of a soft film. Whereas, once WT or Mut 1 was added, ΔD /-Δf ratio decreases drastically with CS-E and HS showing a rigidification induction **(Figure 61.C)**. Mut 2 binds strongly to HS as the WT, but the association to CS-E

is very slower without reaching the equilibrium **(Figure 61.A; Table 13).** Moreover, the binding does not induce any film mechanical property changes **(Figure 61.B; Table 13)**. Mut 3, Mut 4 and Sema3A-65 do not display any binding to any GAG as obtained in SPR **(Figure 61.A and B).**

Table 13: Frequency and dissipation shift resulting from injecting Sema3A-90 WT, Mut-1 and Mut-2 over HS, CS-E and CS-D films in QCM-D.

	Frequency shift (Hz)			**Dissipation shift (X 10^{-6})**		
	HS	CS-E	CS-D	HS	CS-E	CS-D
WT	-20	-28	-11	-1.3	-4.3	-1
Mut 1	-20.5	-42	-11.2	-1.3	-6	-1.2
Mut 2	-34	-9	0	0	0	0

The frequency shift results confirm the binding in SPR, unless for CS-D. No binding to CS-D was observed in SPR, while it is detected in QCM-D. This could be due to the fact that in QCM-D, in contrary to SPR, we saturated the sensor chip surface with GAG, making GAG chains closer to each other. This could promote the binding of Sema3A to GAG chains especially if Sema3A binding is multivalent. In addition, movement of GAG chains on lipid bilayer would also help the binding. Dissipation results indicate that Sema3A-90 binding induces rigidification of the GAG film suggesting that Sema3A could cross-link GAGs chains. This will be confirmed by further investigation as fluorescence recovery after photo bleaching (FRAP). Cluster 2 is not important for binding to GAGs, but it is somehow involved in the rigidification of GAGs film as the WT. This suggests that two mutated amino acids of this cluster are important for an adequate structure allowing crosslink of GAG chains.

It has been reported before that Sema3A is a component of PNNs[130]. Our finding suggests thus another role to Sema3A in PNNs, in addition on its role as a signalling molecule controlling guidance and plasticity. It could also serve as a molecule involved in the building of the highly structured net by crosslinking the CS chains of CSPGs in the PNNs.

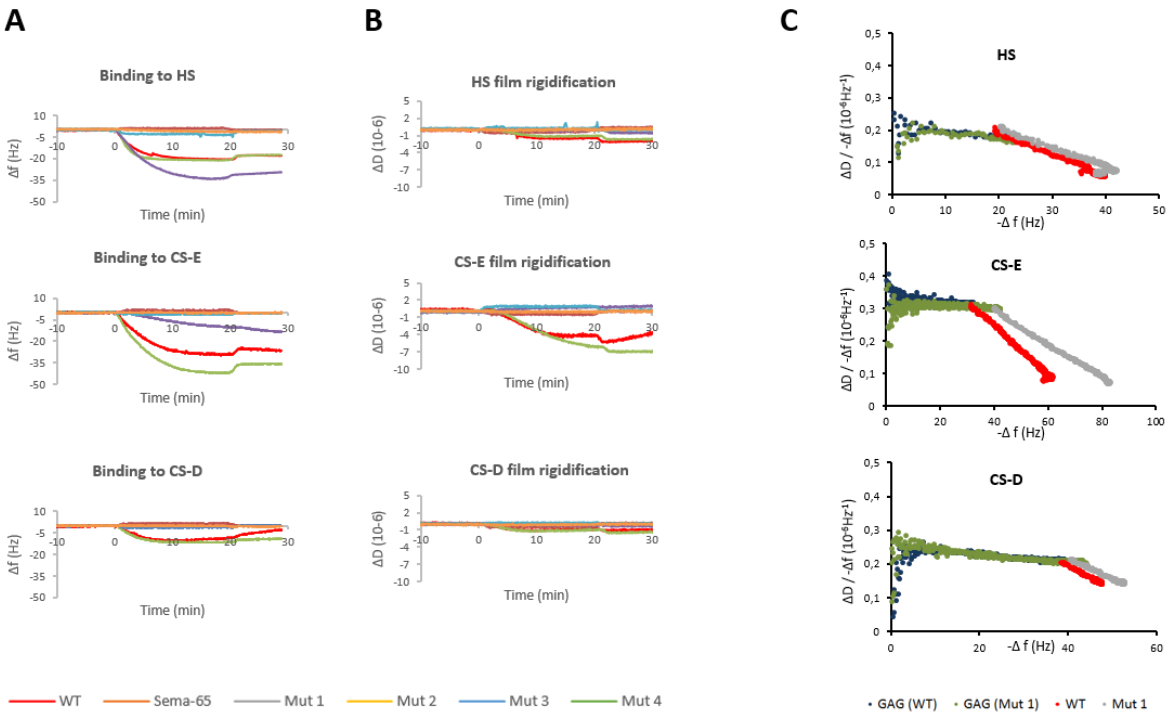

Figure 61: Sema3A WT and mutants - GAGs analysis in QCM-D
(A and B) QCM-D analysis of WT, Mut 1 and Mut 2 binding to HS, CS-E and CS-D measuring the frequency (Δ f, Hz) and dissipation shift (Δ D) induced by the binding of proteins to the GAG film. 20 µg/ml proteins were injected up to the equilibrium at 20 µl/min. A decrease in frequency indicates the binding of the protein and the decrease of dissipation indicates GAG film rigidification. **(C)** Parametric plot indicating the film softness changes, expressed by Δ D / -Δ f versus -Δ f, induced by the binding of Sema3A-WT (red) or Mut 1 (grey) to the GAG film (HS, CS-E or CS-D). The softness for the GAGs film formation, on which Sema3A or Mut 1 were injected is also represented in blue and green, respectively.

1.10 Effect of Sema3A WT and mutants on neurite outgrowth of dorsal root ganglion neurons in culture

Activity of Sema3A is usually evaluated by its ability to induce the collapse of the growth cone or to inhibit the neurites outgrowth of DRG neurons in culture. Here, we assessed the effect of Sema3A and its mutants on inhibition of DRG neurons neurites outgrowth, to check the activity of purified Sema3A and to assess the importance of identified GAG-binding sequences in Sema3A signalling *in vitro*. Dissociated adult rat DRG neurons, which lose their neurites during extraction process, were cultivated in the presence of 100 ng/ml NGF. Neurons were then treated with PBS (negative control), 2 µg/ml of commercial Sema3A (positive control), different concentrations of Sema3A-90 WT and 2 µg/ml of Sema3A-65, Mut 1, Mut 2, Mut 3 and Mut 4 **(Figure 62.A)**. The number of neurons projecting neurites in each condition was quantified and presented as percentage of neurons with neurites **(Figure 62.B)**.

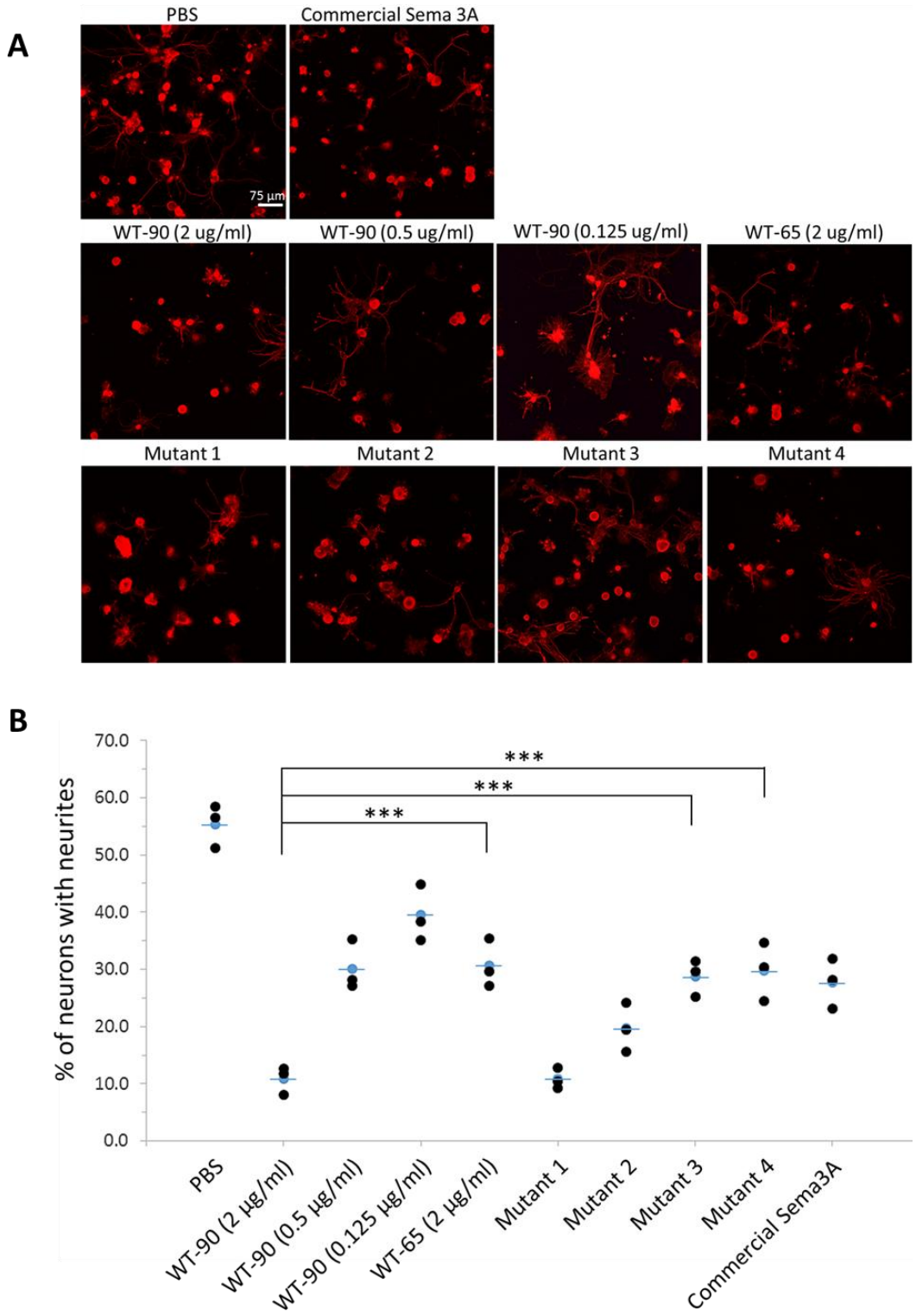

Figure 62 : Effect of Sema3A WT and mutants on neurites outgrowth of dissociated DRG neurons in culture.

(A) DRG neurons were cultured in the presence of various forms of Sema3A (WT concentrations are indicated on the top of each image and the concentration of other proteins is 2 µg/ml) for 48 hours before fixation. Neurons were then stained with beta-III tubulin and DAPI. Confocal images were taken using Zeiss LSM 700 microscope. **(B)** Data were obtained from culture of 3 rats, 3 coverslips per rat and 5 views per coverslip. Percentage of neurons with neurites were counted (*i.e.* the length of neurite is 2 times longer than the cell body) and an average was calculated for every rat (black dots). Blue lines represent the average from the three rats.

The results show firstly that purified Sema3A-90 WT inhibits neurites outgrowth, thus, the purified protein is active. Secondly, this inhibition effect is Sema3A concentration-dependant **(Figure 62.B)**. Sema3A displays an important inhibition effect at 2 µg/ml. This concentration was then used to analyse the effect of other proteins. Sema3A-90 is more inhibitory (three times) than Sema3A-65, indicating thus the importance of C-ter domains to potentiate the inhibitory effect of Sema3A. Mut 1 and Mut 2 induce the same level of inhibition as the Sema3A-90 WT, while Mut 3 and Mut 4 display the same level of inhibition as Sema3A-65 **(Figure 62.B)**.

Results of this functional assay on DRG neurons are proportional to the GAG-binding assays which showed that clusters 3 and 4 of the basic C-ter tail are required for the GAG-binding. These data indicate the importance of GAG-binding sequences to reach an important inhibition of neurites outgrowth, suggesting thus binding of Sema3A to GAGs enhances Sema3A function. It has been already reported that Sema3A-65 has a reduced activity[269]. This diminution in activity could due to the absence of GAG-binding sequences and not to absence of the whole C-ter part. Indeed, GAGs may stabilise the binding of Sema3A to Nrp1-PlxA1 and could be a part of the signalling complex.

2. Rat brain chondroitin sulphates (CSs)

Interaction study of Sema3A with commercial GAGs (which are mainly from marine animal), discussed in the previous sections, enabled us to characterise the Sema3A binding to GAGs: GAG-related specificity, affinity, binding sites on Sema3A and finally minimal required motif on CS. Since we are interested in Sema3A in PNNs context, it would be interesting to evaluate Sema3A interaction with PNNs GAGs, notably CSs. To this purpose, we proceeded by extraction of adult rat brain GAGs.

2.1 Rat brain GAGs extraction

GAGs of each brain ECM compartment (loose matrix, membrane-associated matrix and PNNs) were extracted separately from two 3 months Sprague Dawley rat brains (1 brain ≈ 2 g) using four sequential buffers (B1-B4) as described in material and methods and according to *Kwok et al.*[305] **(Figure 63.A)**. Since the first step of extraction, which consists in

mechanical homogenisation, could induce the releasing of PNNs in earlier buffers[305], the quality of the extraction is checked by WB analysis using an antibody against HAPLN1, a link protein specific to PNNs. In the optimal conditions of extraction and a gentle homogenisation, HAPLN1 appears gradually throughout the extraction and is much more abundant in B4. This analysis confirmed that PNNs were extracted in the right buffer **(Figure 63.B)**. The presence of GAGs at the end of extraction was visualised in PAGE (20% gel) and azure A staining, a basic dye. The staining shows that GAGs are more abundant in the extraction with B1 and B2. The staining of extracted GAGs showed an expanded migration throughout the lane, as compared with the commercial GAGs (CS-A, CS-B and heparin), indicating a large size heterogeneity of rat brain GAG chains **(Figure 63.C)**. The quantity of isolated GAGs was measured using CPC turbidity assay and calculated from the linear regression equation of commercial CS-A standard. As seen in azure A staining, B1 and B2 contain more GAGs (~ 500 and 200 µg, respectively) than B3 and B4 GAGs (~ 100 and 50 µg, respectively) **(Figure 63.D and E)**.

To purify CSs from extracted GAGs, heparinases digestion was performed to separate CS from HS. DNase treatment was also performed to remove potential contaminating DNA. DEAE anion exchange chromatography was then carried out to discard the digested products and hyaluronan. Purified CSs were used for disaccharides analysis and biotinylation for SPR analysis.

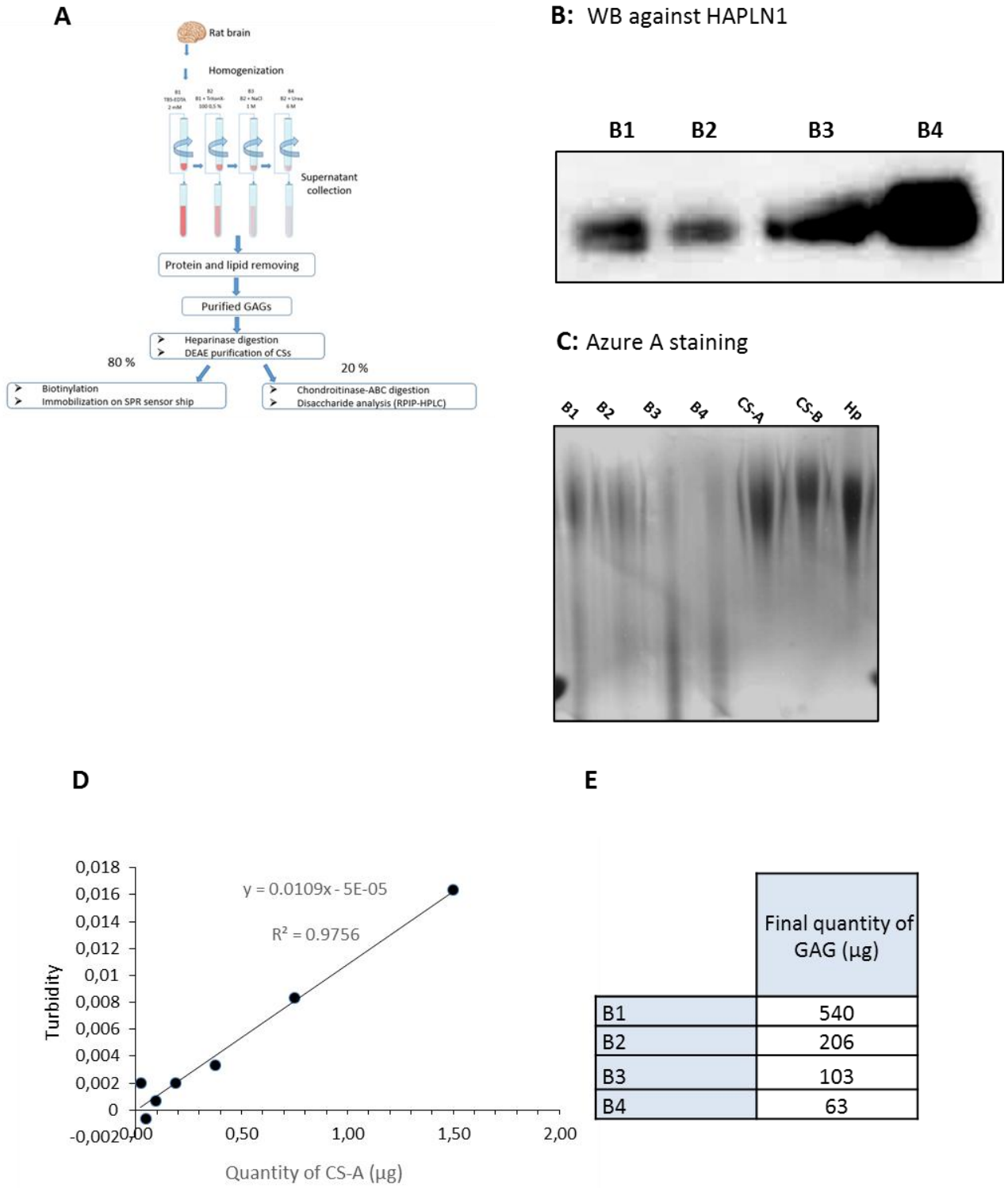

Figure 63: Extraction of GAGs from rat brain.
(A) Schematic representation summarising the protocol followed for CS purification from rat brain. **(B)** Western blot identifying the PNN link protein HAPLN1 in B1-B4, exposition time: 30 s. **(C)** Azure A staining of extracted GAGs (20 % acrylamide gel) with four sequential buffers (B1-B4). Commercial CS-A, CS-B and heparin (Hp) represent positive controls. 5 µg of GAGs are loaded in each well. **(D)** Example of CS-A standard curve resulting from the turbidity assay as measured by absorbance at 405 nm. R^2 represents the coefficient of determination. **(E)** Representative quantities of GAGs extraction with B1-B4 of two rat brains, calculated from the linear regression equation of the standard.

2.2 Disaccharides analysis of brain CSs

2.2.1 Principle

Disaccharides analysis using reversed-phase ion-pair high-performance liquid chromatography (RPIP-HPLC) is a sensitive quantitative method to analyse the disaccharides composition of GAG chains after a complete digestion. This technique is based on resolutive separation in reverse phase chromatography of disaccharides units charged and sulphated differently. An ion pairing agent is added to the mobile phase. The hydrophobic part of this reagent is retained by the apolar stationary phase. The hydrophilic part interacts with the disaccharide units, thus resulting in important retention of the sample. Elution of molecules is performed by NaCl gradient. Eluted molecules undergo then a post-colon labelling by a fluorogenic component which interacts with the reducing end of the disaccharide. The fluorescence is then detected on line and quantified **(Figure 64)**. This method reduces the sample amount from 30 ng in a usual HPLC to 2 ng in the current method. Previous PNNs composition analysis was mainly performed with semi-quantitative fluorophore-associated carbohydrate electrophoresis (FACE) due to its sensitivity. Traditional HPLC is not able to analyse the small amount of glycans isolated from the PNN in a single rat brain. Using RPIP-HPLC method, we could analysis CS content from as less as 0.5 % of the total glycans extracted from one adult rat brain. The method could allow regional analysis of PNN glycans in the brain.

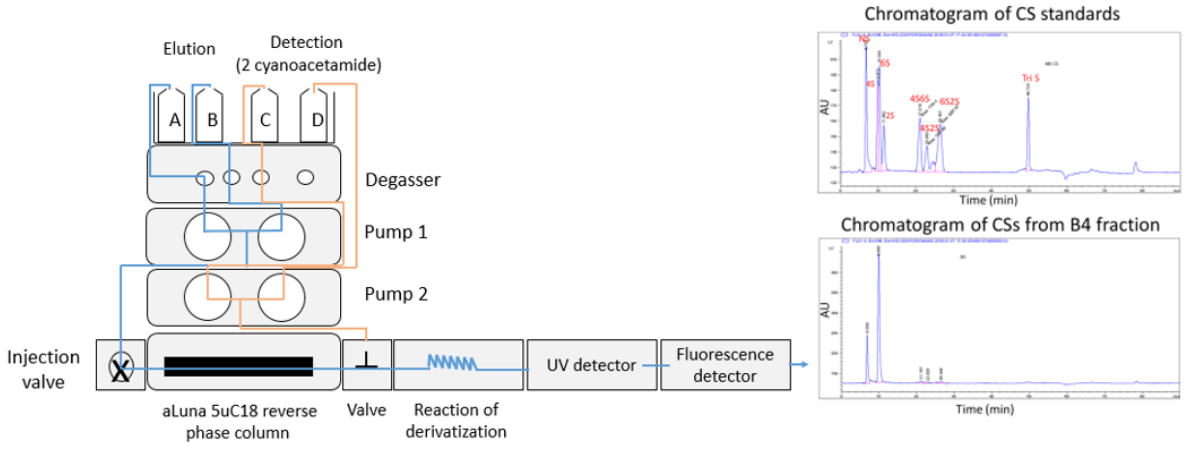

Figure 64: Reverse-phase ion-pair high-performance liquid chromatography (RPIP-HPLC).
(Left) Schematic representation of RPIP-HPLC system and post-column labelling. (Right) Examples of generated chromatograms of standards (top) and samples (bottom).

2.2.2 Disaccharide analysis

20 % (~ 2 µg) of total purified brain CSs (from 2 rat brains) was digested using ChABC to generate CS disaccharide units from which 2% were used for the RPIP-HPLC analysis. The results show that CS-A unit is the predominant isoform and it is more abundant in the soluble ECM and membrane associated-ECM (B1 and B2). The non-sulphated CS unit increased from the soluble ECM to PNNs (B1 to B4). On the contrary, the disulphated CSs: 4S6S and 2S6S (CS-E and CS-D, respectively) are enriched in PNN fraction. Whereas, 2S4S units are the same in all extracts **(Figure 65)**. This disaccharide analysis results are comparable to the observation of *Deepa et al.*[185] It demonstrates that PNN has a specific sulphation pattern which may account for the different functions of PNN-associated CSs.

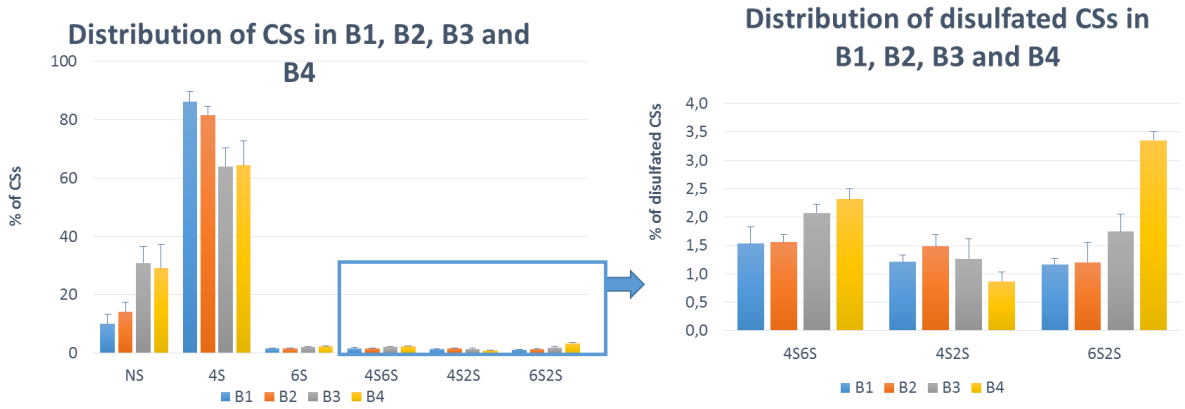

Figure 65: Disaccharide composition of CS in rat brain.
Disaccharide percentage of CS/DS units in B1-B4 extracted from adult rat brain. Results present the mean of 3 different extracts ± SEM. The blue square represents the magnification of the disulphated units; n=4 different samples.

2.3 Biotinylation of rat brain CS and their immobilisation on SPR sensor chip

The 80 % remaining from the purified brain CS was biotinylated using NHS-biotin. Indeed, digestion of the core protein by the pronase, which digests the proteoglycan core protein, left a small peptide containing the serine attached to the GAG *via* it OH. Biotin is then crosslinked with the primary amine of peptide. The success of biotinylation was checked by a dot blot **(Figure 66.A)**. The same intensity was obtained for the same concentration in all conditions, indicating thus all CSs are biotinylated in the same way.

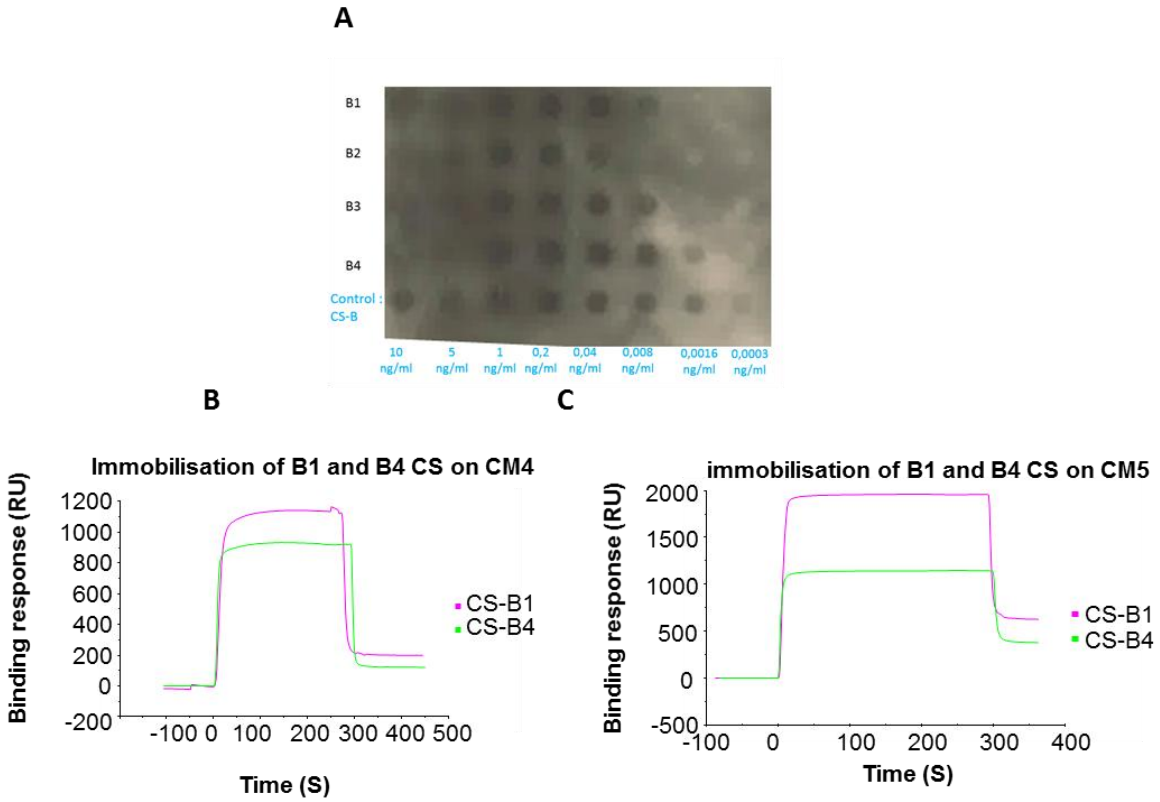

Figure 66: Biotinylation of rat brain CS and their immobilisation on SPR sensor ship.
(A) Dot blot showing the biotinylation of CS extracted with B1-B4 from adult rat brain. Biotinylated CS-B is used as a positive control. Blots of each lane corresponds to a serial dilution of biotinylated CS. **(B-C)** SPR sensorgrams of B1 and B4 CS immobilisation on CM4 and CM5 sensor ship, respectively. CSs were injected until saturation at 10 µl/min flow rate. Immobilisation of B1 CS on CM4 and CM5 results in 223 and 631 RU, respectively. Immobilisation of B4 CS on CM4 and CM5 results in 122 and 377 RU, respectively.

2.4 Sema3A-brain CS interaction analysis using SPR

It has been reported that Sema3A accumulates in PNNs *via* its interaction with CS[204 293]. To analyse this interaction, biotinylated CSs from B1 (as a control) and B4 were immobilised on a CM4 sensor chip to analyse their binding to Sema3A using SPR. SPR data show that biotinylated CS of B1 and B4 are well immobilised on the sensor chip, leading to a shift of 223 and 122 RU, respectively, following the injection over a streptavidin activated surface **(Figure 66.B)**. As CS were injected till saturation, the observed difference in immobilisation level between B1 and B4 extracted CS could be due to a difference in length of CS from loose matrix (B1) and PNN (B4); PNN CS are shorter. Injection of Sema3A, using the conditions set up above, did not result in the formation of a complex. Several hypotheses might explain this absence of interaction:

i) The quantity of CS on the surface is not sufficient for Sema3A binding. To answer this hypothesis, we used CM5 sensor chips that have a higher capture capacity than the CM4 sensor chips used until now. With such surface, we immobilized 16000 RU of streptavidin on which CS 631 and 377 RU of CS from B1 and B4 were captured respectively **(Figure 66.C)**. No binding could be observed on such surfaces, upon Sema3A injection in the 50-375 nM range. Absence of binding is thus due to another phenomenon.

ii) The percentage of CS-E motif (≤2 %) is not sufficient for Sema3A binding. Nevertheless, we demonstrated that a tetrasaccharide of CS-E is sufficient for Sema3A binding. It will be interesting to know in one hand, how the few CS-E units are distributed over the CS chains: individually or organised in domains? On the other hand, how Sema3A binds to PPN CSs: one molecule for one chain or one molecule binds to more than one chain? In this last case, Sema3A could bind and assemble individual units of different chains.

iii) Distribution of different types of CS units in PNNs could not be homogenous. For example, the low percentage of CS-E units carried by different chains could be concentrated in one area allowing the binding of Sema3A in physiological conditions. Extraction of CS from PNN disrupts this local concentration of CS-E motifs leading to a homogenous repartition of CS chains carrying CS-E units. Despite immobilisation of CS on SPR surface mimics the orientation of CS chains in PNNs, The CS-E units might not be sufficiently close to each other to enable Sema3A interaction.

iv) According to Azure A staining **(Figure 63.C)** revealed that the length of extracted CS could be heterologous notably in B4 where the staining is more intense at the bottom of the gel (small size CS). The length of immobilised B4 CS could be not sufficient to Sema3A binding. Especially if Sema3A binding requires more than one CS chain. It will be also interesting to analyse the length of CS chains in PNNs in order to know to which size of CS Sema3A binds and which size of CS is enriched in CS-E units. Therefore, it is very interesting to know if the sulphation pattern is dependent of chain length or vice versa.

Isothermal Titration Calorimetry (ITC) which allows analysis of interaction between molecules in solution could be an alternative for brain CS-Sema3A analysis.

3. Neuropilin 1

Nrp1 is a coreceptor of Sema3A and VEGF. Binding of Sema3A to Nrp 1 is required to trigger a signalling pathway *via* Plxn A, the Sema3A receptor. Interestingly, it has been shown that fraction of Nrp1 could carry a CS type GAG chain and thus that Nrp 1 is a CSPG. CS modification of Nrp1 modulates VEGF signalling[314]. Here, we wanted to analyse the role of this CS chain in Sema3A signalling to attribute a functional role for GAG-binding of Sema3A. To do this, we first produced, purified and analysed the protein

3.1 Nrp1 expression and purification

Recombinant plasmid containing soluble part of mouse Nrp1 (a1/a2, b1/b2 and MAM domain) tagged in C-ter with human Fc Ig-G1 and 6 X His, was expressed in HEK293-F cells growing in suspension. 4 days post-transfection, supernatant containing soluble Nrp1 was collected and purified using Ni-NTA column. Imidazole was exchanged against PBS by dilution-concentration. InstantBlue staining of Ni-NTA eluate reveals existence of two forms of protein: ~ 130 kDa which consists the majority of protein and high MW protein >170 kDa **(Figure 67.A)**. Theoretical MW of the expressed Nrp1 is 120 kDa. This ~10 kDa shift could due to post translational modifications, such as glycosylation. As it is reported before that fraction of Nrp1 could be a CSPG[314], we hypothesised that the upper band of > 170 kDa is gagosylated form of Nrp1. To confirm this, we treated the purified Nrp1 with ChABC to digest the CS chain and then analyse it in SDS-PAGE and WB. Results confirmed that this small fraction is CS-modified Nrp1 **(Figure 67.B)**. This is also confirmed in WB with an antibody directed against poly-His tag **(Figure 67.C)**.

We are here for now. In future experiments, we will separate the gagosylated and non-gagosylated Nrp1 (using DEAE which binds to the negative charges of the GAG) i) to analyse their interaction with Sema3A in SPR and ii) to check if the absence of the chain affects the binding. Whether it is the case, we can suppose that Nrp1 CS chain is thus involved in recruiting and binding of Sema3A to Nrp1. Furthermore, we will also analyse the interaction of Sema3A mutants and Nrp1 to identify maybe the Nrp1-binding site on Sema C-ter. Indeed, in addition to the Sema domain, the C-ter is also involved in Nrp1 binding. In conclusion this analysis would help us to gain insight about the role of GAG-binding in the first step of Sema3A signalling.

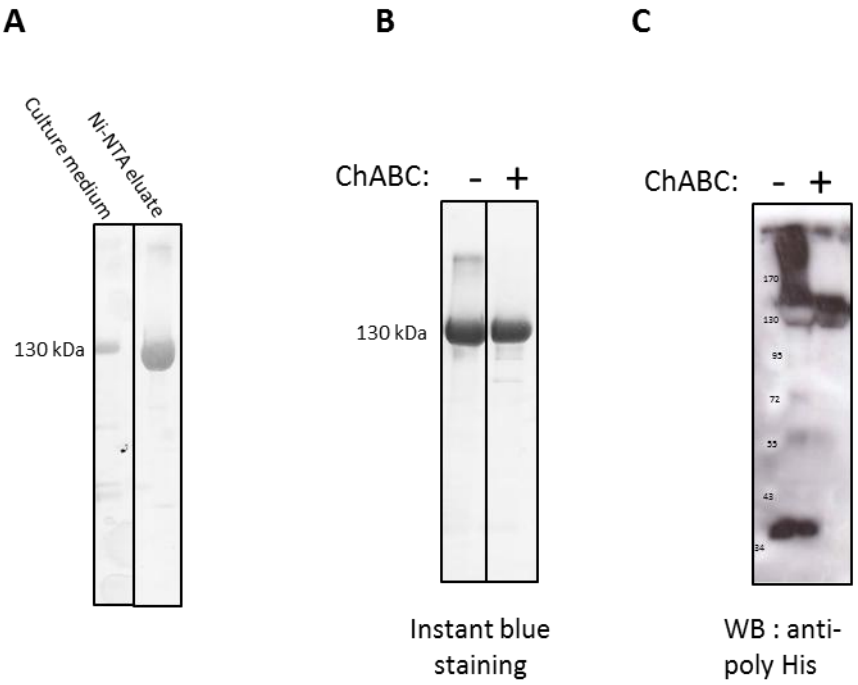

Figure 67: Nrp1 purification and ChABC digestion.
(A) Nrp1 expressed in HEK293-F cells was purified from the culture medium using Ni-NTA chromatography. **(B and C)** Purified Nrp1 was digested with ChABC and analysed in SDS-PAGE/ InstantBlue staining and in western blot with an antibody directed against poly-His tag.

General discussion and perspectives

Several proteins interact with GAGs to achieve their functions. The importance of this interaction is especially investigated and highlighted for the first step of protein signalling (receptor binding)[315]. However, this interaction could be involved in other processes. For example, GAG chains gather several proteins to constitute a reservoir of these molecules, link ECM components to enhance the stability of ECM network, and assembles multimeric complexes [316]. HS-protein interaction is the most investigated GAG-protein interaction due to the abundance of HS in several tissues, *e.g* HS-growth factors[317] and HS-chemokines[318] [319]. CS, the most abundant sulphated GAG in the CNS and cartilage, -protein is less investigated. Nonetheless, several molecules of the CNS are reported to interact with CS to implement their functions and we have listed them in the review *Djerbal et al.2017*[205] **(Appendix 1).** In this project we are interested in characterising the Sema3A-CS interaction interface. Both of these two molecules are found in PNNs which regulate the plasticity of neurons in adult CNS. Sema3A signalling could be involved in the inhibitory mechanisms of PNNs. The role of the interaction of Sema3A with CS is not elucidated. However, at least, CS is responsible of Sema3A accumulation in the PNN. Indeed, ChABC digestion of PNN CS leads to the removal of Sema3A from PNNs[293]. In addition to the proper location of Sema3A in PNN, CS may be involved in the Sema3A signalling and/or Sema3A processing by furin. Hence, the importance of characterising Sema3A-CS interaction.

Sema3A expression and purification protocol

We produced the recombinant Sema3A and its mutant proteins in HEK 293-6E cells. Two major forms are purified: full length Sema3A (90 kDa in reducing conditions) which remains attached to the cell surface and detached with 1 M NaCl and truncated Sema3A (65 kDa comprising Sema domain and a part of the PSI domain) which results from furin cleavage and released in the culture medium. Here for the first time Sema3A full length (Sema3A-90) is purified without resorting to the mutation of the first furin-cleavage site as what has been done to our knowledge in all previous studies analysing full length Sema3A[269] [217]. Moreover, the mutation at the first cleavage site does not protect the cleavage at the second cleavage site. Thus, the C-ter peptide of 1.3 kDa could be missed in the collected Sema3A. Here we set up a simple protocol to collect Sema3A full length and with a good yield (~ 5 mg/L). In addition of producing the protein, Sema3A expression in HEK293-6E

cells informs us about the interaction of the Sema3A and cell surface GAG. Indeed, detaching Sema3A-90 with NaCl ions suggests an ionic interaction between Sema3A and the GAG of the cell surface. Location of Sema3A on the cell surface was already observed in neurons in culture. The treatment of these neurons with ChABC releases full length Sema3A in the culture medium. Moreover, addition of GAG to the culture which competes with GAG of the cell surface, decreases Sema3A on the cell surface[295]. In further experiment, HEK293-6E expressing Sema3A will be treated with heparinases as HEK cells express more HS than CS to show that Sema3A remains attached to the cell surface through GAGs. The presence of Sema3A-90 on the cell surface and Sema3A-65 in the supernatant indicates likewise the importance of the C-ter domain in GAG interaction. Purification step in SP-sepharose indicates also the importance of the C-ter in the interaction with the negative charges of the resin since Sema3A-90 binds to the column, but not Sema3A-65. Furthermore, expression and purification of Sema3A mutants have also indicated the importance of different mutated sequences in GAG-binding. Indeed, mutants missing cluster 3 or cluster 4 which are responsible for the GAG-binding do not bind to the cell surface and bind weakly to the SP-sepharose, unlike the mutants displaying a mutation in cluster 1 or cluster 2 which are not involved in GAG-binding and purified from the cell surface as the WT and eluted at higher salt concentration from SP-sepharose as the WT. Sema3A expression in HEK293-6E cells and purification steps in order to produce the protein is thus also a first indication of the importance of a.a sequences in GAG-binding. The C-ter domain is already been thought to be the GAG-interacting sequence since it has a C-ter basic tail carrying the clusters 3 and 4. Two peptides containing cluster 3 or cluster 4 have been designed in a previous study and show an interaction with GAG. However, an a.a sequence in a peptide does not behave and interact in the same way as in the context of a 3D structured molecule[303].

A key issue in Sema3A expression and purification is the precipitation of full length Sema3A. Indeed, the protein precipitates at physiological salt concentration which causes issues notably in Sema3A-GAG interaction analysis in SPR. Therefore, the injections are performed manually to allow for a fresh and quick dilution before each injection, thus preventing long-term precipitation. Full length Sema3A precipitates also in the Centricon during concentration. This is a limiting factor to obtain a high concentration of this protein for analysis needing a high protein concentration such as SEC and crystallography. This sensibility and instability of the protein is likely due to the disordered C-ter basic tail. Indeed, this issue is not encountered with Sema3A-65. Moreover, Sema3A containing Sema domain,

PSI domain and Ig like domain (without the C-ter basic tail) has been produced for crystallography at a high concentration[217]. This suggests that the C-ter basic tail is responsible for the poor stability of the purified full length Sema3A. The high salt concentration and weak Sema3A-90 concentration in µM range did not perturb our analysis so far. However, further analysis may require finding optimal conditions for a higher stability. Combination Sema3A-90 with GAG could stabilise more the protein to reduce the NaCl concentration.

Another significant issue of purified Sema3A is the heterogeneity of the sample beyond the two common isoforms, Sema3A-90 and Sema3A-65, due to the dimerization of Sema3A and two furin-cleavage sites per monomer. On one hand, most of Sema3A studies use reducing conditions for the analysis. On the other hand, the cleavage at the second furin cleavage site releases a small peptide with negligible MW in SDS-PAGE. Hence, only the existence of the two forms Sema3A-90 (in non-reducing conditions) and Sema3A-65 are reported *in vitro* and even *in vivo*[269] [204]. Analytical ultracentrifugation analysis (AUC) (data not shown) confirmed the heterogeneity in our purified samples which is also observed in SDS-PAGE where we can notice sometimes a superposition of bands. Indeed, the activity of furin on Sema3A is variable from one cell batch to another *e.g* older cells display a high rate of cleavage than younger ones, in addition to other physiological parameters in which we have no control. Thus, the ratio between different isoforms varies from batch to batch. There are two ways of dimerization, the noncovalent dimerization conferred by the Sema domains which dependant of the buffer conditions notably pH and a covalent dimerization conferred by the C-ter disulfide bond. Combination of all these parameters potentially generates numerous isoforms of variable MWs **(Figure 68)**. However, some isoforms have approximately the same MW. Thus, it is not obvious to distinguish between them in SDS-PAGE or to separate them in SEC *e.g* the non-cleaved covalent dimer and the cleaved one in the second furin-cleavage site in one monomer (only 1.3 kDa missed). Does this small difference have an effect on the structure and activity of Sema3A? We do not know yet as the heterogeneity and isoforms resulted from dimerization and furin cleavage was almost not reported and discussed. However, this is an important issue and should be taken in consideration when analysing the importance of an a.a sequence in biochemical or physiological effect.

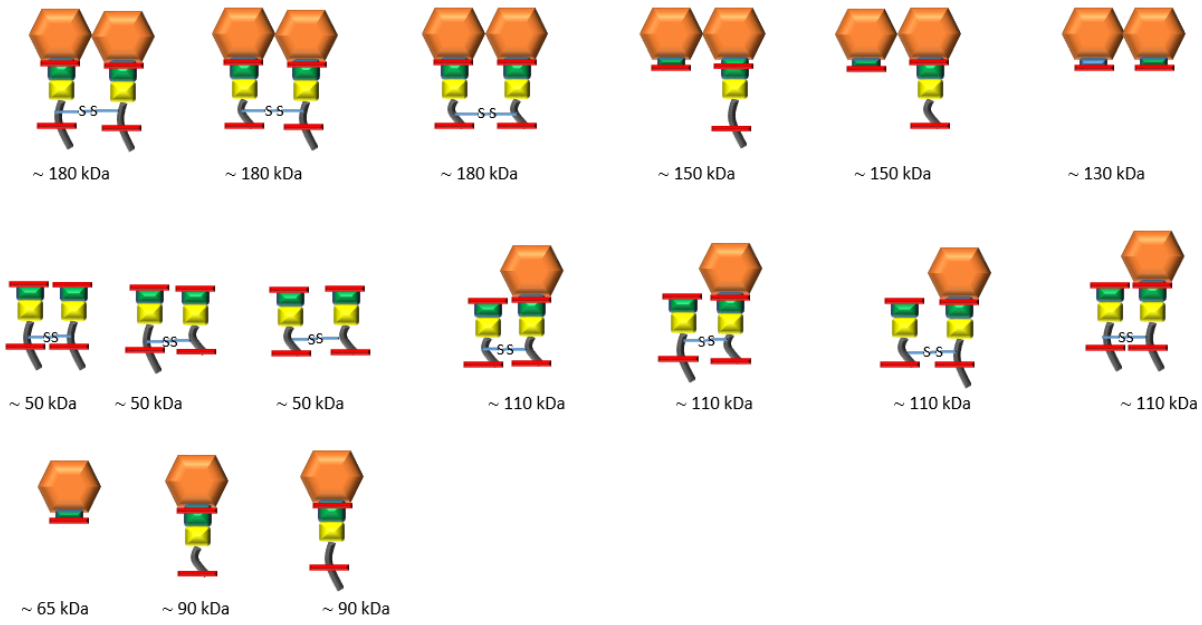

Figure 68: Theoretical Sema3A isoforms and their approximate MWs.
Furin cleavage sites are represented in red lines.

During Sema3A purification we did not pay enough attention to the released C-ter part resulted from furin cleavage at the first site. Indeed, we perform SDS-PAGE analysis in reducing conditions. Hence, the band corresponding to the peptide is at ~25 kDa and usually comes out the gel since we run it for long time to get a better separation. However, in cases that 25 kDa ladder does not exceed the gel, the band corresponding to the C-ter is absent or present in weak intensity. Thus, what is the fate of this peptide, does it remain attached to the cell surface despite 1 M NaCl treatment, or is it degraded? It will be interesting to purify the 25 kDa peptide and analyse its structure, for example using nuclear magnetic resonance (NMR) as the structure of the Sema3A C-ter part is not solved yet. Crystallising full length Sema3A bound to CS may stabilise the C-ter part and thus solving the 3D structure of the entire protein. It is also interesting to use it as a competitor of Sema3A full length for GAG-binding in physiological studies, as it contains the GAG-binding sequences.

Identification of GAG-Sema3A interaction interface

Based on the a.a primary sequence of Sema3A, we identified four potential GAG-binding sites rich in basic a.a which are common to the GAG-binding sites of proteins[205 320]. Only two of them, the two basic clusters on the C-ter basic tail, are validated in “heparin-

beads approach" and in site directed-mutagenesis. Indeed, the mutation of cluster 1 and 2 located on the structured domain, PSI and Ig-like domains, respectively, by a complete or partial substitution of the basic a.a, respectively, does not affect the CS-binding in SPR and QCM-D. In contrary, deletion either of cluster 3 or cluster 4, located at the C-ter basic tail, completely abolishes the CS-binding. Hence both of them are required at the same time for the binding. Cluster 3 sequence of Sema3A "KRDRKQRRQR" [708-717] encompasses a GAG-binding sequence reported in Otx2 "RKQRRER" [36-42] located in its C-ter. More precisely, the first two basic a.a are responsible for the binding as their mutation abolishes the GAG-binding[159]. It will be interesting to know which a.a are exactly involved in the interaction with CS by their individual substitution. Since we have shown that a tetra CS-E motif is sufficient for the binding and both clusters 3 and 4 are required, probably only some basic a.a from these two clusters could participate in the GAG-binding. Indeed, tetra CS-E length is approximately 2 nm and one a.a is about 3.5 Å (~ 7 a.a per tetrasaccharide). Thus, the flexible C-ter basic tail may adapt a conformation to involve a.a from both clusters separated by 17 a.a to interact with an oligosaccharide as small as a tetrasaccharide. In fact, it is common to find GAG-binding sites in flexible regions of the protein such as loops, whose positioning can adapt according to the structure of the opposite GAG *e.g* the GAG binding site of CC chemokine ligand 5 (CCL5) is located in loop strucutre[321].

The heterogeneity of the sulphation within GAG motifs as well as the distribution of different motifs throughout the GAG chain complicate the characterisation of protein-GAG interaction. The synthetic oligosaccharides with defined size, of which sulphation pattern are controlled, enables us to characterise confidently the required sulphate number and motif. We determined that CS-E tetrasaccharide as the minimal motif required for the binding. Interestingly, this length of CS-E is already reported to be required and sufficient to trigger physiological mechanisms such as neurites outgrowth of neurons through its interaction with growth factors such as midkine/pleiotrophin, already shown to interact with CS chains[181 202]. Structural analysis of CS-E tetrasaccharide revealed that all four sulphate groups are presented along a single face[181]. That may concentrate the negative charges in one side and may favour interaction with proteins. We reported that the disaccharide CS-E is not sufficient to make an interaction with protein. Is the length, the number of sulphate or both are not sufficient for the binding? For example, what about a monosaccharide CS-E in non-sulphated tetra or hexasaccharide? How much the negative charges of the two CS-E disaccharides should be close in order to mediate an interaction with protein? For example, two

disaccharide CS-E separated by another disaccharide would interact with protein? A lot of combination can be resulted from the diversity of motifs and their length and could be found within CS chains on the cell surface. However, for now, only some oligosaccharides of CS with homogeneous sulphation are synthetized, given the complexity of the synthesis processes[308 322]. In coming years, advances in synthesis chemistry should open opportunities to design a range of oligosaccharides with desired sulphation.

It is also in perspectives to analyse the minimal required sequence in HS, since Sema3A interacts with HS with the same affinity as with CS. Moreover, HSs are not as much abundant in brain as CSs but they represent a significant percentage in PNN (~30 %). HS may also participate in retaining Sema3A on the cell surface. Here we only purified and characterised CS of the rat brain. It is important to also purify the rat brain PNN HSs and analyse their binding to Sema3A in SPR. We characterised the binding of Sema3A mutants to only CS-E chains. It will be relevant, to analyse their interaction with commercial HS chains in SPR to know whether Sema3A binding to CS and HS involves the same binding sites.

Potential roles of GAG in Sema3A signalling and processing

Nrp1 could carry a single CS chain (CSPG). The role of this CS chain in VEGF signalling was already reported. GAG chain enhances the binding of VEGF to Nrp[241]. Moreover, the presence of heparin improves 100-fold the binding of VEGF to Nrp, suggesting thus that HS could help in bridging or stabilizing the VEGF-Nrp interaction[238]. It will be interesting to investigate this in Sema3A-Nrp1 interaction, *i.e.* whether the CS chain of Nrp 1 is important for recruiting Sema3A and help its binding to Nrp1 and whether the CS chains of CSPGs of the CNS matrix are involved in the binding of Sema3A to its receptor? This would enable to assign a role of Sema3A-GAG interaction in binding to the receptor, thus in Sema3A signalling, and this will be investigated in future studies.

Despite furin is mostly found in *trans*-Golgi, Sema3A is probably cleaved on the cell surface, after its secretion. Indeed, deletion of cluster 1, or deletion or substitution of all basic a.a of cluster 2 resulted in non-secreted protein. WB analysis of this non-secreted Sema3A showed the existence of only the full length Sema3A. In contrary, *Adams et al.*, in their suggested model of Sema3A cleavage by furin, mentioned that Sema3A could undergo a furin cleavage during secretion process[269]. However, they did not analyse the intracellular Sema3A[269]. All these raise an interesting question, how Sema3A is protected from furin

cleavage in Golgi? Do GAGs on the cell surface required for the optimal and differential cleavage of Sema3A by furin? Indeed, it is already reported that GAGs enhances the furin cleavage of viral proteins such as HIV-1 gp160 peptides and papillomavirus[323 324]. Moreover, usually furin cleavage site and GAG-binding site frequently overlap in proteins[325 326] as in Sema3A where the cluster 4 is the second furin cleavage site. In addition, we showed that GAG does not protect Sema3A from furin cleavage as we hypothesized it in the beginning. Further experiments should be performed to investigate whether Sema3A binding to GAG influences furin activity. This would enable to assign a role of Sema3A binding to GAGs in Sema3A activation/inactivation.

Interests of Sema3A-GAG interaction characterization

Characterisation of GAG binding site of Sema3A-GAG interaction interface would enable to design inhibitors, which could be of GAG or protein nature, to block the interaction. Some inhibitors blocking Sema3A effect were already reported. We have mentioned the existence of SICHI peptoid which blocks the Sema3A-GAG interaction and inhibits the Sema3A effects *in vitro*[302 303]. No *in vivo* analysis is reported yet on SICHI. Peptoids are synthetic molecules exogenous to the organisms, thus could be toxic as they are resistant to enzymes. In addition, the affinity of SICHI to GAG is not that high (K_D = 17 ± 2 µM)[303]. Using oligosaccharides of tetrasaccharide in size to block Sema3A could be more relevant since CS is naturally present in the organisms, thus availability of its catabolism machinery. CS chains and CS oligosaccharides are already used in treatment of osteoarthritis and knee joint pain and do not show any toxicity so far[327 328]. Moreover, Sema3A binds to CS oligosaccharides with a very high affinity, in pM range (K_D of tetra CS-E=96.72 ± 35.16 pM).

CS oligosaccharides are more stable and resistant to degradation and denaturation, contrary to peptides which are very sensitive to the degradation. Indeed, Nrp1-derived peptides have been already reported to inhibit the Sema3A effect. The first ones are peptides mimicking MAM domain of Nrp1 or Ig-like domain of Sema3A which inhibit Sema3A response, but at higher concentrations[329]. Soluble part of Nrp1 composing of a1/a2, b1/b2 and MAM domain is also reported to interfere with Sema3A binding to Nrp1 and inhibits growth cone collapse mediated by Sema3A *in vitro*[330]. However, soluble Nrp 1 is a high MW protein (~120 kDa) for administration and it is more subjected to degradation and denaturation. Thus, it is not the most recommended inhibitor for therapeutic use.

Finally, designing small probes, based on CS-binding sites identified in the C-ter basic tail of Sema3A that would enable *in vivo* imaging of PNNs using magnetic resonance imaging (MRI) will be very interesting. Indeed, the probes will interact with Sema-binding motif of PNN CS and would allow following the PNN development with age, changes within disease and comparison between different regions of the CNS.

Conclusion

To gain insight about how PNNs regulate plasticity, we aimed at characterising the interaction between Sema3A and CS. In fact, binding of Sema3A to CS is believed to potentiate Sema3A signalling to modulate plasticity. Characterizing this interaction may enable the design of new strategies aiming at enhancing plasticity and thus regeneration for neurodegenerative diseases or spinal cord injury.

For this purpose, we set up a protocol to express and purify full length Sema3A (90 kDa) as well as the furin-cleaved form composed of the N-ter part (65 kDa). We analysed the binding of the purified proteins to different type of GAGs: CS-E, CS-D and HS in SPR and Q-CMD. Full length Sema3A binds selectively and with a high affinity in the pM range to CS-E and HS, while truncated form does not. We then identified potential GAG-binding sites in the C-ter that we mutated using site directed mutagenesis and analysed their binding to CS-E to validate their importance in GAG-binding. Indeed, two basic clusters referred as cluster 3 and cluster 4 located in the C-ter basic tail are both required in the Sema3A binding to CS-E. Thus they constitute the CS-E-binding sites. Furthermore, using CS-E oligosaccharides produced by synthetic chemistry, we showed that the minimal binding sequence of CS-E for Sema3A binding is a tetrasaccharide. Thus the CS-Sema3A interaction interface is characterized.

To validate the importance of these GAG-binding sequences in Sema3A signalling *in vitro*, we analysed the effect of their mutation on DRG neurons in culture. Mutation of cluster 3 as well as cluster 4 reduces the inhibition effect of Sema3A on neurites outgrowth of DRG neurons. Thus, binding to CS may potentiate Sema3A signalling. Further experiments analysing interaction of Sema3A and its mutants with NRP1 containing a single CS chain (that we already expressed and purified) would highlight more the first signalling step of Sema3A. Moreover, we demonstrated that GAGs do not protect Sema3A from furin cleavage as hypothesised in the begging. It will be very interesting and relevant to highlight the relationship between furin-cleavage, CS-binding and receptors-binding of Sema3A to trigger a cell signal. This would determine the action of Sema3A not only in the CNS but also in other tissues where Sema3A is involved.

We also analysed Sema3A WT and mutants effect on CS-E, CS-D and HS films in QCM-D. Resulted data showed that Sema3A binding to CS-E and HS induces a decrease of dissipation which suggests that Sema3A may induce a crosslink of GAG chains. This hypothesis is supported by our observation of the clustering phenomenon of HEK-293-6E cells expressing Sema3A. However, furthers assays such as FRAP would confirm the crosslinking effect of Sema3A. Hence, Sema3A could participate in stabilizing the PNN network by crosslinking CS.

We extracted and purified CSs from different brain ECM compartments and analysed their sulphation pattern. CS from PNN displays a different sulphation pattern than that of other ECM compartments. We analysed the interaction of these CS, purified from PNN, with Sema3A but no-binding was observed. As a perspective, we will work in setting up the required conditions to analyse the binding of Sema3A to PNN CSs.

Our data, combined with that of the literature allowed us to propose the following model of Sema3A signalling regulation at extracellular level in PNNs **(Figure 69)**.

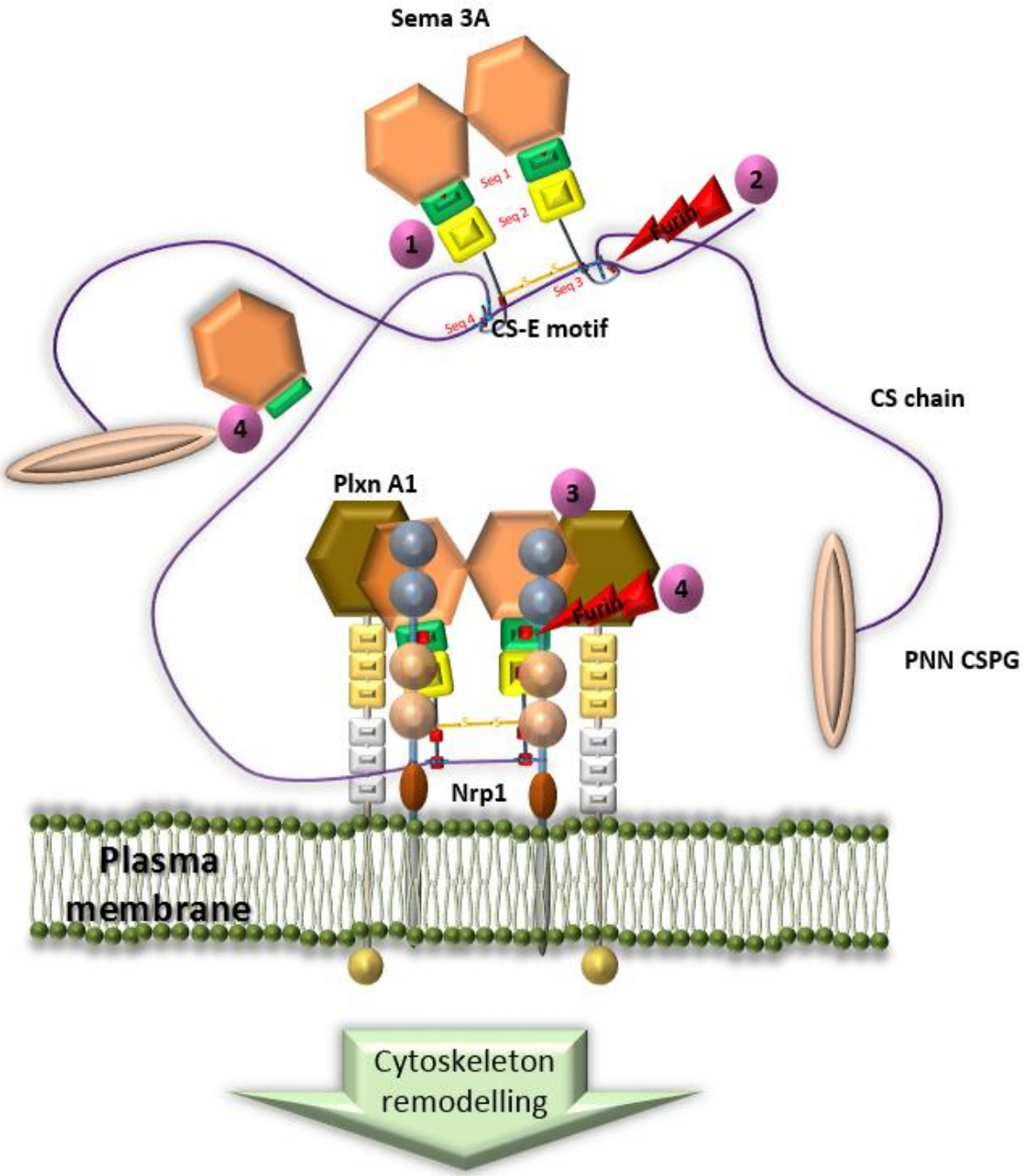

Figure 69: **A schematic model constructed from literature data and our results on Sema3A signalling regulation at extracellular level in PNNs.**
1: Full length Sema3A binds through sequence 3 and 4 mainly to CS-E motif found mostly at the non-reducing end of CS chain(s)[172] of PNN CSPGs or Nrp1, crosslinks them and participates thus in consolidation of the PNN network. **2**: Sema3A binding to CS would enhance furin-cleavage at the second furin cleavage-site (sequence 4) which results in activated Sema3A[269]. **3:** Activated Sema3A binds to Nrp1 and PlxA1 to trigger a signalling pathway which influences the cytoskeleton remodelling[292 331]. CS may also help and stabilise the binding to the receptors**. 4:** Once Sema3A achieved its effect, furin cleaves again in the first furin-cleavage site (sequence 1) which releases the N-ter domain (inactivated form[269]).
Seq: Sequence; **Sema3A**: Semaphorin 3A; **Plxn A1**: Plexin A1; **Nrp1**: Neuropilin 1; **CS**: chondroitin Sulphate; **CSPG**: CS proteoglycan.

Appendices

Glycoconj J (2017) 34:363–376
DOI 10.1007/s10719-017-9761-z

REVIEW

Chondroitin sulfates and their binding molecules in the central nervous system

L Djerbal[1] · H Lortat-Jacob[1] · JCF Kwok[2]

Received: 14 July 2016 / Revised: 31 December 2016 / Accepted: 4 January 2017 / Published online: 18 January 2017

Abstract Chondroitin sulfate (CS) is the most abundant glycosaminoglycan (GAG) in the central nervous system (CNS) matrix. Its sulfation and epimerization patterns give rise to different forms of CS, which enables it to interact specifically and with a significant affinity with various signalling molecules in the matrix including growth factors, receptors and guidance molecules. These interactions control numerous biological and pathological processes, during development and in adulthood. In this review, we describe the specific interactions of different families of proteins involved in various physiological and cognitive mechanisms with CSs in CNS matrix. A better understanding of these interactions could promote a development of inhibitors to treat neurodegenerative diseases.

Keywords Proteoglycans · Glycosaminoglycans · Chondroitin sulfate · Protein-glycosaminoglycan interactions · Central nervous system · Plasticity · Perineuronal nets

Lortat-Jacob H and Kwok JCF contributed equally to this work.

✉ H Lortat-Jacob
hugues.lortat-jacob@ibs.fr

✉ JCF Kwok
j.kwok@leeds.ac.uk

[1] Institut de Biologie Structurale, University Grenoble Alpes, CNRS, CEA, F-38027 Grenoble, France

[2] School of Biomedical Sciences, Faculty of Biological Sciences, University of Leeds, Leeds LS2 9JT, UK

Introduction

Chondroitin sulfate (CS) is an important sulfated carbohydrate belonging to glycosaminoglycan family (GAG). CS was first obtained from cartilage by Fisher and Boedecker in 1861 and was isolated in purer form by Krukenburg in 1884. Seven years later, Schmiedeberg showed that it contains a hexosamine and hexuronic acid but the presence of a sulfuronic group was not mentioned at that time [1]. It was until 1915, Levene and Forge finally resolved the complete structure of CS [2–5]. CS is composed of a D-glucuronic acid (GlcA) and *N*-acetylgalactosamine (GalNAc) [1, 6]. Sulfation is one of the main modification on CSs. The sulfation is often added on C-4 and/or C-6 of GalNAc and/or C-2 of GlcA [7]. The sulfation position results in different forms of CS: CS-A, CS-C, CS-D, CS-E (Fig. 1). This sulfation pattern confers different roles to CSs and allows selective interactions with different molecules. Apart from sulfation, GlcA can be epimerized into L-iduronic acid (idoA) resulting in CS-B, which is also called dermatan sulfate (DS; Fig. 1).

Like most GAGs, CS is located in the extracellular matrix (ECM), at the cell surface or associated to the plasma membrane, in most animal tissues [8]. As such they appeared to be strategically positioned to control various important processes occurring at the cell-tissue interface. It is also found in the intracellular granules of certain cells like mast cells [8–10]. Both in the ECM and at the cell surface, CS is linked to a core protein to form chondroitin sulfate proteoglycan (CSPG). Localization of CSPGs in ECM make them more accessible for different molecules involving in different mechanisms [11].

The expression of CS is tissue dependent and it is present at a high level in the ECM in cartilage and central nervous system (CNS). CS constitutes the most abundant GAG in the

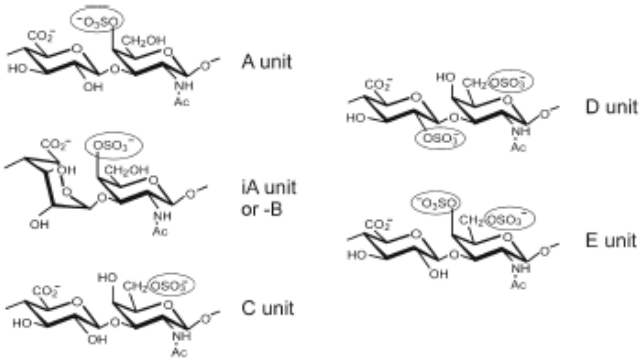

Fig. 1 Structure of disaccharide units of chondroitin sulfate. Chondroitin sulfate consists of repeating disaccharide unit composed of D-glucuronic acid (GlcA) and *N*-acetylgalactosamine (GalNAc). Each monosaccharide may be sulfated on different residues. CS-A: carbon (C) 4 of the GalNAc. CS-C: C6 of the GalNAc. CS-D: C2 of the GlcA and C6 of the GalNAc. CS-E: C4 and C6 of Gal-NAc. GlcA can be epimerized into L-iduronic acid (iA unit) resulting in CS-B

cartilage [12]. Many studies have reported the positive effect of CS in treatment of osteoarthritis [13]. Indeed, CS inhibits the apoptosis of chondrocytes, metalloproteases degradation of cartilage, and activation of pro-inflammatory enzymes [14, 15]. CSPGs are also the major components of ECM in the CNS. They are critical for the formation, development and maintenance of brain morphology and function [16]. CSPGs are highly upregulated in glial scar after CNS injury and they inhibit axonal regeneration [16]. Recently, CSPGs have also been shown to control memory retention in mouse model of Alzheimer's disease. Enzymatic removal of CSPGs enhances memory retention via enhanced plasticity, which would be useful in improving condition such as neurodegeneration [17, 18].

CS composition is also cell-type dependent and changes at different development stages. In nervous system, CS in the ECM changes during ontogenesis. While CS-C is the most expressed CS during embryogenesis, CS-A is the most abundant in adulthood [19, 20]. Apart from biochemical evidence using high performance liquid chromatography, these developmental changes in CSs are also confirmed using immunological techniques. Monoclonal antibodies are developed to specifically recognise different isoforms of CS chain. This tool provides the possibility of mapping the CS distribution during ontogenesis [21]. Furthermore, the spatio-temporal expression of CSs in brain ECM has been investigated. It has been shown that brain CSs exhibit structural diversity and developmental regulation, which suggests that CSs are implicated in diverse functions [22, 23].

The aim of this review is to provide an overview of all reported CS-interacting proteins, with respect to brain function, how they are involved in the maintenance of the ECM structure and their potential functional role. We focus on the interaction of proteins with various CS sulfation pattern and how these promote their signalling to accomplish their function including growth, differentiation, guidance and plasticity within the CNS.

Organization of the CSPG network in the CNS

CSPG is the major component of ECM in the CNS representing as much as ~20% of its total volume [24]. While the ratio of total CS vs heparan sulfate (HS) in the CNS is 9:1, this ratio decreases to 7:3 in the perineuronal net (PNN) matrix [25].

CSPG extraction from the brain ECM, using a sequential method based on different buffers, revealed three distinct compartments: a diffuse matrix, a cell surface-associated matrix and a condensed matrix, which contains different types and amounts of CSPGs [25–27]. Almost all common CSPGs are found in all three compartments, which bear different ECM properties, but in different concentrations and with different molecular characteristics. The use of physiological saline allows the extraction of ECM molecules from the diffuse ECM. Western blotting analysis showed that the diffuse matrix extract contains all forms of neurocan, phosphacan (400 kDa) and brevican (145 kDa) and aggrecan (>500 kDa). The cell surface-associated matrix, which is released with detergent- or high-salt buffer contains membrane associated CSPG – NG2 and also the other CSPGs. Finally the condensed matrix assembly such as PNNs is extracted with 6 M urea buffer and contains almost similar species of neurocan, brevican and aggrecan, but without NG2. This compartment also contains a large amount of versican [25, 27]. Other than core proteins, the sulfation pattern of CS chains is also different in these compartments. Disaccharide analysis has revealed that CS-A is the major CS GAG in adult rat brain ECM and it is more abundant in the diffuse matrix, whereas, the disulfated and/or IdoA containing CSs including CS-B, CS-D and CS-E are more abundant in the PNNs [25].

PNN is a highly organized ECM (Fig. 2) found mainly in parvalbumin (PV) positive GABAergic interneurons in the CNS although PNN is also observed in neurons without PV expression [28–31]. This macromolecular assembly, in addition to CSPGs, is composed of hyaluronan (HA), link proteins

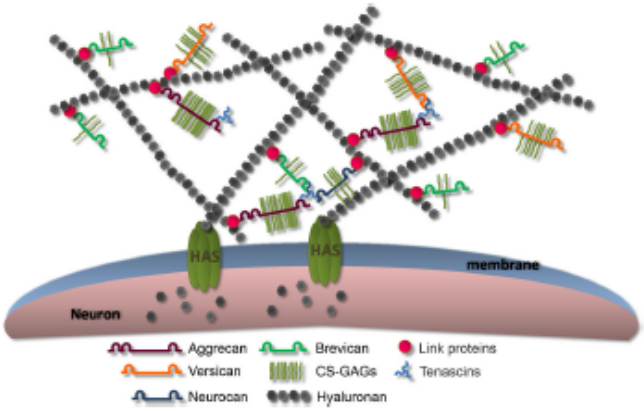

Fig. 2 Structure of PNNs. PNN is composed mainly of CSPGs from the family of lectican (including aggrecan, versican, bervican and neurocan), hyaluronan (HA), link proteins and tenascin-R (Tn-R). HA is the backbone of PNN on which the CSPGs lay. It is anchored by a family of transmembrane enzymes, hyaluronan synthases (HASs). CSPGs bind to HA via a link protein. Tn-R is also involved in the organisation of PNNs by assembling of CSPGs at the C-termini (*Kwok et al. 2011*)

and tenascin-R (Tn-R). HA is the backbone of PNN on which CSPGs interact. It is synthetized by a transmembrane enzyme, hyaluronan synthase (HAS) and is responsible for anchoring PNN on the neuronal surface [32, 33]. Aggrecan is the key CSPG for PNN formation in the cortex although its role can be substituted by other CSPGs in other regions [33–35]. The interaction of CSPGs and HA is stabilised by a family of proteins called link protein, hyaluronan and proteoglycan-binding link proteins (HAPLNs) [36]. This molecular interaction is further stabilized by the trimeric Tn-R which can bind up to three CSPGs [37]. Both HAPLN and Tn-R are crucial for the stabilization and condensed nature of PNN [37, 38].

This unique molecular network looks optimally designed to accomplish very specific functions. It has been proposed that the immature PNNs act like a reservoir of molecules. It attracts the neurotrophic factors responsible for the survival and the growth of the neuronal cells [39]. Moreover, the appearance of the mature form of PNN coincides with the closure of the critical period, a period when experience-dependant plasticity is consolidated [40]. It has been proposed that PNN is important in stabilizing existing synapses and inhibiting further or aberrant synapses formation [38, 40]. In addition, PNNs are described as an ion exchanger in the brain. The two major components of the PNN, HA chain and CSPGs, are highly negatively charged, they can bind to the cations in the ECM and regulate the ion mobility [41].

Proteins-GAGs interaction

GAGs interact with a large array of proteins to implement their functions [42, 43]. This interaction is of great importance to many physiological processes such as cell migration, growth, differentiation, guidance and development [44, 45]. They are also involved in pathological processes such as metastasis, neurodegeneration and inflammation [46–49]. Most GAGs are sulfated, including heparin (Hp), heparan sulfate (HS), keratan sulfate (KS), CS, DS and it was initially assumed that GAG-protein interaction is based on charge interaction. Multiple consensus amino acid sequences on the various GAG-binding proteins were later discovered on this basis [50]. Cardin and Weintraub identified that heparin binds to heparin-binding proteins through peptide sequences enriched in basic residues such as X-B-B-X-B-X and X-B-B-B-X-X-B-X where B is a basic residue and X is a hydropathic residue [51]. A third heparin specific sequence X-B-B-B-X-X-B-B-B-X-X-B-B-X was later reported, first in Willebrand factor and then in other proteins [52]. Further investigation has showed the importance of secondary and tertiary structure or the spatial distribution of basic residues. It has been shown, for example, that a distance of about 20 Å frequently separates two basic amino acids in a number of heparin-binding peptides, facing opposite directions of an alpha-helix [53]. More recent work, however, also demonstrated that GAG binding sites can be well identified by considering neutral hydrogen bond donors, such as asparagine and glutamine, amino acids that importantly contribute to the specificity of the interaction [54]. For CSs, they bind to CNS proteins containing a specific motif rich in arginine and lysine, such as Otx2, which we shall discuss more in the later section [55, 56].

The specificity and selectivity do not confine to protein sequences, but are also dependent on the oligosaccharide sequence and the pattern of sulfation. Chemorepellent molecule semaphorin 3A is found to interact with CS-E and B, but not with CS-D even though these three CSs are all disulfated with the same charge over mass ratio per disaccharide unit [56, 57]. Selective binding of neurotrophic factors like midkine and BDNF to synthetic CS-E tetrasaccharide is observed and lead to neurite outgrouth. Whereas the binding of these factors to CS-R, a synthetic tetrasaccharide with the same number of

sulfate groups as CS-E but distributed differently, is very weak and does not display a neuritogenic activity [58]. Also, different types of HS binds to different types of fibroblast growth factors (FGFs). For example, 2-O sulfate is required for the binding of FGF-2, 6-O sulfate is required for the binding of FGF-10 [59–62]. Recent evidence also shows that sulfation in CS/DS affects the binding and activation of FGF-2 [63–65]. These findings suggest the importance of sulfation pattern of GAGs in the specific binding to various proteins. Since HS is the most abundant GAG in the extracellular environment of many tissues, binding to HS/Hp is more documented than those to CS and KS. Most of interactions proteins-CSs has been characterized in the CNS.

Interactions of CSs with different families of molecules in the CNS ECM

During development, immature neurons elongate their axons through a complex tissue structure to reach their appropriate synaptic partners located millimetres or even centimetres away. Diverse cellular and molecular mechanisms are adopted by embryos to guide the axons to their targets [66]. ECM molecules play a crucial role during this process through the involvement of either the ECM molecules or ECM-binding molecules [67]. CSs interact and cooperate with extracellular signalling proteins and receptors to modulate the axonal outgrowth. Removal of CSs by injection of chondroitinase ABC (ChABC) results in abnormal axonal outgrowth in zebrafish and rat embryos [68, 69] and disruption of retinal axons in mouse embryos [70]. Otherwise, CNS development and CNS injury share certain neural mechanisms including neural outgrowth, guidance and plasticity. Indeed, after CNS injury, the same molecules involved in development are up-regulated again, including CSPGs [71]. They form a chemical barrier, which inhibits axonal projection and regeneration [72]. Enzymatic removal of CSs using ChABC promotes functional recovery after spinal cord injury (SCI) in adult rats [73, 74].

ECM in the CNS is a rich source of signalling molecules involved in different mechanisms of proliferation, differentiation, survival and migration of neurons. Activities and interactions of CSPGs with signalling molecules in ECM depend on many parameters: the core protein, the attached CS chains, their length, the degree and position of sulfates [75]. Composition of CSPGs varies in stages of development and physiological state, and this enables a large families of molecules, as described below, to interact with CSPGs via CSs chains to accomplish their functions (Fig. 3). The degree and position of sulfation on the CS chains confer different specific binding sites to various soluble factors in the ECM. Previous studies have reported an upregulation of CS-E unit and also chondroitin 6-sulfotransferase, an enzyme synthesising CS-C, after spinal cord injury [76, 77]. In the PNNs, CS-E are responsible for the binding of negative guidance molecule semaphorin 3A (Sema3A) and Otx2 [55, 57, 78, 79]. Recently, there are also studies describing the potential involvement of CS-C in epilepsy [80, 81]. These interactions lead to selective activation or inhibition of various signalling pathways. Here, we describe a families of proteins binding to CSs chain of CSPG to modulate the axonal outgrowth and guidance.

i) *Growth factors (GFs)*

GFs are biomolecules which support proliferation, growth, migration and differentiation [82–84]. In addition, they are involved in regulating metabolism, tissue repair and maintaining tissue homeostasis in adult organisms [85]. Some members exist ubiquitously in all tissues but some are expressed in a tissue-specific manner [86, 87]. GFs are usually secreted by neighbouring cells or at nerve terminals into the ECM and act locally due to their short life [88]. The secreted GFs bind to specific receptors on the surface of target cells and induce intracellular signalling pathway. Proteoglycans in the ECM bind to the GFs, facilitate the access and presentation of GFs to the receptor for subsequent signalling pathways [89]. During CNS development, many growth factors are shown to interact with CS chains, which we shall discuss below.

Neurotrophic factors are the family of GFs that promote survival, growth and differentiation of neuronal cells [90, 91]. Different neurotrophic factors, such as fibroblast growth factor, has been postulated to interact with heparin to promote the neurite outgrowth, hence their name "heparin-binding proteins" [92]. Interaction of neurotrophic factors with heparin/HS has attracted much attention similar to the involvement of HS in development [93]. However, these last decades more interest has been diverted to CSs notably in the CNS [94]. Here we describe heparin-binding proteins which interact with CSs in CNS.

Fibroblast growth factors (FGFs) are a large family of proteins, which exert a pleiotropic effects in different tissues. Basic fibroblast growth factor (bFGF) or FGF 2 is a multifunctional growth factor including its effect on survival of neurons and stimulate neurite extension [95]. It has been shown that bFGF binding to HS-, Hp-, or HA-bound surfaces stimulates neurite outgrowth from hippocampal neurons while the binding to CS- or DS-surfaces does not lead to the same observation [96]. On the other hand, Karumbaiah *et al.* has reported the potential of CS-A hydrogel enriched in bFGF in creating an endogenous niche for neural stem cells [97]. Surface plasmon resonance (SPR) analysis shows that CS-A from bovine trachea binds with high affinity to bFGF, brain-derived neurotrophic factor (BDNF) and interleukin 10 [97]. Screening of different GFs including FGF-2, −10, −16, −18

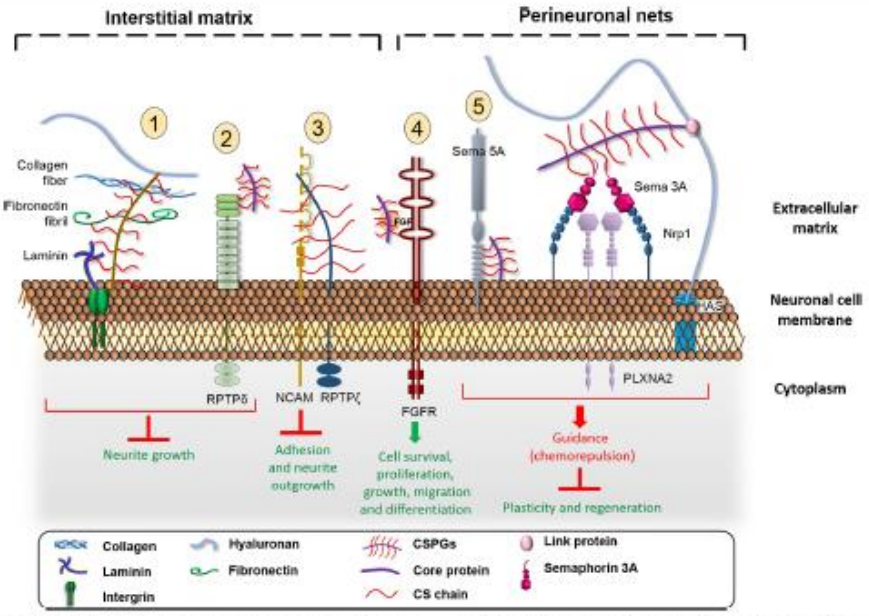

Fig. 3 Interaction of CS glycan chains with different protein families in CNS matrix. CSPGs inhibit the growth cone via the interaction of its CS chain with 1) laminin and collagen and 2) bind its receptor protein tyrosine kinase (RPTP). 3) The neuronal adhesion molecule NCAM interacts with phosphacan (the extracellular part of RPTPζ) by its CS chain and results in an inhibition of adhesion and neurite growth. 4) CS, notably CS-E, acts as a binding partner of FGF to promote growth and differentiation. 5) An interaction of semaphorin 5 A (Sema 5A) with CS chain turns the attractive guidance protein into a repulsive cue. Semaphorin 3A (Sema 3A) is a repulsive guidance protein found in perineuronal nets and interacts specifically with CS-E motif. It exerts its chemorepulsive effect by signalling via plexin-neuropilin receptors. CS could be an additional constituent of sema 3A signalling complex

and Hp-binding epidermal growth factor-like growth factor (HB-EGF) against CS-E using filter binding assay, resonance mirror biosensor IAsys and GAG microarrays showed that these GFs bind to the CS-E from squid cartilage in a dose-dependent manner [64, 65]. FGF-16, FGF-18, and HB-EGF binds to CS-E (Kd ≈ 47.2, 8.9 and 16 nM, respectively) in a comparable affinity to the binding to Hp (Kd ≈ 34.7, 10.8 and 4.7 nM, respectively), while the affinity of FGF-2 and FGF-10 toward CS-E was lower than Hp [64, 65]. Screening of these GFs with oversulfated CS/DS hybrid chain purified from hagfish (CS-H) showed no binding by SPR, suggesting that the binding of the GFs to CS-E is a specific interaction but not due to non-specific charge interaction [98]. The binding of CS to FGF2 is important for the formation of neural spheres, proliferation and self-renewal of neural stem cells through the FGF2/MAPK pathway [99]. Removal of CSs using ChABC reduces neuronal proliferation and differentiation, and on the contrary, it increases the proliferation of astrocytes [100].

Midkine and pleiotrophin are two basic heparin-binding proteins localized in the radial glial fibres in embryonic brain, along which neural stem cells migrate [101]. They mediate neuronal cell adhesion and migration, and promote neurite outgrowth by interacting with cell surface heparin during development [102, 103]. It has been shown that CS-C inhibits the binding of pleiotrophin to its receptor 6B4 Proteoglycan/Phosphacan, which is an extracellular variant of receptor-like protein-tyrosine phosphatase (RPTP) ζ/RPTP β (this receptor family will be discussed in the next section), in rat brain. The binding of CS-C reduces pleiotrophin-induced neuronal migration along radial glial fibres. It has been postulated that CS and a portion of RPTPζ/RPTPβ could constitute the binding site of pleiotrophin [104, 105]. Similarly, Ueoka *et al.* have also shown that the adhesion of embryonic cortical neurons to midkine in culture is specifically inhibited by CS-E [106]. The interaction of midkine to CS-E is as strong as the binding to Hp [106]. The specific and direct interaction between CS-E/CS-H and midkine/pleiotrophin has also been shown by filter binding assay, IAsys and SPR [64, 98, 107]. Midkine and pleiotrophin are involved in neurodegenerative diseases such as Alzheimer's disease. Deposition of midkine and pleiotrophin has been observed in the pathological senile plaque and/or neurofibrillary tangles in Alzheimer's brain [102, 108]. LDL receptor-related protein (LRP) is a receptor of midkine and

pleiotrophin and it is genetically linked to Alzheimer's disease [102]. CS-Midkine/pleiotrophin interaction could be a potential target to treat these diseases. Thus, further understanding of this interaction should be performed. These findings suggest that CSs could be a binding partner or co-receptor for neurotrophic factors in the central nervous system.

ii) *Receptors*

Receptor protein tyrosine phosphatases (RPTPs) are a family of receptor-enzymes that remove phosphate from tyrosine in a protein. RPTPs are commonly found on growth cones [109] and are involved in the control of axon growth, guidance, regeneration and plasticity during development as well as after injury [110–112]. Indeed, a deficit of *O*-mannosylated RPTP ζ contributes to congenital muscular dystrophies [113–115].

Members of class II A RPTP including RPTPσ, RPTPδ and LAR (leukocyte common antigen-related phosphatase) bind with high affinity to CSPGs and HS proteoglycans (HSPGs) [116]. They are postulated to be the receptors of CSPG [117, 118]. RPTPσ knockout mice display a reduced CSPG inhibition after spinal cord injury and an enhanced regeneration after sciatic nerve crush injury [112, 119]. Mimetic peptide of RPTPσ wedge domain releases CSPG-mediated axonal inhibition *in vitro* by binding to RPTPσ and improve the functional recovery after SCI [120]. Binding of CSPG to RPTPσ induces a dephosphorylation of tropomyosin-related kinase B (TrkB), which leads to a down-regulation of dendritic spine formation [121]. TrkB is the BDNF receptor which, in contrast to CSPG, positively regulates the plasticity and spines formation in cortical neurons. Remarkably, binding of RPTPσ to CSPGs or HSPGs induces opposite effect on axonal growth. Cole *et al.* have shown that RPTPσ binding to HSPGs activates axonal growth while binding to CSPGs inhibits it [118]. The binding with CS chains inhibit the oligomerization of RPTPσ which are induced by HSPG [118].

LAR is another CSPG receptor [122]. It has been demonstrated by co-immunoprecipitation that LAR interacts with CSPG directly. This interaction leads to an inactivation of Akt and an activation of RhoA, thus inhibiting axonal growth [122]. Moreover, LAR knockout mice or mice treated with LAR-targeting peptides show an improvement of locomotor function after SCI [122, 123]. PG-RPTPs interaction may be a potential therapeutic target for functional recovery after CNS injuries.

Nogo receptors NgR1 and NgR3 bind to Nogo and induce neurite outgrowth inhibition [124]. It has recently been reported that apart from Nogo, they can also bind to CSPGs and act as CSPGs receptors [125]. Both NgR1 and NgR3 bind specifically to disulfated CS-B, CS-D and CS-E with high affinity. The binding of CSPG to NgR1 and NgR3 inhibit neurite outgrowth. Double knockout of NgR1 and 3 shows increased regeneration after injury, and this is further enhanced with additional ablation of RPTPσ [125].

iii) *Adhesion molecules*

Cell adhesion molecules (CAMs) are surface glycoproteins mediating cell-cell and cell-extracellular interaction. The established connections between cells are important for maintaining tissue integrity and for cell communications [126]. Moreover, CAMs are fundamental for cell migration, notably during development of the CNS [127] and after traumatic brain injury [128]. Neural-CAM (N-CAM) is an adhesion molecule specific to the CNS. It has been implicated in various neuronal mechanisms. Indeed, this molecule is required for motor neuron sprouting, having thus a beneficial role in recovery after SCI. NCAM−/− mice show a significantly reduced locomotor recovery comparing the WT after SCI [129, 130]. N-CAM and neuron-glia CAM (Ng-CAM) bind with high affinity (Kd ≈ 0.5 nM) to the CSPG phosphacan [131]. Treatment with ChABC only reduces this binding by ~15% suggesting that the binding is mostly due to an interaction with the phosphacan core protein. The interaction of phosphacan and N-CAM or Ng-CAM leads to an reduced neurite outgrowth and adhesion *in vitro* [131]. Neurocan, another CSPG in the CNS matrix, also binds to N-CAM and Ng-CAM, and inhibits the neurite outgrowth [132]. Unlike phosphacan, ChABC treatment of neurocan significantly reduces this binding suggesting the interaction is mainly mediated through the CS GAG chains [132]. These findings suggest that N-CAM and Ng-CAM could be the receptors for the two CSPGs phosphacan and neurocan.

CAMs are also involved in other neuronal mechanisms in addition to neuronal migration. Contactin-1 is a glycosylphosphatidyl inositol (GPI)-linked membrane glycoprotein. It is a CAM and implicated in axonal growth, axonal and dendritic interactions of cerebellar interneurons and guidance [133]. With the use of SPR analysis, it has been shown that CS-E binds to contactin-1 with significant affinity (Kd ≈ 1.4 μM) and that this interaction is required for the neurogenesis mediated by CS-E [134].

iv) *Guidance proteins*

Guidance of dendrites and axons to their appropriate targets is a critical process for building a functional CNS during development [135]. These guidance molecules come from different families of proteins including secreted or cell surface guidance molecules and they can be attractive or repulsive [136].

Semaphorin is a large family of secreted and membrane-associated guidance molecules [137]. Initially being identified

as repulsive guidance molecules, several studies in the last decades have reported a chemoattractive role of semaphorins [138–140]. Semaphorins guide the development of peripheral nerve projection and involved in synaptogenesis in the CNS [141, 142]. The persistence of their expression in adulthood suggests a role in the maintenance of pre-established connections and cerebral homeostasis [143].

Semaphorin 3A (Sema 3A) is one of the most studied members in class III semaphorins, which are upregulated after CNS injuries [144]. Owing to its ability in inducing growth cone collapse, Sema 3A is also called collapsin-1 and is the first member being identified in the semaphorin family [138]. It is a secreted protein, signaling via neuropilin-1(Nrp-1) and plexin (Plxn) receptors located at synapses [145–147]. During development, Sema 3A is expressed in a gradient across the cortical layers. It acts as a chemoattractive protein to guide the radial migration of cortical neurons [148]. In adult CNS, Sema 3A is found in the PNNs [78]. It modulates synapse morphology and function [147]. ChABC digestion reduces Sema 3A staining on the PNNs, suggesting an interaction between Sema 3A and CSPG [78]. Further investigations have shown that Sema 3A interacts with CS-E with high affinity [57]. Moreover, Nrp-1 can be modified post-translationally by CS chains, and this modification affects its ability to one of its effector VEGF [149]. These studies suggest that CSPGs could be additional constituents in the Sema 3A–Nrp-Plxn signalling complex. Moreover, Sema 3A is one of the most potent inhibitors to neuronal sprouting after SCI. It inhibits the axonal sprouting induced by nerve growth factor after SCI [150]. Indeed, Sema 3A could be one of the mechanisms which CSPG modulates plasticity. Targeting Sema 3A or its interaction with CSs could be a strategy to improve the plasticity after CNS trauma.

Semaphorin 5A (Sema 5A) is a membrane-associated semaphorin. Like other semaphorins, it is important in the development of the CNS [151]. Semaphorins class 5 is characterized by a specific domain containing two clusters of type-1 thrombospondin repeats (TSRs), which promote neurite outgrowth [152]. TSR displays a basic motif which can interact with the negative chain of HSPG and CSPG [153, 154]. Interestingly, the binding of Sema 5A to HSPG or CSPG triggers opposite responses. Sema 5A mediates neuronal attraction when it binds to HSPG and it becomes repulsive upon binding to CSPG [155]. This study indicates the proteoglycan-dependent function of Sema 5A.

Other than Sema 3A and 5A, Conrad *et al.* have tried to identify other ECM proteins which interact with CNS GAGs to promote the growth and differentiation of embryonic sensory nerve fibres using SPR and microarrays. The results indicate a significant interaction between CS-A and various guidance molecules, including Sema 3E, Sema 6B, ephrin A3 and Robo 2 [156].

Collapsin response mediator protein-4 (CRMP-4) is a 65 kDa phosphoprotein expressed in the CNS during development and in adulthood [157]. Dendrites extension of hippocampal neurons induced by Sema 3A is impaired in CRMP-4−/− hippocampal neurons, suggesting that CRMP-4 belongs to the Sema 3A signalling pathway which induces the growth cone collapse [158]. Moreover, CRMP-4 is identified as crucial protein that overcomes both axonal growth inhibition and scarring after SCI in adult mouse [158]. Interestingly, this intracellular protein interacts with CS. Indeed, CRMP-4 was purified using a CS affinity column [159, 160]. During early development in the CNS, active apoptosis which is essential for the normal development of CNS, causes the release of CRMP-4 into the extracellular space where it binds to CS [161, 162]. The downstream mechanism of the interaction between CRMP-4 and CS remains unknown but the above finding suggests an additional role of CNS ECM in sequestrating intracellular protein (s) released from apoptosis.

Orthodenticle homeobox protein 2 (Otx2) is another intracellular protein found interacting with CS in the ECM. Otx2 is a non-cell-autonomous transcription factor involved in brain morphogenesis [163]. It has been shown to interact with CSs in postnatal development and control plasticity [79]. Indeed, the role of Otx2 in plasticity has been investigated in the visual system in mice during the critical period. During this period, Otx2 is transferred from choroid plexus into the visual cortex and accumulates on the PNN of PV-cells [164]. Otx2 accelerates PV-cells maturation and PNNs formation. In return, PNNs concentrate Otx2 into the surface of PV-cells to be internalized [55]. A positive feedback loop between Otx2 and PNNs, during critical period as well as in maintaining PNN in adulthood, has been proposed [165]. Considering the important role of Otx2 and PNNs in controlling plasticity, further experiments have been performed to characterize the binding site of Otx2 in PNNs. Isothermal titration calorimetry (ITC) experiments show that a specific basic sequence in Otx2, rich in arginine and lysine, interacts specifically and with high affinity with CS-E and CS-D, low affinity with CS-C and not with CS-A [55]. This finding indicates, once more, that the interaction CS-protein is sulfation pattern-dependent, not charge dependent.

v) *Extracellular matrix proteins*

A number of fibrillar and glyco-proteins are also key components of the neuronal ECM in addition to CSPGs. They consist mainly of elastins, collagens, laminins and fibronectins [166]. Despite their small proportion in CNS matrix comparing to CSPGs, these proteins impose significant influence on the growth cone of neurons and regeneration [167, 168]. An addition of laminin to neurons in culture results in a drastic acceleration of neurite outgrowth [168]. Similarly, fibronectin

promotes the neurite outgrowth and axonal regeneration of adult brain neurons *in vitro* [169]. Collagen VI protects the brain from neurodegeneration in ageing [170]. CSPGs and fibrous proteins have a complementary functions. Both work on the maintenance of the ECM homeostasis and the surrounding neurons. An implantation of a collagen/chondroitin 6-sulfate (CS-C) hydrogel containing embryonic striatal neurons allows the reconstruction of matrix and glial repair after a lesion in rat striatum [171]. It is likely that CSPGs and fibrous proteins interact with each other to accomplish their function. Astrochondrin, a CSPG on astrocyte surface and is involved in cerebellar granule cell migration, has been shown to interact specifically with laminin and collagen but not with fibronectin. Implication of CS chain of astrochondrin in this interaction is demonstrated by analysis of the astrochondrin binding to collagen in the presence of soluble CS in a radioligand binding assay. Indeed, soluble CSs are able to compete with astrochondrin to bind to collagen [172]. Snow *et al.* have reported that laminin and fibronectin are responsible for the inhibition effect of CSPGs on the growth cone [173].

Photomedin is another brain ECM protein, interacting with CS, less known comparing to fibronectin and laminin because it is less abundant and its spatiotemporal expression is restricted [174]. Photomedin 1 and 2 are identified as novel members of the olfactomedin family (OLF) [174]. OLFs are glycoproteins expressed mainly in the ECM of olfactory neuroepithelium, while photomedins are expressed mainly in retina ECM. They contain a specific sequence in their C-terminal, called OLF domain which has crucial implications in many neuronal mechanisms, including axonal growth and differentiation of chemosensory cilia [175]. ELISA experiments have shown that photomedins bind to CS-E with high affinity [174]. This is yet another evidence that CS-E interacts with different growth factors involved in neuronal migration and axonal guidance. Taken together, it may suggest that photomedins and growth factors could compete to bind to CS-E. Photomedins are proposed as a reservoir of CS-E and facilitates the localized action of growth factors [174].

vi) *Pathological protein*

Amyloid precursor protein (APP) is a transmembrane glycoprotein. APP undergoes a proteolytic processes giving rise to various peptides. Some of the resulting peptides are involved in neuronal plasticity and neurogenesis, but some of the others are pathological like amyloid beta peptide (Aβ) [176]. Indeed, Aβ is neurotoxic and found accumulated in neurons suffering from Alzheimer's disease [177]. HSs and CSs have been reported to enhance the Aβ aggregation and the sulfate moieties on GAGs are the crucial key for this aggregation [178]. Recent study has reported that an overexpression of heparanase decreases the amyloid burden *in vivo* [179], and that PNN neurons resist neurotoxicity from Aβ and oxidative stress suggesting the neuroprotective role of PNNs [180, 181]. Otherwise, an interaction of APP and PG enhances the neurite outgrowth [182]. The direct interaction of CSPGs and APP has been demonstrated using solid phase binding assay. ChABC digestion of CS reduces the binding by 79%, this confirms the binding is through CS GAG chains [182].

While CSs/CSPGs are abundant in the CNS, study of PGs/GAGs interaction has been focused on HSPGs/HSs instead. Since amyloid beta peptide (Aβ) is accumulated in the extracellular space, which is rich in CSPGs, a specific and significant interaction could be suspected. Further investigation will shed light on the role of CSPG and CS chain in this disease. In addition, CS has been implicated in a number of other neuropathological conditions including epilepsy, stroke, schizophrenia, an in-depth understanding of the role of CS in these diseases will be crucial for targeting CS in the conditions [81, 183, 184].

Conclusion

CS is the most abundant GAG in the CNS matrix. Its diverse pattern of sulfation and epimerization pattern allows precise controls of various physiological processes including the proper development of the CNS and the maintenance of neuronal homeostasis. Moreover, this diversity enables differential binding to a large family of proteins, with different affinities. This huge interaction between CSs and proteins places them at the first position in diverse signalling pathways. Thus, their involvement in various mechanisms during ontogenesis notably the growth cone, regeneration and plasticity.

Targeting the compositional change in CS as well as their interactions could be a promising approach to treat different pathologies. Chemical synthesis of CS oligosaccharides with defined sequences has recently made progresses [185, 186], opening the possibility to use those to manipulate a protein-CS interaction. Meanwhile, a better understanding of CS structure, their organization within the matrix, the mode of interaction with different types of proteins, are essential for targeting the important ECM component in the CNS.

Acknowledgements The authors thank UGA for financial support through "émergence/partenariat stratégique" project.

Compliance with ethical standards

Conflicts of interest The authors declare that they have no conflicts of interest.

Ethical approval This article does not contain any studies with human participants or animals performed by any of the authors.

References

1. Bray, H.G., Gregory, J.E., Stacey, M.: Chemistry of tissues. I. Chondroitin Cartilage. **38**(2), 142–146 (1944). doi:10.1042/bj0380142
2. Levene, P.A., La Forge, F.B.: On chondroitin sulphuric acid: fourth paper. J. Biol. Chem. **20**(3), 433–444 (1915)
3. Levene, P.A., La Forge, F.B.: On chondroitin sulphuric acid: third paper. J. Biol. Chem. **18**(1), 123–130 (1914)
4. Levene, P.A., La Forge, F.B.: On chondroitin sulphuric acid: second paper. J. Biol. Chem. **15**(1), 155–160 (1913)
5. Levene, P.A., La Forge, F.B.: On chondroitin sulphuric acid. J. Biol. Chem. **15**(1), 69–79 (1913)
6. Roseman, S.: Reflections on glycobiology. J. Biol. Chem. **276**(45), 41527–41542 (2001). doi:10.1074/jbc.R100053200
7. Silbert, J.E., Sugumaran, G.: Biosynthesis of chondroitin/dermatan sulfate. IUBMB Life. **54**(4), 177–186 (2002). doi:10.1080/15216540214923
8. Yamada, S., Sugahara, K., Özbek, S.: Evolution of glycosaminoglycans. Commun. Integr. Biol. **4**(2), 150–158 (2011). doi:10.4161/cib.4.2.14547
9. Farrugia, B.L., Whitelock, J.M., O'Grady, R., Caterson, B., Lord, M.S.: Mast cells produce a unique chondroitin sulfate epitope. J. Histochem. Cytochem. **64**(2), 85–98 (2016). doi:10.1369/0022155415620649
10. Thompson, H.L., Schulman, E.S., Metcalfe, D.D.: Identification of chondroitin sulfate E in human lung mast cells. J. Immunol. **140**(8), 2708–2713 (1988)
11. Schwartz, N.B.: Biosynthesis and regulation of expression of proteoglycans. Front. Biosci. **5**, D649–D655 (2000)
12. Hascall, V.C., Sajdera, S.W.: Physical properties and Polydispersity of proteoglycan from bovine nasal cartilage. J. Biol. Chem. **245**(19), 4920–4930 (1970)
13. Bishnoi, M., Jain, A., Hurkat, P., Jain, S.K.: Chondroitin sulphate: a focus on osteoarthritis. Glycoconj. J. 1–13 (2016). doi:10.1007/s10719-016-9665-3
14. Henrotin, Y., Mathy, M., Sanchez, C., Lambert, C.: Chondroitin sulfate in the treatment of osteoarthritis: from *in vitro* studies to clinical recommendations. Ther. Adv. Musculoskelet. Dis. **2**(6), 335–348 (2010). doi:10.1177/1759720x10383076
15. du Souich, P.: Comments on “OARSI guidelines for the non-surgical management of knee osteoarthritis&#x201d. Osteoarthritis and Cartilage **22**(6), 888–889. doi:10.1016/j.joca.2014.03.021
16. Carulli, D., Laabs, T., Geller, H.M., Fawcett, J.W.: Chondroitin sulfate proteoglycans in neural development and regeneration. Curr. Opin. Neurobiol. **15**(1), 116–120 (2005). doi:10.1016/j.conb.2005.01.014
17. Yang, S., Cacquevel, M., Saksida, L.M., Bussey, T.J., Schneider, B.L., Aebischer, P., Melani, R., Pizzorusso, T., Fawcett, J.W., Spillantini, M.G.: Perineuronal net digestion with chondroitinase restores memory in mice with tau pathology. Exp. Neurol. **265**, 48–58 (2015). doi:10.1016/j.expneurol.2014.11.013
18. Kwok, J.C., Yang, S., Fawcett, J.W.: Neural ECM in regeneration and rehabilitation. Prog. Brain Res. **214**, 179–192 (2014). doi:10.1016/B978-0-444-63486-3.00008-6
19. Kitagawa, H., Tsutsumi, K., Tone, Y., Sugahara, K.: Developmental regulation of the sulfation profile of chondroitin sulfate chains in the chicken embryo brain. J. Biol. Chem. **272**(50), 31377–31381 (1997). doi:10.1074/jbc.272.50.31377
20. Miyata, S., Komatsu, Y., Yoshimura, Y., Taya, C., Kitagawa, H.: Persistent cortical plasticity by upregulation of chondroitin 6-sulfation. Nat Neurosci **15**(3), 414–422, S411–412 (2012). doi:10.1038/nn.3023
21. Mark, M.P., Baker, J.R., Kimata, K., Ruch, J.V.: Regulated changes in chondroitin sulfation during embryogenesis: an immunohistochemical approach. Int. J. Dev. Biol. **34**, 191–204 (1990)
22. Herndon, M.E., Lander, A.D.: A diverse set of developmentally regulated proteoglycans is expressed in the rat central nervous system. Neuron. **4**(6), 949–961 (1990). doi:10.1016/0896-6273(90)90148-9
23. Oohira, A., Katoh-Semba, R., Watanabe, E., Matsui, F.: Brain development and multiple molecular species of proteoglycan. Neurosci. Res. **20**(3), 195–207 (1994). doi:10.1016/0168-0102(94)90088-4
24. Nicholson, C., Syková, E.: Extracellular space structure revealed by diffusion analysis. Trends Neurosci. **21**(5), 207–215 (1998). doi:10.1016/S0166-2236(98)01261-2
25. Deepa, S.S., Carulli, D., Galtrey, C., Rhodes, K., Fukuda, J., Mikami, T., Sugahara, K., Fawcett, J.W.: Composition of perineuronal net extracellular matrix in rat brain: a different disaccharide composition for the net-associated proteoglycans. J. Biol. Chem. **281**(26), 17789–17800 (2006). doi:10.1074/jbc.M600544200
26. Kwok, J.F., Foscarin, S., Fawcett, J.: Perineuronal Nets: A Special Structure in the Central Nervous System Extracellular Matrix. In: Leach, J.B., Powell, E.M. (eds.) Extracellular Matrix, vol. 93. Neuromethods, pp. 23–32. Springer New York, (2015)
27. Carulli, D., Rhodes, K.E., Brown, D.J., Bonnert, T.P., Pollack, S.J., Oliver, K., Strata, P., Fawcett, J.W.: Composition of perineuronal nets in the adult rat cerebellum and the cellular origin of their components. J. Comp. Neurol. **494**(4), 559–577 (2006). doi:10.1002/cne.20822
28. Brückner, G., Kacza, J., Grosche, J.: Perineuronal nets characterized by vital Labelling, Confocal and Electron Microscopy in Organotypic Slice Cultures of Rat Parietal Cortex and Hippocampus. J. Mol. Histol. **35**(2), 115–122 (2004). doi:10.1023/b:hijo.0000023374.22298.50
29. Wegner, F., Härtig, W., Bringmann, A., Grosche, J., Wohlfarth, K., Zuschratter, W., Brückner, G.: Diffuse perineuronal nets and modified pyramidal cells immunoreactive for glutamate and the GABAA receptor α1 subunit form a unique entity in rat cerebral cortex. Exp. Neurol. **184**(2), 705–714 (2003). doi:10.1016/s0014-4886(03)00313-3
30. Mueller, A.L., Davis, A., Sovich, S., Carlson, S.S., Robinson, F.R.: Distribution of N-acetylgalactosamine-positive perineuronal nets in the macaque brain: anatomy and implications. Neural Plast. 2016. **2016**, 19. doi:10.1155/2016/6021428
31. Yamada, J., Jinno, S.: Molecular heterogeneity of aggrecan-based perineuronal nets around five subclasses of parvalbumin-expressing neurons in the mouse hippocampus. J. Comp. Neurol., n/a-n/a (2016). doi:10.1002/cne.24132
32. Toole, B.P.: Hyaluronan: from extracellular glue to pericellular cue. Nat. Rev. Cancer. **4**(7), 528–539 (2004)
33. Kwok, J.C.F., Carulli, D., Fawcett, J.W.: *In vitro* modeling of perineuronal nets: hyaluronan synthase and link protein are necessary for their formation and integrity. J. Neurochem. **114**(5), 1447–1459 (2010). doi:10.1111/j.1471-4159.2010.06878.x
34. Giamanco, K.A., Morawski, M., Matthews, R.T.: Perineuronal net formation and structure in aggrecan knockout mice. Neuroscience. **170**(4), 1314–1327 (2010). doi:10.1016/j.neuroscience.2010.08.032

35. Giamanco, K.A., Matthews, R.T.: Deconstructing the perineuronal net: cellular contributions and molecular composition of the neuronal extracellular matrix. Neuroscience. **218**, 367–384 (2012). doi:10.1016/j.neuroscience.2012.05.055
36. Spicer, A.P., Joo, A., Bowling Jr., R.A.: A hyaluronan binding link protein gene family whose members are physically linked adjacent to chondroitin sulfate proteoglycan core protein genes: the missing links. J. Biol. Chem. **278**(23), 21083–21091 (2003). doi:10.1074/jbc.M213100200
37. Morawski, M., Dityatev, A., Hartlage-Rübsamen, M., Blosa, M., Holzer, M., Flach, K., Pavlica, S., Dityateva, G., Grosche, J., Brückner, G., Schachner, M.: Tenascin-R promotes assembly of the extracellular matrix of perineuronal nets via clustering of aggrecan. Philosophical Transactions of the Royal Society of London B. Biol. Sci. **369**(1654), 20140046 (2014). doi:10.1098/rstb.2014.0046
38. Carulli, D., Pizzorusso, T., Kwok, J.C., Putignano, E., Poli, A., Forostyak, S., Andrews, M.R., Deepa, S.S., Glant, T.T., Fawcett, J.W.: Animals lacking link protein have attenuated perineuronal nets and persistent plasticity. Brain. **133**(Pt 8), 2331–2347 (2010). doi:10.1093/brain/awq145
39. Celio, M.R., Blumcke, I.: Perineuronal nets — a specialized form of extracellular matrix in the adult nervous system. Brain Res. Rev. **19**(1), 128–145 (1994). doi:10.1016/0165-0173(94)90006-X
40. Pizzorusso, T., Medini, P., Berardi, N., Chierzi, S., Fawcett, J.W., Maffei, L.: Reactivation of ocular dominance plasticity in the adult visual cortex. Science. **298**(5596), 1248–1251 (2002). doi:10.1126/science.1072699
41. Morawski, M., Reinert, T., Meyer-Klaucke, W., Wagner, F.E., Tröger, W., Reinert, A., Jäger, C., Brückner, G., Arendt, T.: Ion exchanger in the brain: quantitative analysis of perineuronally fixed anionic binding sites suggests diffusion barriers with ion sorting properties. Sci. Report. **5**, 16471 (2015)
42. Sarrazin, S., Lamanna, W.C., Esko, J.D.: Heparan Sulfate Proteoglycans. Cold Spring Harb. Perspect. Biol. **3**(7), (2011). doi:10.1101/cshperspect.a004952
43. Mizumoto, S., Yamada, S., Sugahara, K.: Molecular interactions between chondroitin–dermatan sulfate and growth factors/receptors/matrix proteins. Curr. Opin. Struct. Biol. **34**, 35–42 (2015). doi:10.1016/j.sbi.2015.06.004
44. Gu, W.-L., Fu, S.-L., Wang, Y.-X., Li, Y., Lü, H.-Z., Xu, X.-M., Lu, P.-H.: Chondroitin sulfate proteoglycans regulate the growth, differentiation and migration of multipotent neural precursor cells through the integrin signaling pathway. BMC Neurosci. **10**(1), 1–15 (2009). doi:10.1186/1471-2202-10-128
45. Cui, H., Freeman, C., Jacobson, G.A., Small, D.H.: Proteoglycans in the central nervous system: role in development, neural repair, and Alzheimer's disease. IUBMB Life. **65**(2), 108–120 (2013). doi:10.1002/iub.1118
46. Griffith, J.W., Sokol, C.L., Luster, A.D.: Chemokines and chemokine receptors: positioning cells for host defense and immunity. Annu. Rev. Immunol. **32**(1), 659–702 (2014). doi:10.1146/annurev-immunol-032713-120145
47. Iannuzzi, C., Irace, G., Sirangelo, I.: The effect of glycosaminoglycans (GAGs) on amyloid aggregation and toxicity. Molecules. **20**(2), 2510 (2015)
48. Li, F., ten Dam, G.B., Murugan, S., Yamada, S., Hashiguchi, T., Mizumoto, S., Oguri, K., Okayama, M., van Kuppevelt, T.H., Sugahara, K.: Involvement of highly sulfated chondroitin sulfate in the metastasis of the Lewis lung carcinoma cells. J. Biol. Chem. **283**(49), 34294–34304 (2008). doi:10.1074/jbc.M806015200
49. Monneau, Y., Arenzana-Seisdedos, F., Lortat-Jacob, H.: The sweet spot: how GAGs help chemokines guide migrating cells. J. Leukoc. Biol. **99**(6), 935–953 (2016). doi:10.1189/jlb.3MR0915-440R
50. Hileman, R.E., Fromm, J.R., Weiler, J.M., Linhardt, R.J.: Glycosaminoglycan-protein interactions: definition of consensus sites in glycosaminoglycan binding proteins. BioEssays. **20**(2), 156–167 (1998). doi:10.1002/(SICI)1521-1878(199802)20:2<156::AID-BIES8>3.0.CO;2-R
51. Cardin, A.D., Weintraub, H.J.: Molecular modeling of protein-glycosaminoglycan interactions. Arterioscler. Thromb. Vasc. Biol. **9**(1), 21–32 (1989). doi:10.1161/01.atv.9.1.21
52. Sobel, M., Soler, D.F., Kermode, J.C., Harris, R.B.: Localization and characterization of a heparin binding domain peptide of human von Willebrand factor. J. Biol. Chem. **267**(13), 8857–8862 (1992)
53. Margalit, H., Fischer, N., Ben-Sasson, S.A.: Comparative analysis of structurally defined heparin binding sequences reveals a distinct spatial distribution of basic residues. J. Biol. Chem. **268**(26), 19228–19231 (1993)
54. Sarkar, A., Desai, U.R.: A Simple mMethod for dDiscovering Druggable, Specific Glycosaminoglycan-Protein Systems. Elucidation of Key Principles from Heparin/Heparan Sulfate-Binding Proteins. PLoS ONE. **10**(10), e0141127 (2015). doi:10.1371/journal.pone.0141127
55. Beurdeley, M., Spatazza, J., Lee, H.H., Sugiyama, S., Bernard, C., Di Nardo, A.A., Hensch, T.K., Prochiantz, A.: Otx2 binding to perineuronal nets persistently regulates plasticity in the mature visual cortex. J. Neurosci. **32**(27), 9429–9437 (2012). doi:10.1523/JNEUROSCI.0394-12.2012
56. Corredor, M., Bonet, R., Moure, A., Domingo, C., Bujons, J., Alfonso, I., Pérez, Y., Messeguer, À.: Cationic peptides and Peptidomimetics bind glycosaminoglycans as potential Sema3A pathway inhibitors. Biophys. J. **110**(6), 1291–1303 (2016). doi:10.1016/j.bpj.2016.01.033
57. Dick, G., Tan, C.L., Alves, J.N., Ehlert, E.M., Miller, G.M., Hsieh-Wilson, L.C., Sugahara, K., Oosterhof, A., van Kuppevelt, T.H., Verhaagen, J., Fawcett, J.W., Kwok, J.C.: Semaphorin 3A binds to the perineuronal nets via chondroitin sulfate type E motifs in rodent brains. J. Biol. Chem. **288**(38), 27384–27395 (2013). doi:10.1074/jbc.M111.310029
58. Gama, C.I., Tully, S.E., Sotogaku, N., Clark, P.M., Rawat, M., Vaidehi, N., Goddard, W.A., Nishi, A., Hsieh-Wilson, L.C.: Sulfation patterns of glycosaminoglycans encode molecular recognition and activity. Nat. Chem. Biol. **2**(9), 467–473 (2006). http://www.nature.com/nchembio/journal/v2/n9/suppinfo/nchembio810_SI.html
59. Ashikari-Hada, S., Habuchi, H., Kariya, Y., Itoh, N., Reddi, A.H., Kimata, K.: Characterization of growth factor-binding structures in heparin/heparan sulfate using an Octasaccharide library. J. Biol. Chem. **279**(13), 12346–12354 (2004). doi:10.1074/jbc.M313523200
60. Sun, C., Marcello, M., Li, Y., Mason, D., Lévy, R., Fernig, D.G.: Selectivity in glycosaminoglycan binding dictates the distribution and diffusion of fibroblast growth factors in the pericellular matrix. Open Biol. **6**(3), (2016). doi:10.1098/rsob.150277
61. Qu, X., Carbe, C., Tao, C., Powers, A., Lawrence, R., van Kuppevelt, T.H., Cardoso, W.V., Grobe, K., Esko, J.D., Zhang, X.: Lacrimal gland development and Fgf10-Fgfr2b signaling are controlled by 2-O- and 6-O-sulfated heparan sulfate. J. Biol. Chem. **286**(16), 14435–14444 (2011). doi:10.1074/jbc.M111.225003
62. Ashikari-Hada, S., Habuchi, H., Sugaya, N., Kobayashi, T., Kimata, K.: Specific inhibition of FGF-2 signaling with 2-O-sulfated octasaccharides of heparan sulfate. Glycobiology. **19**(6), 644–654 (2009). doi:10.1093/glycob/cwp031
63. Nikolovska, K., Spillmann, D., Seidler, D.G.: Uronyl 2-O sulfotransferase potentiates Fgf2-induced cell migration. J. Cell Sci. **128**(3), 460–471 (2015). doi:10.1242/jcs.152660

64. Deepa, S.S., Umehara, Y., Higashiyama, S., Itoh, N., Sugahara, K.: Specific molecular interactions of oversulfated chondroitin sulfate E with various heparin-binding growth factors. Implications as a physiological binding partner in the brain and other tissues. J. Biol. Chem. **277**(46), 43707–43716 (2002). doi:10.1074/jbc.M207105200
65. Shipp, E.L., Hsieh-Wilson, L.C.: Profiling the sulfation specificities of glycosaminoglycan interactions with growth factors and chemotactic proteins using microarrays. Chem. Biol. **14**(2), 195–208 (2007). doi:10.1016/j.chembiol.2006.12.009
66. Landis, S.C.: Neuronal Growth Cones. Annu. Rev. Physiol. **45**(1), 567–580 (1983). doi:10.1146/annurev.ph.45.030183.003031
67. Dodd, J., Jessell, T.: Axon guidance and the patterning of neuronal projections in vertebrates. Science. **242**(4879), 692–699 (1988). doi:10.1126/science.3055291
68. Bernhardt, R.R., Schachner, M.: Chondroitin sulfates affect the formation of the segmental motor nerves in zebrafish embryos. Dev. Biol. **221**(1), 206–219 (2000). doi:10.1006/dbio.2000.9673
69. Kwok, J.C., Yuen, Y.L., Lau, W.K., Zhang, F.X., Fawcett, J.W., Chan, Y.S., Shum, D.K.: Chondroitin sulfates in the developing rat hindbrain confine commissural projections of vestibular nuclear neurons. Neural Dev. **7**, 6 (2012). doi:10.1186/1749-8104-7-6
70. Chung, K.Y., Taylor, J.S., Shum, D.K., Chan, S.O.: Axon routing at the optic chiasm after enzymatic removal of chondroitin sulfate in mouse embryos. Development. **127**(12), 2673–2683 (2000)
71. Asher, R.A., Morgenstern, D.A., Moon, L.D.F., Fawcett, J.W.: Chondroitin sulphate proteoglycans: inhibitory components of the glial scar. In: Progress in Brain Research, vol. Volume 132. pp. 611–619. Elsevier, (2001)
72. Silver, J., Miller, J.H.: Regeneration beyond the glial scar. Nat. Rev. Neurosci. **5**(2), 146–156 (2004). doi:10.1038/nrn1326
73. Bradbury, E.J., Moon, L.D.F., Popat, R.J., King, V.R., Bennett, G.S., Patel, P.N., Fawcett, J.W., McMahon, S.B.: Chondroitinase ABC promotes functional recovery after spinal cord injury. Nature. **416**(6881), 636–640 (2002)
74. Zhao, R.R., Fawcett, J.W.: Combination treatment with chondroitinase ABC in spinal cord injury–breaking the barrier. Neurosci. Bull. **29**(4), 477–483 (2013). doi:10.1007/s12264-013-1359-2
75. Kwok, J.C., Dick, G., Wang, D., Fawcett, J.W.: Extracellular matrix and perineuronal nets in CNS repair. Dev. Neurobiol. **71**(11), 1073–1089 (2011). doi:10.1002/dneu.20974
76. Gilbert, R.J., McKeon, R.J., Darr, A., Calabro, A., Hascall, V.C., Bellamkonda, R.V.: CS-4,6 is differentially upregulated in glial scar and is a potent inhibitor of neurite extension. Mol. Cell. Neurosci. **29**(4), 545–558 (2005). doi:10.1016/j.mcn.2005.04.006
77. Properzi, F., Carulli, D., Asher, R.A., Muir, E., Camargo, L.M., Van Kuppevelt, T.H., Ten Dam, G.B., Furukawa, Y., Mikami, T., Sugahara, K., Toida, T., Geller, H.M., Fawcett, J.W.: Chondroitin 6-sulphate synthesis is up-regulated in injured CNS, induced by injury-related cytokines and enhanced in axon-growth inhibitory glia. Eur. J. Neurosci. **21**(2), 378–390 (2005). doi:10.1111/j.1460-9568.2005.03876.x
78. Vo, T., Carulli, D., Ehlert, E.M.E., Kwok, J.C.F., Dick, G., Mecollari, V., Moloney, E.B., Neufeld, G., de Winter, F., Fawcett, J.W., Verhaagen, J.: The chemorepulsive axon guidance protein semaphorin3A is a constituent of perineuronal nets in the adult rodent brain. Mol. Cell. Neurosci. **56**, 186–200 (2013). doi:10.1016/j.mcn.2013.04.009
79. Spatazza, J., Lee, H.H., Di Nardo, A.A., Tibaldi, L., Joliot, A., Hensch, T.K., Prochiantz, A.: Choroid-plexus-derived Otx2 homeoprotein constrains adult cortical plasticity. Cell Rep. **3**(6), 1815–1823 (2013). doi:10.1016/j.celrep.2013.05.014
80. Heck, N., Garwood, J., Loeffler, J.P., Larmet, Y., Faissner, A.: Differential upregulation of extracellular matrix molecules associated with the appearance of granule cell dispersion and mossy fiber sprouting during epileptogenesis in a murine model of temporal lobe epilepsy. Neuroscience. **129**(2), 309–324 (2004). doi:10.1016/j.neuroscience.2004.06.078
81. Yutsudo, N., Kitagawa, H.: Involvement of chondroitin 6-sulfation in temporal lobe epilepsy. Experimental Neurology 274, Part B, 126–133 (2015). doi:10.1016/j.expneurol.2015.07.009
82. Hall, B.K., Ekanayake, S.: Effects of growth factors on the differentiation of neural crest cells and neural crest cell-derivatives. Int. J. Dev. Biol. **35**, 367–387 (1991)
83. Antoniades, H.N., Owen, A.J.: Growth Factors and Regulation of Cell Growth. Annu. Rev. Med. **33**(1), 445–463 (1982). doi:10.1146/annurev.me.33.020182.002305
84. Seeger, M.A., Paller, A.S.: The roles of growth factors in keratinocyte migration. Adv. Wound Care. **4**(4), 213–224 (2015). doi:10.1089/wound.2014.0540
85. Fox, G.M.: The role of growth factors in tissue repair III. In: Clark, R.A.F., Henson, P.M. (eds.) The molecular and cellular biology of wound repair, pp. 265–271. Springer US, Boston (1988)
86. Slavin, J.: Fibroblast growth factors: at the heart of angiogenesis. Cell Biol. Int. **19**(5), 431–444 (1995). doi:10.1006/cbir.1995.1087
87. Yan, Q., Rosenfeld, R.D., Matheson, C.R., Hawkins, N., Lopez, O.T., Bennett, L., Welcher, A.A.: Expression of brain-derived neurotrophic factor protein in the adult rat central nervous system. Neuroscience. **78**(2), 431–448 (1997). doi:10.1016/S0306-4522(96)00613-6
88. Lee, K., Silva, E.A., Mooney, D.J.: Growth factor delivery-based tissue engineering: general approaches and a review of recent developments. J. R. Soc. Interface. **8**(55), 153–170 (2011). doi:10.1098/rsif.2010.0223
89. Forsten-Williams, K., Chu, C.L., Fannon, M., Buczek-Thomas, J.A., Nugent, M.A.: Control of growth factor networks by heparan sulfate proteoglycans. Ann. Biomed. Eng. **36**(12), 2134–2148 (2008). doi:10.1007/s10439-008-9575-z
90. Alderson, R.F., Alterman, A.L., Barde, Y.-A., Lindsay, R.M.: Brain-derived neurotrophic factor increases survival and differentiated functions of rat septal cholinergic neurons in culture. Neuron. **5**(3), 297–306 (1990). doi:10.1016/0896-6273(90)90166-D
91. Oliveira, S.L.B., Pillat, M.M., Cheffer, A., Lameu, C., Schwindt, T.T., Ulrich, H.: Functions of neurotrophins and growth factors in neurogenesis and brain repair. Cytometry. Part A. **83A**(1), 76–89 (2013). doi:10.1002/cyto.a.22161
92. Billings, P.C., Pacifici, M.: Interactions of signaling proteins, growth factors and other proteins with heparan sulfate: mechanisms and mysteries. Connect. Tissue Res. **56**(4), 272–280 (2015). doi:10.3109/03008207.2015.1045066
93. Perrimon, N., Bernfield, M.: Specificities of heparan sulphate proteoglycans in developmental processes. Nature. **404**(6779), 725–728 (2000)
94. Sugahara, K., Kitagawa, H.: Recent advances in the study of the biosynthesis and functions of sulfated glycosaminoglycans. Curr. Opin. Struct. Biol. **10**, 518–527 (2000)
95. Hatten, M.E., Lynch, M., Rydel, R.E., Sanchez, J., Joseph-Silverstein, J., Moscatelli, D., Rifkin, D.B.: *In vitro* neurite extension by granule neurons is dependent upon astroglial-derived fibroblast growth factor. Dev. Biol. **125**(2), 280–289 (1988). doi:10.1016/0012-1606(88)90211-4
96. Walicke, P.A.: Interactions between basic fibroblast growth factor (FGF) and glycosoaminoglycans in promoting neurite outgrowth. Exp. Neurol. **102**(1), 144–148 (1988). doi:10.1016/0014-4886(88)90087-8
97. Karumbaiah, L., Enam, S.F., Brown, A.C., Saxena, T., Betancur, M.I., Barker, T.H., Bellamkonda, R.V.: Chondroitin sulfate glycosaminoglycan hydrogels create endogenous niches for neural

stem cells. Bioconjug. Chem. **26**(12), 2336–2349 (2015). doi:10.1021/acs.bioconjchem.5b00397
98. Nandini, C.D., Mikami, T., Ohta, M., Itoh, N., Akiyama-Nambu, F., Sugahara, K.: Structural and functional characterization of oversulfated chondroitin sulfate/dermatan sulfate hybrid chains from the notochord of hagfish: neuritogenic and binding activities for growth factors and neurotrophic factors. J. Biol. Chem. **279**(49), 50799–50809 (2004). doi:10.1074/jbc.M404746200
99. Sirko, S., Akita, K., Von Holst, A., Faissner, A.: Structural and Functional Analysis of Chondroitin Sulfate Proteoglycans in the Neural Stem Cell Niche. Methods Enzymol. **479**, 37–71 (2010). doi:10.1016/s0076-6879(10)79003-0
100. Sirko, S., von Holst, A., Wizenmann, A., Götz, M., Faissner, A.: Chondroitin sulfate glycosaminoglycans control proliferation, radial glia cell differentiation and neurogenesis in neural stem/progenitor cells. Development. **134**(15), 2727–2738 (2007). doi:10.1242/dev.02871
101. Matsumoto, K., Wanaka, A., Takatsuji, K., Muramatsu, H., Muramatsu, T., Tohyama, M.: A novel family of heparin-binding growth factors, pleiotrophin and midkine, is expressed in the developing rat cerebral cortex. Dev. Brain Res. **79**(2), 229–241 (1994). doi:10.1016/0165-3806(94)90127-9
102. Kadomatsu, K., Muramatsu, T.: Midkine and pleiotrophin in neural development and cancer. Cancer Lett. **204**(2), 127–143 (2004). doi:10.1016/S0304-3835(03)00450-6
103. Muramatsu, H., Shirahama, H., Yonezawa, S., Maruta, H., Muramatsu, T.: Midkine, A Retinoic Acid-Inducible Growth/Differentiation Factor: Immunochemical Evidence for the Function and Distribution. Dev. Biol. **159**(2), 392–402 (1993). doi:10.1006/dbio.1993.1250
104. Maeda, N., Nishiwaki, T., Shintani, T., Hamanaka, H., Noda, M.: 6B4 proteoglycan/phosphacan, an extracellular variant of receptor-like protein-tyrosine phosphatase ζ/RPTPβ, binds pleiotrophin/heparin-binding growth-associated molecule (HB-GAM). J. Biol. Chem. **271**(35), 21446–21452 (1996). doi:10.1074/jbc.271.35.21446
105. Maeda, N., Noda, M.: Involvement of receptor-like protein tyrosine phosphatase ζ/RPTPβ and its ligand pleiotrophin/heparin-binding growth-associated molecule (HB-GAM) in neuronal migration. J. Cell Biol. **142**(1), 203–216 (1998). doi:10.1083/jcb.142.1.203
106. Ueoka, C., Kaneda, N., Okazaki, I., Nadanaka, S., Muramatsu, T., Sugahara, K.: Neuronal cell adhesion, mediated by the heparin-binding neuroregulatory factor midkine, is specifically inhibited by chondroitin sulfate E. Structural ans functional implications of the over-sulfated chondroitin sulfate. J. Biol. Chem. **275**(48), 37407–37413 (2000). doi:10.1074/jbc.M002538200
107. Mizumoto, S., Fongmoon, D., Sugahara, K.: Interaction of chondroitin sulfate and dermatan sulfate from various biological sources with heparin-binding growth factors and cytokines. Glycoconj. J. **30**(6), 619–632 (2013). doi:10.1007/s10719-012-9463-5
108. Yasuhara, O., Muramatsu, H., Kim, S.U., Muramatsu, T., Maruta, H., McGeer, P.L.: Midkine, a novel neurotrophic factor, is present in senile plaques of alzheimer disease. Biochem. Biophys. Res. Commun. **192**(1), 246–251 (1993). doi:10.1006/bbrc.1993.1406
109. Ensslen-Craig, S.E., Brady-Kalnay, S.M.: Receptor protein tyrosine phosphatases regulate neural development and axon guidance. Dev. Biol. **275**(1), 12–22 (2004). doi:10.1016/j.ydbio.2004.08.009
110. Stoker, A.W.: RPTPs in axons, synapses and neurology. Semin. Cell Dev. Biol. **37**, 90–97 (2015). doi:10.1016/j.semcdb.2014.09.006
111. Fry, E.J., Chagnon, M.J., López-Vales, R., Tremblay, M.L., David, S.: Corticospinal tract regeneration after spinal cord injury in receptor protein tyrosine phosphatase sigma deficient mice. Glia. **58**(4), 423–433 (2010). doi:10.1002/glia.20934
112. Shen, Y., Tenney, A.P., Busch, S.A., Horn, K.P., Cuascut, F.X., Liu, K., He, Z., Silver, J., Flanagan, J.G.: PTPsigma is a receptor for chondroitin sulfate proteoglycan, an inhibitor of neural regeneration. Science. **326**(5952), 592–596 (2009). doi:10.1126/science.1178310
113. Dwyer, C.A., Baker, E., Hu, H., Matthews, R.T.: RPTPζ/phosphacan is abnormally glycosylated in a model of muscle–eye–brain disease lacking functional POMGnT1. Neuroscience. **220**, 47–61 (2012). doi:10.1016/j.neuroscience.2012.06.026
114. Dwyer, C.A., Katoh, T., Tiemeyer, M., Matthews, R.T.: Neurons and glia modify receptor protein-tyrosine phosphatase ζ (RPTPζ)/phosphacan with cell-specific O-Mannosyl Glycans in the developing brain. J. Biol. Chem. **290**(16), 10256–10273 (2015). doi:10.1074/jbc.M114.614099
115. Dino, M.R., Harroch, S., Hockfield, S., Matthews, R.T.: Monoclonal antibody cat-315 detects a glycoform of receptor protein tyrosine phosphatase beta/phosphacan early in CNS development that localizes to extrasynaptic sites prior to synapse formation. Neuroscience. **142**(4), 1055–1069 (2006). doi:10.1016/j.neuroscience.2006.07.054
116. Aricescu, A.R., McKinnell, I.W., Halfter, W., Stoker, A.W.: Heparan sulfate proteoglycans are ligands for receptor protein tyrosine phosphatase σ. Mol. Cell. Biol. **22**(6), 1881–1892 (2002). doi:10.1128/mcb.22.6.1881-1892.2002
117. Shen, Y.: Traffic lights for axon growth: proteoglycans and their neuronal receptors. Neural Regen. Res. **9**, 356–361 (2014). doi:10.4103/1673-5374.128236
118. Coles, C.H., Shen, Y., Tenney, A.P., Siebold, C., Sutton, G.C., Lu, W., Gallagher, J.T., Jones, E.Y., Flanagan, J.G., Aricescu, A.R.: Proteoglycan-specific molecular switch for RPTPsigma clustering and neuronal extension. Science. **332**(6028), 484–488 (2011). doi:10.1126/science.1200840
119. McLean, J., Batt, J., Doering, L.C., Rotin, D., Bain, J.R.: Enhanced rate of nerve regeneration and directional errors after sciatic nerve injury in receptor protein tyrosine phosphatase ς knock-out mice. J. Neurosci. **22**(13), 5481–5491 (2002)
120. Lang, B.T., Cregg, J.M., DePaul, M.A., Tran, A.P., Xu, K., Dyck, S.M., Madalena, K.M., Brown, B.P., Weng, Y.L., Li, S., Karimi-Abdolrezaee, S., Busch, S.A., Shen, Y., Silver, J.: Modulation of the proteoglycan receptor PTPsigma promotes recovery after spinal cord injury. Nature. **518**(7539), 404–408 (2015). doi:10.1038/nature13974
121. Kurihara, D., Yamashita, T.: Chondroitin sulfate proteoglycans down-regulate spine formation in cortical neurons by targeting tropomyosin-related kinase B (TrkB) protein. J. Biol. Chem. **287**(17), 13822–13828 (2012). doi:10.1074/jbc.M111.314070
122. Fisher, D., Xing, B., Dill, J., Li, H., Hoang, H.H., Zhao, Z., Yang, X.L., Bachoo, R., Cannon, S., Longo, F.M., Sheng, M., Silver, J., Li, S.: Leukocyte common antigen-related phosphatase is a functional receptor for chondroitin sulfate proteoglycan axon growth inhibitors. J. Neurosci. **31**(40), 14051–14066 (2011). doi:10.1523/JNEUROSCI.1737-11.2011
123. Xu, B., Park, D., Ohtake, Y., Li, H., Hayat, U., Liu, J., Selzer, M.E., Longo, F.M., Li, S.: Role of CSPG receptor LAR phosphatase in restricting axon regeneration after CNS injury. Neurobiol. Dis. **73**, 36–48 (2015). doi:10.1016/j.nbd.2014.08.030
124. Schwab, M.E.: Functions of Nogo proteins and their receptors in the nervous system. Nat. Rev. Neurosci. **11**(12), 799–811 (2010)
125. Dickendesher, T.L., Baldwin, K.T., Mironova, Y.A., Koriyama, Y., Raiker, S.J., Askew, K.L., Wood, A., Geoffroy, C.G., Zheng, B., Liepmann, C.D., Katagiri, Y., Benowitz, L.I., Geller, H.M., Giger, R.J.: NgR1 and NgR3 are receptors for chondroitin sulfate proteoglycans. Nat. Neurosci. **15**(5), 703–712 (2012). doi:10.1038/nn.3070
126. Lodish, H., Berk, A., Zipursky, S.L., Matsudaira, P., Baltimore, D., Darnell, J.: Cell-cell adhesion and communication. In: Lodish, H.e.a. (ed.) Molecular Cell Biology. W.H. Freeman, New York (2000)

127. Schmid, R.S., Maness, P.F.: L1 and NCAM adhesion molecules as signaling coreceptors in neuronal migration and process outgrowth. Curr. Opin. Neurobiol. **18**(3), 245–250 (2008). doi:10.1016/j.conb.2008.07.015
128. Park, K., Biederer, T.: Neuronal adhesion and synapse organization in recovery after brain injury. Future Neurol. **8**(5), 555–567 (2013). doi:10.2217/fnl.13.35
129. Chipman, P.H., Schachner, M., Rafuse, V.F.: Presynaptic NCAM is required for motor neurons to functionally expand their peripheral field of innervation in partially Denervated muscles. J. Neurosci. **34**(32), 10497–10510 (2014). doi:10.1523/jneurosci.0697-14.2014
130. Saini, V., Loers, G., Kaur, G., Schachner, M., Jakovcevski, I.: Impact of neural cell adhesion molecule deletion on regeneration after mouse spinal cord injury. Eur. J. Neurosci. **44**(1), 1734–1746 (2016). doi:10.1111/ejn.13271
131. Milev, P., Friedlander, D.R., Sakurai, T., Karthikeyan, L., Flad, M., Margolis, R.K., Grumet, M., Margolis, R.U.: Interactions of the chondroitin sulfate proteoglycan phosphacan, the extracellular domain of a receptor-type protein tyrosine phosphatase, with neurons, glia, and neural cell adhesion molecules. J. Cell Biol. **127**(6), 1703–1715 (1994). doi:10.1083/jcb.127.6.1703
132. Friedlander, D.R., Milev, P., Karthikeyan, L., Margolis, R.K., Margolis, R.U., Grumet, M.: The neuronal chondroitin sulfate proteoglycan neurocan binds to the neural cell adhesion molecules Ng-CAM/L1/NILE and N-CAM, and inhibits neuronal adhesion and neurite outgrowth. J. Cell Biol. **125**(3), 669–680 (1994). doi:10.1083/jcb.125.3.669
133. Berglund, E.O., Murai, K.K., Fredette, B., Sekerková, G., Marturano, B., Weber, L., Mugnaini, E., Ranscht, B.: Ataxia and abnormal cerebellar Microorganization in mice with ablated contactin Gene expression. Neuron. **24**(3), 739–750 (1999). doi:10.1016/S0896-6273(00)81126-5
134. Mikami, T., Yasunaga, D., Kitagawa, H.: Contactin-1 is a functional receptor for neuroregulatory chondroitin sulfate-E. J. Biol. Chem. **284**(7), 4494–4499 (2009). doi:10.1074/jbc.M809227200
135. Nugent, A.A., Kolpak, A.L., Engle, E.C.: Human disorders of axon guidance. Curr. Opin. Neurobiol. **22**(5), 837–843 (2012). doi:10.1016/j.conb.2012.02.006
136. Goodman, C.S.: Mechanisms and molecules that control growth cone guidance. Annu. Rev. Neurosci. **19**(1), 341–377 (1996). doi:10.1146/annurev.ne.19.030196.002013
137. Dewit, J., Verhaagen, J.: Role of semaphorins in the adult nervous system. Prog. Neurobiol. **71**(2–3), 249–267 (2003). doi:10.1016/j.pneurobio.2003.06.001
138. Luo, Y., Raible, D., Raper, J.A.: Collapsin: a protein in brain that induces the collapse and paralysis of neuronal growth cones. Cell. **75**(2), 217–227 (1993). doi:10.1016/0092-8674(93)80064-L
139. Bagnard, D., Lohrum, M., Uziel, D., Puschel, A.W., Bolz, J.: Semaphorins act as attractive and repulsive guidance signals during the development of cortical projections. Development. **125**(24), 5043–5053 (1998)
140. Polleux, F., Morrow, T., Ghosh, A.: Semaphorin 3A is a chemoattractant for cortical apical dendrites. Nature **404**(6778), 567–573 (2000). http://www.nature.com/nature/journal/v404/n6778/suppinfo/404567a0_S1.html
141. Murphey, R.K., Froggett, S.J., Caruccio, P., Shan-Crofts, X., Kitamoto, T., Godenschwege, T.A.: Targeted expression of shibirets and semaphorin 1a reveals critical periods for synapse formation in the giant fiber of drosophila. Development. **130**(16), 3671–3682 (2003). doi:10.1242/dev.00598
142. Taniguchi, M., Yuasa, S., Fujisawa, H., Naruse, I., Saga, S., Mishina, M., Yagi, T.: Disruption of semaphorin III/D Gene causes severe abnormality in peripheral nerve projection. Neuron. **19**(3), 519–530 (1997). doi:10.1016/S0896-6273(00)80368-2
143. Yazdani, U., Terman, J.R.: The semaphorins. Genome Biol. **7**(3), 1–14 (2006). doi:10.1186/gb-2006-7-3-211
144. Mecollari, V., Nieuwenhuis, B., Verhaagen, J.: A perspective on the role of class III semaphorin signaling in central nervous system trauma. Front. Cell. Neurosci. **8**, (2014). doi:10.3389/fncel.2014.00328
145. Tamagnone, L., Artigiani, S., Chen, H., He, Z., Ming, G.-L., Song, H.-J., Chedotal, A., Winberg, M.L., Goodman, C.S., Poo, M.-M., Tessier-Lavigne, M., Comoglio, P.M.: Plexins Are a Large Family of Receptors for Transmembrane, Secreted, and GPI-Anchored Semaphorins in Vertebrates. Cell. **99**(1), 71–80. doi:10.1016/S0092-8674(00)80063-X
146. Winberg, M.L., Noordermeer, J.N., Tamagnone, L., Comoglio, P.M., Spriggs, M.K., Tessier-Lavigne, M., Goodman, C.S.: Plexin A Is a Neuronal Semaphorin Receptor that Controls Axon Guidance. Cell. **95**(7), 903–916. doi:10.1016/S0092-8674(00)81715-8
147. Bouzioukh, F., Daoudal, G., Falk, J., Debanne, D., Rougon, G., Castellani, V.: Semaphorin3A regulates synaptic function of differentiated hippocampal neurons. Eur. J. Neurosci. **23**(9), 2247–2254 (2006). doi:10.1111/j.1460-9568.2006.04783.x
148. Chen, G., Sima, J., Jin, M., Wang, K.-Y., Xue, X.-J., Zheng, W., Ding, Y.-Q., Yuan, X.-B.: Semaphorin-3A guides radial migration of cortical neurons during development. Nat. Neurosci. **11**(1), 36–44 (2008). http://www.nature.com/neuro/journal/v11/n1/suppinfo/nn2018_S1.html
149. Shintani, Y., Takashima, S., Asano, Y., Kato, H., Liao, Y., Yamazaki, S., Tsukamoto, O., Seguchi, O., Yamamoto, H., Fukushima, T., Sugahara, K., Kitakaze, M., Hori, M.: Glycosaminoglycan modification of neuropilin-1 modulates VEGFR2 signaling. EMBO J. **25**(13), 3045–3055 (2006). doi:10.1038/sj.emboj.7601188
150. Tang, X.-Q., Tanelian, D.L., Smith, G.M.: Semaphorin3A inhibits nerve growth factor-induced sprouting of nociceptive afferents in adult rat spinal cord. J. Neurosci. **24**(4), 819–827 (2004). doi:10.1523/jneurosci.1263-03.2004
151. Purohit, A., Sadanandam, A., Myneni, P., Singh, R.K.: Semaphorin 5A mediated cellular navigation: connecting nervous system and cancer. Biochim. et Biophys. Acta (BBA) – Rev. Cancer. **1846**(2), 485–493 (2014). doi:10.1016/j.bbcan.2014.09.006
152. Adams, R.H., Betz, H., Püschel, A.W.: A novel class of murine semaphorins with homology to thrombospondin is differentially expressed during early embryogenesis. Mech. Dev. **57**(1), 33–45 (1996). doi:10.1016/0925-4773(96)00525-4
153. Adams, J.C., Tucker, R.P.: The thrombospondin type 1 repeat (TSR) superfamily: diverse proteins with related roles in neuronal development. Dev. Dyn. **218**(2), 280–299 (2000). doi:10.1002/(SICI)1097-0177(200006)218:2<280::AID-DVDY4>3.0.CO;2-0
154. Gantt, S.M., Clavijo, P., Bai, X., Esko, J.D., Simnis, P.: Cell adhesion to a motif shared by the malaria Circumsporozoite protein and thrombospondin is mediated by its glycosaminoglycan-binding region and not by CSVTCG. J. Biol. Chem. **272**(31), 19205–19213 (1997). doi:10.1074/jbc.272.31.19205
155. Kantor, D.B., Chivatakarn, O., Peer, K.L., Oster, S.F., Inatani, M., Hansen, M.J., Flanagan, J.G., Yamaguchi, Y., Sretavan, D.W., Giger, R.J., Kolodkin, A.L.: Semaphorin 5A is a bifunctional axon guidance cue regulated by heparan and chondroitin sulfate proteoglycans. Neuron. **44**(6), 961–975 (2004). doi:10.1016/j.neuron.2004.12.002
156. Conrad, A.H., Zhang, Y., Tasheva, E.S., Conrad, G.W.: Proteomic analysis of potential keratan sulfate, chondroitin sulfate a, and hyaluronic acid molecular interactions. Invest. Ophthalmol. Vis. Sci. **51**(9), 4500–4515 (2010). doi:10.1167/iovs.09-4914

157. Wang, L.-H., Strittmatter, S.M.: A family of rat CRMP genes is differentially expressed in the nervous system. J. Neurosci. **16**(19), 6197–6207 (1996)
158. Nagai, J., Kitamura, Y., Owada, K., Yamashita, N., Takei, K., Goshima, Y., Ohshima, T.: Crmp4 deletion promotes recovery from spinal cord injury by neuroprotection and limited scar formation. Sci. Report. **5**, 8269 (2015). doi:10.1038/srep08269 http://www.nature.com/articles/srep08269#supplementary-information
159. Franken, S., Junghans, U., Rosslenbroich, V., Baader, S.L., Hoffmann, R., Gieselmann, V., Viebahn, C., Kappler, J.: Collapsin response mediator proteins of neonatal rat brain interact with chondroitin sulfate. J. Biol. Chem. **278**(5), 3241–3250 (2003). doi:10.1074/jbc.M210181200
160. Junghans, U., Franken, S., Pommer, A., Müller, H., Viebahn, C., Kappler, J.: A monoclonal antibody against a neuron-specific 65-kDa protein with laminar expression in the developing cerebral cortex. Histochem. Cell Biol. **117**(4), 317–325 (2002). doi:10.1007/s00418-002-0394-2
161. Ferrer, I., Tortosa, A., Blanco, R., Martín, F., Serrano, T., Planas, A., Macaya, A.: Naturally occurring cell death in the developing cerebral cortex of the rat. Evidence of apoptosis-associated internucleosomal DNA fragmentation. Neurosci. Lett. **182**(1), 77–79 (1994). doi:10.1016/0304-3940(94)90210-0
162. Oppenheim, R.W.: Cell death during development of the nervous system. Annu. Rev. Neurosci. **14**(1), 453–501 (1991). doi:10.1146/annurev.ne.14.030191.002321
163. Acampora, D., Gulisano, M., Broccoli, V., Simeone, A.: Otx genes in brain morphogenesis. Prog. Neurobiol. **64**(1), 69–95 (2001). doi:10.1016/S0301-0082(00)00042-3
164. Sugiyama, S., Di Nardo, A.A., Aizawa, S., Matsuo, I., Volovitch, M., Prochiantz, A., Hensch, T.K.: Experience-dependent transfer of Otx2 homeoprotein into the visual cortex activates postnatal plasticity. Cell. **134**(3), 508–520 (2008). doi:10.1016/j.cell.2008.05.054
165. Bernard, C., Prochiantz, A.: Otx2-PNN interaction to regulate cortical plasticity. Neural Plast. 2016. **7**, (2016). doi:10.1155/2016/7931693
166. Alberts, B., Johnson, A., Lewis, J., Morgan, D., Raff, M., Roberts, K., Walter, P.: Cell Junctions and the Extracellular Matrix. In: Molecular Biology of the Cell. Garland Science, (2015)
167. Gundersen, R.W.: Response of sensory neurites and growth cones to patterned substrata of laminin and fibronectin *in vitro*. Dev. Biol. **121**(2), 423–431 (1987). doi:10.1016/0012-1606(87)90179-5
168. Rivas, R.J., Burmeister, D.W., Goldberg, D.J.: Rapid effects of laminin on the growth cone. Neuron. **8**(1), 107–115 (1992). doi:10.1016/0896-6273(92)90112-Q
169. Tonge, D.A., de Burgh, H.T., Docherty, R., Humphries, M.J., Craig, S.E., Pizzey, J.: Fibronectin supports neurite outgrowth and axonal regeneration of adult brain neurons *in vitro*. Brain Res. **1453**, 8–16 (2012). doi:10.1016/j.brainres.2012.03.024
170. Cescon, M., Chen, P., Castagnaro, S., Gregorio, S., Bonaldo, P.: Lack of collagen VI promotes neurodegeneration by impairing autophagy and inducing apoptosis during aging. Aging. **8**(5), 1083–1101 (2016)
171. Woerly, S., Marchand, R.: Collagen-cliondroitin-6-sulfate hydrogel implants in CNS lesion cavities favor glial repair, the differentiation of co-implanted neurons and the growth of axons. Restor. Neurol. Neurosci. **3**(2), 95–99 (1991)
172. Streit, A., Nolte, C., Rásony, T., Schachner, M.: Interaction of astrochondrin with extracellular matrix components and its involvement in astrocyte process formation and cerebellar granule cell migration. J. Cell Biol. **120**(3), 799–814 (1993). doi:10.1083/jcb.120.3.799
173. Snow, D.M., Brown, E.M., Letourneau, P.C.: Growth cone behaviour in the presence of soluble chondroitin sulfate proteoglycan (CSPG), compared to behaviour on CSPG bound to laminin or fibronectin. Int. J. Dev. Neurosci. **14**(3), 331–349 (1996). doi:10.1016/0736-5748(96)00017-2
174. Furutani, Y., Manabe, R.-I., Tsutsui, K., Yamada, T., Sugimoto, N., Fukuda, S., Kawsi, J., Sugiura, N., Kimata, K., Hayashizaki, Y., Sekiguchi, K.: Identification and characterization of photomedins: novel olfactomedin-domain-containing proteins with chondroitin sulphate-E-binding activity. Biochem. J. **389**(3), 675–684 (2005). doi:10.1042/bj20050120
175. Bal, R.S., Anholt, R.R.: Formation of the extracellular mucous matrix of olfactory neuroepithelium: identification of partially glycosylated and nonglycosylated precursors of olfactomedin. Biochemistry. **32**(4), 1047–1053 (1993)
176. Nalivaeva, N.N., Turner, A.J.: The amyloid precursor protein: a biochemical enigma in brain development, function and disease. FEBS Lett. **587**(13), 2046–2054 (2013). doi:10.1016/j.febslet.2013.05.010
177. Lazarov, O., Demars, M.P.: All in the Family: How the APPs Regulate Neurogenesis. Front. Neurosci. **6**, (2012). doi:10.3389/fnins.2012.00081
178. Castillo, G.M., Lukito, W., Wight, T.N., Snow, A.D.: The sulfate moieties of glycosaminoglycans are critical for the enhancement of beta-amyloid protein fibril formation. J. Neurochem. **72**(4), 1681–1687 (1999)
179. Jendresen, C.B., Cui, H., Zhang, X., Vlodavsky, I., Nilsson, L.N.G., Li, J.-P.: Overexpression of heparanase lowers the amyloid burden in amyloid-β precursor protein transgenic mice. J. Biol. Chem. **290**(8), 5053–5064 (2015). doi:10.1074/jbc.M114.600569
180. Morawski, M., Brückner, G., Jäger, C., Seeger, G., Matthews, R.T., Arendt, T.: Involvement of perineuronal and Perisynaptic extracellular matrix in Alzheimer's disease neuropathology. Brain Pathol. **22**(4), 547–561 (2012). doi:10.1111/j.1750-3639.2011.00557.x
181. Morawski, M., Brückner, M.K., Riederer, P., Brückner, G., Arendt, T.: Perineuronal nets potentially protect against oxidative stress. Exp. Neurol. **188**(2), 309–315 (2004). doi:10.1016/j.expneurol.2004.04.017
182. Williamson, T.G., Nurcombe, V., Beyreuther, K., Masters, C.L., Small, D.H.: Affinity purification of proteoglycans that bind to the amyloid protein precursor of Alzheimer's disease. J. Neurochem. **65**(5), 2201–2208 (1995). doi:10.1046/j.1471-4159.1995.65052201.x
183. Soleman, S., Yip, P.K., Duricki, D.A., Moon, L.D.F.: Delayed treatment with chondroitinase ABC promotes sensorimotor recovery and plasticity after stroke in aged rats. Brain. **135**(4), 1210–1223 (2012). doi:10.1093/brain/aws027
184. Pantazopoulos, H., Woo, T.W., Lim, M.P., Lange, N., Berretta, S.: Extracellular matrix-glial abnormalities in the amygdala and entorhinal cortex of subjects diagnosed with schizophrenia. Arch. Gen. Psychiatry. **67**(2), 155–166 (2010). doi:10.1001/archgenpsychiatry.2009.196
185. Despras, G., Bernard, C., Perrot, A., Cattiaux, L., Prochiantz, A., Lortat-Jacob, H., Mallet, J.M.: Toward libraries of biotinylated chondroitin sulfate analogues: from synthesis to *in vivo* studies. Chemistry. **19**(2), 531–540 (2013). doi:10.1002/chem.201202173
186. Solera, C., Macchione, G., Maza, S., Kayser, M.M., Corzana, F., de Paz, J.L., Nieto, P.M.: Chondroitin sulfate tetrasaccharides: synthesis, Three-Dimensional Structure and Interaction with Midkine. Chem. Eur. J. **22**(7), 2356–2369 (2016). doi:10.1002/chem.201504440

Appendix 1: Chondroitin sulphates and their binding molecules in the central nervous system. (*Djerbal et al., 2017*[205]).

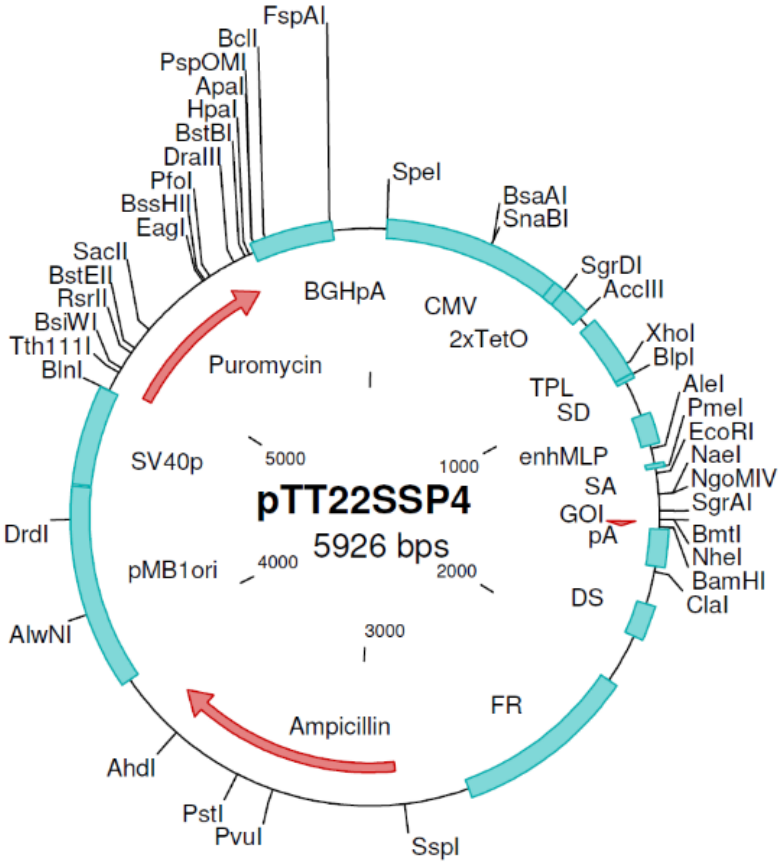


```
1349  atg gga gaa ctg ctg ctg ctc ctt ctg ctg ggg ctg cgg ctt cag ctg agt ctt gga gcc
                                    signal peptide
        m   g   e   l   l   l   l   l   l   l   g   l   r   l   q   l   s   l   g   a

1409  ggc gct cct ggc tcc tcc acc ggc cac cac cat cac cat cat cac cac ggc tcc acc ggc
                link                                H8G
        g   a   p   g   s   s   t   g   h   h   h   h   h   h   h   h   g   s   t   g

                                    NheI                                BamHI
                                  -+-----                             -+-----
1469  gag aac ctg tac ttt cag ggc gct agc nnn nnn nnn nnn nnn nnn gga tcc
                TEV
        e   n   l   y   f   q   g   a   s   ?   ?   ?   ?   ?   ?   g   s
                                        >>........GOI........>>
```

Appendix 2: pTT22SSP4 expression vector.
pTT22SSP4 was from NRC biotechnology research institute, Cananda. Sema3A sequence was sub-cloned between NheI and BamHI sites.

M G E L L L L L L L L G L R L Q L S L G A G A P G S S T G H H H H H H H H G S T G E N L Y F Q G A S
A N G K N N V P R L K L S Y K E M L E S N N V I T F N G L A N S S S Y H T F L L D E E R S R L Y V G
A K D H I F S F N L V N I K D F Q K I V W P V S Y T R R D E C K W A G K D I L K E C A N F I K V L K
A Y N Q T H L Y A C G T G A F H P I C T Y I E V G H H P E D N I F K L Q D S H F E N G R G K S P Y D
P K L L T A S L L I D G E L Y S G T A A D F M G R D F A I F R T L G H H H P I R T E Q H D S R W L N
D P R F I S A H L I P E S D N P E D D K V Y F F F R E N A I D G E H S G K A T H A R I G Q I C K N D F
G G H R S L V N K W T T F L K A R L I C S V P G P N G I D T H F D E L Q D V F L M N S K D P K N P I
V Y G V F T T S S N I F K G S A V C M Y S M S D V R R V F L G P Y A H R D G P N Y Q W V P Y Q G R
V P Y P R P G T C P S K T F G G F D S T K D L P D D V I T F A R S H P A M Y N P V F P I N N R P I M I
K T D V N Y Q F T Q I V V D R V D A E D G Q Y D V M F I G T D V G T V L K V V S V P K E T W H D L
E E V L L E E M T V F R E P T T I S A M E L S T K Q Q Q L Y I G S T A G V A Q L P L H R C D I Y G K
A C A E C C L A R D P Y C A W D G S S C S R Y F P T A K R R T R R Q D I R N G D P L T H C S D L Q
H H D N H H G H S L E E R I I Y G V E N S S T F L E C S P K S Q R A L V Y W Q F Q R R N E D R K E E
I R V G D H I I R T E Q G L L L R S L Q K K D S G N Y L C H A V E H G F M Q T L L K V T L E V I D T
E H L E E L L H K D D D G D G S K T K E M S S S M T P S Q K V W Y R D F M Q L I N H P N L N T M D
E F C E Q V W K R D R K Q R R Q R P G H S Q G S S N K W K H M Q E S K K G R N R R T H E F E R
A P R S V

Appendix 3: Amino acids sequence of expressed Sema3A protein.
Signal peptide Link 8X His TEV cleavage site NheI Sema3Adomain (a.a residues: 3-752) PSI domain Ig-like C2-type domain C_{ter} **Defined potential GAG-binding sites** **Cystein responsible of the disulfide bond**

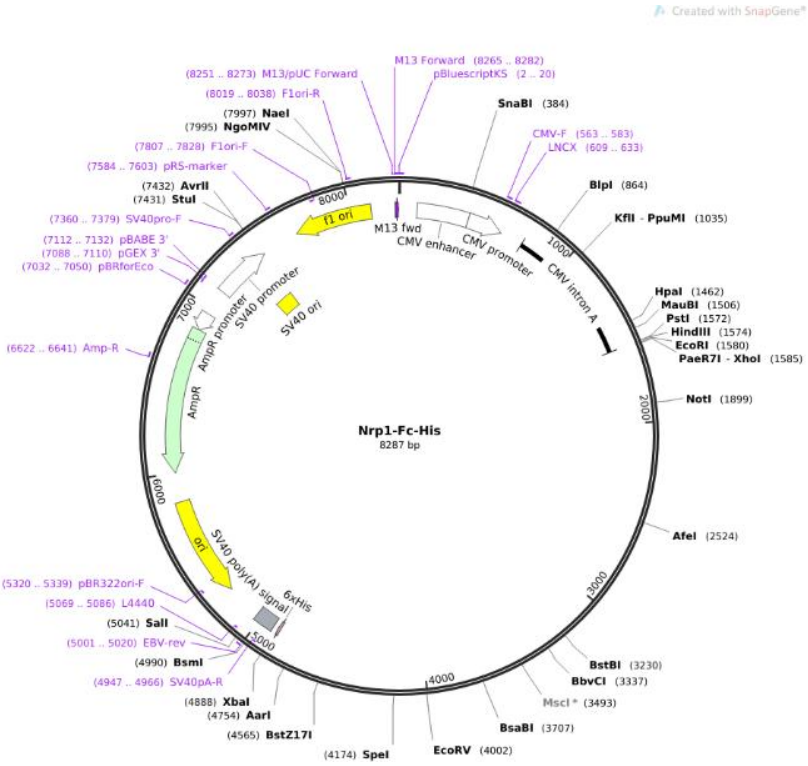

Appendix 4 : Nrp1-FC-His expression vector
Mouse Nrp1-Fc-His was a gift from Woj Wojtowicz (Addgene plasmid # 72097). Vector backbone is pCMVi-SV40ori. It expresses the extracellular region of the Neuropilin 1 protein, C-terly fused to the Fc region of human IgG1 + 6X histidine tag. More information is available in: https://www.addgene.org/72097/.

MERGLPLLCATLALALALAGAFRSDKCGGTIKIENPGYLTSPGYPHSYHPSEKCEWLIQAPEPYQRIMIN
FNPHFDLEDRDCKYDYVEVIDGENEGGRLWGKFCGKIAPSPVVSSGPFLFIKFVSDYETHGAGFSIRYEIF
KRGPECSQNYTAPTGVIKSPGFPEKYPNSLECTYIIFAPKMSEIILEFESFDLEQDSNPPGGMFCRYDRLEI
WDGFPEVGPHIGRYCGQKTPGRIRSSSGVLSMVFYTDSAIAKEGFSANYSVLQSSISEDFKCMEALGMES
GEIHSDQITASSQYGTNWSVERSRLNYPENGWTPGEDSYKEWIQVDLGLLRFVTAVGTQGAISKETKKK
YYVKTYRVDISSNGEDWISLKEGNKAIIFQGNTNPTDVVLGVFSKPLITRFVRIKPVSWETGISMRFEVY
GCKITDYPCSGMLGMVSGLISDSQITASNQADRNWMPENIRLVTSRTGWALPPSPHPYTNEWLQVDLG
DEKIVRGVIIQGGKHRENKVFMRKFKIAYSNNGSDWKTIMDDSKRKAKSFEGNNNYDTPELRTFSPLST
RFIRIYPERATHSGLGLRMELLGCEVEAPTAGPTTPNGNPVDECDDDQANCHSGTGDDFQLTGGTTVLA
TEKPTIIDSTIQSEFPTYGFNCEFGWGSHKTFCHWEHDSHAQLRWSVLTSKTGPIQDHTGDGNFIYSQAD
ENQKGKVARLVSPVVYSQSSAHCMTFWYHMSGSHVGTLRVKLRYQKPEEYDQLVWMVVGHQGDH
WKEGRVLLHKSLKLYQVIFEGEIGKGNLGGIAVDDISINNHISQEDCAKPTDLDKKNTEIKIDETGSTPGY
EGEGEGDKNISRKPGNVLKTLTSDKTHTCPPCPAPELLGGPSVFLFPPKPKDTLMISRTPEVTCVVVDVS
HEDPEVKFNWYVDGVEVHNAKTKPREEQYNSTYRVVSVLTVLHQDWLNGKEYKCKVSNKALPAPIE
KTISKAKGQPREPQVYTLPPSRDELTKNQVSLTCLVKGFYPSDIAVEWESNGQPENNYKTTPPVLDSDG
SFFLYSKLTVDKSRWQQGNVFSCSVMHEALHNHYTQKSLSLSPGKGGHHHHHH

Appendix 5: Amino acids sequence of expressed Nrp1 protein.
Signal peptid CUB 1 CUB 2 F5/8 type C 1 F5/8 type C2 MAM Human Fc Ig G1 6X His

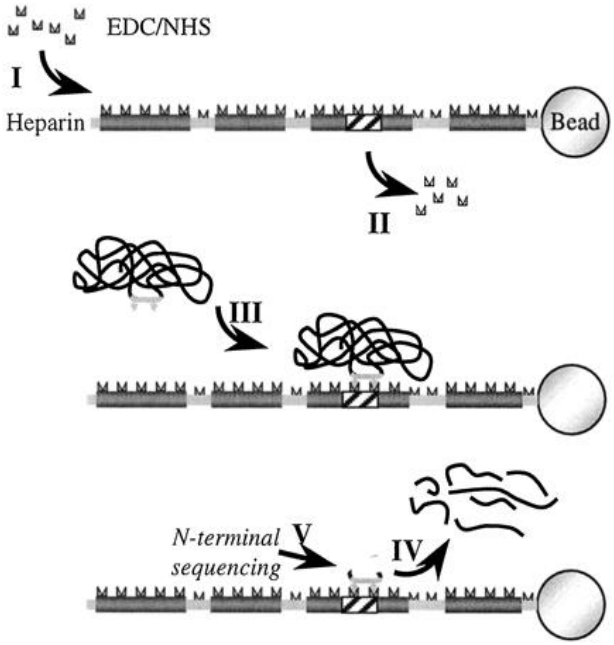

Vives et al.(2004)

Appendix 6 : Strategy of the beads approach.
Heparin immobilized beads are first incubated with EDC/NHS resulting in the activation of the polysaccharide carboxylic groups (I). After washing to remove ex- cess of cross-linking reagents (II), Heparin-beads are incubated with the protein of interest that will interact with the heparin chain at the level of a defined oligosaccharide motif. This interaction causes contacts between amine-bearing amino acids of the protein (pale grey arrow- heads) and activated carboxyl groups of the heparin, resulting in the formation of covalent linkages (III). After washing to remove unbound protein, beads are submitted to proteolysis. Protein fragments released are cleared away by extensive washing (IV), while those remaining trapped on the heparin, i.e. containing the heparin binding site, can be identified by solid phase N-ter protein sequencing performed directly on the beads (V) *(from Vivès et al. 2004*[304]).

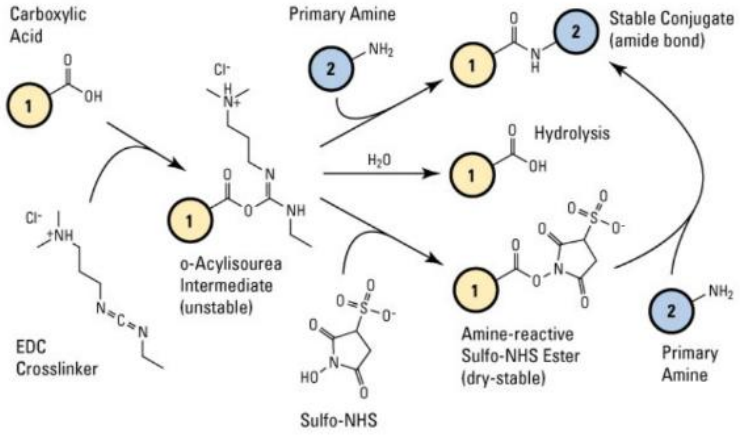

Appendix 7: Sulfo-NHS plus EDC (carbodiimide) crosslinking reaction scheme.
Carboxyl-to-amine crosslinking using the carbodiimide EDC and Sulfo-NHS. Addition of NHS or Sulfo-NHS to EDC reactions (bottom-most pathway) increases efficiency and enables molecule (1) to be activated for storage and later use.

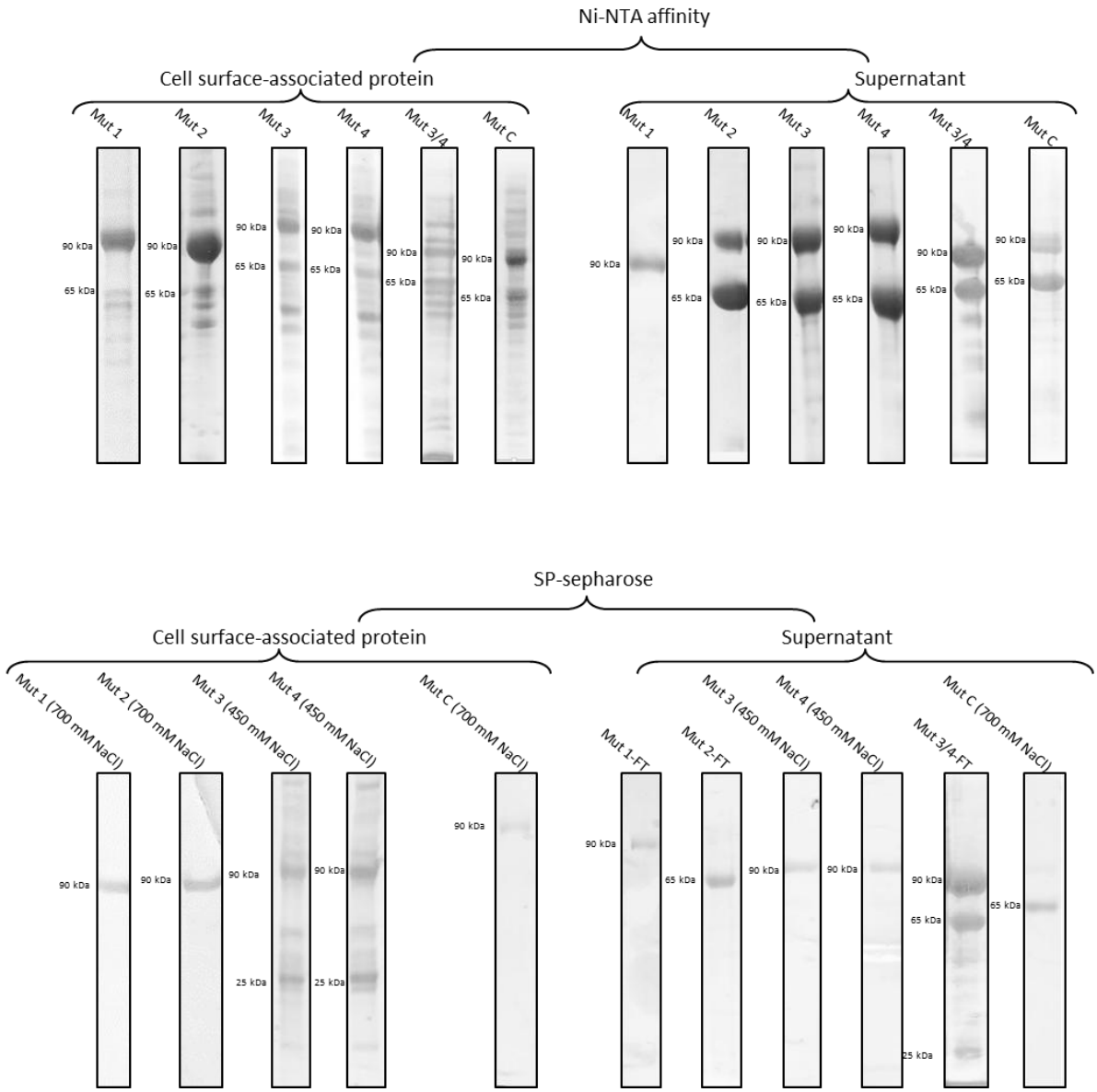

Appendix 8: Examples of elution profile in Ni-NTA and SP-sepharose of cell surface-associated protein and culture medium of all mutants.

Version française

Caractérisation de l'interaction semaphorine 3A-chondroitine sulfate dans le système nerveux central

Résumé

Les réseaux périneuronaux (PNN) sont des régulateurs clé de la plasticité et de la régénération des neurones au niveau du système nerveux central chez l'adulte. Le PNN est une matrice extracellulaire hautement organisée, qui entoure des populations spécifiques de neurones, enrichie en protéoglycanes à chondroïtine sulfate (CSPG). La chondroïtine sulfate (CS) est un polysaccharide linéaire, appartenant à la famille des glycosaminoglycanes (GAG), qui peut être sulfaté à différentes positions et donner lieu à plusieurs isoformes. Ces isoformes interagissent de manière spécifique avec de nombreuses molécules de signalisation dont la semaphorine 3A (Sema3A). Sema3A est une protéine secrétée, qui interagit avec les CS et s'accumule ainsi dans les PNN. Elle est impliquée dans la guidance des neurones sur lesquels elle agit par chimio-répulsion. Les aspects structuraux et fonctionnels de l'interaction entre Sema3A et CS sont encore mal connus, mais celle-ci pourrait être requise pour renforcer la liaison de la Sema3A avec ses récepteurs et déclencher une voie de signalisation qui aboutit à l'inhibition de la plasticité synaptique. Le but du projet est donc de caractériser biochimiquement l'interface d'interaction Sema3A-CS. Il a pour perspective d'élaborer des molécules interférant avec cette interaction qui pourraient permettre une amélioration de la plasticité neuronale après une maladie neurodégénérative ou une lésion de la moelle épinière.

Pour ce faire, la Sema3A est exprimée dans un système hétérologue de cellules eucaryotes pour être purifiée. Deux formes ont été purifiées : une forme entière de 90 kDa qui reste accrochée à la surface cellulaire et une forme clivée de 65 kDa secrétée dans le milieu de culture. La Sema3A-90 interagit d'une manière sélective et avec une très haute affinité avec la CS-E (chondroitine disulfatée en position 4 et 6) et l'héparane sulfate, alors que, la forme clivée n'interagit avec aucun GAG, comme observé par résonance plasmonique de surface (SPR). Quatre sites, situés dans le domaine C-terminal de la protéine, susceptibles d'interagir avec les GAG ont été identifiés et analysés par mutagenèse. Deux d'entre eux sont impliqués dans la reconnaissance des GAG et sont nécessaires à la Sema3A pour inhiber la croissance de neurites sur des cultures de neurones issus de ganglion de la racine dorsale de cerveaux de rats. En parallèle, nos travaux montrent qu'un tetrasaccharide de CS-E est la taille minimale requise pour l'interaction avec la Sema 3A. Enfin, des analyses réalisées en utilisant une

microbalance à cristal de quartz avec dissipation ont montré que la Sema3A pourrait réticuler les chaines de GAG, participant ainsi à la stabilisation du réseau périneuronal.

Introduction

La matrice extracellulaire du système nerveux central et les réseaux périneuronaux

La matrice extracellulaire (ECM) est le ciment qui connecte les cellules entre elles afin de former un tissu. Elle est composée de nombreuses molécules secrétées par les cellules environnantes. En plus de son rôle structural, l'ECM est impliquée dans plusieurs processus physiologiques et pathologiques pendant le développement et chez l'adulte. L'ECM du système nerveux central (SNC) est unique par sa composition. En effet, contrairement aux autres ECM, celle du SNC contient plus de protéoglycanes (PG) que de protéines fibreuses. D'ailleurs le ratio glycosaminoglycanes (GAG): collagène est de 10 :1.

Les principaux composants de la matrice du SNC

1. Acide hyaluronique (HA)

HA est un polysaccharide linéaire composé d'une répétition de l'unité disaccharidique acide glucuronique (GlcA) and N-acetylglucosamine (GlcNAc) [-β(1,4)-GlcA-β(1,3)-GlcNAc-]$_n$. HA constitue le squelette de l'ECM sur lequel toutes les autres molécules s'assemblent.

2. Protéoglycanes (PG)

Les PG sont les composants clés la matrice neuronale. Un PG est constitué d'un core protéique et une ou plusieurs chaines de GAG attachées d'une manière covalente. Ces chaines de GAG sont souvent de nature héparane sulfate (HS) et/ou chondroitine sulfate (CS) et donnant lieu à des HSPG (*e.g* syndecan) ou des CSPG (*e.g* lecticans), respectivement. Les CSPG sont plus abondants dans le SNC. Les PG sont impliqués dans la régulation de nombreux processus physiologique pendant le développement et chez l'adulte telle que la croissance des neurites.

3. Tenascine-C et R

Les tenascines (TN) sont une famille de cinq glycoprotéines dont TN-C et TN-R qui sont exprimés dans le SNC. Elles sont impliquées dans les processus de chimio-attraction et chimio-répulsion.

4. Protéine de liaison des hyaluronanes et des protéoglycanes (HAPLN)

Les HAPLN est une famille de quatre membres (HAPLN 1-4). Ces protéines sont surtout impliquées dans la stabilisation de l'interaction entre HA et CSPG, comme leur nom l'indique.

Les types de matrices dans le SNC

La matrice du SNC est organisée sur plusieurs niveaux **(Figure 11)** i) **la membrane basale** qui entoure les vaisseaux sanguins et toute la surface piale du SNC ; ii) **la matrice interstitielle** (matrice classique) composée de molécules remplissant l'espace intercellulaire et elle peut être solubilisée facilement avec NaCl 150 mM; iii) **les réseaux perineuronaux (PNN)** qui est une matrice hautement organisée et condensée, qui a pour rôle principal « la régulation de la plasticité neuronale ». Les PNN sont solubilisés seulement avec une combinaison de NaCl 1 M, tritionX-100 0.5% et urée 6 M. Nous nous intéressons aux PNN.

Les réseaux périneuronaux

Les PNN ont été découverts par Camillo Golgi en 1882 bien avant la découverte de l'appareil de Golgi. Ils sont souvent visualisés grâce à une agglutinine extraite de la plante *Wisteria floribunda* (WFA) qui a une affinité pour les CS enrichie dans les PNN. Les PNN sont composés de HA, de CSPG (aggrecan, versican, neurocan et brevican), TN-R et HAPLN **(Figure 13)**. Ces différents constituants sont secrétés soit par les neurones ou/et les cellules gliales. Les PNN sont spécifiques à des populations particulières de neurones qui sont souvent les neurones à parvalbumine (neurones PV) inhibiteurs. Ils sont exprimés dans des régions telles que le cortex, les amygdales, hippocampe, le cervelet et la moelle épinière[9]. L'apparition des PNN coïncident avec la fin de la période critique qui a lieu pendant les derniers stades du développement du SNC. Cette dernière est la période de maturation pendant laquelle le cerveau est très sensible aux stimuli de l'environnement, donc l'apprentissage. A la fin de la période critique, après l'établissement des connexions entre neurones, les PNN entourent les neurones sous forme de nid d'abeilles stabilisant ainsi les connexions mises en place.

La structure des PNN hautement organisée est certainement conçue pour accomplir des fonctions bien spécifiques. Les PNN sont surtout connus pour leurs dans la régulation de la plasticité neuronale dans le SNC mature. La perturbation des PNN par chondroitinase ABC (ChABC) restore la plasticité neuronale, montrant ainsi l'importance des PNN dans la

plasticité. Trois mécanismes sur la régulation de la plasticité par les PNN ont été proposés : les PNN i) agissent comme une barrière physique inhibant la formation de nouvelles synapses ; ii) restreint la mobilité latérale des récepteurs du glutamate (un neurotransmetteur excitateur) AMPA (acide alpha-amino-3-hydroxy-5méthyl1-4-isoxazolepropionique) et iii) retiennent les molécules de signalisation inhibitrices telles que la semaphorine 3A (Sema3A) *via* les chaines CS des PG, par exemple.

Les chondroitine sulfates du système nerveux central

Les chondroitine sulfates (CS) appartiennent à la famille des GAG. Les GAG sont des polysaccharides linéaires composés d'une répétions d'unités disaccharidiques qui peuvent subir des modifications telles que la sulfatation et l'épimerisation. Les GAG sont organisés en cinq familles distinctes : acide hyaluronique, héparane sulfate/héparine, kératane sulfate et chondroitine sulfate. L'unité disaccharidique du CS est composée de β (1,4) acide glucuronique (GlcA)-β (1,3) N-acetylgalactosamine (GalNAc) qui peut être sulfatée à différentes positions et épimerisée en carbone C5 de GlcA. Cela donne lieu à différents isoformes et les plus communs sont présentés dans la **Figure 27**. Les CS constituent le GAG sulfaté le plus abondant dans l'ECM du SNC, notamment les PNN[11]. Son expression et sa sulfatation varie en fonction du temps et de l'espace. Ce qui permet aux CS d'interagir avec une large gamme de protéines de signalisation dont la Sema3A, requises pour chaque condition.

La semaphorine 3A

La semaphorine 3A (Sema3A) est une protéine de guidance axonale par chimio-répulsion appartenant à la classe 3 de la grande famille des semaphorines. La signalisation de la Sema3A se fait via son récepteur plexinA1 (PlxnA1) et son corécepteur neuropiline1 (Nrp1). Sema3A est un homodimère covalent grâce à un pont disulfure situé dans sa région C-ter. Le monomère est de 90 kDa, composé d'un domaine Sema (qui peut se dimériser d'une manière non-covalente avec un autre domaine Sema) en N-ter suivi d'un domaine PSI, Ig-like et d'un domaine C-ter basique. Sema3A contient deux sites de clivage pour la furine, une protéase ubiquitaire. Le premier site est situé au niveau du PSI domaine et le deuxième site est situé au niveau du domaine C-ter basique. Le clivage au niveau du premier site a pour conséquence un fragment N-ter de 65 kDa **(Figure 38).**

Le but du projet

La Sema3A s'accumule au niveau des PNN par son interaction avec la CS, contribuant ainsi à la régulation de la plasticité neuronale. En effet, la digestion de la CS des PNN par une enzyme spécifique (ChABC) entraine la suppression de la Sema3A. Dans ce contexte, le but du projet consiste d'une part à caractériser l'interaction entre la Sema3A et la CS : caractériser le site d'interaction de la Sema 3A avec les CS et vice versa ; et d'autre part comprendre le rôle de cette interaction : effet de la Sema sur les GAG et vice versa. Tout cela permettrait de développer des stratégies dans le but d'inhiber cette interaction et améliorer la plasticité et la régénération des neurones, notamment après une lésion de la moelle épinière.

Résultats et discussion

Semaphorine 3A

Expression et purification de la Sema3A

La Sema3A a été clonée dans un vecteur d'expression en cellules de mammifères, qui contient une étiquette poly-His au niveau de son N-ter, pour être ensuite surexprimée dans des cellules HEK293-E. Deux formes de Sema3A ont été obtenues **(Figure 44.C).** Une forme de 90 kDa qui reste accrochée à la surface cellulaire et une forme 65 kDa secrétée dans le milieu de culture. Sema3A-90, qui constitue la forme entière de la protéine, reste accrochée à la surface cellulaire en interagissant via son C-ter basique avec les GAG de la surface des HEK. Cette forme est décrochée par du PBS contenant 1 M NaCl pour être purifiée par la suite. La forme 65 correspond au N-ter de la Sema3A clivée par la furine au niveau du premier site du clivage. Cette forme ne contient pas les domaines C-ter qui pourront interagir avec les charges négatives des GAG. Ce qui explique son relargage dans le milieu de culture. Ces deux formes ont subi deux étapes de purification **(Figure 46).** La première étape consiste en purification sur une colonne d'affinité Ni-NTA, puisque la protéine contient une étiquette poly-His. La deuxième étape consiste en chromatographie échangeuse de cations (SP-sépharose) pour séparer les deux formes. La Sema3A-90 est éluée avec 700 mM de NaCl, alors que la Sema3A-65 ne s'accroche pas à la colonne. Ces résultats de purification constituent une première indication sur l'importance du C-ter de la Sema3A dans l'interaction avec les GAG de la surface cellulaire des HEK et avec les charges négatives de l'échangeuse de cations.

Identification des sites d'interaction avec la CS sur la Sema3A

Dans le but d'identifier de potentiels sites d'interaction avec les GAG sur la Sema3A, nous avons d'abord analysé la séquence primaire d'a.a de la Sema3A. Nous avons identifié quatre sites potentiels, riches en acides aminés basiques: KRRTRR [résidus: 530-535], RRNEDRK [résidus: 593-599], KRDRKQRRQR [résidus: 708-717] et KKGRNRR [résidus: 735-741] localisés au niveau du domaine PSI, Ig-like et la queue C-ter basique, respectivement **(Figure 47.A)**. Ce genre de séquences est souvent retrouvé dans les sites d'interaction des protéines avec les GAG. Pour confirmer leur interaction avec les GAG, nous avons utilisé une méthode basée sur des billes liées d'une manière covalente à l'héparine. Nous avons analysée l'interaction de la Sema3A et l'héparine. Les résultats montrent que deux des sites identifiés par l'analyse de la séquence primaire (les deux localisées au niveau de la queue C-ter) interagissent avec l'héparine **(Figure 47.B)**.

Puisque le but était de trouver les sites interagissant avec la CS, nous avons mutés individuellement les quatre sites potentiels par mutagenèse dirigée. Quatre mutants appelés, Mut 1, Mut 2, Mut 3 et Mut 4, respectivement, sont obtenus **(Figure 49)**. Mut 1 et Mut 2, comme le WT, sont purifiés à partir de la surface cellulaire. Alors que, Mut 3 et Mut 4 sont purifiés à partir du milieu de culture. Ces résultats de purification indiquent l'importance de ces deux sites mutés (3 et 4) pour rester accroché aux GAG de la surface cellulaire.

Analyse de l'interaction Sema3A WT et ses mutants – chondroitine sulfate en SPR

Nous avons analysé l'interaction de la Sema3A purifiée (Sema3A-65 et Sema3A-90) avec les chaines de CS enrichie d'unités disulfatés (CS-D et CS-E) en SPR. La Sema3A-90 interagit avec la CS-E avec une très haute affinité de l'ordre du pM. Par contre, elle n'interagit pas avec la CS-D **(Figure 52 A et B)**. Cela indique que l'interaction de la Sema3A-90 avec la CS serait dépendante de la sulfatation. La Sema3A-65 n'interagit avec aucune CS **(Figure 55).** Cela confirme l'importance du domaine C-ter dans l'interaction avec les CS.

Nous avons également analysé l'interaction des mutants (Mut 1, Mut 2, Mut 3 et Mut 4) avec la CS-E en SPR **(Figure 56).** Les résultats obtenus montrent que Mut 1 et Mut 2 interagissent fortement avec la CS-E, comme ce qui a été vu avec le WT. Alors que, le Mut 3 et le Mut 4 ne présentent aucune interaction avec la CS-E dans la gamme de concentrations analysées. Cela confirme que les sites 3 et 4 mutés sont tous les deux sites importants pour

interagir avec la CS-E. Les sites d'interaction de la Sema3A avec la CS-E sont ainsi identifiés.

Analyse de l'interaction Sema3A– oligosaccharides de la chondroitine sulfate-E en SPR

Nous avons analysé en SPR l'interaction de la Sema 3A et des oligosaccharides de CS-E de différentes tailles : disaccharide, tetrasaccharide et hexasaccharide **(Figure 57)**. La Sema3A n'interagit pas avec le disaccharide. Cependant, elle interagit avec une très haute affinité, du même ordre qu'une longue chaine, avec le tetra- et le hexasaccharide. Ces résultats montrent que le tetrasaccharide CS-E est suffisant pour interagir avec la Sema3A et c'est le motif minimal requis pour cette interaction.

Analyse de l'interaction Sema3A WT et mutants – chondroitine sulfate en QCM-D

Nous avons analysé l'interaction de la Sema3A et la CS-E en QCM-D **(Figure 61)**. Le QCM-D est une technique qui permet de mesurer l'interaction entre deux molécules, comme en SPR. En plus, il peut mesurer l'épaisseur des films et suggérer un effet de réticulation des chaines de GAG par la Sema3A. Le QCM-D mesure deux paramètres : la fréquence et la dissipation. La fréquence nous renseigne sur une éventuelle interaction entre les deux molécules. La dissipation nous renseigne sur l'épaisseur du film. L'addition de la Sema3A sur le film de CS entraine une diminution de l'épaisseur (diminution de la dissipation). Cette diminution pourrait être due à un effet de réticulation des chaines de CS par la Sema3A. Par conséquent, la Sema3A pourrait interagir avec différentes chaines de CS-E et entrainer ainsi leur réticulation. La Sema3A participerait ainsi à la stabilisation du PNN.

Effet de la Sema3A et ses mutants sur la croissance des neurites de neurones du ganglion de la racine dorsale

La Sema 3A est connue pour son effet inhibiteur sur la croissance des neurites de neurones du ganglion de la racine dorsale (DRG) en culture. Dans le but de savoir si l'interaction de la Sema3A avec les GAG est importante pour son activité, Nous avons traité des neurones de DRG avec la Sema3A WT et les mutants **(Figure 62)**. Ensuite, nous avons quantifié le nombre de neurones possédant des neurites. Les résultats obtenus montrent que le Mut 1 et le Mut 2 présentent le même effet (une forte inhibition) que le WT. Alors que, le Mut 3 et le Mut 4 présentent un effet d'inhibition moins important que le WT. Cela indique que les séquences 3 et 4 mutées, requises pour l'interaction avec la CS-E, sont requises pour

une activité importante de la Sema3A (l'inhibition). Cela suggère que l'interaction de la Sema3A avec les GAG pourrait renforcer l'activité de la Sema 3A.

Chondroitine sulfates du cerveau de rat

Nous avons extrait des CS des différents compartiments de l'ECM, dont les PNN, du cerveau de rat adulte. Nous avons analysé leur composition disaccharidique en RPIP-HPLC **(Figure 65)**. Les résultats obtenues révèlent un pattern de sulfatation diffèrent d'un compartiment a un autre. Les PNN ont donc une sulfatation propre à eux, ce qui leur confère une interaction spécifique avec les molécules de signalisation.

Conclusion et perspectives

En conclusion, la forme entière de la Sema3A a été purifiée pour la première fois sans avoir recours à la mutation des sites de clivage de la furine. Nous avons par la suite caractérisé d'une part les sites d'interaction des CS sur la Sema3A. Et d'autre part, le motif d'interaction de la Sema3A sur la CS-E. Nous avons également mis en évidence les rôles potentiels de cette interaction Sema3A-CS qui peuvent être potentiellement l'effet de réticulation de la Sema3A sur les chaines de CS, participant ainsi à la stabilisation du PNN. Le second rôle pourrait consister dans l'effet des CS sur l'augmentation de l'activité de la Sema3A. En perspective, il serait intéressant d'analyser de plus près le rôle physiologique de cette interaction Sema3A-CS. Par ailleurs, chercher des inhibiteurs de cette interaction serait d'un très grand intérêt sur l'amélioration de la plasticité et la régénération des neurones.

References

1. Reichardt and Prokop. Introduction: The Role of Extracellular Matrix in Nervous System Development and Maintenance. *Dev. Neurobiol.* (2011). doi:10.1002/dneu.20975
2. Piez, K. A. History of extracellular matrix: A personal view. *Matrix Biol.* **16,** 85–92 (1997).
3. Robert, L. Éditorial Matrix biology: past, present and future. *Pathol Biol* **49,** 279–83 (2001).
4. Borel, J. P., Maquart, F. X., Robert, A. M., Labat-Robert, J. & Robert, L. Celebration of the 50th anniversary of the foundation of the French society for connective tissue research. Its short history in the frame of the origin and development of this discipline. *Pathol. Biol.* **60,** 2–6 (2011).
5. Tani, E. & Ametani, T. Extracellular distribution of ruthenium red-positive substance in the cerebral cortex. *J. Ultrasructure Res.* **34,** 1–14 (1971).
6. Dityatev, A., Seidenbecher, C. I. & Schachner, M. Compartmentalization from the outside: The extracellular matrix and functional microdomains in the brain. *Trends in Neurosciences* **33,** 503–512 (2010).
7. Bonneh-Barkay, D. & Wiley, C. A. Brain extracellular matrix in neurodegeneration. *Brain Pathology* **19,** 573–585 (2009).
8. Lau, L. W., Cua, R., Keough, M. B., Haylock-Jacobs, S. & Yong, V. W. Pathophysiology of the brain extracellular matrix: A new target for remyelination. *Nature Reviews Neuroscience* **14,** 722–729 (2013).
9. Benarroch, E. E. Extracellular matrix in the CNS. *Neurology* **85,** 1417–1427 (2015).
10. Ruoslahti, E. Brain extracellular matrix. *Glycobiology* **6,** 489–192 (1996).
11. Sood, D. *et al.* Fetal brain extracellular matrix boosts neuronal network formation in 3D bioengineered model of cortical brain tissue. *ACS Biomater Sci Eng* **2,** 131–140 (2016).
12. Galtrey, C. M. & Fawcett, J. W. The role of chondroitin sulfate proteoglycans in regeneration and plasticity in the central nervous system. *Brain Res. Rev.* **54,** 1–18 (2007).
13. Barros, C. S., Franco, S. J. & Müller, U. Extracellular matrix: functions in the nervous system. *Cold Spring Harb. Perspect. Biol.* **3,** a005108 (2011).
14. Meyer, K., Linker, A. & Rapport, M. M. The production of monosaccharides from hyaluronic acid by. *J. Biol. Chem.* **192,** 275–281 (1951).
15. Toole, B. P. Hyaluronan is not just a goo! *Journal of Clinical Investigation* **106,** 335–336 (2000).
16. Toole, B. P. Hyaluronan: from extracellular glue to pericellular cue. *Nat. Rev. Cancer* **4,** 528–539 (2004).
17. Kwok, J. C. F., Dick, G., Wang, D. & Fawcett, J. W. Extracellular matrix and perineuronal nets in CNS repair. *Dev. Neurobiol.* **71,** 1073–1089 (2011).
18. Tammi, M. I., Day, A. J. & Turley, E. A. Hyaluronan and homeostasis: A balancing act. *Journal of Biological Chemistry* **277,** 4581–4584 (2002).
19. Richter, R. P., Baranova, N. S., Day, A. J. & Kwok, J. C. Glycosaminoglycans in extracellular matrix organisation: are concepts from soft matter physics key to understanding the formation of perineuronal nets? *Curr. Opin. Struct. Biol.* **50,** 65–74 (2018).
20. Allison, D. D. & Grande-Allen, K. J. Review. Hyaluronan: A Powerful Tissue Engineering Tool. *Tissue Eng.* **12,** 2131–2140 (2006).
21. Diogo Escudero. HAS2 (hyaluronan synthase 2). *Atlas of genetics and cytogenetics in oncology and Haematology* (2009). Available at: http://atlasgeneticsoncology.org/Genes/HAS2ID412ch8q24.html. (Accessed: 25th July 2018)
22. Rapraeger, A. C. & Ott, V. L. Molecular interactions of the syndecan core proteins. *Current Opinion in Cell Biology* **10,** 620–628 (1998).
23. Rauch, U. *et al.* Isolation and characterization of developmentally regulated chondroitin sulfate and chondroitin/keratan sulfate proteoglycans of brain identified with monoclonal antibodies. *J. Biol. Chem.* **266,** 14785–14801 (1991).
24. Cole, G. J. & Mccabe, C. F. Identification of a Developmentally Regulated Keratan Sulfate Proteoglycan That Inhibits Cell Adhesion and Neurite Outgrowth. *Neuron* **7,** 1007–1018 (1991).
25. Klinger, M. M., Margolis, R. U. & Margolis, R. K. Isolation and characterization of the heparan sulfate proteoglycans of brain. Use of affinity chromatography on lipoprotein lipase-agarose. *J. Biol. Chem.* **260,** 4082–4090 (1985).
26. Lander, A. D. Proteoglycans in the nervous system. *Curr. Opin. Neurobiol.* **3,** 71–723 (1993).
27. Herndon, M. E. & Lander, a D. A diverse set of developmentally regulated proteoglycans is expressed in the rat central nervous system. *Neuron* **4,** 949–61 (1990).
28. Cui, H., Freeman, C., Jacobson, G. A. & Small, D. H. Proteoglycans in the Central Nervous System: Role in Development, Neural Repair, and Alzheimer's Disease. *Int. Union Biochem. Mol. Biol.* **65,** 108–120 (2013).
29. Maurel, P., Rauch, U., Fladt, M., Margolist, R. K. & Margolis, R. U. Phosphacan, a chondroitin sulfate

proteoglycan of brain that interacts with neurons and neural cell-adhesion molecules, is an extracellular variant of a receptor-type protein tyrosine phosphatase. *Biochemistry* **91,** 2512–2516 (1994).
30. Yamaguchi, Y. Lecticans: organizers of the brain extracellular matrix. *C. Cell. Mol. Life Sci* **57,** 276–289 (2000).
31. Hocking, A. M., Shinomura, T. & McQuillan, D. J. Leucine-rich repeat glycoproteins of the extracellular matrix. *Matrix Biology* **17,** 1–19 (1998).
32. Staub, E., Hinzmann, B. & Rosenthal, A. A novel repeat in the melanoma-associated chondroitin sulfate proteoglycan defines a new protein family. *FEBS Lett.* **527,** 114–8 (2002).
33. Klaus Elenius and Markku Jalkanen. Function of the syndecans - a family of cell surface proteoglycans. *J. Cell Sci. 107,* **107,** 2975–2982 (1994).
34. Kim, M.-S., Saunders, A. M., Hamaoka, B. Y., Beachy, P. A. & Leahy, D. J. Structure of the protein core of the glypican Dally-like and localization of a region important for hedgehog signaling. *PNAS* **108,** 13112–13117 (2011).
35. Filmus, J., Capurro, M. & Rast, J. Glypicans. *Genome Biol.* **9,** (2008).
36. Victor Nurcombe,* Miriam D. Ford, Jason A. Wildschut, P. F. B. Developmental Regulation of Neural Response to FGF-1 and FGF-2 by Heparan Sulfate Proteoglycan. *Science (80-.).* **260,** (1993).
37. McKeon, R. J., Jurynec, M. J. & Buck, C. R. The Chondroitin Sulfate Proteoglycans Neurocan and Phosphacan Are Expressed by Reactive Astrocytes in the Chronic CNS Glial Scar. *J. Neurosci.* **19,** 10778–10788 (1999).
38. Sango, K. *et al.* Phosphacan and neurocan are repulsive substrata for adhesion and neurite extension of adult rat dorsal root ganglion neurons in vitro. *Exp. Neurol.* **182,** 1–11 (2003).
39. Michael Schmalfeldt, Christine E. Bandtlow, María T. Dours-Zimmermann, K. H. W. and D. R. Z. Brain derived versican V2 is a potent inhibitor of axonal growth. *J. Cell Sci.* **113,** 807–816 (2000).
40. Yamada, H. *et al.* The Brain Chondroitin Sulfate Proteoglycan Brevican Associates with Astrocytes Ensheathing Cerebellar Glomeruli and Inhibits Neurite Outgrowth from Granule Neurons. *J. Neurosci.* **20,** :7784–7795 (1997).
41. Kurihara, D. & Yamashita, T. Chondroitin sulfate proteoglycans down-regulate spine formation in cortical neurons by targeting tropomyosin-related kinase B (TrkB) protein. *J. Biol. Chem.* **287,** 13822–13828 (2012).
42. Oohira, A., Matsui, F., Tokita, Y., Yamauchi, S. & Aono, S. Molecular interactions of neural chondroitin sulfate proteoglycans in the brain development. *Arch. Biochem. Biophys.* **374,** 24–34 (2000).
43. Joester, A. & Faissner, A. The structure and function of tenascins in the nervous system. *Matrix Biol.* **20,** 13–22 (2001).
44. Jakovcevski, I., Miljkovic, D., Schachner, M. & Andjus, P. R. Tenascins and inflammation in disorders of the nervous system. *Amino Acids* **44,** 1115–1127 (2013).
45. Kammerer, R. A. *et al.* Tenascin-C hexabrachion assembly is a sequential two-step process initiated by coiled-coil α-helices. *J. Biol. Chem.* **273,** 10602–10608 (1998).
46. Jones, P. L. & Jones, F. S. Mini review Tenascin-C in development and disease: gene regulation and cell function. *Matrix Biol.* **19,** 581596 (2000).
47. Garcion, E., Halilagic, A., Faissner, A. & Ffrench-Constant, C. Generation of an environmental niche for neural stem cell development bythe extracellular matrix molecule tenascin C. *Development* **131,** 3423–3432 (2004).
48. Strekalova, T. *et al.* Fibronectin domains of extracellular matrix molecule tenascin-C modulate hippocampal learning and synaptic plasticity. *Mol. Cell. Neurosci.* **21,** 173–187 (2002).
49. Reinhard, J., Roll, L. & Faissner, A. Tenascins in Retinal and Optic Nerve Neurodegeneration. *Front. Integr. Neurosci.* **11,** 30 (2017).
50. Woodworth, A., Pesheva, P., Fiete, D. & Baenziger, J. U. Neuronal-specific Synthesis and Glycosylation of Tenascin-R. *J. Biol. Chem.* **279,** 10413–10421 (2004).
51. Anlar, B. & Gunel-Ozcan, A. Tenascin-R: Role in the central nervous system. *Int. J. Biochem. Cell Biol.* **44,** 1385–1389 (2012).
52. Liao, H., Huang, W., Niu, R., Sun, L. & Zhang, L. Cross-talk between the epidermal growth factor-like repeats/fibronectin 6-8 repeats domains of Tenascin-R and microglia modulates neural stem/progenitor cell proliferation and differentiation. *J. Neurosci. Res.* **86,** 27–34 (2008).
53. Liao, H., Bu, W. Y., Wang, T. H., Ahmed, S. & Xiao, Z. C. Tenascin-R plays a role in neuroprotection via its distinct domains that coordinate to modulate the microglia function. *J. Biol. Chem.* **280,** 8316–8323 (2005).
54. Spicer, A. P., Joo, A. & Bowling, R. A. A Hyaluronan Binding Link Protein Gene Family Whose Members Are Physically Linked Adjacent to Chrondroitin Sulfate Proteoglycan Core Protein Genes. *J. Biol. Chem.* **278,** 21083–21091 (2003).
55. Carulli, D. *et al.* Animals lacking link protein have attenuated perineuronal nets and persistent plasticity.

Brain a J. Neurol. J. Neurol. **133,** 2331–2347 (2010).
56. Bekku, Y. *et al.* Bral2 is Indispensable for the Proper Localization of Brevican and the Structural Integrity of the Perineuronal Net in the Brainstem and Cerebellum. *J. Comp. Neurol* **520,** 1721–1736 (2012).
57. Oohira, A., Matsui, F., Matsuda, M. & Shoji, R. Developmental Change in the Glycosaminoglycan Composition of the Rat Brain. *J. Neurochem.* **47,** 588–593 (1986).
58. Mészár, Z. *et al.* Hyaluronan accumulates around differentiating neurons in spinal cord of chicken embryos. *Brain Res. Bull.* **75,** 414–418 (2008).
59. Fraser, J. R., Laurent, T. C. & Laurent, U. B. Hyaluronan: its nature, distribution, functions and turnover. *J. Intern. Med.* **242,** 27–33 (1997).
60. Bignami, A. & Asher, R. Some observations on the localization of hyaluronic acid in adult, newborn and embryonal rat brain. *Int. J. Dev. Neurosci.* **10,** 45–57 (1992).
61. Sorg, B. A. *et al.* Casting a Wide Net: Role of Perineuronal Nets in Neural Plasticity. *J. Neurosci.* **36,** 11459–11468 (2016).
62. Faissner, A. *et al.* Isolation of a neural chondroitin sulfate proteoglycan with neurite outgrowth promoting properties. *J. Cell Biol.* **126,** 783–799 (1994).
63. Schmalfeldt, M., Dours-Zimmermann, M. T., Winterhalter, K. H. & Zimmermann, D. R. Versican V2is a major extracellular matrix component of the mature bovine brain. *J. Biol. Chem.* **273,** 15758–15764 (1998).
64. Zhou, X.-H. *et al.* Neurocan Is Dispensable for Brain Development. *Mol. Cell. Biol.* **21,** 5970–5978 (2001).
65. Niisato, K. Age-Dependent Enhancement of Hippocampal Long-Term Potentiation and Impairment of Spatial Learning through the Rho-Associated Kinase Pathway in Protein Tyrosine Phosphatase Receptor Type Z-Deficient Mice. *J. Neurosci.* **25,** 1081–1088 (2005).
66. Saksela, O. & Rifkin, D. B. Release of basic fibroblast growth factor-heparan sulfate complexes from endothelial cells by plasminogen activator-mediated proteolytic activity. *J. Cell Biol.* **110,** 767–775 (1990).
67. Rusnati, M and Presta, M. Interaction of angiogenic basic fibroblast growth factor with endothelial cell heparan sulfate proteoglycans Biological implications in neovascularization. *Int. J. Clin. Lab. Res.* **26,** 15–23 (1996).
68. BRachel K. Okolicsanyi, Lotta E. Oikari, Chieh Yu, L. R. G. and L. M. H. Heparan Sulfate Proteoglycans as Drivers of Neural Progenitors Derived From Human Mesenchymal Stem Cells. *Front. Neurosci.* **11,** (2018).
69. Condomitti, G. & de Wit, J. Heparan Sulfate Proteoglycans as Emerging Players in Synaptic Specificity. *Front. Mol. Neurosci.* **11,** (2018).
70. Hsueh, Y. P. & Sheng, M. Regulated expression and subcellular localization of syndecan heparan sulfate proteoglycans and the syndecan-binding protein CASK/LIN-2 during rat brain development. *J. Neurosci.* **19,** 7415–25 (1999).
71. Luo, N. *et al.* Syndecan-4 modulates the proliferation of neural cells and the formation of CaP axons during zebrafish embryonic neurogenesis. *Sci. Rep.* **6,** (2016).
72. Bartsch, U., Pesheva, P., Raff, M. & Schachner, M. Expression of janusin (J1–160/180) in the retina and optic nerve of the developing and adult mouse. *Glia* **9,** 57–69 (1993).
73. David, L. S., Schachner, M. & Saghatelyan, A. The Extracellular Matrix Glycoprotein Tenascin-R Affects Adult But Not Developmental Neurogenesis in the Olfactory Bulb. *J. Neurosci.* **33,** 10324–10339 (2013).
74. Probstmeier, R., Rg Nellen, J., Gloor, S., Wernig, A. & Pesheva, P. Tenascin-R is Expressed by Schwann Cells in the Peripheral Nervous System. *J. Neurosci. Res.* **64,** 70–78 (2001).
75. Rauch, U. Review Extracellular matrix components associated with remodeling processes in brain. *C. Cell. Mol. Life Sci* **61,** 2031–2045 (2004).
76. von Holst, A. Tenascin C in Stem Cell Niches: Redundant, Permissive or Instructive? *Cells Tissues Organs* **188,** 170–177 (2008).
77. O'Keefe, P., Westgate, K. & Wisner, B. Taking the naturalness out of natural disasters. *Nature* **260,** 566–567 (1976).
78. Coles, E. G., Gammill, L. S., Miner, J. H. & Bronner-Fraser, M. Abnormalities in neural crest cell migration in laminin α5 mutant mice. *Dev. Biol.* **289,** 218–228 (2006).
79. Loulier, K. *et al.* β1 integrin maintains integrity of the embryonic neocortical stem cell niche. *PLoS Biol.* **7,** 1000176 (2009).
80. Thomas Pietri1,*, Olivier Eder1, Marie Anne Breau1, Piotr Topilko2, Martine Blanche1, Cord Brakebusch3, Reinhard Fässler3, J.-P. T. and S. D. Conditional β1-integrin gene deletion in neural crest cells causes severe developmental alterations of the peripheral nervous system. *Development* **131,** 3871–

3883 (2004).
81. Salzer1, J. L. & Zalc, and B. *Myelination J.L. Current Biology* **26,** (2016).
82. Podratz, J. L., Rodriguez, E. & Windebank, A. J. Role of the extracellular matrix in myelination of peripheral nerve. *Glia* **35,** 35–40 (2001).
83. Chernousov, M. A., Yu, W.-M., Chen, Z.-L., Carey, D. J. & Strickland, S. Regulation of Schwann cell function by the extracellular matrix. *Glia* **56,** 1498–1507 (2008).
84. Barros, C. S. *et al.* 1 integrins are required for normal CNS myelination and promote AKT-dependent myelin outgrowth. *Development* **136,** 2717–2724 (2009).
85. Pendleton, J. C. *et al.* Chondroitin sulfate proteoglycans inhibit oligodendrocyte myelination through PTPσ. *Exp. Neurol.* **247,** 113–121 (2013).
86. Stern, R., Asari, A. A. & Sugahara, K. N. Hyaluronan fragments: An information-rich system. *Eur. J. Cell Biol.* **85,** 699–715 (2006).
87. Dobbertin, A. *et al.* Analysis of combinatorial variability reveals selective accumulation of the fibronectin type III domains B and D of tenascin-C in injured brain. *Exp. Neurol.* **225,** 60–73 (2010).
88. Properzi, F. *et al.* Chondroitin 6-sulphate synthesis is up-regulated in injured CNS, induced by injury-related cytokines and enhanced in axon-growth inhibitory glia. *Eur. J. Neurosci.* **21,** 378–390 (2005).
89. George, N. & Geller, H. M. Extracellular matrix and traumatic brain injury. *J. Neurosci. Res.* **96,** 573–588 (2018).
90. Choi, B. H. Role of the basement membrane in neurogenesis and repair of injury in the central nervous system. *Microsc. Res. Tech.* **28,** 193–203 (1994).
91. Mjg, R., García Medrano, B. & Bravo, J. The Role of the Basal Lamina in Nerve Regeneration. *J Cytol Histol* **7,** 438 (2016).
92. Engelhardt, B. Development of the blood-brain barrier The blood-brain barrier from a historical perspective. *Cell Tissue Res* **314,** 119–129 (2003).
93. Deepa, S. S. *et al.* Composition of perineuronal net extracellular matrix in rat brain: A different disaccharide composition for the net-associated proteoglycans. *J. Biol. Chem.* **281,** 17789–17800 (2006).
94. Celio, M. R., Spreafico, R., De Biasi, S. & Vitellaro-Zuccarello, L. Perineuronal nets: past and present. *Trends Neurosci.* **21,** 510–515 (1998).
95. Spreafico, R., De Biasi, S. & Vitellaro-Zuccarello, L. The Perineuronal Net: A Weapon for a Challenge. *J. Hist. Neurosci.* **8,** 179–185 (1999).
96. Atoji, Y., Hori, Y., Sugimura, M. & Suzuki, Y. Extracellular matrix of the superior olivary nuclei in the dog. *J. Neurocytol.* **18,** 599–610 (1989).
97. Bignami, A., Asher, R., Perides, G. & Rahemtulla, F. The extracellular matrix of cerebral gray matter: Golgi's pericellular net and nissl's nervösen Grau revisited. *Int. J. Dev. Neurosci.* **10,** 291–299 (1992).
98. Perides, G., Erickson, H. P., Rahemtulla, F. & Bignami, A. Colocalization of tenascin with versican, a hyaluronate-binding chondroitin sulfate proteoglycan. *Anat. Embryol. (Berl).* **188,** 467–79 (1993).
99. Celio, M. R. & Blümcke, I. Perineuronal nets--a specialized form of extracellular matrix in the adult nervous system. *Brain Res. Brain Res. Rev.* **19,** 128–45 (1994).
100. Vitellaro-Zuccarello, L., Bosisio, P., Mazzetti, S., Monti, C. & De Biasi, S. Differential expression of several molecules of the extracellular matrix in functionally and developmentally distinct regions of rat spinal cord. *Cell Tissue Res.* **327,** 433–447 (2007).
101. Carulli, D. *et al.* Composition of Perineuronal Nets in the Adult Rat Cerebellum and the Cellular Origin of Their Components. *J. Comp. Neurol* **494,** 559–577 (2006).
102. Galtrey, C. M., Kwok, J. C. F., Carulli, D., Rhodes, K. E. & Fawcett, J. W. Distribution and synthesis of extracellular matrix proteoglycans, hyaluronan, link proteins and tenascin-R in the rat spinal cord. *Eur. J. Neurosci.* **27,** 1373–1390 (2008).
103. Bekku, Y. *et al.* Molecular cloning of Bral2, a novel brain-specific link protein, and immunohistochemical colocalization with brevican in perineuronal nets. *Mol. Cell. Neurosci.* **24,** 148–159 (2003).
104. Müller, T. Methylene blue supravital staining: an evaluation of its applicability to the mammalian brain and pineal gland. *Histol. Histopathol.* **13,** 1019–26 (1998).
105. Härtig, W., Brauer, K. & Brückner, G. Wisteria floribunda agglutinin-labelled nets surround parvalbumin-containing neurons. *Neuroreport* **3,** 869–72 (1992).
106. Seeger, G., Brauer, K., Härtig, W. & Brückner, G. Mapping of perineuronal nets in the rat brain stained by colloidal iron hydroxide histochemistry and lectin cytochemistry. *Neuroscience* **58,** 371–388 (1994).
107. Wang, D. & Fawcett, J. The perineuronal net and the control of CNS plasticity. *Cell Tissue Res* **349,** 147–160 (2012).
108. Irvine, S. F. & Kwok, J. C. F. Perineuronal nets in spinal motoneurones: Chondroitin sulphate proteoglycan around alpha motoneurones. *Int. J. Mol. Sci.* **19,** (2018).
109. Brückner, G., Kacza, J. & Grosche, J. Perineuronal nets characterized by vital labelling, confocal and

electron microscopy in organotypic slice cultures of rat parietal cortex and hippocampus. *J. Mol. Histol.* **35,** 115–22 (2004).
110. Pantazopoulos, H. *et al.* A Sweet Talk: The Molecular Systems of Perineuronal Nets in Controlling Neuronal Communication. *Front. Integr. Neurosci* **11,** 33 (2017).
111. Kosaka, T. & Heizmann, C. W. Selective staining of a population of parvalbumin-containing GABAergic neurons in the rat cerebral cortex by lectins with specific affinity for terminal N-acetylgalactosamine. *Brain Res.* **483,** 158–163 (1989).
112. Baig, S., Wilcock, G. K. & Love, S. Loss of perineuronal net N-acetylgalactosamine in Alzheimer's disease. *Acta Neuropathol.* **110,** 393–401 (2005).
113. National Academy of Sciences. Perineuronal nets and recall of distant fear memories. *PNA* **115,** 433–434 (2018).
114. Morikawa, S., Ikegaya, Y., Narita, M. & Tamura, H. Activation of perineuronal net-expressing excitatory neurons during associative memory encoding and retrieval. *Sci. Rep.* **7,** (2017).
115. Carstens, K. E., Phillips, M. L., Pozzo-Miller, L., Weinberg, R. J. & Dudek, S. M. Perineuronal Nets Suppress Plasticity of Excitatory Synapses on CA2 Pyramidal Neurons. *J. Neurosci.* **36,** 6312–6320 (2016).
116. Smith, C. C. *et al.* Differential regulation of perineuronal nets in the brain and spinal cord with exercise training. *Brain Res. Bull.* **111,** 20–26 (2015).
117. Pizzorusso, T. *et al.* Reactivation of ocular dominance plasticity in the adult visual cortex. *Science* **298,** 1248–51 (2002).
118. Cabulli, D., Rhodes, K. E. & Fawcett, J. W. Upregulation of aggrecan, link protein 1, and hyaluronan synthases during formation of perineuronal nets in the rat cerebellum. *J. Comp. Neurol.* **501,** 83–94 (2007).
119. Brauer, K., Werner, L. & Leibnitz, L. Perineuronal nets of glia. *J. Hirnforsch.* **23,** 701–8 (1982).
120. Sorg, B. A. *et al.* Casting a Wide Net : Role of Perineuronal Nets in Neural Plasticity. *J. Neurosci.* **36,** 11459–11468 (2016).
121. Tommaso Pizzorusso, Paolo Medini, Nicoletta Berardi, Sabrina Chierzi, James W. Fawcett, L. M. Reactivation of Ocular Dominance Plasticity in the Adult Visual Cortex. *Science (80-.).* **298,** (2002).
122. Barritt, A. W. *et al.* Chondroitinase ABC promotes sprouting of intact and injured spinal systems after spinal cord injury Europe PMC Funders Group. *J Neurosci* **26,** 10856–10867 (2006).
123. Fawcett, J. W. & Asher, R. . The glial scar and central nervous system repair. *Brain Res. Bull.* **49,** 377–391 (1999).
124. Celio, M. R. & Blumcke, I. Perineuronal nets — a specialized form of extracellular matrix in the adult nervous system. *Brain Res. Rev.* **19,** 128–145 (1994).
125. Miyata, S., Nishimura, Y. & Nakashima, T. Perineuronal nets protect against amyloid β-protein neurotoxicity in cultured cortical neurons. *Brain Res.* **1150,** 200–206 (2007).
126. Morawski, M. *et al.* Ion exchanger in the brain: Quantitative analysis of perineuronally fixed anionic binding sites suggests diffusion barriers with ion sorting properties. *Sci. Rep.* **5,** 16471 (2015).
127. Brückner, G. *et al.* Perineuronal nets provide a polyanionic, glia- associated form of microenvironment around certain neurons in many parts of the rat brain. *Glia* **8,** 183–200 (1993).
128. Suttkus, A. *et al.* Aggrecan, link protein and tenascin-R are essential components of the perineuronal net to protect neurons against iron-induced oxidative stress. **5,** (2014).
129. Frischknecht, R. *et al.* Brain extracellular matrix affects AMPA receptor lateral mobility and short-term synaptic plasticity. (2009). doi:10.1038/nn.2338
130. De Winter, F. *et al.* The Chemorepulsive Protein Semaphorin 3A and Perineuronal Net-Mediated Plasticity. *Neural Plasticity* **2016,** (2016).
131. Bernard, C. & Prochiantz, A. Otx2-PNN Interaction to Regulate Cortical Plasticity. *Neural Plast.* **2016,** 7931693 (2016).
132. Sugiyama, S. *et al.* Experience-dependent transfer of Otx2 homeoprotein into the visual cortex activates postnatal plasticity. *Cell* **134,** 508–20 (2008).
133. Chang, M. C. *et al.* Narp regulates homeostatic scaling of excitatory synapses on Parvalbumin interneurons. *Nat. Neurosci.* **13,** 1090–1097 (2010).
134. Gao, H.-M. & Hong, J.-S. Why neurodegenerative diseases are progressive: uncontrolled inflammation drives disease progression. *Trends Immunol.* **29,** 357–65 (2008).
135. Suttkus, A., Holzer, M., Morawski, M. & Arendt, T. The neuronal extracellular matrix restricts distribution and internalization of aggregated Tau-protein. *Neuroscience* **313,** 225–235 (2016).
136. Brückner, G. *et al.* Cortical areas abundant in extracellular matrix chondroitin sulphate proteoglycans are less affected by cytoskeletal changes in Alzheimer's disease. *Neuroscience* **92,** 791–805 (1999).
137. Suttkus, A., Morawski, M. & Arendt, T. Protective Properties of Neural Extracellular Matrix. *Mol. Neurobiol.* **53,** 73–82 (2016).

138. Okamoto, M., Mori, S., Ichimura, M. & Endo, H. Chondroitin sulfate proteoglycans protect cultured rat's cortical and hippocampal neurons from delayed cell death induced by excitatory amino acids. *Neurosci. Lett.* **172,** 51–54 (1994).
139. Lendvai, D. *et al.* Neurochemical mapping of the human hippocampus reveals perisynaptic matrix around functional synapses in Alzheimer's disease. *Acta Neuropathol* **125,** 215–229 (2013).
140. Morawski, M., Brückner, M. K., Riederer, P., Brückner, G. & Arendt, T. Perineuronal nets potentially protect against oxidative stress. *Exp. Neurol.* **188,** 309–315 (2004).
141. Végh, M. J. *et al.* Reducing hippocampal extracellular matrix reverses early memory deficits in a mouse model of Alzheimer's disease. *Acta Neuropathol. Commun.* **2,** 76 (2014).
142. Yang, S. *et al.* Perineuronal net digestion with chondroitinase restores memory in mice with tau pathology. *Exp. Neurol.* **265,** 48–58 (2015).
143. Romberg, C. *et al.* Depletion of perineuronal nets enhances recognition memory and long-term depression in the perirhinal cortex. *J. Neurosci.* **33,** 7057–7065 (2013).
144. Perry, G. *et al.* Association of heparan sulfate proteoglycan with the neurofibrillary tangles of Alzheimer's disease. *J. Neurosci.* **11,** 3679–83 (1991).
145. Castillo, G. M., Ngo, C., Cummings, J., Wight, T. N. & Snow, A. D. Perlecan Binds to the β-Amyloid Proteins (Aβ) of Alzheimer's Disease, Accelerates Aβ Fibril Formation, and Maintains Aβ Fibril Stability. *J. Neurochem.* **69,** 2452–2465 (2002).
146. Kanekiyo, T. *et al.* Heparan Sulphate Proteoglycan and the Low-Density Lipoprotein Receptor-Related Protein 1 Constitute Major Pathways for Neuronal Amyloid- Uptake. *J. Neurosci.* **31,** 1644–1651 (2011).
147. KWON, B., Tetzlaff, W., Grauer, J. N., Beiner, J. & Vaccaro, A. R. Pathophysiology and pharmacologic treatment of acute spinal cord injury. *Spine J.* **4,** 451–464 (2004).
148. Hurlbert, R. J. Strategies of Medical Intervention in the Management of Acute Spinal Cord Injury. *Spine (Phila. Pa. 1976).* **31,** S16–S21 (2006).
149. Cajal, S. R. y. *Degeneration & Regeneration of the Nervous System, Volume 2*. (Oxford University Press Humphrey Milford, 1928).
150. Mueller, B. K., Mueller, R. & Schoemaker, H. Stimulating neuroregeneration as a therapeutic drug approach for traumatic brain injury. *Br. J. Pharmacol.* **157,** 675–85 (2009).
151. Fidler, P. S. *et al.* Comparing astrocytic cell lines that are inhibitory or permissive for axon growth: the major axon-inhibitory proteoglycan is NG2. *J. Neurosci.* **19,** 8778–8788 (1999).
152. Jones, L. L., Margolis, R. U. & Tuszynski, M. H. The chondroitin sulfate proteoglycans neurocan, brevican, phosphacan, and versican are differentially regulated following spinal cord injury. *Exp. Neurol.* **182,** 399–411 (2003).
153. Tang, X., Davies, J. E. & Davies, S. J. A. Changes in distribution, cell associations, and protein expression levels of NG2, neurocan, phosphacan, brevican, versican V2, and tenascin-C during acute to chronic maturation of spinal cord scar tissue. *J. Neurosci. Res.* **71,** 427–44 (2003).
154. Moon, L. D. F., Asher, R. A., Rhodes, K. E. & Fawcett, J. W. Regeneration of CNS axons backto their target following treatment of adult rat brain with chondroitinase ABC. *Nature neuroscience* **4,** 465–466 (2001).
155. Bradbury, E. J. *et al.* Chondroitinase ABC promotes functional recovery after spinal cord injury. *Nature* **416,** 636–640 (2002).
156. Karetko, M. & Skangiel-Kramska, J. Diverse functions of perineuronal nets. *Acta Neurobiol. Exp. (Wars).* **69,** 564–77 (2009).
157. Wang, D., Ichiyama, R. M., Zhao, R., Andrews, M. R. & Fawcett, J. W. Chondroitinase Combined with Rehabilitation Promotes Recovery of Forelimb Function in Rats with Chronic Spinal Cord Injury. *J. Neurosci.* **31,** 9332–9344 (2011).
158. Fox, K. & Caterson, B. Neuroscience: Freeing the brain from the perineuronal net. *Science* **298,** 1187–1189 (2002).
159. Beurdeley, M. *et al.* Otx2 binding to perineuronal nets persistently regulates plasticity in the mature visual cortex. *J. Neurosci.* **32,** 9429–37 (2012).
160. Bray, B. Y. H. G., Gregory, J. E. & Stacey, M. chemistry of tissues. *Biochem. J.* **38,** 142–146 (1944).
161. Levene, B. Y. P. A. On chondroitin. (1913).
162. Roseman, S. Reflections on Glycobiology * 1. *J. Biol. Chem.* **276,** 41527–41542 (2001).
163. Lindahl, U. & Rodén, L. The chondroitin 4-sulfate-protein linkage. *J. Biol. Chem.* **241,** 2113–2119 (1966).
164. Winter, W. T., Arnott, S., Isaac, D. H. & Atkins, E. D. T. Chondroitin 4-sulfate: The structure of a sulfated glycosaminoglycan. *J. Mol. Biol.* **125,** 1–19 (1978).
165. Connell, B. J. & Lortat-Jacob, H. Human Immunodeficiency Virus and Heparan Sulfate: From Attachment to Entry Inhibition. *Front. Immunol.* **4,** 385 (2013).

166. Soares da Costa, D., Reis, R. L. & Pashkuleva, I. Sulfation of Glycosaminoglycans and Its Implications in Human Health and Disorders. *Annu. Rev. Biomed. Eng.* **19,** annurev–bioeng–071516–044610 (2017).
167. Ishan Capila and Robert J. Linhardt*. Heparin- Protein Interactions. *Angew. Chem. Int.* **41,** 390 ± 412 [1] (2002).
168. Maccarana, M., Sakura, Y., Tawada, A., Yoshida, K. & Lindahl, U. Domain structure of heparan sulfates from bovine organs. *J. Biol. Chem.* **271,** 17804–17810 (1996).
169. Maeda, N., Ishii, M., Nishimura, K. & Kamimura, K. Functions of chondroitin sulfate and heparan sulfate in the developing brain. *Neurochem. Res.* **36,** 1228–1240 (2011).
170. Liu, C. C. *et al.* Neuronal heparan sulfates promote amyloid pathology by modulating brain amyloid-β clearance and aggregation in Alzheimer's disease. *Sci. Transl. Med.* **8,** 332ra44 (2016).
171. Funderburgh, J. L. Keratan sulfate biosynthesis. *IUBMB Life* **54,** 187–194 (2002).
172. August, J. T., Granner, D. & Murad, F. *Chondroitin Sulfate: Structure, Role and Pharmacological Activity*. (2006).
173. Silbert, J. E. & Reppucci, A. C. Biosynthesis of chondroitin sulfate. Independent addition of glucuronic acid and N acetylgalactosamine to oligosaccharides. *J. Biol. Chem.* **251,** 3942–3947 (1976).
174. Silbert, J. E. & Sugumaran, G. Biosynthesis of Chondroitin/Dermatan Sulfate. *IUBMB Life (International Union Biochem. Mol. Biol. Life)* **54,** 177–186 (2002).
175. Mikami, T. & Kitagawa, H. Biosynthesis and function of chondroitin sulfate. *Biochim. Biophys. Acta* **1830,** 4719–33 (2013).
176. Kearns, A. E., Vertel, B. M. & Schwartz, N. B. Topography of glycosylation and UDP-xylose production. *J. Biol. Chem.* **268,** 11097–11104 (1993).
177. Sugahara, K. & Kitagawa, H. Recent advances in the study of the biosynthesis and functions of sulfated glycosaminoglycans. *Curr. Opin. Struct. Biol.* **10,** 518–527 (2000).
178. Pacheco, B., Malmström, A. & Maccarana, M. Two dermatan sulfate epimerases form iduronic acid domains in dermatan sulfate. *J. Biol. Chem.* **284,** 9788–9795 (2009).
179. Midura, R. J., Calabro, A., Yanagishita, M. & Hascall, V. C. Nonreducing end structures of chondroitin sulfate chains on aggrecan isolated from swarm rat chondrosarcoma cultures. *J. Biol. Chem.* **270,** 8009–8015 (1995).
180. Ohtake-Niimi, S. *et al.* Mice deficient in N-acetylgalactosamine 4-sulfate 6-o-sulfotransferase are unable to synthesize chondroitin/dermatan sulfate containing N-acetylgalactosamine 4,6-bissulfate residues and exhibit decreased protease activity in bone marrow-derived mast cells. *J. Biol. Chem.* **285,** 20793–805 (2010).
181. Gama, C. I. *et al.* Sulfation patterns of glycosaminoglycans encode molecular recognition and activity. *Nat. Chem. Biol.* **2,** 467–473 (2006).
182. Prabhakar, V. & Sasisekharan, R. The Biosynthesis and Catabolism of Galactosaminoglycans. *Adv. Pharmacol.* **53,** 69–115 (2006).
183. Kaneiwa, T., Mizumoto, S., Sugahara, K. & Yamada, S. Identification of human hyaluronidase-4 as a novel chondroitin sulfate hydrolase that preferentially cleaves the galactosaminidic linkage in the trisulfated tetrasaccharide sequence. *Glycobiology* **20,** 300–309 (2010).
184. Tachi, Y. *et al.* Expression of hyaluronidase-4 in a rat spinal cord hemisection model. *Asian Spine J.* **9,** 7–13 (2015).
185. Deepa, S. S. *et al.* Composition of Perineuronal Net Extracellular Matrix in Rat Brain. *J. Biol. Chem.* **281,** 17789–17800 (2006).
186. Kitagawa, H., Tsutsumi, K., Tone, Y. & Sugahara, K. Developmental regulation of the sulfation profile of chondroitin sulfate chains in the chicken embryo brain. *J. Biol. Chem.* **272,** 31377–31381 (1997).
187. Maeda, N. Structural variation of chondroitin sulfate and its roles in the central nervous system. *Cent. Nerv. Syst. Agents Med. Chem.* **10,** 22–31 (2010).
188. Ishii, M. & Maeda, N. Spatiotemporal expression of chondroitin sulfate sulfotransferases in the postnatal developing mouse cerebellum. *Glycobiology* **18,** 602–614 (2008).
189. Foscarin, S., Raha-Chowdhury, R., Fawcett, J. W. & Kwok, J. C. F. Brain ageing changes proteoglycan sulfation, rendering perineuronal nets more inhibitory. *Aging (Albany. NY).* **9,** 1607–1622 (2017).
190. Miyata, S., Komatsu, Y., Yoshimura, Y., Taya, C. & Kitagawa, H. Persistent cortical plasticity by upregulation of chondroitin 6-sulfation. *Nat. Neurosci.* **15,** 414–422 (2012).
191. Gilbert, R. J. *et al.* CS-4,6 is differentially upregulated in glial scar and is a potent inhibitor of neurite extension. *Mol. Cell. Neurosci.* **29,** 545–558 (2005).
192. Brown, J. M. *et al.* A sulfated carbohydrate epitope inhibits axon regeneration after injury. *Proc. Natl. Acad. Sci.* **109,** 4768–4773 (2012).
193. Hikino, M. *et al.* Oversulfated Dermatan Sulfate Exhibits Neurite Outgrowth-promoting Activity toward Embryonic Mouse Hippocampal Neurons. *J. Biol. Chem.* **278,** 43744–43754 (2003).
194. Mikami, T., Yasunaga, D. & Kitagawa, H. Contactin-1 Is a Functional Receptor for Neuroregulatory

Chondroitin Sulfate-E. *J. Biol. Chem.* **284,** 4494–4499 (2009).
195. Ida, M. *et al.* Identification and functions of chondroitin sulfate in the milieu of neural stem cells. *J. Biol. Chem.* **281,** 5982–5991 (2006).
196. Takeda, A., Shuto, M. & Funakoshi, K. Chondroitin Sulfate Expression in Perineuronal Nets After Goldfish Spinal Cord Lesion. *Front. Cell. Neurosci.* **12,** 63 (2018).
197. Maeda, N. *et al.* Heterogeneity of the chondroitin sulfate portion of phosphacan/6B4 proteoglycan regulates its binding affinity for pleiotrophin/heparin binding growth-associated molecule. *J. Biol. Chem.* **278,** 35805–35811 (2003).
198. Bradbury, E. J. *et al.* Chondroitinase ABC promotes functional recovery after spinal cord injury. *Nature* **416,** 636–640 (2002).
199. Chung, K. Y., Taylor, J. S., Shum, D. K. & Chan, S. O. Axon routing at the optic chiasm after enzymatic removal of chondroitin sulfate in mouse embryos. *Development* **127,** 2673–2683 (2000).
200. Swarup, V. P. *et al.* Exploiting Differential Surface Display of Chondroitin Sulfate Variants for Directing Neuronal Outgrowth NIH Public Access. *J Am Chem Soc* **135,** 13488–13494 (2013).
201. Shimazaki, Y. *et al.* Developmental change and function of chondroitin sulfate deposited around cerebellar Purkinje cells. *J. Neurosci. Res.* **82,** 172–183 (2005).
202. Sotogaku, N. *et al.* Activation of phospholipase C pathways by a synthetic chondroitin sulfate-E tetrasaccharide promotes neurite outgrowth of dopaminergic neurons. *J. Neurochem.* **103,** 749–60 (2007).
203. Grimpe, B. & Silver, J. A novel DNA enzyme reduces glycosaminoglycan chains in the glial scar and allows microtransplanted dorsal root ganglia axons to regenerate beyond lesions in the spinal cord. *J. Neurosci.* **24,** 1393–7 (2004).
204. Dick, G. *et al.* Semaphorin 3A binds to the perineuronal nets via chondroitin sulfate type E motifs in rodent brains. *J. Biol. Chem.* **288,** 27384–27395 (2013).
205. Djerbal, L., Lortat-Jacob, H. & Kwok, J. Chondroitin sulfates and their binding molecules in the central nervous system. *Glycoconjugate Journal* **34,** 363–376 (2017).
206. Yazdani, U. & Terman, J. R. The semaphorins. *Genome Biol.* **7,** 211 (2006).
207. Kolodkin, A. L. *et al.* Fasciclin IV: Sequence, expression, and function during growth cone guidance in the grasshopper embryo. *Neuron* **9,** 831–845 (1992).
208. Luo, Y., Raible, D. & Raper, J. A. Collapsin: A Protein in Brain That Induces the Collapse and Paralysis of Neuronal Growth Cones. *Cell* **75,** 217–227 (1993).
209. Kolodkin, A. L., Matthes, D. J. & Goodman, C. S. The semaphorin genes encode a family of transmembrane and secreted growth cone guidance molecules. *Cell* **75,** 1389–1399 (1993).
210. Püschel, A. W., Adams, R. H. & Betz, H. Murine semaphorin D/collapsin is a member of a diverse gene family and creates domains inhibitory for axonal extension. *Neuron* **14,** 941–948 (1995).
211. Adams, R. H., Betz, H. & Püschel, A. W. A novel class of murine semaphorins with homology to thrombospondin is differentially expressed during early embryogenesis. *Mech. Dev.* **57,** 33–45 (1996).
212. Zhu, L. *et al.* Regulated surface expression and shedding support a dual role for semaphorin 4D in platelet responses to vascular injury. *Proc. Natl. Acad. Sci.* **104,** 1621–1626 (2007).
213. Browne, K., Wang, W., Liu, R. Q., Piva, M. & O'Connor, T. P. Transmembrane semaphorin5B is proteolytically processed into a repulsive neural guidance cue. *J. Neurochem.* **123,** 135–146 (2012).
214. Holmes, S. *et al.* Sema7A is a potent monocyte stimulator. *Scand. J. Immunol.* **56,** 270–5 (2002).
215. Antipenko, A. *et al.* Structure of the Semaphorin-3A Receptor Binding Module. *Neuron* **39,** 589–598 (2003).
216. Love, C. A. *et al.* The ligand-binding face of the semaphorins revealed by the high-resolution crystal structure of SEMA4D. *Nat. Struct. Biol.* **10,** 843–848 (2003).
217. Janssen, B. J. C. *et al.* Neuropilins lock secreted semaphorins onto plexins in a ternary signaling complex. *Nat. Struct. Mol. Biol.* **19,** 1293–1299 (2012).
218. Janssen, B. J. C. *et al.* Structural basis of semaphorin-plexin signalling. *Nature* **467,** (2010).
219. Liu, H. *et al.* Structural Basis of Semaphorin-Plexin Recognition and Viral Mimicry from Sema7A and A39R Complexes with PlexinC1. *Cell* **142,** 749–761 (2010).
220. Alto, L. T. & Terman, J. R. Semaphorins and their Signaling Mechanisms. *Methods Mol Biol* **1493,** 1–25 (2017).
221. Yazdani, U. & Terman, J. R. The semaphorins. *Genome Biol.* **7,** 211 (2006).
222. Siebold, C. & Jones, E. Y. Structural insights into semaphorins and their receptors. *Semin. Cell Dev. Biol.* **24,** 139–145 (2013).
223. Nogi, T. *et al.* Structural basis for semaphorin signalling through the plexin receptor. *Nature* **467,** (2010).
224. Wang, Y. *et al. Plexins Are GTPase-Activating Proteins for Rap and Are Activated by Induced Dimerization*. (2012).
225. Bell, C. H., Aricescu, A. R., Jones, E. Y. & Siebold, C. Dual Binding Mode for RhoGTPases in Plexin

Signalling. *PLoS Biol* **9,** 1001134 (2011).
226. Terman, J. R., Mao, T., Pasterkamp, R. J., Yu, H.-H. & Kolodkin, A. L. MICALs, a family of conserved flavoprotein oxidoreductases, function in plexin-mediated axonal repulsion. *Cell* **109,** 887–900 (2002).
227. Kolodkin, A. L. *et al.* Neuropilin Is a Semaphorin III Receptor. *Cell* **90,** 753–762 (1997).
228. Feiner, L. & Koppel, A. M. Secreted Chick Semaphorins Bind Recombinant Neuropilin with Similar Affinities but Bind Different Subsets of Neurons In Situ. *Neuron* **19,** 539–545 (1997).
229. Appleton, B. A. *et al.* Structural studies of neuropilin/antibody complexes provide insights into semaphorin and VEGF binding. *EMBO J.* **26,** 4902–4912 (2007).
230. Yelland, T. & Djordjevic, S. Crystal Structure of the Neuropilin-1 MAM Domain: Completing the Neuropilin-1 Ectodomain Picture. *Structure* **24,** 2008–2015 (2016).
231. Chen, H., He, Z., Bagri, A. & Tessier-Lavigne, M. Semaphorin-neuropilin interactions underlying sympathetic axon responses to class III semaphorins. *Neuron* (1998). doi:10.1016/S0896-6273(00)80648-0
232. Roth, L. *et al.* Transmembrane Domain Interactions Control Biological Functions of Neuropilin-1. *Mol. Biol. Cell* **19,** 646–654 (2008).
233. Nakamura, F., Kalb, R. G. & Strittmatter, S. M. Molecular basis of semaphorin-mediated axon guidance. *J. Neurobiol.* **44,** 219–29 (2000).
234. Nasarre, P., Gemmill, R. M. & Drabkin, H. A. The emerging role of class-3 semaphorins and their neuropilin receptors in oncology. *OncoTargets and Therapy* **7,** 1663–1687 (2014).
235. Kitsukawa, T. *et al.* Neuropilin-semaphorin III/D-mediated chemorepulsive signals play a crucial role in peripheral nerve projection in mice. *Neuron* **19,** 995–1005 (1997).
236. Lee, C. C., Kreusch, A., Mcmullan, D., Ng, K. & Spraggon, G. Crystal Structure of the Human Neuropilin-1 b1 Domain Neuropilins and Axon Guidance Neuropilin-1 is one of two family members initially identi- fied as high-affinity cell surface receptors for secreted. *Structure* **11,** 99–108 (2003).
237. Ruiz de Almodovar, C. *et al.* VEGF mediates commissural axon chemoattraction through its receptor Flk1. *Neuron* **70,** 966–78 (2011).
238. Mamluk, R. *et al.* Neuropilin-1 binds vascular endothelial growth factor 165, placenta growth factor-2, and heparin via its b1b2 domain. *J. Biol. Chem.* **277,** 24818–24825 (2002).
239. Gu, C. *et al.* Characterization of neuropilin-1 structural features that confer binding to semaphorin 3A and vascular endothelial growth factor 165. *J. Biol. Chem.* **277,** 18069–18076 (2002).
240. Gagnon, M. L. *et al.* Identification of a natural soluble neuropilin-1 that binds vascular endothelial growth factor: In vivo expression and antitumor activity. *Proc. Natl. Acad. Sci. U. S. A.* **97,** 2573–8 (2000).
241. Shintani, Y. *et al.* Glycosaminoglycan modification of neuropilin-1 modulates VEGFR2 signaling. *EMBO J.* **25,** 3045–55 (2006).
242. Elpek, G. Ö. Neuropilins and liver. *World J. Gastroenterol.* **21,** 7065–7073 (2015).
243. Dodd, J. & Jessell, T. M. Axon guidance and the patterning of neuronal projections in vertebrates. *Science* **242,** 692–699 (1988).
244. Nugent, A. A., Kolpak, A. L. & Engle, E. C. Human disorders of axon guidance. *Curr. Opin. Neurobiol.* **22,** 837–43 (2012).
245. Stoeckli, E. T. Understanding axon guidance: are we nearly there yet? *Development* **145,** dev151415 (2018).
246. de Ramon Francàs, G., Zuñiga, N. R. & Stoeckli, E. T. The spinal cord shows the way – How axons navigate intermediate targets. *Dev. Biol.* **432,** 43–52 (2017).
247. Gamboa, N. T. *et al.* Neurovascular patterning cues and implications for central and peripheral neurological disease. *Surg. Neurol. Int.* **8,** 208 (2017).
248. Landis, S. C. Neuronal growth cones. *Ann.Rev.Physiol.* **45,** 567–580 (1983).
249. Chauvet, S. *et al.* Gating of Sema3E/PlexinD1 Signaling by Neuropilin-1 Switches Axonal Repulsion to Attraction during Brain Development. *Neuron* **56,** 807–822 (2007).
250. Kolk, S. M. *et al.* Semaphorin 3F is a bifunctional guidance cue for dopaminergic axons and controls their fasciculation, channeling, rostral growth, and intracortical targeting. *J. Neurosci.* **29,** 12542–57 (2009).
251. Kantor, D. B. *et al.* Semaphorin 5A Is a Bifunctional Axon Guidance Cue Regulated by Heparan and Chondroitin Sulfate Proteoglycans. *Neuron* **44,** 961–975 (2004).
252. Matsuoka, R. L. *et al.* Class5 transmembrane semaphorins control selective mammalian retinal lamination and function. *Neuron* **71,** 460–473 (2011).
253. Matsuoka, R. L. *et al.* Transmembrane semaphorin signalling controls laminar stratification in the mammalian retina. *Nature* **470,** 259–264 (2011).
254. Baudet, M.-L. *et al.* miR-124 acts through CoREST to control onset of Sema3A sensitivity in navigating retinal growth cones. *Nat. Neurosci.* **15,** 29–38 (2012).

255. Matsuo, T., Rossier, D. A., Kan, C. & Rodriguez, I. The wiring of Grueneberg ganglion axons is dependent on neuropilin 1. *Development* **139,** 2783–2791 (2012).
256. Messersmith, E. K. *et al. Semaphorin III Can Function as a Selective Chemorepellent to Pattern Sensory Projections in the Spinal Cord*. *Neuron* **14,** (1995).
257. Reza, J. N., Gavazzi, I. & Cohen, J. Neuropilin-1 Is Expressed on Adult Mammalian Dorsal Root Ganglion Neurons and Mediates Semaphorin3a/Collapsin-1-Induced Growth Cone Collapse by Small Diameter Sensory Afferents. *Mol. Cell. Neurosci.* **14,** 317–326 (1999).
258. Tang, X.-Q. Semaphorin3A Inhibits Nerve Growth Factor-Induced Sprouting of Nociceptive Afferents in Adult Rat Spinal Cord. *J. Neurosci.* **24,** 819–827 (2004).
259. Moret, F., Renaudot, C., Bozon, M. & Castellani, V. Semaphorin and neuropilin co-expression in motoneurons sets axon sensitivity to environmental semaphorin sources during motor axon pathfinding. *Development* **134,** 4491–4501 (2007).
260. Chen, G. *et al.* Semaphorin-3A guides radial migration of cortical neurons during development. *Nat. Neurosci.* **11,** 36–44 (2008).
261. Giacobini, P. *et al.* Semaphorin 4D regulates gonadotropin hormonereleasing hormone-1 neuronal migration through PlexinBl-Met complex. *J. Cell Biol.* **183,** 555–566 (2008).
262. Kumanogoh, A. *Semaphorins a diversity of emerging physiological and pathological activities*. *Springer* (2015). doi:10.1007/978-4-431-54385-5
263. Takamatsu, H., Okuno, T. & Kumanogoh, A. Regulation of immune cell responses by semaphorins and their receptors. *Cell. Mol. Immunol.* **7,** 83–8 (2010).
264. Sterling, J. A. *et al.* The Role of Semaphorin 4D in Bone Remodeling and Cancer Metastasis. **9,** 1 (2018).
265. Xu, R. Semaphorin 3A a new player in bone remodeling. *Cell Adhesion and Migration* **8,** 5–10 (2014).
266. Sakurai, A., Doci, C. & Gutkind, J. S. Semaphorin signaling in angiogenesis, lymphangiogenesis and cancer. *Cell Res.* **22,** 23–32 (2011).
267. Palodetto, B. *et al.* SEMA3A partially reverses VEGF effects through binding to neuropilin-1. *Stem Cell Res.* **22,** 70–78 (2017).
268. Neufeld, G., Sabag, A. D., Rabinovicz, N. & Kessler, O. Semaphorins in angiogenesis and tumor progression. *Cold Spring Harb. Perspect. Med.* **2,** a006718 (2012).
269. Adams, R. H., Lohrum, M., Klostermann, A., Betz, H. & Püschel, A. W. The chemorepulsive activity of secreted semaphorins is regulated by furin-dependent proteolytic processing. *EMBO J.* **16,** 6077–6086 (1997).
270. Bravo, D. A., Gleason, J. B., Sanchez, R. I., Roth, R. A. & Fuller, R. S. Accurate and efficient cleavage of the human insulin proreceptor by the human proprotein-processing protease furin. Characterization and kinetic parameters using the purified, secreted soluble protease expressed by a recombinant baculovirus. *J. Biol. Chem.* **269,** 25830–7 (1994).
271. Nakayama, K. Furin: a mammalian subtilisin/Kex2p-like endoprotease involved in processing of a wide variety of precursor proteins. *Biochem. J.* **327,** 625–35 (1997).
272. Molloy, S. S., Thomas, L., VanSlyke, J. K., Stenberg, P. E. & Thomas, G. Intracellular trafficking and activation of the furin proprotein convertase: localization to the TGN and recycling from the cell surface. *EMBO J.* **13,** 18–33 (1994).
273. Klostermann, A., Lohrum, M., Adams, R. H. & Püschel, A. W. The chemorepulsive activity of the axonal guidance signal semaphorin D requires dimerization. *J. Biol. Chem.* **273,** 7326–31 (1998).
274. Nakamura, F., Tanaka, M., Takahashi, T., Kalb, R. G. & Strittmatter, S. M. *NNeuropilin-1 Extracellular Domains Mediate Semaphorin D/III-Induced Growth Cone Collapse*. *Neuron* **21,** (1998).
275. Comeau, M. R. *et al.* A poxvirus-encoded semaphorin induces cytokine production from monocytes and binds to a novel cellular semaphorin receptor, VESPR. *Immunity* **8,** 473–482 (1998).
276. Winberg, M. L. *et al.* Plexin A is a neuronal semaphorin receptor that controls axon guidance. *Cell* **95,** 903–916 (1998).
277. Plexin-Neuropilin-1 Complexes Form Functional Semaphorin-3A Receptors. *Cell* **99,** 59–69 (1999).
278. Takahashi, T. & Strittmatter, S. M. PlexinA1 autoinhibition by the Plexin sema domain. *Neuron* **29,** 429–439 (2001).
279. Sabag, A. D. *et al.* The role of the plexin-A2 receptor in Sema3A and Sema3B signal transduction. *J. Cell Sci.* **127,** 5240–5252 (2014).
280. Yaron, A., Huang, P.-H., Cheng, H.-J. & Tessier-Lavigne, M. Differential Requirement for Plexin-A3 and -A4 in Mediating Responses of Sensory and Sympathetic Neurons to Distinct Class 3 Semaphorins. *Neuron* **45,** 513–523 (2005).
281. Wen, H., Lei, Y., Eun, S.-Y. & Ting, J. P.-Y. Plexin-A4-semaphorin 3A signaling is required for Toll-like receptor- and sepsis-induced cytokine storm. *J. Exp. Med.* **207,** 2943–57 (2010).
282. Zygmunt, T. *et al.* Semaphorin-PlexinD1 Signaling Limits Angiogenic Potential via the VEGF Decoy

Receptor sFlt1. *Dev. Cell* **21,** 301–314 (2011).
283. Neufeld, G. & Kessler, O. The semaphorins: Versatile regulators of tumour progression and tumour angiogenesis. *Nature Reviews Cancer* **8,** 632–645 (2008).
284. Goshima, Y., Nakamura, F., Strittmatter, P. & Strittmatter, S. M. Collapsin-induced growth cone collapse mediated by an intracellular protein related to UNC-33. *Nature* **376,** 509–514 (1995).
285. Mitsui, N. *et al.* Involvement of Fes / Fps tyrosine kinase in semaphorin3A signaling. *EMBO J.* **21,** (2002).
286. Inatome, R. *et al.* Identification of CRAM, a novel unc-33 gene family protien that associates with CRMP3 and protein-tyrosine kinase(s) in the developing rat brain. *J. Biol. Chem.* **275,** 27291–27302 (2000).
287. Fukata, Y. *et al.* CRMP-2 binds to tubulin heterodimers to promote microtubule assembly. *Nat. Cell Biol.* **4,** 583–591 (2002).
288. Jin, Z. & Strittmatter, S. M. Rac1 mediates collapsin-1-induced growth cone collapse. *J. Neurosci.* **17,** 6256–6263 (1997).
289. Sasaki, Y. *et al.* Fyn and Cdk5 mediate semaphorin-3A signaling, which is involved in regulation of dendrite orientation in cerebral cortex. *Neuron* **35,** 907–20 (2002).
290. Fan, J., Mansfield, S. G., Redmond, T., Gordon-Weeks, P. R. & Raper, J. A. The organization of F-actin and microtubules in growth cones exposed to a brain-derived collapsing factor. *J. Cell Biol.* **121,** 867–878 (1993).
291. Chadborn, N. H. PTEN couples Sema3A signalling to growth cone collapse. *J. Cell Sci.* **119,** 951–957 (2006).
292. Brown, J. A., Wysolmerski, R. B. & Bridgman, P. C. Dorsal Root Ganglion Neurons React to Semaphorin 3A Application through a Biphasic Response that Requires Multiple Myosin II Isoforms. *Mol. Biol. Cell* **20,** 1167–1179 (2009).
293. Vo, T. *et al.* The chemorepulsive axon guidance protein semaphorin3A is a constituent of perineuronal nets in the adult rodent brain. *Mol. Cell. Neurosci.* **56,** 186–200 (2013).
294. de Wit, J., Toonen, R. F., Verhaagen, J. & Verhage, M. Vesicular trafficking of semaphorin 3A is activity-dependent and differs between axons and dendrites. *Traffic* **7,** 1060–77 (2006).
295. De Wit, J., De Winter, F., Klooster, J. & Verhaagen, J. Semaphorin 3A displays a punctate distribution on the surface of neuronal cells and interacts with proteoglycans in the extracellular matrix. *Mol. Cell. Neurosci.* **29,** 40–55 (2005).
296. Treps, L. *et al.* Extracellular vesicle-transported Semaphorin3A promotes vascular permeability in glioblastoma. *Oncogene* **35,** 2615–2623 (2016).
297. Mecollari, V., Nieuwenhuis, B. & Verhaagen, J. A perspective on the role of class III semaphorin signaling in central nervous system trauma. *Front. Cell. Neurosci.* **8,** 328 (2014).
298. Pasterkamp, R. J. & Verhaagen, J. Semaphorins in axon regeneration: Developmental guidance molecules gone wrong? *Philosophical Transactions of the Royal Society B: Biological Sciences* **361,** 1499–1511 (2006).
299. Minor, K. H., Bournat, J. C., Toscano, N., Giger, R. J. & Davies, S. J. A. Decorin, erythroblastic leukaemia viral oncogene homologue B4 and signal transducer and activator of transcription 3 regulation of semaphorin 3A in central nervous system scar tissue. *Brain* **134,** 1140–1155 (2011).
300. Syed, Y. A. *et al.* Inhibition of CNS Remyelination by the Presence of Semaphorin 3A. *J. Neurosci.* **31,** 3719–3728 (2011).
301. Zimmer, G. *et al.* Chondroitin Sulfate Acts in Concert with Semaphorin 3A to Guide Tangential Migration of Cortical Interneurons in the Ventral Telencephalon. *Cereb. Cortex Oct.* **20,** 2411–2422 (2010).
302. Montolio, M. *et al.* A Semaphorin 3A Inhibitor Blocks Axonal Chemorepulsion and Enhances Axon Regeneration. *Chem. Biol.* **16,** 691–701 (2009).
303. Corredor, M. *et al.* Cationic Peptides and Peptidomimetics Bind Glycosaminoglycans as Potential Sema3A Pathway Inhibitors. *Biophys. J.* **110,** 1291–303 (2016).
304. Vives, R. R. *et al.* A Novel Strategy for Defining Critical Amino Acid Residues Involved in Protein/Glycosaminoglycan Interactions. *J. Biol. Chem.* **279,** 54327–54333 (2004).
305. Kwok, J. C. F., Foscarin, S. & Fawcett, J. W. *Extracellular Matrix, Neuromethods*. **93,** (2015).
306. Saesen, E. *et al.* Insights into the Mechanism by Which Interferon-γ Basic Amino Acid Clusters Mediate Protein Binding to Heparan Sulfate. *J. Am. Chem. Soc.* **135,** 9384–9390 (2013).
307. Jacquinet, J.-C., Lopin-Bon, C. & Vibert, A. From polymer to size-defined oligomers: a highly divergent and stereocontrolled construction of chondroitin sulfate A, C, D, E, K, L, and M oligomers from a single precursor: part 2. *Chem. A Eur. J.* **15,** 9579–9595 (2009).
308. Jacquinet, J.-C. & Lopin-Bon, C. Stereocontrolled preparation of biotinylated chondroitin sulfate E di-, tetra-, and hexasaccharide conjugates. *Carbohydr. Res.* **402,** 35–43 (2015).

309. Migliorini, E. *et al.* Well-defined biomimetic surfaces to characterize glycosaminoglycan-mediated interactions on the molecular, supramolecular and cellular levels. *Biomaterials* **35,** 8903–8915 (2014).
310. Cardin, A. D. & Weintraub, H. J. Molecular modeling of protein-glycosaminoglycan interactions. *Arteriosclerosis* **9,** 21–32 (1989).
311. Sobel, M., Soler, D. F., Kermode, J. C. & Harris, R. B. Localization and characterization of a heparin binding domain peptide of human von Willebrand factor. *J. Biol. Chem.* **267,** 8857–62 (1992).
312. Anton Van Der Merwe, P. Surface plasmon resonance.
313. Dubacheva, G. V *et al.* Controlling Multivalent Binding through Surface Chemistry: Model Study on Streptavidin. *J. Am. Chem. Soc.* **139,** 4157–4167 (2017).
314. Shintani, Y. *et al.* Glycosaminoglycan modification of neuropilin-1 modulates VEGFR2 signaling. *EMBO J.* **25,** 3045–55 (2006).
315. Esko, J. D. & Linhardt, R. J. *Proteins that Bind Sulfated Glycosaminoglycans*. *Essentials of Glycobiology* 1–13 (Cold Spring Harbor Laboratory Press, 2009). doi:10.1101/glycobiology.3e.038
316. Rogers, C. J. *et al.* Elucidating glycosaminoglycan-protein-protein interactions using carbohydrate microarray and computational approaches. *Proc. Natl. Acad. Sci.* **108,** 9747–9752 (2011).
317. Ashikari-Hada, S. *et al.* Characterization of growth factor-binding structures in heparin/heparan sulfate using an octasaccharide library. *J. Biol. Chem.* **279,** 12346–54 (2004).
318. Lortat-Jacob, H. The molecular basis and functional implications of chemokine interactions with heparan sulphate. *Curr. Opin. Struct. Biol.* **19,** 543–548 (2009).
319. Monneau, Y., Arenzana-Seisdedos, F. & Lortat-Jacob, H. The sweet spot: how GAGs help chemokines guide migrating cells. *J. Leukoc. Biol.* **99,** 935–953 (2016).
320. Lindahl, U. & Li, J. ping. Interactions Between Heparan Sulfate and Proteins-Design and Functional Implications. *International Review of Cell and Molecular Biology* **276,** 105–159 (2009).
321. Liang, W. G. *et al.* Structural basis for oligomerization and glycosaminoglycan binding of CCL5 and CCL3. *Proc. Natl. Acad. Sci.* **113,** 5000–5005 (2016).
322. Yang, S. *et al.* An Approach to Synthesize Chondroitin Sulfate-E (CS-E) Oligosaccharide Precursors. *J. Org. Chem.* **83,** 5897–5908 (2018).
323. Pasquato, A. *et al.* Heparin enhances the furin cleavage of HIV-1 gp160 peptides. *FEBS Lett.* **581,** 5807–5813 (2007).
324. Day, P. M., Lowy, D. R. & Schiller, J. T. Heparan Sulfate-Independent Cell Binding and Infection with Furin-Precleaved Papillomavirus Capsids. *J. Virol.* **82,** 12565–12568 (2008).
325. Rawling, J., Cano, O., Garcin, D., Kolakofsky, D. & Melero, J. A. Recombinant Sendai Viruses Expressing Fusion Proteins with Two Furin Cleavage Sites Mimic the Syncytial and Receptor-Independent Infection Properties of Respiratory Syncytial Virus. *J. Virol.* **85,** 2771–2780 (2011).
326. Klimstra, W. B., Heidner, H. W. & Johnston, R. E. The furin protease cleavage recognition sequence of Sindbis virus PE2 can mediate virion attachment to cell surface heparan sulfate. *J. Virol.* **73,** 6299–6306 (1999).
327. Henrotin, Y., Mathy, M., Sanchez, C. & Lambert, C. Chondroitin sulfate in the treatment of osteoarthritis: From in vitro studies to clinical recommendations. *Therapeutic Advances in Musculoskeletal Disease* **2,** 335–348 (2010).
328. Mie Nishimura, Nobuyuki Miyamoto, Jun Nishihira. Daily Oral Chondroitin Sulfate Oligosaccharides for Knee Joint Pain in Healthy Subjects: A Randomized, Blinded, Placebo-Controlled Study. *Open Nutr. J.* **12,** (2018).
329. Williams, G. *et al.* A complementary peptide approach applied to the design of novel semaphorin/neuropilin antagonists. *J. Neurochem.* **92,** 1180–90 (2005).
330. Moloney, E. B., Mecollari, V., Blits, B., De Winter, F. & Verhaagen, J. Neuropilin-derived scavenger molecules with specificity for semaphorin 3A. *Unpublished*
331. Guan, K. L. & Rao, Y. Signalling mechanisms mediating neuronal responses to guidance cues. *Nature Reviews Neuroscience* **4,** 941–956 (2003).